Winter 12-15-2022

Using Proteomics to Discover New Connections in the Arabidopsis Circadian Clock

Maria Lynn Sorkin
Washington University in St. Louis

WASHINGTON UNIVERSITY IN ST. LOUIS

Division of Biology and Biomedical Sciences
Plant and Microbial Biosciences

Dissertation Examination Committee:
Dmitri Nusinow, Chair
Ram Dixit
Malia Gehan
Elizabeth Haswell
Erik Herzog

Using Proteomics to Discover New Connections in the Arabidopsis Circadian Clock

by

Maria Lynn Sorkin

A dissertation presented to
The Graduate School
of Washington University in
partial fulfillment of the
requirements for the degree
of Doctor of Philosophy

August 2022
St. Louis, Missouri

Table of Contents

List of Figures

List of Supplemental Figures

List of Tables

List of Supplemental Tables

Acknowledgements

I have so much gratitude for the friends, mentors, and lab mates who have helped and supported me while I completed my dissertation work. First, I am grateful to Washington University in St. Louis and the Donald Danforth Plant Science Center for serving equally as my home institutions. My graduate stipend was funded by the National Science Foundation Graduate Research Fellowship Program and the William H. Danforth Plant Science Fellowship.

I am so grateful to my graduate mentor, Dr. Dmitri (“meter”) Nusinow. Meter was the kind, excited, patient, and down-to-earth advisor that I needed in graduate school. He curbed my worst research habits and encouraged me to grow in and outside of the laboratory. Advisors often wear many hats. Meter’s included but were not limited to: mentor, therapist, and friend. Meter—Thank you for always being my biggest cheerleader.

I would also like to thank Dr. Karen Hicks, Dr. Colleen Doherty and the members of my thesis committee, Drs. Elizabeth Haswell, Malia Gehan, Erik Herzog, and Ram Dixit, for their invaluable mentorship and commitment to my education as a research scientist. I hope to pay forward the time and effort you spent helping me and the lessons I’ve learned from you.

I do not think it would have been possible for me to finish graduate school without my cohort, friends, and lab mates. Thanks to Tricia Walker, Jenny Codjoe, Ginger Johnson, Ryan Calcutt, Andrew Lin, Emma Frawley, and especially Dennis Zhu for their friendship and love. I have so much gratitude for all the current and past members of the Nusinow Lab, especially to Dr. He Huang, Sarah Pardi, Becca Bindbeutel, Dr.

Vanessica Jawahir, Kristen Edgeworth, Sunita Pathak, Andrew Lin, Dr. Dong-Yeon Lee, Adele Ayers, and Austin Morgan. Thank you to Dr. Margaret Wilson, who was not only a second graduate school mentor to me, but also a coworker, role model, and friend.

Finally, I would like to thank my girlfriend, Shelby Nash, my brother, Michael Sorkin, my cat, Freddie Mercury, and my parents, Kathie and Bruce Sorkin, for their unwavering love and support. Shelby—you make me feel right. Michael—I look up to you more than you know. Mom and Dad—you raised me to believe I was capable of anything I set my mind to. I am here because of your love and support.

Maria Lynn Sorkin

Washington University in St. Louis

August 2022

Dedicated to my parents.

ABSTRACT OF THE DISSERTATION

Using Proteomics to Discover New Connections in the Arabidopsis Circadian Clock

by

Maria Lynn Sorkin

Doctor of Philosophy in Biology and Biomedical Sciences

Plant and Microbial Biosciences

Washington University in St. Louis, 2022

Dr. Dmitri Nusinow, Chair

The plant circadian clock is an endogenous timekeeping mechanism that uses daylength and temperature cycles to synchronize internal physiology with the external environment. Much of our understanding of the clock in the model plant *Arabidopsis thaliana* comes from genetic approaches. In this thesis, I use affinity purification coupled with mass spectrometry (APMS) to identify protein-protein interactions for core clock components on a proteomic scale. I developed and optimized a protocol to perform APMS on a core set of circadian clock proteins: CIRCADIAN CLOCK ASSOCIATED 1 (CCA1), LATE ELONGATED HYPOCOTYL (LHY), PSEUDORESPONSE REGULATOR 5 (PRR5), PRR7, PRR9, TIMING OF CAB 1 (TOC1)/PRR1, FIONA 1 (FIO1), JUMONJI DOMAIN CONTAINING 5 (JMJD5), NIGHT LIGHT-INDUCIBLE AND CLOCK-REGULATED 1 (LNK1), LNK2, and REVEILLE 8 (RVE8). The combined dataset of proteins coprecipitated with these clock factors represents a circadian clock “interactome” that is publicly available for future studies. I chose to follow up on an interaction between RVE8/LNK1/LNK2 and two proteins previously unrelated to these

clock components, COLD-REGULATED PROTEIN 27 (COR27) and COR28. I found that these proteins form a complex in the early evening that serves to regulate RVE8 protein stability and to block the transcriptional activity of RVE8-LNK1/2. Together, this work demonstrates the power of proteomics to make new discoveries in the plant circadian clock and I hope that my datasets will be a useful tool for future studies.

1. Introduction — Overview of Circadian Rhythms in Plants

1.1 Fundamental Properties of Circadian Rhythms Across Kingdoms

In an otherwise ever-changing environment, the rise and fall of the sun each day is a constant. The basic consequences of the Earth's rotation include the absence of the sun's light during the night and the temperature fluctuations that accompany the day-night cycle. These environmental cues have been stable points of reference for organisms since the origins of life. As such, it is unsurprising that biological timekeeping mechanisms have evolved in all kingdoms of life (Rosbash, 2009; Saini et al., 2019). For plants, which evolved to harness the sun's energy to grow, this basic distinction between day and night served as a powerful synchronization cue for numerous processes; for example, during the day, plants capture carbon through photosynthesis; at night, the plant can redirect its energy on non-photosynthetic activities. This internal timekeeping mechanism has been termed the circadian clock. The word "circadian" stems from the Latin phrase "circa diem" or "about a day" and is used to describe processes that exhibit a ~24-hour rhythm.

The clock is not a physical structure but rather exists as a network of genes that typically participate in interlocking transcription-translation feedback loops (TTFLs) that drive rhythms of circadian outputs (Pokhilko et al., 2012a; Hsu et al., 2013a). These gene components make up what is thought of as the "core oscillator" of the clock—they can be likened to the gears in a grandfather clock. The basic clock signaling pathway consists of environmental input cues such as daylength and temperature that feed into the core oscillator, which then uses these cues to synchronize the timing of various phenotypic outputs. There are three primary characteristics that are used to define circadian clocks that we will discuss in the following paragraphs.

The first characteristic common to all circadian clocks is that they generate rhythms of approximately 24 hours (McClung, 2006). The time that it takes to complete one full cycle of a circadian rhythm is termed the “period”. By definition, the period of circadian-regulated outputs is ~24 hours. When the clock is internally (genetically) or externally (environmentally) perturbed, these influences can manifest in a deviation of the period from 24 hours to be shorter or longer(Pittendrigh, 1960). The second characteristic is that these rhythms are self-sustaining and endogenously generated. This means that circadian rhythms are maintained even in the absence of entrainment—or synchronization—cues like daylength and temperature, at least for a short period of time(Pittendrigh, 1960). The third characteristic of circadian clocks is that it is a temperature-compensated system. The rate of most biological reactions is influenced by the temperature of the system(Elias et al., 2014). The Q_{10} temperature coefficient defines the factor by which the rate of a reaction increases for every 10-degree Celsius increase in temperature. In most biological systems, the rate of a given biological reaction roughly doubles with a 10-degree increase in temperature, or $Q_{10} = 2$ (Elias et al., 2014). As the 24-hour cycling of the Earth is not influenced by ambient temperature, it is advantageous for circadian systems to be buffered against changes in temperature to maintain a period of 24 hours. Thus, a temperature-compensation mechanism has evolved for circadian systems across kingdoms(Colin Pittendrigh and by N Harvey, 1954; Pittendrigh, 1960; Gould et al., 2006; O’neill and Reddy, 2011; Cohen and Golden, 2015). Modeling efforts have shown that temperature compensation in the Arabidopsis circadian system is achieved through temperature-induced changes in the rates of transcription, translation, and degradation of clock factors (Avello et al., 2019).

While circadian systems are present across kingdoms of life and share these three defining characteristics, the lack of homology between the cyanobacterial, fungal, plant, and animals oscillators suggests that these clocks have evolved independently (Bell-Pedersen et al., 2005; Rosbash, 2009). The cyanobacterial *Synechococcus elongatus PCC 7942* clock, for example, is centered around the 24-hour cycle of the phosphorylation state of the *kaiABC* system. This system is self-contained and can be reconstituted *in vitro* to sustain *kaiC* phosphorylation rhythms for several weeks (Tomita et al.; Nakajima et al., 2005). In contrast, the circadian oscillators in fungi, plants and animals feature complicated interlocking transcription-translation feedback loops (Brunner and Káldi, 2008; Mohawk et al., 2012; Pokhilko et al., 2012a; Hsu and Harmer, 2014). In summary, circadian clocks are present in all kingdoms of life, share three defining criteria, but otherwise are thought to have evolved independently in cyanobacteria, plants, and animals.

1.2 The Plant Circadian Oscillator: Inputs, Outputs, and Core Feedback Loops

The plant circadian system can be broken down into three main components: 1) environmental inputs, 2) core oscillator genes, and 3) circadian-regulated physiological outputs (Creux and Harmer, 2019). In general, core oscillator components are those that participate in the interlocking transcription-translation feedback loops involving other oscillator factors. Oscillator components also typically exhibit circadian rhythms in gene expression and produce a change in circadian period, phase, or amplitude when mutated. In contrast, mutation of an output gene should not affect clock function. Input genes might not exhibit circadian gene expression but will have a clock mutant phenotype.

While these categorizations can be helpful for compartmentalizing the complicated circadian network in plants, it is not a perfect system; it is difficult to definitively categorize genes into a single one of these groups. For example, some genes, such as *PHYTOCHROME B* ***(****PHYB*), can be considered both input and output components, for example(Millar et al., 1995b; Bognár et al., 1999). Additionally, there are an increasing number of circadian-associated genes that do not fit neatly into any of these categories but clearly play a role in circadian rhythms. For example, the family of four MUT9-LIKE KINASES (MLK1-4) lengthen circadian period when mutated, co-precipitate with circadian clock proteins, and interact with the core oscillator protein CCA1 to modulate flowering time (Huang et al., 2016; Su et al., 2017; Zheng et al., 2018). Yet, there are no publications that have labeled the MLKs as core oscillator components or inputs and it is not clear which category the MLKs should fall into. This lack of clarity around what is considered an input, output, or an oscillator muddies our understanding of the plant circadian system and potentially encourages researchers to view important clock-associated factors such as the MLKs as less significant to clock function than those components that have been definitively labeled.

Having acknowledged these shortcomings, we will provide an overview of the circadian system in Arabidopsis through the traditional lens of these three general categories in the following sections.

Oscillator. The plant clock core oscillator consists of several transcription-translation feedback loops (Pokhilko et al., 2012a) (**Figure 1**). In the morning, the partially redundant MYB-like transcription factors *CIRCADIAN CLOCK ASSOCIATED 1*

(CCA1) and *LATE ELONGATED HYPOCOTYL* (LHY) heterodimerize and directly bind a *cis*-regulatory motif called the Evening Element to repress evening-phased genes, including *PSEUDORESPONSE REGULATOR 5 (PRR5), TIMING OF CAB 1* (*TOC1/PRR1*) and the components of the Evening Complex (EC): *EARLY FLOWERING 3* (*ELF3*), *EARLY FLOWERING 4* (*ELF4*), and *LUX ARRHYTHMO* (*LUX*) (Harmer et al., 2000; Alabadí et al., 2001; Nusinow et al., 2011; Kamioka et al., 2016). As the day progresses, *TOC1* expression increases and reciprocally represses the expression of *CCA1*/*LHY* (Gendron et al., 2012; Pokhilko et al., 2012b), forming a negative feedback loop. While *CCA1* and *LHY* are generally considered repressors, there is evidence that they are activators of *PRR7/9* (Farré et al., 2005), which themselves repress *CCA1/LHY* around midday (Nakamichi et al., 2010). The sequential repression of CCA1/LHY by the PRRs then allows for the expression of evening-phased genes.

The EC is named as such due to the evening-phased peak in expression levels of its three constituents: *ELF3*, *ELF4*, and *LUX* (Nusinow et al., 2011). Loss-of-function mutations in any of the EC components (*elf3, elf4,* or *lux*) causes arrhythmicity, indicating the importance of this complex for the overall function of the clock (Hicks et al., 1996; Doyle et al., 2002; Hazen et al., 2005; Onai and Ishiura, 2005). CCA1 occupies the promoter regions of all three EC components, which contain evening elements or CCA1 Binding SitesIn the late evening, the EC represses *PRR7* and *PRR9*, relieving repression on *CCA1* and *LHY*, enabling these transcription factors to be expressed once again at dawn (Dixon et al., 2011; Helfer et al., 2011; Chow et al., 2012; Mizuno et al., 2014b; Ezer et al., 2017).

While most of these feedback loops involve transcriptional repressors, a group of eight LHY/CCA1-like (LCL) proteins called the *REVEILLE*s (RVE1-8) serve as activators in the clock (Rawat et al., 2011; Hsu et al., 2013b). The *RVEs* contain a conserved LCL domain that shares sequence similarity with *CCA1* and *LHY* and bind to the same Evening Element binding motif. RVE4/8 interact with a group of 4 transcriptional co-regulators called NIGHT LIGHT INDUCIBLE AND CLOCK-REGULATED 1-4 (LNK1-4) that co-activate the expression of evening-phased circadian clock genes including *PRR5* and *TOC1*(Farinas and Mas, 2011; Rugnone et al., 2013; Xie et al., 2014). This coactivation activity is mediated through recruitment of the basal transcriptional machinery by LNK1/2 to RVE8 target gene promoters (Ma et al., 2018). PRR5 and other evening clock genes in turn repress the expression of RVE8, forming another negative feedback loop (Rawat et al., 2011). It is interesting that despite their similarities, CCA1/LHY and the RVEs perform opposing roles while regulating the same target genes. This balance between activator and repressor MYB-like transcription factors has been shown to be essential for proper clock function (Shalit-Kaneh et al., 2018).

Two other genes that appear to be important for oscillator function but have not been definitively placed in any specific feedback loop are *FIONA* 1 (*FIO1*) and *JUMONJI DOMAIN CONTAINING 5* (*JMJD5; AKA JUMONJI-C DOMAIN-CONTAINING PROTEIN 30, JMJ30*). Mutations in *fio1* cause early flowering and lengthening of the circadian period of leaf movement and the expression of core oscillator genes *CCA1*, *LHY*, *TOC1*, and *LUX* (Kim et al., 2008). This mutant phenotype is not dependent on light or temperature conditions, indicating that *FIO1* is not an input to the clock—at least not in the light or temperature pathways. Recent work has shown that *FIO1* is an ortholog of

human *METTL16*, an N^6-methyladenosine (m^6A) methyltransferase, and regulates photoperiod-independent flowering and phytochrome-dependent hypocotyl elongation through deposition of m^6A at target at U6 snRNA and at some poly(A)$^+$ RNAs including the important flowering regulator *SUPPRESSOR OF OVEREXPRESSION OF CONSTANS 1* (*SOC1*) (Wang et al., 2022; Xu et al., 2022).

JMJD5 is an evening-expressed putative histone demethylase that is a conserved circadian clock gene in plants and humans (Jones et al., 2010). *jmjd5* mutant plants exhibit early flowering (when paired with a mutation in its homolog *jmj32*) and a short period mutant phenotype in *CCR2*::*LUC* reporter expression (Jones et al., 2010; Gan et al., 2014). Interestingly, ambient temperature plays a critical role in both of these *jmjd5* phenotypes; loss-of-function *jmjd5* mutant plants have defective temperature compensation and early flowering occurs only under elevated temperatures (29℃) (Gan et al., 2014; Jones et al., 2019). While global levels of H3K36me3 and H3K79me3 are altered in *JMJD5* over-expressors or loss-of-function mutants, direct demethylase activity has not been demonstrated *in vivo* and histone methylation at circadian loci is not substantially altered (Gan et al., 2014; Lee et al., 2018; Jones et al., 2019). This suggests that while *JMJD5* does not directly modify histone methylation of clock gene loci, its effects on the clock could be related to demethylation of other target genes that have downstream effects on the clock. While there is little overlap in general between the plant and mammalian circadian systems, it is notable that both FIO1 and JMJD5 appear to have conserved functions in the clocks in both of these kingdoms.

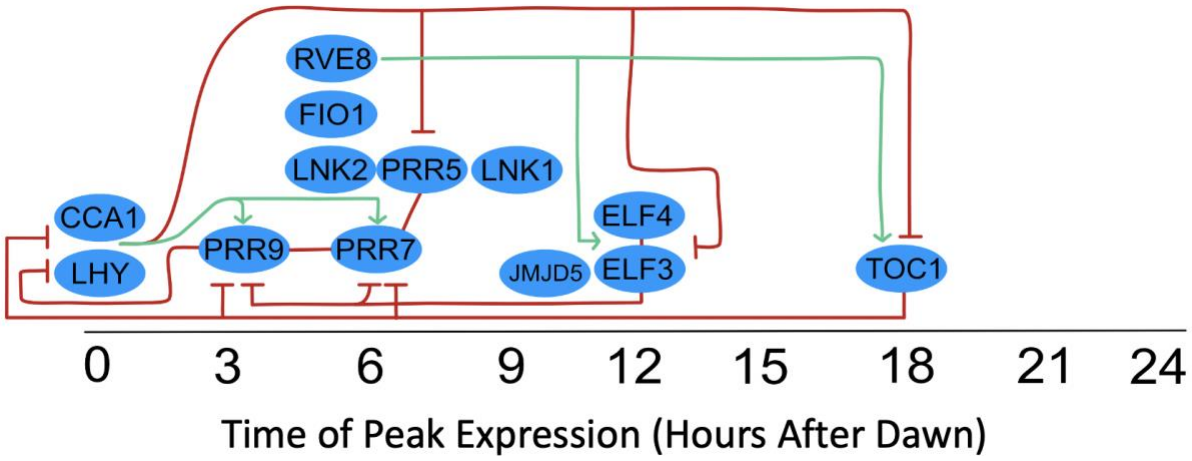

Figure 1.1 Partial model of the core circadian oscillator in Arabidopsis
A subset of circadian clock genes are plotted along a time axis depending on the time of peak protein expression. Transcriptional activation or repression is shown in green and red lines.

While not formally considered part of the core oscillator, several kinase families are important for circadian rhythms in plants. A key regulator of CCA1/LHY activity is the Ser/Thr kinase CK2 (also known as casein kinase II), which interacts with and phosphorylates these transcription factors (Sugano et al., 1998; Sugano et al., 1999; Daniel et al., 2004). While early work suggested that CK2-mediated phosphorylation of CCA1 enhances its ability to bind target promoters(Sugano et al., 1998; Daniel et al., 2004), there is also evidence that CCA1 phosphorylation antagonizes its DNA-binding activity and that reduced phosphorylation leads to increased CCA1 protein stability(Portolés and Más, 2010; Lu et al., 2011). Mutation of the subunits of CK2, which are encoded by discrete loci, results in a change in circadian period of several oscillator genes including CCA1/LHY, further indicating the role for this kinase in circadian rhythms(Sugano et al., 1999; Perales et al., 2006; Lu et al., 2011). Additionally, recent work has demonstrated a role for the Arabidopsis *CASEIN KINASE 1 LIKE (CKL)* family

in phosphorylation of circadian clock proteins including PRR5 and TOC1 (Uehara et al., 2019). Casein kinase homologs are important for circadian clocks across multiple kingdoms of life, making them one of the only known genetic components that is common between independently-evolved clocks (Lowrey et al., 2000; He et al., 2006).

The *MUT9-LIKE KINASES 1-4 (MLK1-4)* form another class of important circadian-associated CK1-like kinases that phosphorylate histones H3 at threonine 3 and H2A at serine 95(Wang et al., 2015b; Su et al., 2017) . The MLKs interact with the EC via PHYTOCHROME B (PhyB) as well as with CCA1, although it does not appear that they are phosphorylating these components(Huang et al., 2016; Su et al., 2017; Zheng et al., 2018; Wilson et al., 2021). Rather, it is possible that the MLKs are recruited to target loci through these clock transcription factors(Su et al., 2017). Loss-of-function mutations in the MLKs results in delayed flowering and period lengthening, further indicating their importance for circadian rhythms (Huang et al., 2016).

Inputs. The primary input cues for the plant clock are daylength and temperature (Pittendrigh, 1960). While the endogenous clock mechanism serves to sustain rhythms of ~24 hours, external environmental cues are still necessary to ensure clock rhythms are synchronized with the environment (Millar). After all, daylength and temperature cycles do change over the course of the year, especially at latitudes further from the equator. Thus, plants and other organisms have evolved to track these two important stimuli and adjust their circadian rhythms accordingly. In this section, we focus on the input of light and temperature to the clock, but it should be noted that other inputs have been identified including photosynthate, calcium, and ethylene(Bläsing et al., 2005; Haydon et al., 2013; Haydon et al., 2017; Ruiz et al., 2018).

Inputs can typically be identified by their stimulus-dependent clock mutant phenotypes. For example, loss-of-function *phyB* mutants exhibit lengthened circadian period when grown under red light, but show no circadian defect under blue light (Millar et al., 1995b). This is because PhyB feeds into the circadian oscillator via its function as a red-light photoreceptor and does not affect the clock outside of this role.

Light Input. The daily cycle of sunrise and sunset is a powerful synchronizing cue to circadian clocks (Pittendrigh, 1960). Increasing light intensity shortens the circadian period of diurnal organisms while it lengthens the period of nocturnal species, a phenomenon known as Aschoff's Rule (Pittendrigh, 1960; Aschoff, 1979) that holds true in the plant kingdom as well (Somers et al., 1998a; Devlin and Kay, 2000). As light is one of the most important cues for circadian entrainment, the proteins that sense light, called photoreceptors, are key input components in the clock(Casal, 2000). Red and far-red light are sensed by the phytochromes while blue light and UV radiation are received by cryptochromes and LIGHT-OXYGEN-VOLTAGE(LOV)-domain-containing proteins like the phototropins. With the exception of the phototropins, all of these classes of photoreceptors are known inputs to the circadian clock in Arabidopsis (Chen et al., 2004). While light is clearly an important input to the plant clock, we know surprisingly little about how, mechanistically, the photoreceptors input to the central oscillator. This is in part due to the challenge of isolating the effects of a single photoreceptor when there is high redundancy and overlap in the action of phytochromes, cryptochromes, LOV-domain-containing photoreceptors, and UV receptors. Indeed, a *phyA phyB cry1 cry2* quadruple mutant plant can still use light signals to entrain the circadian clock (Yanovsky et al.,

2000). The majority of our knowledge about how light affects the clock is via transcriptomic analyses in photoreceptor mutant backgrounds.

The red-light photoreceptors make up a five-member family of proteins called the phytochromes (PhyA-E) that mediate red-light input to the circadian clock (Millar et al., 1995b; Somers et al., 1998a; Devlin and Kay, 2000). Upon red-light exposure, the Phys photoconvert from an inactive red-light absorbing form to an active, far-red light absorbing conformer that can translocate from the cytosol into the nucleus (Sakamoto and Nagatani, 1996; Yamaguchi et al., 1999). In the nucleus, the Phys regulate a vast number of genes through the PHYTOCHROME INTERACTING FACTOR (PIF) transcription factors, including circadian clock or clock-associated genes (Martínez-García et al., 2000; Tepperman et al., 2001). Additionally, PhyB interacts with several circadian clock proteins including ELF3 (Xing Liang Liu et al., 2001; Yeom et al., 2014; Huang et al., 2016). Consistent with a connection between PhyB and ELF3, ELF3 appears to be important for phytochrome-mediate input to the clock (Wenden et al., 2011). In summary, the phytochromes detect red and far-red light in the environment and relay this information to the circadian clock to propagate rhythms.

Cryptochrome 1 (CRY1) and CRY2 are the blue-light photoreceptors that feed into the plant clock(Casal, 2000). CRYs are highly conserved across kingdoms of life(Lucas-Lledó and Lynch, 2009) and CRY homologs in mammals are core oscillator components (Miyamoto and Sancar, 1998; Van Der Horst et al., 1999). While CRYs do not appear to be core oscillator components in plants, the conservation of the CRYs in plant and animal clocks serves as one of the few instances of conservation between plant and mammalian

circadian systems (Somers et al., 1998a). While the CRYs absorb only in the blue region of the light spectrum, Arabidopsis c*ry1* and *cry2* mutants exhibit lengthened circadian period under blue, red and white light (Somers et al., 1998a; Devlin and Kay, 2000), suggesting that while the CRYs play a role in blue-light input to the clock, they may also be targets of downstream signaling from other photoreceptors that respond to other wavelengths of light.

One mechanism by which CRY1/2 regulate photomorphogenesis and circadian rhythms is through its binding to the E3 ubiquitin ligase CONSTITUTIVE PHOTOMORPHOGENIC 1 (COP1) in a blue-light-dependent fashion (Liu et al., 2011). COP1 targets photomorphogenesis and circadian clock proteins for degradation by the 26S proteasome in darkness (Wang et al., 2015a; Hoecker, 2017). To promote light-mediated growth and circadian rhythms, photo-activated CRY1/2 compete for COP1 binding, thus blocking COP1 from binding target substrates (Wang et al., 2001; Yang et al., 2001; Liu et al., 2011; Ponnu et al., 2019). For instance, ELF3 is degraded in a COP1-dependent manner and this degradation is possibly antagonized by photoactivated CRY1/2(Wang et al., 2015a). Beyond this mechanistic insight and the initial observations of the effect of *cry* mutations on clock period, the little else we understand of how these photoreceptors regulate the clock is through transcriptomic studies(Facella et al., 2008; Zhang et al., 2008).

In addition to the phototropins, there is another family of blue-light-responsive LOV-domain genes that consists of *ZEITLUPE* (*ZTL*), *FLAVIN-BINDING*, *KELCH REPEAT, F-BOX 1* (*FKF1*), and *LOV KELCH PROTEIN 2* (*LKP2*) that are well known to

regulate photoperiodic flowering time and circadian rhythms (Baudry et al., 2010; Ito et al., 2012). Upon blue-light exposure, FKF1 interacts with the floral regulator and core circadian clock protein GIGANTEA (GI) to form a complex at the end of the day(Sawa et al., 2007). The GI-FKF1 complex targets the floral repressor CDF1 for degradation, thus allowing for the expression of photoperiodic floral development genes (Sawa et al., 2007). Similarly, GI and ZTL also form a blue-light dependent complex that sequesters ZTL away from oscillator components PRR5 and TOC allowing these proteins to accumulate over the course of the day (Fujiwara et al., 2008)F. At night, the GI-ZTL complex disassociates and allows for ZTL to target PRR5/TOC1 for degradation by the 26S proteasome (Más et al., 2003; Kiba et al., 2007). A similar mechanism of ZTL regulation has been proposed for *HEAT SHOCK PROTEIN 90* (*HSP90*) wherein HSP90 stabilizes ZTL, leading to increased degradation of PRR5 and TOC1 (Kim et al., 2011).

Temperature Input. While our mechanistic knowledge of light input to the circadian clock is lacking, there is even less known about temperature input. The synchronization of the clock with temperature cycles is termed temperature entrainment. Temperature cycles of as little as a 4℃ difference in day-night temperature can entrain the plant circadian clock even in the absence of light-dark cycles (Somers et al., 1998b; Salomé and Robertson Mcclung, 2005). Two members of the PRR family of transcription factors, PRR7 and PRR9, are known to be essential for temperature entrainment of the clock; in *prr7-3 prr9-1* double mutants, plants are unable to maintain free-running rhythms after entrainment to temperature cycles (Salomé and Robertson Mcclung, 2005). Similarly, the evening expressed *ELF3* gene also appears to be necessary for proper temperature entrainment and recent work has demonstrated that a prion-like domain found in ELF3

serves as a thermosensor (Thines and Harmon, 2010; Jung et al., 2020). While the factors that sense temperature in plants are not fully understood, it is interesting to note that proteins known for their role in light signaling such as PhyB and the cryptochromes also appear to participate in temperature perception in *Arabidopsis* (Mazzella et al., 2000; Halliday et al., 2003; Legris et al., 2016).

Cold temperature response is regulated largely through the transcriptional effects driven by the C-repeat (CRT)/drought-responsive element (DRE) binding factor (CBF/DREB) family of transcription factors (Zhao et al., 2016; Shi et al., 2018). CBF1-CBF3 are massively upregulated upon exposure to cold temperatures, which prompts the activation of downstream target genes known as cold-regulated (COR) genes (Gilmour et al., 1998; Medina et al., 1999). The EC transcription factor, LUX, is upregulated by CBF1 upon exposure to cold temperatures and *lux* loss-of-function mutants exhibit decreased survival upon freezing at -5 ℃ for 5 hours, demonstrating how cold temperature can feed into the (Chow et al., 2014). The influence of the CBFs extends beyond LUX, as core oscillator genes LNK1, LNK3, LNK4, and JMJD5 are differentially expressed in a CBF1/2/3 overexpression line RNA-seq (Park et al., 2015). However, no formal studies have been made to validate the connection between these clock components and the CBFs.

Outputs. There are numerous phenotypes that have been linked to circadian rhythms over the years. Estimates for the percentage of the Arabidopsis genome that is under circadian regulation generally agree that ~10-30% of transcripts are circadian-regulated, suggesting the clock regulates a wide variety of pathways (Harmer et al., 2000;

Covington et al., 2008; Filichkin et al., 2011; Nagel et al., 2015). The list of known circadian outputs includes abiotic and biotic stress responses, reproductive development, growth, photosynthesis, and gene expression, to name a few (Harmer et al., 2000; Covington et al., 2008; Creux and Harmer, 2019). For the purposes of this thesis, we will focus this section of the role of the clock in temperature response, as this is a central part of this work.

Temperature Response. In addition to using temperature as an input cue, the clock also regulates temperature response as an output. The *CBFs* play a role in the clock-regulated response to cold. *CBF* expression is circadian regulated and cold-induction of the *CBFs* is gated by the circadian clock with peak and trough induction at ZT4 and ZT16, respectively (Harmer et al., 2000; Fowler et al., 2005). This circadian regulation and gated induction is driven largely by *CCA1/LHY*, as *cca1-11 lhy-21* double mutants are highly impaired in these activities (Dong et al., 2011). The CCA1/LHY-like transcription factors *RVE4* and *RVE8* also contribute to circadian regulation of *CBF*-mediated freezing tolerance. Under non-stressed conditions, CCA1/LHY suppress the expression of the CBFs and are rapidly degraded in response to cold stress, relieving repression and allowing downstream activation of cold tolerance genes (Kidokoro et al., 2021). Meanwhile, RVE4/8 rapidly translocate from the cytosol to the nucleus upon cold treatment and activate *CBF3* (Kidokoro et al., 2021). Thus, *rve4*/8 mutants show decreased cold tolerance. Together, CCA1/LHY and their related transcription factor cousins RVE4/8 regulate cold tolerance via transcriptional control of the CBFs.

The clock is also important for the response to warm temperatures. The EC—particularly ELF3—appears to play a central role in the response to temperature (Mizuno et al., 2014a; Box et al., 2015; Ezer et al., 2017). ELF3 does not have a known DNA-binding domain but represses target gene expression through formation of the EC with its partners ELF4 and LUX (Helfer et al., 2011; Nusinow et al., 2011). Under warm temperatures, ELF3 occupancy at target gene promoters is decreased, relieving repression of these targets (Mizuno et al., 2014a; Box et al., 2015). Recent work has demonstrated that an ELF3 prion-like domain containing a polyglutamine repeat contributes to warm temperature-induced formation of ELF3 nuclear speckles that exhibit characteristics of liquid-liquid phase-separated bodies (Jung et al., 2020). Formation of ELF speckles and decreased ELF3 promoter occupancy are positively correlated with increased temperature, suggesting that ELF3 could be sequestered in phase-separated nuclear bodies under warm temperatures, relieving repression of growth related factors like PIF4 (Mizuno et al., 2014a; Box et al., 2015).

The RVE-LNK transcriptional module has also been linked to the response to warm temperatures. LNK1 is repressed through direct binding of the EC to its promotor (Mizuno et al., 2014c). The existing role of the EC in warm temperature response prompted Mizuno et al. to examine whether LNK1 could be a downstream-acting component of this response. Indeed, the authors found that LNK1 expression is induced by warm temperatures in a EC-dependent manner, specifically in the evening (Mizuno et al., 2014c). Together with the recent mechanistic findings regarding EC inhibition under warm temperatures (Box et al., 2015; Jung et al., 2020), it is likely that LNK1 is induced under warm temperatures due to relieved repression by the EC. Additionally, another study

found that a large portion of heat-shock regulated gene promoters contain the cis-binding motifs for RVE4/8 (Li et al., 2019). This study demonstrated that RVE4/8 are important for the induction of the first wave of heat-shock induced gene expression, especially in the hours around midday (Li et al., 2019). In summary, the RVE-LNK transcriptional unit has been linked to the regulation of both warm and cool temperatures, with the EC as an upstream regulator of LNK1, if not also RVE4/8, warm-induced expression. The strong connection between the RVEs and LNKs and temperature output suggests these oscillator components may also be important for temperature input to the clock, though this question has not yet been addressed.

1.3 Circadian Regulation of Agriculturally Relevant Traits

The plant circadian clock regulates numerous agriculturally relevant traits and is thus an appropriate target to manipulate when developing or domesticating crop species. Prior to scientific understanding of the plant clock, farmers unknowingly placed clock genes under artificial selection, preferring plants that flowered at a specific time of year or were adapted to a specific climate. Now, with our mechanistic understanding of clock function, we can perform targeted manipulation or employ breeding programs that target circadian rhythms to improve crop traits like stress tolerance and yield.

Flowering time is a trait of high importance for crop breeders that is strongly regulated by circadian rhythms. The transition from vegetative growth to reproductive development is one of the most complex and critical phase transitions for a plant. In general, farmers have selected for crop species that have synchronous flowering and that flower at a particularly time of year to optimize yield (Purugganan and Fuller, 2009). There

are three main reproductive categories of plants: long-day plants that flower when daylength exceeds a critical length, short-day plants that flower when daylength is shorter than a critical length, and day-neutral plants that flower regardless of daylength (Garner and Allard, 1920). As the clock is the biological timekeeper that tracks daylength, it follows that it is vital for proper timing of reproductive development. Briefly, the clock regulates flowering time primarily through the time-of-day-specific expression of floral regulator genes such as *CONSTANS* (*CO*), which activates the expression of the master floral activator *FLOWERING LOCUS T* (*FT*) (Putterill et al., 2004; Andrés and Coupland, 2012). In the long-day plant Arabidopsis, the oscillator protein GI and ubiquitin ligase FKF1 dimer is stabilized by light at the end of the day and targets the CYCLING DOF FACTORS (CDFs) for degradation. Once degraded, the CDFs can no longer perform their canonical activity of repressing *CO* expression, allowing for *CO*-mediated activation of *FT* and floral development (Andrés and Coupland, 2012). An additional way the clock regulates flowering time is through the control of vernalization—the process of acquiring flowering competence through exposure to a prolonged period of cold temperatures (Andrés and Coupland, 2012). Recent work has shown that a key vernalization gene, VIN3, is activated by the oscillator components CCA1/LHY, directly connecting the clock and vernalization (Hepworth et al., 2018; Kyung et al., 2022).

As daylength is dependent on latitudinal location, clock genes have been targets of natural and artificial selection, especially when a species has spread or was physically relocated to a new latitude. For example, wild tomato was originally domesticated in the Andean region of South America (modern day Peru/Ecuador) and was later introduced into Mesoamerica (modern day Central America and parts of the Southern portion of

North America), where it was grown under longer days compared to its ancestral equatorial environment (Blanca et al., 2012). A study that examined the genetic differences between wild Andean and domesticated Mesoamerican cultivars of tomato found that the circadian clock in the domesticated plants was decelerated (had a longer intrinsic circadian period of 26 hours and a phase shift from ~17 to ~20 hours after dawn) (Müller et al., 2015). Further investigation identified mutations in *EMPFINDLICHER IM DUNKELROTEN LICHT 1* (*EID1*) and *LNK2* as the causative allelic changes that produced the delayed phase and long period, respectively, in domesticated tomato (Müller et al., 2015; Müller et al., 2018) There is some evidence that longer periods are advantageous at higher latitudes (Michael et al., 2003). Another possible explanation for why mutation of *EID1* and *LNK2* was selected for is that these mutations produced plants that were more plastic and thus able to adapt to a sudden change in daylength patterns. This has the interesting implication that relaxation of circadian control in the plant could be a key target for adapting crop species to new latitudes or climates. Apart from flowering time, breeders and genetic engineers can also look to the circadian clock for producing plants that are more tolerant to abiotic and biotic stress.

1.4 Affinity Purification-Mass Spectrometry as a Tool for Clock Discovery

Most of our knowledge of the circadian system in plants has come from forward and reverse genetic screens (**Table 1.1**). The development of clock gene promoter-driven firefly luciferase reporters was incredibly useful for discovery of novel clock components and clock-associated loci (Millar et al., 1992; Millar et al., 1995a). By mutagenizing seeds carrying a clock reporter such as CCA1::Firefly Luciferase, one can quickly identify mutant

lines that exhibit altered circadian period, phase, or amplitude of the reporter. However, genetic approaches have their shortcomings: genetic redundancy, lethality, and conditional mutant phenotypes can limit the pool of clock-associated genes that can be identified by this method. A proteomics-based approach offers another avenue for discovering novel clock-associated factors and functions that comes with its own advantages and disadvantages. We have chosen to use protein-protein interactions as a tool for examining the Arabidopsis circadian clock.

Table 1.1 Most of oscillator genes were identified through forward and reverse genetics
A subset of known circadian clock oscillator genes and how they were first identified.

AGI Locus Number	Gene Name	Method of Identification	Reference
AT2G46830	CCA1	Promoter/Promoter-Element Pull-Down	Wang et al. (1997) *The Plant Cell* Kenigsbuch and Tobin (1995) *Plant Physiology*
AT1G01060	LHY	Forward/Reverse Genetics	Schaffer, R. (1997) Ph.D. Thesis Schaffer et al. (1998) *Cell*
AT5G61380	TOC1	Forward/Reverse Genetics	Millar et al. (1995) *Science*
AT5G24470	PRR5	Forward/Reverse Genetics	Nakamichi et al. (2005) *Plant Cell Physiology*
AT5G02810	PRR7	Forward/Reverse Genetics	Nakamichi et al. (2005) Plant Cell Physiology Farré et al. (2005) *Current Biology*
AT2G46790	PRR9	Forward/Reverse Genetics	Nakamichi et al. (2005) Plant Cell Physiology Farré et al. (2005) Current Biology
AT3G09600	RVE8	Promoter/Promoter-Element Pull-Down	Rawat et al. (2011) *PLoS Genetics*
AT5G64170	LNK1	Transcriptomics	Rugnone et al. (2013) *PNAS*
AT3G54500	LNK2	Transcriptomics	Rugnone et al. (2013) *PNAS*
AT2G21070	FIO1	Forward/Reverse Genetics	Kim et al. (2008) *The Plant Cell*
AT2G25930	ELF3	Forward/Reverse Genetics	Zagotta et al. (1992) *Aust. J. Plant Physiology*
AT2G40080	ELF4	Forward/Reverse Genetics	Doyle et al. (2002) *Nature*
AT3G20810	JMJD5	Transcriptomics	Jones et al. (2010) *PNAS*

Proteins do not function in isolation. Rather, they are dynamically binding and releasing interacting partners, forming homodimers, heterodimers, and higher order complexes. The functional roles of protein interactions include but are not limited to adding/removing post-translational modifications, changing the conformation of a binding partner, increasing/decreasing enzymatic or other functional activities, inducing subcellular translocation, promoting recruitment to target chromatin, and sequestration. By identifying the protein interacting partners of known clock-associated factors, we can thus potentially identify new clock-associated proteins and also form hypotheses about what purpose these protein interactions serve on a mechanistic level.

We use affinity purification coupled with mass spectrometry (APMS) to identify protein-protein interactions on a proteomic scale. In this method, bait proteins of interest are tagged with an affinity epitope such as the FLAG tag and expressed in their respective mutant background, effectively eliminating any wild-type bait protein from depleting the pool of interactors. Bait proteins and any interacting prey proteins are co-precipitated using immunoprecipitation or affinity resins such as nickel-coated beads to capture His-tagged proteins. The co-precipitated proteins are identified by their mass-to-charge ratio using liquid chromatography-mass spectrometry (LCMS).

APMS has been used effectively in the past to discover new connections within the clock (Huang et al., 2016; Krahmer et al., 2018). A previous study from the Nusinow Lab used APMS to identify novel connections between the EC and other clock and light signaling proteins including TOC1, TIME FOR COFFEE (TIC), the family of phytochromes, TANDEM ZINC KNUCKLE/PLUS 3 (TZP), and the family of MUT9-LIKE

KINASES (MLKs) (Huang et al., 2016). The MLKs, which were previously unlinked to the clock, were shown to have mutant phenotypes in flowering time, circadian period length, and hypocotyl elongation, demonstrating how APMS can be used to identify new clock-associated factors (Huang et al., 2016). Another study that demonstrated how APMS can be used for circadian clock discovery focused on the enigmatic protein GIGANTEA (GI) (Krahmer et al., 2018). In their study, Krahmer et al. collected tissue expression affinity-tagged GI at six timepoints over the course of the 24-hour day to identify time-of-day-specific protein interactions. Similarly to our 2016 study, the authors identified an interaction between this their clock bait protein and a previously uncharacterized protein, CYCLING DOF FACTOR6 (CDF6). Further characterization showed that CDF6 plays a role in photoperiodic flowering time (Krahmer et al., 2018). Among other studies, these two papers demonstrate the power of APMS to identify novel connections within the circadian network and between the clock and other signaling pathways.

This dissertation discusses our application of APMS to make new discoveries within the Arabidopsis circadian system. In Chapter 1, we will discuss the optimization of this method and report a cautionary tale of avoiding non-specific binding proteins in APMS datasets. In Chapter 2, we report a near-comprehensive protein-protein interactome for the Arabidopsis circadian clock that was assembled from the APMS of 11 core circadian clock proteins: CCA1, LHY, RVE8, LNK1, LNK2, TOC1, PRR5, PRR7, PRR9, JMJD5, and FIONA 1 (FIO1). Chapter 3 focuses in on the interaction we identified between RVE8, LNK1/2, and COLD RESPONSE PROTEIN 27 (COR27) and COR28 and how this complex regulates circadian and cold-tolerance pathways. We hope this dissertation provides technical expertise on using APMS for proteomic interactome studies and that

our near-comprehensive circadian interactome will serve as an invaluable tool for future clock studies. Additionally, our identification of the novel RVE-LNK-COR complex opens several new avenues of investigation to further characterize this new clock and cold-regulatory mechanism. We hope this research will bolster future studies investigating the underlying fundamental biology of circadian rhythms in plants and also inform applied research programs aimed at improving crop performance via circadian-regulated traits.

1.5 References

Alabadí D, Oyama T, Yanovsky MJ, Harmon FG, Más P, Kay SA (2001) Reciprocal Regulation Between TOC1 and LHY / CCA1 Within the Arabidopsis Circadian Clock. Science (80-) **293**: 880–883

Andrés F, Coupland G (2012) The genetic basis of flowering responses to seasonal cues. Nat Rev Genet **13**: 627–39

Aschoff J (1979) Circadian Rhythms: Influences of Internal and External Factors on the Period Measured in Constant Conditions. Z Tierpsychol **49**: 225–249

Avello PA, Davis SJ, Ronald J, Pitchford JW (2019) Heat the Clock: Entrainment and Compensation in Arabidopsis Circadian Rhythms. J Circadian Rhythms **17**: 1–11

Baudry A, Ito S, Song YH, Strait AA, Kiba T, Lu S, Henriques R, Pruneda-Paz JL, Chua NH, Tobin EM, et al (2010) F-Box Proteins FKF1 and LKP2 Act in Concert with ZEITLUPE to Control Arabidopsis Clock Progression. Plant Cell **22**: 606–622

Bell-Pedersen D, Cassone VM, Earnest DJ, Golden SS, Hardin PE, Thomas TL, Zoran MJ (2005) Circadian rhythms from multiple oscillators: Lessons from diverse organisms. Nat Rev Genet **6**: 544–556

Blanca J, Cañizares J, Cordero L, Pascual L, Diez MJ, Nuez F (2012) Variation Revealed by SNP Genotyping and Morphology Provides Insight into the Origin of the Tomato. PLoS One **7**: e48198

Bläsing OE, Gibon Y, Günther M, Höhne M, Morcuende R, Osuna D, Thimm O, Usadel B, Scheible WR, Stitt M (2005) Sugars and Circadian Regulation Make Major Contributions to the Global Regulation of Diurnal Gene Expression in Arabidopsis. Plant Cell **17**: 3257

Bognár LK, Hall A, Ádám É, Thain SC, Nagy F, Millar AJ (1999) The circadian clock controls the expression pattern of the circadian input photoreceptor, phytochrome B. Proc Natl Acad Sci **96**: 14652–14657

Box MS, Huang BE, Domijan M, Jaeger KE, Khattak AK, Yoo SJ, Sedivy EL, Jones DM, Hearn TJ, Webb AAR, et al (2015) ELF3 controls thermoresponsive growth in Arabidopsis. Curr Biol **25**: 194–199

Brunner M, Káldi K (2008) Interlocked feedback loops of the circadian clock of Neurospora crassa. Mol Microbiol **68**: 255–262

Casal JJ (2000) Phytochromes, Cryptochromes, Phototropin: Photoreceptor Interactions in Plants. Photochem Photobiol **71**: 1–11

Chen M, Chory J, Fankhauser C (2004) Light Signal Transduction in Higher Plants. Annu Rev Genet **38**: 87–117

Chow BBY, Helfer A, Nusinow D a., Kay S a. (2012) ELF3 recruitment to the PRR9 promoter requires other Evening Complex members in the Arabidopsis circadian clock. Plant Signal Behav **7**: 170–173

Chow BY, Sanchez SE, Breton G, Pruneda-Paz JL, Krogan NT, Kay SA (2014) Transcriptional Regulation of LUX by CBF1 Mediates Cold Input to the Circadian Clock in Arabidopsis. Curr Biol **24**: 1518–1524

Cohen SE, Golden SS (2015) Circadian Rhythms in Cyanobacteria. Microbiol Mol Biol Rev **79**: 373–385

Colin Pittendrigh BS, by N Harvey CE (1954) ON TEMPERATURE INDEPENDENCE IN THE CLOCK SYSTEM CONTROLLING EMERGENCE TIME IN DROSOPHILA. Proc Natl Acad Sci **40**: 1018–1029

Covington MF, Maloof JN, Straume M, Kay SA, Harmer SL (2008) Global transcriptome analysis reveals circadian regulation of key pathways in plant growth and development. Genome Biol **9**: 10.1186/gb-2008-9-8-r130

Creux N, Harmer S (2019) Circadian Rhythms in Plants. Cold Spring Harb Perspect Biol. doi: 10.1101/cshperspect.a034611

Daniel X, Sugano S, Tobin EM (2004) CK2 phosphorylation of CCA1 is necessary for its circadian oscillator function in Arabidopsis. Proc Natl Acad Sci U S A **101**: 3292–3297

Devlin PF, Kay SA (2000) Cryptochromes Are Required for Phytochrome Signaling to the Circadian Clock but Not for Rhythmicity. Plant Cell **12**: 2499

Dixon LE, Knox K, Kozma-Bognar L, Southern MM, Pokhilko A, Millar AJ (2011) Temporal repression of core circadian genes is mediated through EARLY FLOWERING 3 in Arabidopsis. Curr Biol **21**: 120–125

Dong MA, Farré EM, Thomashow MF (2011) CIRCADIAN CLOCK-ASSOCIATED 1 and LATE ELONGATED HYPOCOTYL regulate expression of the C-REPEAT BINDING FACTOR (CBF) pathway in Arabidopsis. Proc Natl Acad Sci **108**: 7241–7246

Doyle MR, Davis SJ, Bastow RM, McWatters HG, Kozma-Bognár L, Nagy F, Millar AJ (2002) The ELF4 gene controls circadian rhythms and flowering time in Arabidopsis thaliana. Nature **419**: 74–77

Elias M, Wieczorek G, Rosenne S, Tawfik DS (2014) The universality of enzymatic rate-temperature dependency. Trends Biochem Sci. doi: 10.1016/j.tibs.2013.11.001

Ezer D, Jung J-H, Lan H, Biswas S, Gregoire L, Box MS, Charoensawan V, Cortijo S, Lai X, Stöckle D, et al (2017) The evening complex coordinates environmental

and endogenous signals in Arabidopsis. Nat Plants. doi: 10.1038/nplants.2017.87

Facella P, Lopez L, Carbone F, Galbraith DW, Giuliano G, Perrotta G (2008) Diurnal and circadian rhythms in the tomato transcriptome and their modulation by cryptochrome photoreceptors. PLoS One **3**: e2798

Farinas B, Mas P (2011) Functional implication of the MYB transcription factor RVE8/LCL5 in the circadian control of histone acetylation. Plant J **66**: 318–329

Farré EM, Harmer SL, Harmon FG, Yanovsky MJ, Kay SA (2005) Overlapping and Distinct Roles of PRR7 and PRR9 in the Arabidopsis Circadian Clock. Curr Biol **15**: 47–54

Filichkin SA, Breton G, Priest HD, Dharmawardhana P, Jaiswal P, Fox SE, Michael TP, Chory J, Kay SA, Mockler TC (2011) Global Profiling Of Rice And Poplar Transcriptomes Highlights Key Conserved Circadian-Controlled Pathways and cis-Regulatory Modules. PLoS One **6**: e16907

Fowler SG, Cook D, Thomashow MF (2005) Low Temperature Induction of Arabidopsis CBF1, 2, and 3 Is Gated by the Circadian Clock 1. Plant Physiol **137**: 961–968

Fujiwara S, Wang L, Han L, Suh SS, Salomé PA, McClung CR, Somers DE (2008) Post-translational regulation of the Arabidopsis circadian clock through selective proteolysis and phosphorylation of pseudo-response regulator proteins. J Biol Chem **283**: 23073–23083

Gan ES, Xu Y, Wong JY, Geraldine Goh J, Sun B, Wee WY, Huang J, Ito T (2014) Jumonji demethylases moderate precocious flowering at elevated temperature via regulation of FLC in Arabidopsis. Nat Commun. doi: 10.1038/ncomms6098

Garner WW, Allard HA (1920) Effect of the relative length of day and night and other factors of the environment on growth and reproduction in plants. J Agric Res **18**: 553–606

Gendron JM, Pruneda-Paz JL, Doherty CJ, Gross AM, Kang SE, Kay SA (2012) Arabidopsis circadian clock protein, TOC1, is a DNA-binding transcription factor. Proc Natl Acad Sci **109**: 3167–3172

Gilmour SJ, Zarka DG, Stockinger EJ, Salazar MP, Houghton JM, Thomashow MF (1998) Low temperature regulation of the Arabidopsis CBF family of AP2 transcriptional activators as an early step in cold-induced COR gene expression. Plant J **16**: 433–442

Gould PD, Locke JCW, Larue C, Southern MM, Davis SJ, Hanano S, Moyle R, Milich R, Putterill J, Millar AJ, et al (2006) The molecular basis of temperature compensation in the *Arabidopsis* circadian clock. Plant Cell **18**: 1177–1187

Halliday KJ, Salter MG, Thingnaes E, Whitelam GC (2003) Phytochrome control of flowering is temperature sensitive and correlates with expression of the floral integrator FT. Plant J **33**: 875–885

Harmer SL, Hogenesch JB, Straume M, Chang H-S, Han B, Zhu T, Wang X, Kreps JA, Kay SA (2000) Orchestrated Transcription of Key Pathways in Arabidopsis by the Circadian Clock. Science **290**: 2110–2113

Haydon MJ, Mielczarek O, Frank A, Román Á, Webb AAR (2017) Sucrose and Ethylene Signaling Interact to Modulate the Circadian Clock. Plant Physiol **175**: 947–958

Haydon MJ, Mielczarek O, Robertson FC, Hubbard KE, Webb A a R (2013) Photosynthetic entrainment of the Arabidopsis thaliana circadian clock. Nature **502**: 689–92

Hazen SP, Schultz TF, Pruneda-Paz JL, Borevitz JO, Ecker JR, Kay SA (2005) LUX ARRHYTHMO encodes a Myb domain protein essential for circadian rhythms. Proc Natl Acad Sci **102**: 10387–10392

He Q, Cha J, He Q, Lee HC, Yang Y, Liu Y (2006) CKI and CKII mediate the FREQUENCY-dependent phosphorylation of the WHITE COLLAR complex to close the Neurospora circadian negative feedback loop. Genes Dev **20**: 2552–2565

Helfer A, Nusinow DA, Chow BY, Gehrke AR, Bulyk ML, Kay SA (2011) LUX ARRHYTHMO Encodes a Nighttime Repressor of Circadian Gene Expression in the Arabidopsis Core Clock. Curr Biol **21**: 126–133

Hepworth J, Antoniou-Kourounioti RL, Bloomer RH, Selga C, Berggren K, Cox D, Collier Harris BR, Irwin JA, Holm S, Säll T, et al (2018) Absence of warmth permits epigenetic memory of winter in Arabidopsis. Nat Commun. doi: 10.1038/S41467-018-03065-7

Hicks KA, Millar AJ, Carré IA, Somers DE, Straume M, Ry Meeks-Wagner D, Kay SA (1996) Conditional Circadian Dysfunction of the Arabidopsis early-flowering 3 Mutant.

Hoecker U (2017) The activities of the E3 ubiquitin ligase COP1/SPA, a key repressor in light signaling. Curr Opin Plant Biol **37**: 63–69

Van Der Horst GTJ, Muijtjens M, Kobayashi K, Takano R, Kanno SI, Takao M, De Wit J, Verkerk A, Eker APM, Van Leenen D, et al (1999) Mammalian Cry1 and Cry2 are essential for maintenance of circadian rhythms. Nature **398**: 627–630

Hsu PY, Devisetty UK, Harmer SL (2013a) Accurate timekeeping is controlled by a cycling activator in Arabidopsis. Elife. doi: 10.7554/eLife.00473

Hsu PY, Devisetty UK, Harmer SL (2013b) Accurate timekeeping is controlled by a cycling activator in Arabidopsis. Elife **2**: e00473

Hsu PY, Harmer SL (2014) Wheels within wheels: The plant circadian system. Trends Plant Sci. doi: 10.1016/j.tplants.2013.11.007

Huang H, Alvarez S, Bindbeutel R, Shen Z, Naldrett MJ, Evans BS, Briggs SP, Hicks LM, Kay SA, Nusinow DA, et al (2016) Identification of Evening Complex Associated Proteins in Arabidopsis by Affinity Purification and Mass Spectrometry. Mol Cell Proteomics **15**: 201–217

Ito S, Song YH, Imaizumi T (2012) LOV Domain-Containing F-Box Proteins: Light-Dependent Protein Degradation Modules in Arabidopsis. Mol Plant **5**: 573–582

Jones MA, Covington MF, DiTacchio L, Vollmers C, Panda S, Harmer SL (2010) Jumonji domain protein JMJD5 functions in both the plant and human circadian

systems. Proc Natl Acad Sci U S A **107**: 21623–21628

Jones MA, Morohashi K, Grotewold E, Harmer SL (2019) Arabidopsis JMJD5/JMJ30 Acts Independently of LUX ARRHYTHMO Within the Plant Circadian Clock to Enable Temperature Compensation. Front Plant Sci **10**: 1–12

Jung J-H, Barbosa AD, Hutin S, Kumita JR, Gao M, Derwort D, Silva CS, Lai X, Pierre E, Geng F, et al (2020) A prion-like domain in ELF3 functions as a thermosensor in Arabidopsis. Nature. doi: 10.1038/s41586-020-2644-7

Kamioka M, Takao S, Suzuki T, Taki K, Higashiyama T, Kinoshita T, Nakamichi N (2016) Direct Repression of Evening Genes by CIRCADIAN CLOCK-ASSOCIATED1 in the Arabidopsis Circadian Clock. Plant Cell **28**: 696–711

Kiba T, Henriques R, Sakakibara H, Chua NH (2007) Targeted Degradation of PSEUDO-RESPONSE REGULATOR5 by an SCFZTL Complex Regulates Clock Function and Photomorphogenesis in Arabidopsis thaliana. Plant Cell **19**: 2516–2530

Kidokoro S, Hayashi K, Haraguchi H, Ishikawa T, Soma F, Konoura I, Toda S, Mizoi J, Suzuki T, Shinozaki K, et al (2021) Posttranslational regulation of multiple clock-related transcription factors triggers cold-inducible gene expression in Arabidopsis. Proc Natl Acad Sci. doi: 10.1073/PNAS.2021048118

Kim J, Kim Y, Yeom M, Kim JH, Nam HG (2008) FIONA1 is essential for regulating period length in the Arabidopsis circadian clock. Plant Cell **20**: 307–319

Kim TS, Kim WY, Fujiwara S, Kim J, Cha JY, Park JH, Lee SY, Somers DE (2011) HSP90 functions in the circadian clock through stabilization of the client F-box protein ZEITLUPE. Proc Natl Acad Sci U S A **108**: 16843–16848

Krahmer J, Goralogia GS, Kubota A, Zardilis A, Johnson RS, Song YH, MacCoss MJ, LeBihan T, Halliday KJ, Imaizumi T, et al (2018) Time-resolved Interaction Proteomics of the GIGANTEA Protein Under Diurnal Cycles in Arabidopsis. FEBS Lett 1873-3468.13311

Kyung J, Jeon M, Jeong G, Shin Y, Seo E, Yu J, Kim H, Park C-M, Hwang D, Lee I (2022) The two clock proteins CCA1 and LHY activate VIN3 transcription during vernalization through the vernalization-responsive cis-element. Plant Cell **34**: 1020–1037

Lee K, Park OS, Seo PJ (2018) JMJ30-mediated demethylation of H3K9me3 drives tissue identity changes to promote callus formation in Arabidopsis. Plant J **95**: 961–975

Legris M, Klose C, Burgie ES, Rojas CCR, Neme M, Hiltbrunner A, Wigge PA, Schäfer E, Vierstra RD, Casal JJ (2016) Phytochrome B integrates light and temperature signals in Arabidopsis. Science **354**: 897–900

Li B, Gao Z, Liu X, Sun D, Tang W (2019) Transcriptional Profiling Reveals a Time-of-Day-Specific Role of REVEILLE 4/8 in Regulating the First Wave of Heat Shock-Induced Gene Expression in Arabidopsis. Plant Cell **31**: 2353–2369

Liu B, Zuo Z, Liu H, Liu X, Lin C (2011) Arabidopsis cryptochrome 1 interacts with SPA1 to suppress COP1 activity in response to blue light. Genes Dev **25**: 1029–

1034

Lowrey PL, Shimomura K, Antoch MP, Yamazaki S, Zemenides PD, Ralph MR, Menaker M, Takahashi JS (2000) Positional syntenic cloning and functional characterization of the mammalian circadian mutation tau. Science (80-) **288**: 483–491

Lu SX, Liu H, Knowles SM, Li J, Ma L, Tobin EM, Lin C (2011) A Role for Protein Kinase Casein Kinase2 a-Subunits in the Arabidopsis Circadian Clock. Plant Physiol **157**: 1537–1545

Lucas-Lledó JI, Lynch M (2009) Evolution of mutation rates: Phylogenomic analysis of the photolyase/cryptochrome family. Mol Biol Evol **26**: 1143–1153

Ma Y, Gil S, Grasser KD, Mas P (2018) Targeted Recruitment of the Basal Transcriptional Machinery by LNK Clock Components Controls the Circadian Rhythms of Nascent RNAs in Arabidopsis. Plant Cell **30**: 907–924

Martínez-García JF, Huq E, Quail PH (2000) Direct targeting of light signals to a promoter element-bound transcription factor. Science (80-) **288**: 859–863

Más P, Kim W-Y, Somers DE, Kay SA (2003) Targeted degradation of TOC1 by ZTL modulates circadian function in Arabidopsis thaliana. Nature **426**: 567–570

Mazzella MA, Bertero D, Casal JJ (2000) Temperature-dependent internode elongation in vegetative plants of Arabidopsis thaliana lacking phytochrome B and cryptochrome 1. Planta **210**: 497–501

McClung CR (2006) Plant circadian rhythms. Plant Cell **18**: 792–803

Medina J, Bargues M, Terol J, Pérez-Alonso M, Salinas J (1999) The Arabidopsis CBF gene family is composed of three genes encoding AP2 domain-containing proteins whose expression is regulated by low temperature but not by abscisic acid or dehydration. Plant Physiol **119**: 463–469

Michael TP, Salome PA, Yu HJ, Spencer TR, Sharp EL, McPeek MA, Alonso JM, Ecker JR, McClung CR (2003) Enhanced Fitness Conferred by Naturally Occurring Variation in the Circadian Clock. Science (80-) **302**: 1049–1053

Millar AJ Input signals to the plant circadian clock. doi: 10.1093/jxb/erh034

Millar AJ, Carré IA, Strayer CA, Chua N-H, Kay SA (1995a) Circadian Clock Mutants in Arabidopsis Identified by Luciferase Imaging.

Millar AJ, Short SR, Chua N-H, Kay SA (1992) A Novel Circadian Phenotype Based on Firefly Luciferase Expression in Transgenic Plants. Plant Cell **4**: 1075–1087

Millar AJ, Straume M, Chory J, Chua N-H, Kay SA (1995b) The Regulation of Circadian Period by Phototransduction Pathways in Arabidopsis. Cold Spring Harbor Laboratory Press

Miyamoto Y, Sancar A (1998) Vitamin B2-based blue-light photoreceptors in the retinohypothalamic tract as the photoactive pigments for setting the circadian clock in mammals. Proc Natl Acad Sci U S A **95**: 6097–6102

Mizuno T, Kitayama M, Oka H, Tsubouchi M, Takayama C, Nomoto Y, Yamashino T (2014a) The EC Night-Time Repressor Plays a Crucial Role in Modulating

Circadian Clock Transcriptional Circuitry by Conservatively Double-Checking Both Warm-Night and Night-Time-Light Signals in a Synergistic Manner in Arabidopsis thaliana. Plant Cell Physiol **55**: 2139–2151

Mizuno T, Nomoto Y, Oka H, Kitayama M, Takeuchi A, Tsubouchi M, Yamashino T (2014b) Ambient Temperature Signal Feeds into the Circadian Clock Transcriptional Circuitry Through the EC Night-Time Repressor in Arabidopsis thaliana. Plant Cell Physiol **55**: 958–976

Mizuno T, Takeuchi A, Nomoto Y, Nakamichi N, Yamashino T (2014c) The LNK1 night light-inducible and clock-regulated gene is induced also in response to warm-night through the circadian clock nighttime repressor in Arabidopsis thaliana. Plant Signal Behav. doi: 10.4161/psb.28505

Mohawk JA, Green CB, Takahashi JS (2012) Central and peripheral circadian clocks in mammals. Annu Rev Neurosci **35**: 445–462

Müller NA, Wijnen CL, Srinivasan A, Ryngajllo M, Ofner I, Lin T, Ranjan A, West D, Maloof JN, Sinha NR, et al (2015) Domestication selected for deceleration of the circadian clock in cultivated tomato. Nat Genet **48**: 89–93

Müller NA, Zhang L, Koornneef M, Jiménez-Gómez JM (2018) Mutations in EID1 and LNK2 caused light-conditional clock deceleration during tomato domestication. Proc Natl Acad Sci U S A **115**: 7135–7140

Nagel DH, Doherty CJ, Pruneda-Paz JL, Schmitz RJ, Ecker JR, Kay SA (2015) Genome-wide identification of CCA1 targets uncovers an expanded clock network in Arabidopsis. Proc Natl Acad Sci 4802–4810

Nakajima M, Imai K, Ito H, Nishiwaki T, Murayama Y, Iwasaki H, Oyama T, Kondo T (2005) Reconstitution of circadian oscillation of cyanobacterial KaiC phosphorylation in vitro. Science (80-) **308**: 414–415

Nakamichi N, Kiba T, Henriques R, Mizuno T, Chua N-H, Sakakibara H (2010) PSEUDO-RESPONSE REGULATORS 9, 7, and 5 Are Transcriptional Repressors in the Arabidopsis Circadian Clock. Plant Cell **22**: 594–605

Nusinow DA, Helfer A, Hamilton EE, King JJ, Imaizumi T, Schultz TF, Farré EM, Kay SA (2011) The ELF4–ELF3–LUX complex links the circadian clock to diurnal control of hypocotyl growth. Nature **475**: 398–402

O'neill JS, Reddy AB (2011) Circadian clocks in human red blood cells. Nature **469**: 498–502

Onai K, Ishiura M (2005) PHYTOCLOCK 1 encoding a novel GARP protein essential for the Arabidopsis circadian clock. Genes to Cells **10**: 963–972

Park S, Lee C-M, Doherty CJ, Gilmour SJ, Kim Y, Thomashow MF (2015) Regulation of the Arabidopsis CBF regulon by a complex low-temperature regulatory network. Plant J **82**: 193–207

Perales M, Portolés S, Más P (2006) The proteasome-dependent degradation of CKB4 is regulated by the Arabidopsis biological clock. Plant J **46**: 849–860

Pittendrigh CS (1960) Circadian rhythms and the circadian organization of living

systems. Cold Spring Harb Symp Quant Biol **25**: 159–184

Pokhilko A, Fernández AP, Edwards KD, Southern MM, Halliday KJ, Millar AJ (2012a) The clock gene circuit in Arabidopsis includes a repressilator with additional feedback loops. Mol Syst Biol **8**: 1–13

Pokhilko A, Fernández AP, Edwards KD, Southern MM, Halliday KJ, Millar AJ (2012b) The clock gene circuit in Arabidopsis includes a repressilator with additional feedback loops. Mol Syst Biol **8**: 574

Ponnu J, Riedel T, Penner E, Schrader A, Hoecker U (2019) Cryptochrome 2 competes with COP1 substrates to repress COP1 ubiquitin ligase activity during Arabidopsis photomorphogenesis. Proc Natl Acad Sci U S A **116**: 27133–27141

Portolés S, Más P (2010) The Functional Interplay between Protein Kinase CK2 and CCA1 Transcriptional Activity Is Essential for Clock Temperature Compensation in Arabidopsis. PLoS Genet **6**: e1001201

Purugganan MD, Fuller DQ (2009) The nature of selection during plant domestication. Nature **457**: 843–8

Putterill J, Laurie R, Macknight R (2004) It's time to flower: The genetic control of flowering time. BioEssays **26**: 363–373

Rawat R, Takahashi N, Hsu PY, Jones MA, Schwartz J, Salemi MR, Phinney BS, Harmer SL (2011) REVEILLE8 and PSEUDO-REPONSE REGULATOR5 Form a Negative Feedback Loop within the Arabidopsis Circadian Clock. PLoS Genet **7**: e1001350

Rosbash M (2009) The Implications of Multiple Circadian Clock Origins. PLoS Biol **7**: e1000062

Rugnone ML, Faigón Soverna A, Sanchez SE, Schlaen RG, Hernando CE, Seymour DK, Mancini E, Chernomoretz A, Weigel D, Más P, et al (2013) LNK genes integrate light and clock signaling networks at the core of the Arabidopsis oscillator. Proc Natl Acad Sci U S A **110**: 12120–5

Ruiz MCM, Hubbard KE, Gardner MJ, Jung HJ, Aubry S, Hotta CT, Mohd-Noh NI, Robertson FC, Hearn TJ, Tsai Y-C, et al (2018) Circadian oscillations of cytosolic free calcium regulate the Arabidopsis circadian clock. Nat Plants **4**: 690–698

Saini R, Jaskolski M, Davis SJ (2019) Circadian oscillator proteins across the kingdoms of life: structural aspects. BMC Biol. doi: 10.1186/s12915-018-0623-3

Sakamoto K, Nagatani A (1996) Nuclear localization activity of phytochrome B. Plant J **10**: 859–868

Salomé PA, Robertson Mcclung C (2005) PSEUDO-RESPONSE REGULATOR 7 and 9 Are Partially Redundant Genes Essential for the Temperature Responsiveness of the Arabidopsis Circadian Clock. Plant Cell **17**: 791–803

Sawa M, Nusinow DA, Kay SA, Imaizumi T (2007) FKF1 and GIGANTEA Complex Formation is Required for Day-Length Measurement in Arabidopsis. Science (80-) **318**: 261–265

Shalit-Kaneh A, Kumimoto RW, Filkov V, Harmer SL (2018) Multiple feedback loops

of the Arabidopsis circadian clock provide rhythmic robustness across environmental conditions. Proc Natl Acad Sci U S A **115**: 7147–7152

Shi Y, Ding Y, Yang S (2018) Molecular Regulation of CBF Signaling in Cold Acclimation. Trends Plant Sci **23**: 623–637

Somers DE, Devlin PF, Kay SA (1998a) Phytochromes and cryptochromes in the entrainment of the Arabidopsis circadian clock. Science (80-) **282**: 1488–1490

Somers DE, Webb AAR, Pearson M, Kay SA (1998b) The short-period mutant, toc1-1, alters circadian clock regulation of multiple outputs throughout development in Arabidopsis thaliana. Development **125**: 485–494

Su Y, Wang S, Zhang F, Zheng H, Liu Y, Huang T, Ding Y (2017) Phosphorylation of Histone H2A at Serine 95: A Plant-Specific Mark Involved in Flowering Time Regulation and H2A.Z Deposition. Plant Cell **29**: 2197–2213

Sugano S, Andronis C, Green RM, Wang ZY, Tobin EM (1998) Protein kinase CK2 interacts with and phosphorylates the Arabidopsis circadian clock-associated 1 protein. Proc Natl Acad Sci U S A **95**: 11020–11025

Sugano S, Andronis C, Ong MS, Green RM, Tobin EM (1999) The protein kinase CK2 is involved in regulation of circadian rhythms in Arabidopsis. Proc Natl Acad Sci U S A **96**: 12362–12366

Tepperman JM, Zhu T, Chang HS, Wang X, Quail PH (2001) Multiple transcription-factor genes are early targets of phytochrome A signaling. Proc Natl Acad Sci U S A **98**: 9437–9442

Thines B, Harmon FG (2010) Ambient temperature response establishes ELF3 as a required component of the core Arabidopsis circadian clock. Proc Natl Acad Sci **107**: 3257–3262

Tomita J, Nakajima M, Kondo T, Iwasaki H No Transcription-Translation Feedback in Circadian Rhythm of KaiC Phosphorylation.

Uehara TN, Mizutani Y, Kuwata K, Hirota T, Sato A, Mizoi J, Takao S, Matsuo H, Suzuki T, Ito S, et al (2019) Casein kinase 1 family regulates PRR5 and TOC1 in the Arabidopsis circadian clock. Proc Natl Acad Sci U S A **166**: 11528–11536

Wang C, Yang J, Song P, Zhang W, Lu Q, Yu Q, Jia G (2022) FIONA1 is an RNA N 6-methyladenosine methyltransferase affecting Arabidopsis photomorphogenesis and flowering. Genome Biol. doi: 10.1186/s13059-022-02612-2

Wang CQ, Khoshhal Sarmast M, Jiang J, Dehesh K (2015a) The transcriptional regulator BBX19 promotes hypocotyl growth by facilitating COP1-mediated EARLY FLOWERING3 degradation in arabidopsis. Plant Cell **27**: 1128–1139

Wang H, Ma LG, Li JM, Zhao HY, Xing Wang Deng (2001) Direct interaction of Arabidopsis cryptochromes with COP1 in light control development. Science (80-) **294**: 154–158

Wang Z, Casas-Mollano JA, Xu J, Riethoven JJM, Zhang C, Cerutti H (2015b) Osmotic stress induces phosphorylation of histone H3 at threonine 3 in pericentromeric regions of Arabidopsis thaliana. Proc Natl Acad Sci U S A **112**:

8487–8492

Wenden B, Kozma-Bognár L, Edwards KD, Hall AJW, Locke JCW, Millar AJ (2011) Light inputs shape the Arabidopsis circadian system. Plant J **66**: 480–491

Wilson ME, Tzeng SC, Augustin MM, Meyer M, Jiang X, Choi JH, Rogers JC, Evans BS, Kutchan TM, Nusinow DA (2021) Quantitative proteomics and phosphoproteomics support a role for mut9-like kinases in multiple metabolic and signaling pathways in Arabidopsis. Mol Cell Proteomics **20**: 100063

Xie Q, Wang P, Liu X, Yuan L, Wang L, Zhang C, Li Y, Xing H, Zhi L, Yue Z, et al (2014) LNK1 and LNK2 Are Transcriptional Coactivators in the Arabidopsis Circadian Oscillator. Plant Cell **26**: 2843–2857

Xing Liang Liu, Covington MF, Fankhauser C, Chory J, Wagner DR (2001) ELF3 Encodes a Circadian Clock–Regulated Nuclear Protein That Functions in an Arabidopsis PHYB Signal Transduction Pathway. Plant Cell **13**: 1293

Xu T, Wu X, Eng Wong C, Fan S, Zhang Y, Zhang S, Liang Z, Yu H, Shen L, Xu T, et al (2022) FIONA1-Mediated m6A Modification Regulates the Floral Transition in Arabidopsis. Adv Sci **9**: 2103628

Yamaguchi R, Nakamura M, Mochizuki N, Kay SA, Nagatani A (1999) Light-dependent Translocation of a Phytochrome B-GFP Fusion Protein to the Nucleus in Transgenic Arabidopsis. J Cell Biol **145**: 437–445

Yang H-Q, Tang R-H, Cashmore AR (2001) The Signaling Mechanism of Arabidopsis CRY1 Involves Direct Interaction with COP1. Plant Cell **13**: 2573–2587

Yanovsky MJ, Mazzella MA, Casal JJ (2000) A quadruple photoreceptor mutant still keeps track of time. Curr Biol **10**: 1013–1015

Yeom M, Kim H, Lim J, Shin A-Y, Hong S, Kim J-I, Gil Nam H (2014) How Do Phytochromes Transmit the Light Quality Information to the Circadian Clock in Arabidopsis? Mol Plant **7**: 1701–1704

Zhang XN, Wu Y, Tobias JW, Brunk BP, Deitzer GF, Liu D (2008) HFR1 is crucial for transcriptome regulation in the cryptochrome 1-mediated early response to blue light in Arabidopsis thaliana. PLoS One **3**: e3563

Zhao C, Zhang Z, Xie S, Si T, Li Y, Zhu J-K (2016) Mutational Evidence for the Critical Role of CBF Transcription Factors in Cold Acclimation in Arabidopsis. Plant Physiol **171**: 2744–2759

Zheng H, Zhang F, Wang S, Su Y, Ji X, Jiang P, Chen R, Hou S, Ding Y (2018) MLK1 and MLK2 Coordinate RGA and CCA1 Activity to Regulate Hypocotyl Elongation in Arabidopsis thaliana. Plant Cell **30**: 67–82

2 Optimization of Affinity-Purification Mass-Spectrometry

Portions of this chapter were originally published as Sorkin and Nusinow (2022) *Plant Circadian Networks*, Chapter 15 “Using Tandem Affinity Purification to Identify Circadian Clock Protein Complexes from *Arabidopsis*” Editors: Dorothee Staiger, Seth Davis, Amanda Melaragno Davis

2.1 Abstract

Proteins rarely function in isolation. Identifying the interacting partners of a given protein can help define its function by assuming that interacting partners share a joint function with the protein of interest. Our lab has developed a tandem affinity purification-mass spectrometry (APMS) protocol to identify protein-protein interactions on a proteomic scale for circadian clock factors. Here, we describe a protocol for the affinity purification of 3x-FLAG-6X-His (HFC)-tagged proteins and best practices for avoiding non-specific binding proteins. Together, we present this analysis as a guide to trainees interested in performing APMS on any bait protein of interest, although the majority of this study focuses on the identification of novel circadian clock-associated factors.

2.2 Introduction: Overview of Methodology

Tandem affinity purification coupled with mass spectrometry (APMS) is a powerful method to identify protein-protein interactions on a proteomic level. While most clock proteins have been identified via forward and reverse genetic screens, taking a proteomic approach to studying the clock may illuminate novel clock components and roles for clock proteins that were overlooked previously. By engineering a plant with an affinity-tagged version of a protein of interest, one can effectively capture near-native, direct and indirect protein interactions with the tagged protein *in vivo*.

One challenge of APMS is the difficulty of identifying and eliminating false positive proteins that are coprecipitated with the protein of interest. Co-precipitation of false positives is often due to the abundance of the contaminating protein or the native affinity of that protein for the antibody or resin you are using during the protocol. The protocol

supplied here includes two immunoprecipitation steps for each epitope tag in the purification of a 6x-His-3x-FLAG tandem affinity tagged bait protein in *Arabidopsis thaliana*. The use of two different affinity tags significantly reduces the number of false positives, as it is increasingly unlikely that a contaminating protein has a high affinity for two different antibodies or resins. We also recommend using both 1) a GFP-6x-His-3x-FLAG and 2) a wild-type no-tag background as negative controls. Any protein coprecipitated in these control immunoprecipitations can likely be deprioritized as a true interacting partner of the bait protein of interest. One may also use localization data to deprioritize proteins that are located in a separate compartment from the protein of interest; for example, a chloroplast-localized protein that is coprecipitated with a nuclear-localized transcription factor could be a false positive. Lastly, several datasets, including Van Leene et al. (2015) (Van Leene et al., 2015) and Besbrugge et al. (2018) (Besbrugge et al., 2018), contain lists of common contaminants in APMS experiments and can also be used to filter out non-specific binding proteins.

The circadian clock is made up of approximately 25 core oscillator proteins that participate in interlocking transcription-translation feedback loops to regulate numerous and diverse physiological outputs (Creux and Harmer, 2019). Identification and compilation of protein-protein interactions for circadian clock-associated proteins will be a valuable resource for understanding how the clock connects to environmental input pathways and how it coordinates appropriate physiological responses in the plant. APMS is an ideal method for probing complex signaling networks such as the circadian clock because of its effective capture of direct and indirect interacting proteins on a proteomic scale. Additionally, APMS is conducted *in vivo* in an engineered plant that can be grown

under specific environmental conditions that are known to affect clock activity. Thus, APMS allows for the identification of protein-protein interactions under physiologically relevant conditions for the plant and is higher throughput compared to other techniques such as the yeast 2-hybrid system.

Our method effectively captures protein-protein interactions *in vivo* and has been used to identify both established and novel protein interactions (Huang et al., 2016a) (*see* **Note 1** for details on designing and characterizing engineered bait proteins). Additionally, we detail a cost-effective method for crosslinking an antibody of interest to Protein G magnetic beads from scratch, eliminating the need to buy expensive pre-crosslinked antibody beads.

2.3 Materials

Prepare all solutions using ultrapure deionized water (18 MPa at 25 °C).

Crosslinking antibodies to protein G beads

1. Dynabeads™ Protein G for Immunoprecipitation (Invitrogen, catalog number: 10003D).
2. Monoclonal ANTI-FLAG M2 antibody produced in mouse (Sigma-Aldrich, catalog number: F1804).
3. Magnetic stand for microcentrifuge tubes.
4. Protein G Wash Buffer: 0.1 M $Na_3C_6H_5O_7$ pH 5.0, 0.01% NP-40.
5. Crosslinking Sensitization Buffer: 0.2 M triethanolamine, pH 8.2.

6. Crosslinking Buffer :10 mM dimethyl pimelimidate (DMP) in 0.2 M triethanolamine, pH 8.2. Prepare fresh.
7. Crosslinking Quench Buffer: 0.2 M ethanolamine, pH 8.2.
8. Tris-Buffered Saline: 50 mM Tris-HCl, pH 7.5, 150 mM NaCl, 0.01% Triton x-100.
9. Dynabeads™ Storage Buffer: 50% Glycerol, 50 mM Tris-HCl, pH 8.0, 150 mM NaCl, 0.01%, Triton x-100, 0.03% Na-Azide.
10. 4x SDS-PAGE Sample Buffer: For 10 mL of sample buffer, mix 5 mL 0.5 M Tris-HCl pH 6.8, 1.0 g SDS, 0.8 mL 0.1% Bromophenol Blue, and 4 mL of 100% glycerol. Adjust the final volume to 10 mL with ultrapure water. Aliquot into 10 tubes containing 950 µL of this solution. When ready to use an aliquot, add 2-mercaptoethanol to a final concentration of 5%; so add 50 µL. Heat and mix tube to dissolve mixture if necessary.

Plant Growth and Tissue Homogenization

1. MS agar medium: Add 2.205 g Murashige and Skoog medium and 7.0 g agar to ~500 mL of water. Add water to a volume of 1 L. Autoclave and dispense ~40 mL per 15 cm dish.
2. 15 cm petri dish.
3. Filter paper.
4. Gas sterilization chamber
5. Liquid N_2.
6. Mixer Mill MM 400 Tissue Homogenizer (Retsch).
7. 35 mL stainless steel grinding jar (Retsch, catalog number: 01.462.0214).

8. 3.2 mm stainless steel balls (Bio Spec Products, catalog number: 11079132ss).
9. Dry ice.

Affinity Purification

1. Magnetic stand for microcentrifuge tubes.
2. Magnetic stand for 15-mL conical tubes.
3. Sonic Dismembrator.
4. Low protein-binding microcentrifuge tubes.
5. 50-mL round-bottom tube.
6. Dynabeads™ His-Tag Isolation and Pulldown (Invitrogen, catalog number: 10104D).
7. 3x FLAG peptide (Sigma-Aldrich, catalog number: F4799).
8. Dry ice.
9. SII buffer: 100 mM Na-phosphate, pH 8.0, 150 mM NaCl, 5 mM EDTA, 5 mM EGTA, 0.1% Triton X-100 (see Note 2). Filter through a 0.22 μm filter syringe to sterilize and store at 4 °C.
10. SII buffer plus inhibitors: Make just before use. Use filter-sterilized SII buffer made in the previous step. Add 1 mM phenylmethylsulfonyl fluoride (PMSF) (see Note **3**), 1x protease inhibitor tablet (EDTA-free) (Thermo Fisher Scientific, catalog number: 88266), 1x phosphatase inhibitor cocktail II (Sigma-Aldrich, catalog number: P5726), 1x phosphatase inhibitor cocktail III (Sigma-Aldrich, catalog number: P0044), and 50 μM MG-132.

11. Protein concentration assay that is compatible with detergent, such as the Bio-Rad DC Protein Assay (Bio-Rad, catalog number: 5000111).
12. His Immunoprecipitation (IP) Buffer (*see* **Note 4**): 100 mM Na-phosphate, pH 8.0, 150 mM NaCl, 0.025% Triton X-100 (*see* **Note 2**). Filter through a 0.22 µm filter syringe to sterilize. Store at 4 °C.
13. 3x FLAG peptide: 50 mg/mL MDYKDHDGDYKDHDIDYKDDDDK resuspended in 100 mM Na-phosphate, pH 8.0. Store at -80 °C.
14. FLAG Elution Buffer: 500 µg/mL 3x FLAG peptide in His IP Buffer.
15. Ammonium bicarbonate buffer: Make fresh the day of purification. Solution is 25 mM ammonium bicarbonate in ultrapure deionized water. Filter through a 0.22 µm filter syringe to sterilize.

2.4 Methods

Cross-linking antibody to protein G beads (*see* **Notes 5 and 6**)

1. Rotate Dynabeads™ Protein G to fully resuspend beads in solution (*see* **Notes 7** *and* **8**).
2. Pipette 1.2 mL of resuspended Protein G Dynabeads™ into a microcentrifuge tube. Place tubes on a magnetic stand to collect beads for 1 minute. Remove supernatant with a pipette and discard.
3. Add 900 µL of protein G wash buffer to beads and rotate to wash for 5 minutes. Spin down the tube briefly in a microcentrifuge to collect liquid from cap, place in magnetic stand for 1 minute, and remove wash without disturbing beads. Repeat

this wash step once for a total of two washes to complete buffer exchange of the bead solution.

4. Add 700 µL of protein G wash buffer to washed beads and then add exactly 200 µL of anti-FLAG M2 antibody to the tube (*see* **Note 9**).
5. Rotate tube at 4 °C for 1 hour to allow antibody to bind to Dynabeads™ (*see* **Note 10**).
6. After the 1 hour incubation, remove 1% (9 µL) of resuspended bead solution for the “input” control sample that will be analyzed via SDS-PAGE gel (**Fig. 2.1**).
7. Spin down tube to gather all liquid from cap and place on magnetic stand for 1 minute. Remove 1% (9 µL) of supernatant for “flow through” control sample that will be analyzed via SDS-PAGE gel (**Fig. 2.1**). Remove remaining flow through from beads and discard.
8. Wash beads by adding 900 µL of protein G wash buffer and rotating for 5 minutes at room temperature. All following steps are performed at room temperature.
9. Repeat wash once for a total of two washes.
10. Wash beads twice with 900 µL 0.2 M NaBorate, pH 8.0. Rotate each wash for 3 minutes.
11. Wash beads three times with 900 µL 0.2 M triethanolamine, pH 8.2 (crosslinking sensitization buffer), to sensitize beads for cross-linking. Rotate each wash for 3 minutes. On the last wash, save 1% (9 µL) of resuspended beads in a microcentrifuge tube for the pre-crosslink control sample.

12. Cross-link antibody to beads by adding 900 µL of freshly prepared 0.01 M dimethyl pimelimidate (DMP) in 0.2 M triethanolamine, pH 8.2 (crosslinking buffer). Incubate with rotation for 30 minutes at room temperature (*see* **Note 11**).
13. Spin down tube to capture liquid from cap, then place tube on magnetic stand for 1 minute to capture beads. Remove supernatant.
14. Add 900 µL of 0.2 M ethanolamine, pH 8.2 (crosslinking quench buffer) to quench DMP crosslinker. Incubate with rotation for 30 minutes at room temperature.
15. Spin down tube to capture liquid from cap, then place tube on magnetic stand for 1 minute to capture beads. Remove ethanolamine supernatant and discard.
16. Wash beads twice with 900 µL of 0.1 M glycine, pH 2.5 to strip off non-covalently linked antibody. Invert by hand for exactly 1 minute each time to wash beads quickly (*see* **Note 12**).
17. Wash twice with 900 µL of 1x tris-buffered saline to neutralize pH. Rotate each wash for 3 minutes. During the second saline wash, fully resuspend beads and remove 1% (9 µL) as the post-crosslink control sample.
18. Remove saline wash and resuspend beads in 1.2 mL Dynabeads™ storage buffer. Beads can be stored at -20 °C for at least one year.
19. Add 4x SDS sample buffer to quality control samples (input, flow through, pre-crosslink, post-crosslink) and boil for 10 minutes to denature.
20. Test for effective crosslinking by running an SDS-PAGE gel of the input, flow through, pre-crosslink and post-crosslink control samples taken. Stain the SDS-PAGE gel with Coomassie blue to show abundance of antibody in each sample.

An example of successful crosslinking is shown in **Figure 2.1** (*see* **Notes 10** and **11**).

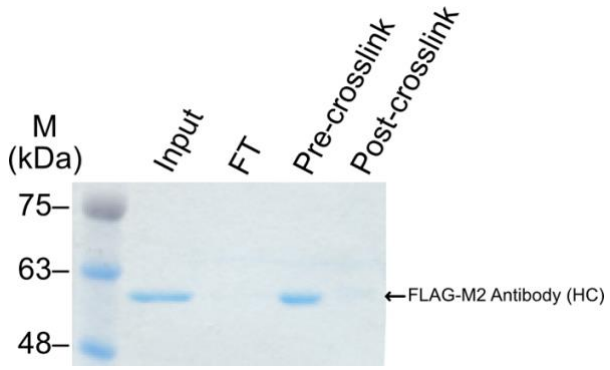

Figure 2.1 Coomassie blue stain of quality control samples from crosslinking FLAG-M2 antibody to Protein G Dynabeads.
Samples have been boiled; therefore, the antibody will dissociate from the beads and will result in a ~60 kDa band representing the heavy chain of the antibody unless effectively crosslinked. HC = heavy chain, FT= flow through.

Plant Growth and Tissue Collection

1. For each genotype, gas sterilize 18 tubes containing ~50 μL of seeds. Spread 2 tubes of seed evenly per 15-cm diameter plates, totaling 9 plates per genotype. This should be enough seed to collect 3x ~5 g of tissue from 10-day-old *Arabidopsis thaliana* seedlings expressing the 6x-His-3x-FLAG-tagged protein of interest in the null mutant background. Three packets of 5 g of tissue will serve as 3 biological replicates. Tubes containing ~50 μL of seed can be gas sterilized in 1.5 mL tubes for 4-5 hours in a sterilization chamber after adding 3 mL of hydrochloric acid to 100 mL of bleach.
2. Scatter seeds evenly on 15-cm diameter round plates with 15-cm round filter paper placed on top of 1/2x Murashige and Skoog media containing 1% sucrose. Seal

plates with micropore tape to allow gas exchange and place in darkness at 4 °C for 2-3 days.

3. Transfer plates to the appropriate growth conditions. Typical collections are grown under 12-hour light, 12-hour dark photoperiods (12:12) at 22 °C. Grow plants under white light at 100 μmol•m^{-2}•sec^{-1} (*see* **Note 13**).
4. On the 10th day of growth, collect 5 g of tissue into tin foil packets at the peak time of protein expression or at the zeitgeber time of interest (*see* **Notes 14** *and* **15**). 5 g of tissue can typically be obtained from collecting tissue from 2-3 plates. Flash freeze tissue in tinfoil in liquid N_2.
5. Tissue packets can be stored at -80 °C for at least 6 months.

Tissue Homogenization

1. Cool steel grinding jars in liquid nitrogen. Each jar can hold up to 5g of tissue.
2. Pre-crush 5 g packets of tissue as much as possible in tin foil while frozen before transferring into pre-cooled 35-mL steel grinding jars compatible with a Rosche Mixer Mill 400 or other similar device. Ensure O-ring and steel ball are in place before sealing jar. Use sterile, liquid nitrogen-cooled spatulas to help transfer tissue. Perform the transfer on dry ice to keep grinding cassettes cold.
3. The first set of grinding is performed for 45 seconds at 25/sec frequency. Then, repeat grinding 3x at 45 seconds at 30/sec frequency. Cool steel grinding jars in liquid nitrogen in between each set of tissue homogenization to ensure tissue remains frozen.

4. After a total of 4 rounds of homogenization, open steel jars and use a pre-cooled spatula to transfer powdered tissue to a well-labeled, sterile 50-mL conical tube on dry ice.
5. You can store tissue powder in 50-mL conical tubes at -80 °C for up to 1 month.

Protein Extraction and Sonication (*see* **Note 16**)

All subsequent steps should be performed in a 4 °C cold room unless otherwise noted.

1. Add ~12 mL of SII buffer plus inhibitors to 5 g of frozen tissue powder in a 50-mL conical tube on dry ice. Remove the tube from dry ice. Allow bubbles to release before closing the lid of the 50-mL conical.
2. Incubate frozen tissue in SII buffer for 10-15 minutes with rotation, or until all ground powder is in solution and there are no chunks.
3. Use a Fisherbrand Model 505 Sonic Dismembrator probe sonicator or similar to homogenize and lyse cells for 20 seconds (2 seconds on, 2 seconds off, total of 40 seconds, to prevent heat generation) at 50% power. Place sample on ice to cool, then repeat sonication once.

Extract Clarification

1. Transfer extract to a clean, 50-mL round-bottom centrifuge tube and centrifuge for 10 minutes at ≥ 20,000 *x g* at 4 °C.
2. Transfer supernatant to a second clean 50-mL round-bottom centrifuge tube by using a serological pipet, avoiding disturbing the pellet.
3. Repeat the centrifugation step, spinning for 10 minutes at ≥ 20,000 *x g* at 4 °C.

4. Remove and save the green supernatant using a 10 mL serological pipette tip with a p1000 pipette tip attached to the end and filter this extract through a 0.45 µm syringe filter into a sterile 15 mL conical tube, avoiding disturbance of the pellet. Save 90 µL of clarified extract for the “total input” quality control sample that will be analyzed via Western blot (**Fig. 2.2**).
5. Measure protein concentration of clarified extract (*see* **Note 17**).

Pre-wash anti-FLAG Dynabeads™

1. For 5 g of tissue from 10-day-old plants, you will use 250 µL of crosslinked anti-FLAG Dynabeads™ (*see* **Note 18**).
2. During the centrifugation steps, fully resuspend crosslinked anti-FLAG Dynabeads™ (made in section 3.1) with rotation at 4 °C.
3. Add 500 µL of SII buffer without inhibitors to a microcentrifuge then add exactly 250 µL of crosslinked anti-FLAG Dynabeads™ to the buffer (*see* **Note 18**).
4. Spin down tube to collect any liquid from cap and place on magnetic stand for 1 minute to capture beads. Remove supernatant.
5. Complete buffer exchange by washing beads twice more for 3 minutes in 900 µL SII buffer without inhibitors in a microcentrifuge tube. Always spin down tubes to collect liquid from caps then place tubes on the magnetic stand to capture beads for 1 minute before removing washes, making sure to not disturb the beads.
6. After two washes, resuspend beads in 400 µL of SII buffer and keep on ice until ready for the immunoprecipitation step.

FLAG Immunoprecipitation

1. Place pre-washed anti-FLAG Dynabeads™ (made in section 3.7) on magnetic stand for 1 minute and remove supernatant.
2. Use ~500 µL of extract to resuspend and transfer all washed anti-FLAG Dynabeads™ back into the clarified extract in the 15 mL conical tube.
3. Rinse the 1.5 mL tube that contained washed anti-FLAG Dynabeads™ twice with ~500 µL extract to ensure that all beads have been transferred to the 15 mL conical tube.
4. Incubate extract with anti-FLAG beads for 60 minutes with rotation at 4 °C (*see* **Note 19**).
5. Prepare the FLAG elution buffer during the IP. A volume of 3.6 mL of FLAG elution buffer should be enough for two samples.

Bead Capture and Washes

1. Spin down 15 mL tubes to collect liquid from caps at 1000 *x* g at 4˚C for 10 seconds.
2. Place 15 mL conical tube on a magnetic stand to capture beads.
3. Remove flow through using a 10 mL serological pipette tip with a p1000 pipette tip attached to the end to reduce flow rate and chance of disturbing beads. Save 90 µL of the depleted extract for the “FLAG IP flow through” quality control sample.
4. Wash Dynabeads™ with 10 mL of His IP buffer without inhibitors for 5 minutes with rotation (*see* **Note 4**).
5. Spin down 15 mL tube at 1000 *x* g at 4˚C for 10 seconds and place on magnetic stand to capture beads. Remove wash using a 10 mL serological pipette tip with a p1000 tip attached to the end.

6. Repeat wash once more with 10 mL of His IP buffer.
7. On the third wash, use 900 µL of His IP buffer to wash beads off the side of the 15 mL tube and transfer to a 1.5 mL low protein-binding tube. Repeat the wash to transfer all magnetic beads from the 15 mL conical tube to the 1.5 mL tube. Discard wash each time.
8. Wash one more time with 900 µL of His IP buffer in the 1.5 mL tube for a total of three 900 µL washes.

Elution of immunoprecipitated proteins off anti-FLAG beads

1. After removing the last wash from beads, add 400 µL of FLAG elution buffer to beads. Rotate at 4 °C for 15 minutes.
2. Spin down tubes briefly to collect liquid from caps. Place tubes in magnetic stand to capture beads for 1 minute. Remove 1/10th of elution (40 µL) and save in a tube labeled “Elution 1” for quality control. Pipette remaining elution into a low-protein binding 1.5 mL tube labeled “Combined Elution”.
3. Repeat steps 1-2 at 4 °C one more time, each time saving 1/10th of elution (Elutions 1 and 2) and transferring the remaining elution into the “Combined Elutions” tube.
4. Repeat steps 1-2 at 30 °C twice. Each time save 1/10th of elution (Elutions 3 and 4) and transferring the remaining elution into the “Combined Elutions” tube.
5. After all elution steps, remove 1/20th (~72 µL) of the “Combined Elutions” for the “Combined Elutions” quality control sample.

Wash His-Tag Isolation Dynabeads™

1. Fully resuspend the Dynabeads™ His-Tag Isolation and Pulldown magnetic beads by rotating bottle at 4 °C.

2. During the elution incubation steps, begin performing wash steps for the Dynabeads™ His-Tag Isolation and Pulldown magnetic beads. For 5 g tissue sample, use 90 µL of His Dynabeads™ (*see* **Note 20**).
3. Add exactly 90 µL of His Dynabeads™ to 500 µL of His IP buffer in a low-protein binding microcentrifuge tube that is well labeled (this is the final tube) and pipette up and down to wash all beads from the pipette tip.
4. Place the tube on the magnetic stand to capture beads for 1 minute. Remove wash, making sure not to disrupt beads.
5. Complete buffer exchange by washing beads with 500 µL of His IP buffer for 5 minutes with rotation. Remove wash.
6. Add 500 µL of His IP buffer to beads and let sit on ice until ready for use.

His-tag immunoprecipitation and washes

1. Once all elutions are combined into one tube, remove the supernatant from the washed His Dynabeads™ (prepared in Section 3.11) and add the combined elutions to beads.
2. Incubate elutions with His beads for 20 minutes at 4 °C with rotation.
3. Place tube on magnetic stand to capture beads for 1 minute. Remove 1/20th of His IP flow through (~72 µL) for quality control. Remove and discard remaining flow through from beads.
4. Wash beads with 900 µL of His IP buffer for 5 minutes with rotation at 4 °C.
5. Spin down tube to collect liquid from the lid. Place tube on magnetic stand for 1 minute to capture beads. Remove wash, making sure not to disrupt beads.
6. Repeat wash two more times for a total of three 900 µL washes in His IP buffer.

7. For the fourth wash, add 900 µL of sterile-filtered 25 mM ammonium bicarbonate and rotate for 3 minutes at 4 °C.
8. Repeat ammonium bicarbonate wash 3 more times, for a total of 4 washes in ammonium bicarbonate.
9. On the 4th ammonium bicarbonate wash, completely resuspend beads in the buffer. Remove 1/10th of bead suspension (90 µL) for quality control.
10. Spin down tube for 1 minute to collect liquid from the lid. Place tube on magnetic stand for 1 minute to capture beads. Remove wash.
11. Spin down tube for 1 minute a second time, place on magnetic stand, and remove any remaining ammonium bicarbonate buffer from tube.
12. Flash freeze tube in liquid N_2. Samples can be stored at -80 °C for up to one year. Samples are now ready for trypsin digest and analysis by LC-MS.

Quality Control Western Blot

1. Before sending samples for LC-MS analysis, it is good practice to perform a Western blot on quality control samples to ensure bait proteins were effectively immunoprecipitated.
2. We recommend running the following samples for the quality control gel: total input, FLAG IP flow through, FLAG elutions 1 through 4, Combined FLAG elutions, His IP ammonium bicarb suspension, and His IP flow-through. For the His IP suspension sample, spin down tube and remove supernatant from beads. Resuspend beads in 30 µL of 2x SDS sample buffer. Add 4x SDS sample buffer to all other quality control samples to 1x concentration and boil for 10 minutes to denature.

3. Run the quality control samples on an SDS-PAGE gel and transfer to nitrocellulose membrane. Probe for your bait protein using either a native antibody, anti-His antibody, or anti-FLAG antibody. If possible, use another antibody to detect a known protein interactor to ensure protein-protein interactions were maintained and coprecipitated throughout procedure.
4. **Figure 2.2** shows a sample Western blot from a successful tandem affinity purification using this protocol.

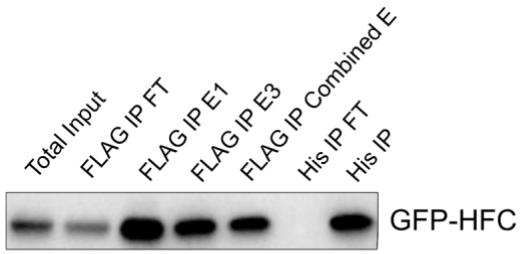

Figure 2.2 Western blot of quality control samples from an affinity purification. Immunoblot treated with anti-FLAG antibody at 1:10,000 concentration. Figure shows quality control samples from a tandem affinity purification of 35S::GFP-6x-His-3x-FLAG (HFC). Ideally, there is little HFC-fusion protein observed in the flow through samples, and the final His IP sample contains the majority of the original input. FT= flow through, E= elution, IP= immunoprecipitation.

2.5 Notes

1. Recommendations for the design of affinity-tagged proteins:
    a. We recommend using a 6x-His-3x-FLAG tandem affinity tag at the C-terminus of your protein unless the modification of the C-terminus will likely result in functional disruption.

b. Transform your affinity-tagged protein into a null mutant background so that the native protein is absent to maximize interaction between your tagged protein and its partners.

c. Expression level of the transgene can affect the level of non-specific binding in your immunoprecipitation; we recommend testing the ability of the affinity-tagged plant in rescuing the mutant background. Ideally, the tagged protein should rescue mutant phenotypes back to wild type levels.

2. Use of detergents in buffers used for sample preparation for mass spectrometry can cause damage to mass spectrometer equipment and interfere with proper quantification of peptides. Conversely, complete removal of detergents from these buffers inhibits immunoprecipitation of bait proteins and co-immunoprecipitation of interacting proteins using Dynabeads™ in our experience. The detergent concentrations used in these buffers have yielded effective protein extraction and binding to affinity beads without causing damage or interference while using the LTQ-Velos Pro Orbitrap LC-MS/MS.
3. Once dissolved in isopropanol solution, PMSF has a short half-life. Use within 1 hour.
4. The His IP buffer does not contain chelating agents EDTA and EGTA as these agents can chelate the cobalt-based coating on the His-isolation Dynabeads™ and render them inactive. Do not use chelating agents in any steps involving the His-isolation Dynabeads™. Note that SII buffer therefore cannot be used in any steps involving His Dynabeads™.

5. Instead of crosslinking your antibody to Protein G beads from scratch, you may purchase Dynabeads™ that are pre-crosslinked to the antibody. If purchasing pre-crosslinked beads, avoid beads made of or coated in sepharose, amylose or any other carbohydrate. Many plant proteins will bind to carbohydrate resins, which will increase non-specific binding.
6. The crosslinking protocol takes approximately 2.5 hours to complete, not including running the SDS-PAGE quality control gel.
7. A regular scale preparation is 1.2 mL cross-linked bead solution per tube. Therefore, 200 µL of 1 µg/mL anti-FLAG M2 antibody will be added to 1.2 mL of Protein G beads.
8. For affinity purification using antibodies generated in rabbits, Protein A Dynabeads™ can be substituted. For Protein A crosslinking, replace Na-Citrate pH 5.0 with Na-Phosphate pH 8.0 buffer in the Protein A Wash Buffer.
9. It is important to add exactly 200 µL of antibody to each tube to maintain an identical background of crosslinked beads for all immunoprecipitations.
10. If you are seeing flowthrough of antibody after incubation with Protein G beads (as determined by Coomassie stain of an SDS-PAGE gel), you may need to decrease the amount of antibody added or increase the time of incubation with the beads. See **Figure 2.1** for an example of a successful crosslinking quality control gel.
11. If antibody is dissociating from Protein G Dynabeads™ (there is a heavy chain band in the post-crosslink sample on the Coomassie stain of the quality control SDS-PAGE gel), increase crosslinking time with DMP or purchase new DMP if

stock is old. See **Figure 2.1** for an example of a successful crosslinking quality control gel.

12. Do not incubate crosslinked Dynabeads™ in 0.2 M glycine for more than 1 minute. Overexposure to glycine can cause the crosslinked antibody to strip off the beads.
13. Expression and stability of clock-associated proteins is often modulated by the intensity, wavelength and duration of light as well as temperature. Consider these factors when selecting growth conditions.
14. If collecting tissue at a dawn or dusk transition, collect the tissue under the light condition prior to the transition. For example, if collecting at dawn—the time of the dark-light transition—then collect tissue under darkness. This will prevent accumulation of transient light-induced proteins that would not normally be abundant.
15. If collecting during the dark-period, tissue may be collected under dim green light. Ensure that all other sources of light are blacked out to ensure full darkness and to avoid activation of photoreceptor light-signaling pathways.
16. The affinity purification protocol starting from the protein extraction and sonication step typically takes between 6-9 hours to complete.
17. For 5 g of tissue resuspended in 12 mL of SII buffer, we typically measure between 2-5 mg/mL of total protein content. You can measure protein concentration using a detergent-compatible method such as the DC Protein Assay from Bio-Rad.
18. You may need to optimize the volume of beads used during the IPs. If there is a high amount of flow through of the tagged bait protein observed in the quality control immunoblot, we recommend increasing the bead volume from 250 µL. You

may also experiment with using fewer beads to find the lowest bead input you can use to deplete your bait protein.

19. You may need to optimize the incubation time of your extract with the anti-FLAG beads. We recommend incubation for 60 minutes to capture your bait protein and any interacting proteins. However, if you notice there is high flow through of your bait protein after a 60-minute incubation (as determined in your quality control Western blot (**Fig. 2.2**)), you may want to increase the time of your FLAG IP.
20. The binding capacity of the His Dynabeads™ is listed as 40 µg of a 28 kDa histidine-tagged protein / mg (25 µL) of beads. You may want to adjust the volume of His beads used depending on the total protein content measured from the extract and your estimates of total His-tagged bait protein.

2.6 Results

Use of detergents. The use of detergents in APMS experiments must be delicately balanced. Surfactants such as NP-40, Triton X-100, sodium dodecyl sulfate (SDS), and 3-[(3-cholamidopropyl)dimethylammonio]-1-propanesulfonate (CHAPS) are commonly incorporated into protein extraction buffers to facilitate the solubilization of hydrophobic proteins. However, these detergents can interfere with enzymatic peptide digestion, disrupt protein-protein interactions, and damage expensive mass spectrometry equipment (Zhang and Li, 2004). We thus sought to test the efficacy of different surfactants in protein extraction and co-precipitation.

We first tested the effect of eliminating detergent upon protein extraction and purification *in planta*. To test this, we performed a small-scale tandem affinity purification

on ~300 mg of tissue overexpressing PHOTOPERIODIC CONTROL OF HYPOCOTYL 1 (PCH1) tagged with 3x-FLAG and 6x-His (HFC) (35S::PCH1-HFC, (Huang et al., 2016b)). Protein extracts made in buffers without detergent were noticeably lighter in color (less green) than their + detergent counterparts. When we quantified protein concentration, indeed, the -detergent samples contained less protein (3.56 mg/mL) than +detergent samples (5.3 mg/mL), despite starting with equal tissue quantities. We normalized protein concentration to 2.0 mg/mL for the affinity purifications and found that the amount of PCH1-HFC in the FLAG flow-through was visibly higher in the sample without detergent (**Lane 2, Figure 2.3**). Additionally, the amount of PCH1-HFC in the HIS IP was noticeably lower in the -detergent sample versus the +detergent sample (**Lane 4, Figure 2.3**), indicating that some detergent is important for proper extraction and capture of proteins by affinity purification. We additionally wanted to test whether co-precipitation of interacting proteins was compromised in the absence of detergent. PCH1 is known to interact with the protein Phytochrome B (PhyB) (Huang et al., 2016b). Thus, we looked at the abundance of PhyB throughout the tandem affinity purification process by Western blotting and probing with a PhyB-specific antibody. We saw a similar result as observed for PCH1-HFC levels: there was more PhyB lost in the FLAG flow-through and much less PhyB coprecipitated in the His IP in the -detergent sample versus +detergent (**Figure 2.3**). Together, this experiment demonstrated that the absence of detergent is highly detrimental to the complete capture of affinity-tagged proteins and their interacting partners during APMS. This experiment only examined PCH1-HFC and PhyB purification in +/- detergent; however, the effect of detergent levels on affinity purification of other

plant proteins would likely be affected by a particular protein's hydrophobicity or the type of affinity resin being used.

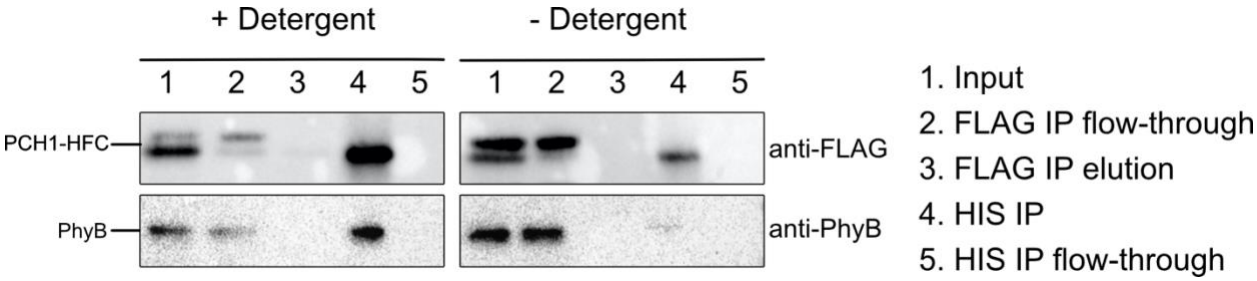

Figure 2.3 The absence of detergent decreases immunoprecipitation of tagged proteins and coprecipitation of interacting partners.
Protein extracts from plants overexpressing PHOTOPERIODIC CONTROL OF HYPOCOTYL 1 (PCH1) tagged with 3x-FLAG-6x-HIS (HFC) were subjected to tandem affinity purification consisting of FLAG-tag immunoprecipitation followed by His-tag affinity purification. Protein extraction and affinity purifications were performed in buffer with detergent (+ Detergent, 0.1% Triton X-100 in FLAG IP buffer, 0.05% Triton x-100 in His-tag isolation buffer) or without detergent (- Detergent, no Triton X-100 in FLAG nor His-tag buffers). PCH1-HFC was tracked throughout extraction and purification steps via Western blotting probing for the FLAG epitope. A PCH1-interacting protein, Phytochrome B (PhyB) was also tracked via Western blotting probing with an antibody specific for native PhyB.

While Western blotting showed clear decreases in purified proteins in the small-scale APMS (**Figure 2.3**), we wanted to confirm that this decrease corresponded to fewer overall peptides identified in a large-scale APMS. We thus performed tandem affinity purification on a line expressing LATE ELONGATED HYPOCOTYL (LHY) from its endogenous promoter and tagged with the HFC tag and transformed into an *lhy* loss-of-function mutant background: pB7 LHYp::LHY-HFC in *lhy-20* CCA1::LUC. We performed side-by-side affinity purifications on 5g tissue with our typical buffer recipe (+Detergent, 0.1% Triton X-100 in the FLAG IP buffer and 0.025% Triton X-100 in the HIS IP Buffer) or with no detergent in the HIS IP buffer (-Detergent, 0.1% Triton X-100 in the FLAG IP buffer and 0.0% Triton X-100 in the HIS IP Buffer). We saw equivalent levels of LHY-HFC in the total input and FLAG flow-through samples via Western blotting (**Figure 2.4**).

However, the amount of LHY-HFC in the FLAG elutions (which are performed in HIS IP Buffer) was severely decreased in the -detergent treatment, highlighting the importance of detergent for eluting proteins from the FLAG Dynabeads. Following, much less LHY-HFC bait was observed in the final HIS IP sample in -detergent (**Figure 2.4**).

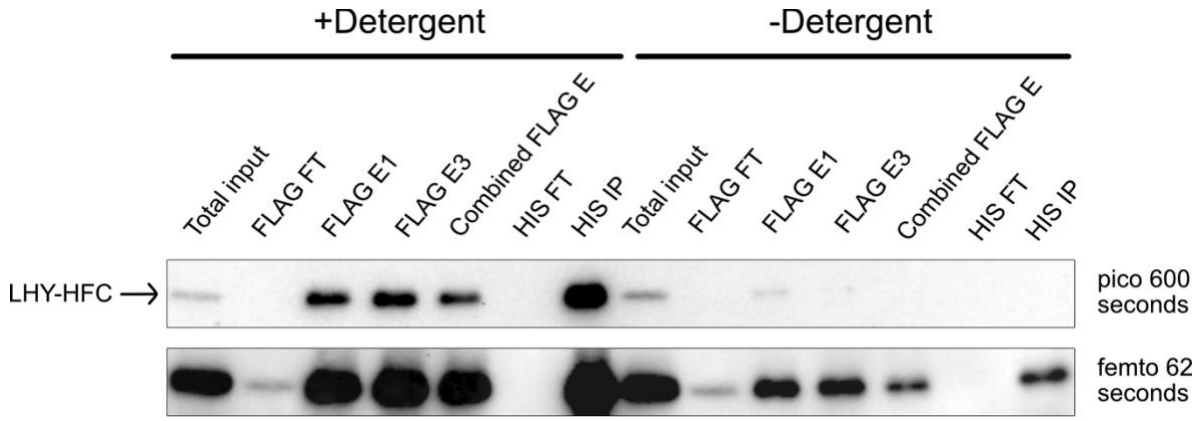

Figure 2.4 The absence of detergent decreases immunoprecipitation of tagged proteins in large-scale affinity purification.
Protein extracts from plants expressing LHY-HFC were subjected to tandem affinity purification consisting of FLAG-tag immunoprecipitation followed by His-tag affinity purification. Protein extraction and affinity purifications were performed in buffer with (+ Detergent, 0.1% Triton X-100 in FLAG IP buffer, 0.025% Triton x-100 in His-tag isolation buffer) or without detergent (- Detergent, 0.1% Triton X-100 in FLAG and 0.0% Triton X-100 in His-tag buffers). LHY-HFC was tracked throughout extraction and purification steps via Western blotting probing for the FLAG epitope using an anti-FLAG antibody. Two exposure times are included to show low abundance bands. FT= flow through, E= Elution.

We submitted the +/- detergent samples for analysis by LCMS and found that the no detergent sample indeed contained fewer identifiable proteins (38 proteins) compared to the +detergent sample (265 proteins). In terms of total spectrum count for the LHY-HFC bait protein in each of these APs, we identified 94 total spectra mapped to LHY-HFC in the no detergent sample, while the +detergent sample showed 394. This trend of fewer spectra in the no detergent sample was maintained for all identified proteins, such as the family of casein kinase (CK) subunits which are known LHY-binding factors (**Table 2.1**). This indicates the lack of detergent negatively affects co-precipitation of all proteins

equally. This massive difference in the overall number of proteins identified and bait protein spectra captured demonstrated that indeed, the absence of detergent—while optimal for the functioning of a mass spectrometer—was highly detrimental to the goal of identifying protein-protein interactions. While excluding detergent from APMS is thus not a suitable option, thoroughly washing the HIS-tag isolation beads (or other final bead product) at least four times with 25 mM ammonium bicarbonate (resuspended in water, no detergent) is an effective way of depleting detergent from the sample before downstream peptide digestion and LCMS.

Identified Protein	Accession Number	LHY-HFC_No Detergent	LHY-HFC_Detergent
LHY-HFC	AT1G01060	82	336
CKA2	AT3G50000	37	83
CKA4	AT2G23070	34	71
CKB4	AT2G44680	5	21
CKB1	AT5G47080	9	22
CKA1	AT5G67380	32	75
CKB3	AT3G60250	7	23
CKB2	AT4G17640	7	15

Table 2.1 Absence of detergent decreases capture of relevant proteins in LHY-HFC APMS
Total spectra for a given identified protein are provided from one replicate of LHY-HFC No Detergent and one replicate of LHY-HFC performed with detergent. The Casein Kinases (CK) are known LHY-interacting partners. Total spectra identified for CKs and LHY-HFC bait protein decreases in the no detergent sample.

Having determined the importance of including detergent in the affinity purification of HFC tagged proteins, we next sought to test the efficacy of different types of detergent in our protocol. Our original protocol uses 0.1% triton X-100 for the protein extraction and FLAG IP steps and 0.025% triton X-100 for the HIS IP (beginning at the FLAG elution step). Triton X-100 is a non-ionic surfactant that is commonly used for the solubilization of hydrophobic proteins and for lysing cells by disrupting lipid membranes. We also included NP-40, Empigen BB (N,N-Dimethyl-N-dodecylglycine betaine, N-(Alkyl C10-

C16)-N,N-dimethylglycine betaine), and a styrene-maleic acid lipid particle (SMALP) detergent in our studies. NP-40 is also a non-ionic detergent very similar in nature to triton X-100 and these two are often used interchangeably. Empigen BB is a zwitterionic detergent, which means it contains both positive and negatively charged particles at its headgroup. Lastly, SMALPs are a newer technology being used as an alternative to conventional detergents for their ability to separate intact sections of membranes without disrupting embedded protein complexes. For our purposes, we require a detergent that effectively disrupts cell and nuclear membranes and solubilizes proteins. However, as we are interested in protein-protein interactions, we do not want the detergent to disrupt the bonds between proteins in complex. Thus, ionic detergents such as SDS (sodium dodecyl sulfate) should not be used for capturing native protein interactions. Zwitterionic detergents such as Empigen BB are ideal for their lack of net charge and conductivity, making them ideal detergents for ion-exchange chromatography and electrophoresis, but can have negative effects on maintaining protein-protein interactions. As SMALP technology is still in the early stages of development, we were curious to see if it could be an effective alternative to non-ionic detergents like triton X-100 and NP-40 in our APMS.

We tested these four types of surfactants in their ability to extract total protein and IP PCH1-HFC using a FLAG IP. We tested our original protocol (0.1% triton X-100), 0.1% Empigen BB, 0.25% XIRAN SMALP (SL30010 P20 (2.3:1 ratio of styrene:maleic acid)), and 0.05% NP-40. Although we started with equal amounts of tissue for the protein extraction, we found that the SMALP detergent was much more effective at extracting total protein, as indicated by the input level of PCH1-HFC (**Figure 2.5**). For the FLAG IP, triton X-100 and NP-40 behaved very similarly in their ability to IP PCH1-HFC (**Figure**

2.5). Empigen BB detergent, while effective at extracting total protein, showed decreased PCH1-HFC in the IP sample compared to the other detergents, suggesting that this zwitterionic surfactant may be disrupting the ability of the immunobeads to capture the FLAG epitope on PCH1 (**Figure 2.5**). The SMALP detergent, while superior in its ability to extract total protein, seemed to limit the amount of PCH1-HFC that was immunoprecipitated, as suggested by the increased amount of PCH1-HFC in the flow-through (**Figure 2.5**). This might suggest that the SMALP detergents, too, decrease the ability of the tagged protein to be captured by immunobeads. Thus, while the SMALP detergent presents an interesting alternative to non-ionic detergents, we concluded that our original protocol using 0.1% triton X-100 in the FLAG IP and 0.025% triton X-100 in the His IP was the most effective method for our APMS purposes.

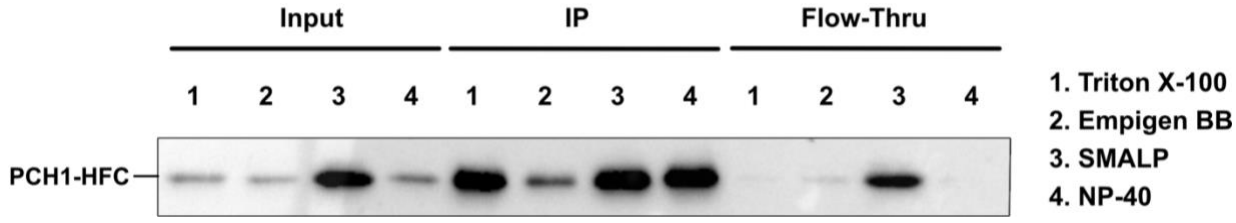

Figure 2.5 Type of detergent impacts protein extraction and FLAG immunoprecipitation.
Protein extracts from plants overexpressing PHOTOPERIODIC CONTROL OF HYPOCOTYL 1 (PCH1) tagged with 3x-FLAG-6x-HIS (HFC) were subjected to FLAG immunoprecipitation (IP). Protein extraction and IP purifications were performed in buffer with different detergents (1= 0.1% triton X-100, 2= 0.1% Empigen BB Zwitterionic detergent, 3= 0.25% XIRAN SMALP detergent, 4= 0.05% NP-40. Western blot shows PCH1-HFC via probing for the FLAG epitope using anti-FLAG antibody.

Prioritization criteria for interacting proteins. One of the most challenging aspects of APMS experiments is discerning true binding factors from non-specific binding proteins. By performing a tandem affinity purification by first targeting the FLAG epitope and subsequently targeting the His-tag, we can decrease the number of non-specific

binding proteins; a protein that has affinity for the FLAG antibody will likely not also have affinity for the His-tag isolation beads. Thus, a promiscuous binding protein carried over from the FLAG IP will hopefully be eliminated in the His-tag isolation.

Despite this effort to limit non-specific binding proteins from our APMS samples, we suspect that a large portion of our interactor lists contains false positives. While the use of two tags decreases the number of non-specific proteins that simply bind to our affinity beads, this does not address the problem of proteins that might bind to the affinity tags themselves or to the bait protein of interest in a non-specific manner. Additionally, some proteins may simply be extremely abundant in the cell and fail to be sufficiently depleted from our samples during wash steps. To combat this, we have defined several criteria by which we have prioritized interactors. We prioritize interactors that 1) were assigned > 1 spectrum in a given clock bait APMS, 2) were assigned 0 spectra in GFP-HFC negative control APMS, 3) have rhythmic mRNA abundance patterns under diurnal LDHC conditions, 4) have rhythmic mRNA abundance patterns under constant light conditions, 5) are localized to the same subcellular compartment as bait protein, and 6) are already associated with circadian rhythms in the literature.

To eliminate proteins that bind to our FLAG or His epitopes or to any given protein non-specifically, we perform a control APMS using tissue from a line that constitutively expresses GFP-HFC (35S::GFP-HFC). Among the top interacting proteins identified in our GFP-HFC control APMS samples were the alpha subunit of ATP synthase (ATPA), glyceraldehyde-3-phosphate dehydrogenase C2 (GAPC2), ribulose-bisphosphate carboxylase (RBCL), and several actin family members (**Dataset S1**). These proteins are

likely extremely highly abundant in the cell and potentially bind non-specifically to our bait proteins or do not get sufficiently washed off the affinity beads. Indeed, we see between 3-49 spectra mapping to GAPC2 in all our clock protein APMS samples submitted (**Dataset S1**). If not for the GFP-HFC negative control sample, we would not have an effective way of knowing whether GAPC2 is a true binding partner of these clock proteins. Of the 1039 proteins identified across our affinity purification experiments, we were able to eliminate 144 proteins (13.8%) as non-specific binding proteins that were coprecipitated with GFP-HFC (**Dataset S1**).

Finally, as demonstrated by our investigation of FTIP1 (**Appendix I**), inclusion of a wild type, no-tag background APMS is a critical control. By including a no-tag control, one can capture non-specific binding proteins that have affinity for the resins used during the immunoprecipitation. Of the total number of proteins identified, we eliminated 102 proteins (9.8%) as non-specific binding proteins that coprecipitated with Col-0 (**Dataset S1**). Together, the inclusion of GFP-HFC and Col-0 negative controls helped eliminate non-specific binding proteins from our list of interactors, allowing us to focus instead on a smaller list of proteins that were more likely to be true positive interactors.

2.7 Summary

In this chapter, we have detailed a protocol for affinity purification-mass spectrometry (APMS) of 6X-His-3X-FLAG-(HFC-) tagged proteins from Arabidopsis protein extracts. We additionally address two challenges of APMS: the use of detergents and elimination of false-positive or non-specific binding proteins from interactor lists. We discuss how best to avoid false positives, which includes use of both a wild type no-tag control as well as a

GFP-tag control. We hope that this discussion will be a useful lesson to scientists-in-training in how to critically assess their data and question confounding results.

2.8 Relative Contributions

Shin-Cheng (Newcity) Tzeng performed the LC/MS of affinity-purified samples and was instrumental for the completion of this work. He Huang and Rebecca Bindbeutel created the PCH1p::PCH1-HFC line used during detergent testing (Huang et al., 2016b). MLS, He Huang, and DAN designed the experimental approach. MLS performed the experiments, made the figures, and wrote this chapter.

2.9 References

Besbrugge N, Van Leene J, Eeckhout D, Cannoot B, Kulkarni SR, De Winne N, Persiau G, Van De Slijke E, Bontinck M, Aesaert S, et al (2018) GSyellow, a Multifaceted Tag for Functional Protein Analysis in Monocot and Dicot Plants. Plant Physiol **177**: 447–464

Bonnot T, Gillard MB, Nagel DH CAST-R: An application to visualize circadian and heat stress-responsive genes in plants. doi: 10.1093/plphys/kiac121

Covington MF, Maloof JN, Straume M, Kay SA, Harmer SL (2008) Global transcriptome analysis reveals circadian regulation of key pathways in plant growth and development. Genome Biol **9**: 10.1186/gb-2008-9-8-r130

Creux N, Harmer S (2019) Circadian Rhythms in Plants. Cold Spring Harb Perspect Biol. doi: 10.1101/cshperspect.a034611

Endo M (2016) Tissue-specific circadian clocks in plants. Curr Opin Plant Biol **29**: 44–49

Hsu PY, Harmer SL (2012) Circadian Phase Has Profound Effects on Differential Expression Analysis. PLoS One **7**: e49853

Hsu PY, Harmer SL (2014) Wheels within wheels: The plant circadian system. Trends Plant Sci **19**: 240–249

Huang H, Alvarez S, Bindbeutel R, Shen Z, Naldrett MJ, Evans BS, Briggs SP, Hicks LM, Kay SA, Nusinow DA, et al (2016a) Identification of Evening Complex Associated Proteins in Arabidopsis by Affinity Purification and Mass Spectrometry. Mol Cell Proteomics **15**: 201–217

Huang H, Nusinow DA (2016) Into the Evening: Complex Interactions in the Arabidopsis Circadian Clock. Trends Genet **32**: 674–686

Huang H, Yoo CY, Bindbeutel R, Goldsworthy J, Tielking A, Alvarez S, Naldrett MJ, Evans BS, Chen M, Nusinow DA (2016b) PCH1 integrates circadian and light-signaling pathways to control photoperiod-responsive growth in Arabidopsis. Elife **5**: 1–27

Kim J, Kim Y, Yeom M, Kim JH, Nam HG (2008) FIONA1 is essential for regulating period length in the Arabidopsis circadian clock. Plant Cell **20**: 307–319

Van Leene J, Eeckhout D, Cannoot B, De Winne N, Persiau G, Van De Slijke E, Vercruysse L, Dedecker M, Verkest A, Vandepoele K, et al (2015) An improved toolbox to unravel the plant cellular machinery by tandem affinity purification of Arabidopsis protein complexes. Nat Protoc **10**: 169–187

Lek A, Evesson FJ, Sutton RB, North KN, Cooper ST (2012) Ferlins: Regulators of Vesicle Fusion for Auditory Neurotransmission, Receptor Trafficking and Membrane Repair. Traffic **13**: 185–194

Liu L, Li C, Liang Z, Yu H (2018a) Characterization of Multiple C2 Domain and Transmembrane Region Proteins in Arabidopsis. Plant Physiol **176**: 2119–2132

Liu L, Li C, Song S, Teo ZWN, Shen L, Wang Y, Jackson D, Yu H (2018b) FTIP-Dependent STM Trafficking Regulates Shoot Meristem Development in Arabidopsis. Cell Rep **23**: 1879–1890

Liu L, Liu C, Hou X, Xi W, Shen L, Tao Z, Wang Y, Yu H (2012) FTIP1 is an essential regulator required for florigen transport. PLoS Biol **10**: e1001313

Romanowski A, Schlaen RG, Perez-Santangelo S, Mancini E, Yanovsky MJ (2020) Global transcriptome analysis reveals circadian control of splicing events in Arabidopsis thaliana . Plant J **3**: 1–14

Shimizu H, Katayama K, Koto T, Torii K, Araki T, Endo M, Doherty CJ, Kay SA, Barclay JL, Tsang AH, et al (2015) Decentralized circadian clocks process thermal and photoperiodic cues in specific tissues. Nat Plants **1**: 10.1038/NPLANTS.2015.163

Sorkin ML, Nusinow DA (2021) Time Will Tell: Intercellular Communication in the Plant Clock. Trends Plant Sci **26**: 706–719

Sorkin ML, Nusinow DA (2022) Using Tandem Affinity Purification to Identify Circadian Clock Protein Complexes from Arabidopsis. *In* D Staiger, S Davis, AM Davis, eds, Plant Circadian Networks Methods Protoc. Springer US, New York, NY, pp 189–203

Südhof TC, Rizo J (1996) Synaptotagmins: C2-Domain Proteins That Regulate Membrane Traffic. Neuron **17**: 379–388

Zhang N, Li L (2004) Effects of common surfactants on protein digestion and matrix-assisted laser desorption/ionization mass spectrometric analysis of the digested peptides using two-layer sample preparation. Rapid Commun Mass Spectrom **18**: 889–896

3 A Protein-Protein Interactome for the Arabidopsis Circadian Clock

3.1 Abstract

The Arabidopsis circadian clock consists of several interlocking transcription-translation feedback loops and approximately 20-30 protein components. This highly interconnected network has primarily been studied using genetic means such as forward and reverse genetic screens. Here, we present an alternative approach to clock discovery using proteomics. Using affinity-purification coupled with mass-spectrometry (APMS), we identified hundreds of putative interacting partners for eight of the core circadian clock proteins in Arabidopsis thaliana: CIRCADIAN CLOCK ASSOCIATED 1 (CCA1), LATE ELONGATED HYPOCOTYL (LHY), FIONA 1 (FIO1), JUMONJI DOMAIN CONTAINING 5 (JMJD5), TIMING OF CAB 1 (TOC1), PSEUDORESPONSE REGULATOR 5 (PRR5), PRR7, and PRR9. We validated a novel interaction between CCA1/LHY and CYCLING DOF FACTOR 2 (CDF2) via yeast 2-hybrid and highlight several high priority interactions to follow up on for each circadian clock bait protein studied. To make our dataset publicly available and easily interpretable, we have uploaded our interactome data to the STRING database (www.string-db.org), which we hope users will apply to form and support new research hypotheses concerning the Arabidopsis circadian clock.

3.2 Introduction

Most of the components that are part of the core clock oscillator in Arabidopsis thaliana were first identified through genetic methods. The clock genes *LATE ELONGATED HYPOCOTYL* (*LHY*), *EARLY FLOWERING* (*ELF*) *3*, *ELF4*, *FIONA 1* (*FIO1*), *PSEUDORESPONSE REGULATOR* (*PRR*) *1* (aka *TIMING OF CAB EXPRESSION 1* (*TOC1*)), *PRR5*, *PRR7*, and *PRR9* were all identified using forward or reverse genetic screens (Millar et al., 1995; Schaffer et al., 1998; Doyle et al., 2002; Farré

et al., 2005; Nakamichi et al., 2005). *JUMONJI DOMAIN CONTAINING 5* (*JMJD5*), and *NIGHT LIGHT-INDUCIBLE AND CLOCK-REGULATED 1* (*LNK*) and *LNK2* were identified by transcriptomics (Jones et al., 2010; Rugnone et al., 2013) and *CIRCADIAN CLOCK ASSOCIATED 1* (*CCA1*) and REVEILLE 8 were identified through promoter/promoter-element pull-down assays (Kenigsbuch and Tobin, 1995; Wang et al., 1997). While much insight has been gained into the clock mechanism through genetic means, examining the clock through a proteomic lens presents a relatively unexplored avenue of discovery. Here, we use affinity purification-mass spectrometry (APMS) to discover protein-protein interactions for the core clock proteins CCA1, LHY, PRR1/TOC1, PRR5, PRR7, PRR9, FIO1, and JMJD5.

CCA1 and LHY are morning-expressed MYB-like transcriptional repressors that function at the heart of the circadian oscillator in Arabidopsis (Wang and Tobin, 1998b; Alabadí et al., 2001; Mizoguchi et al., 2002). Phosphorylation of CCA1/LHY by CASEIN KINASE 2 (CK2) is required for protein-DNA complex formation (Daniel et al., 2004) and direct interactions between these clock proteins and CASEIN KINASE ALPHA 1 (CKA1), CKA2, CASEIN KINASE BETA 1 (CKB1), CKB2, and CKB3 have been previously established (Sugano et al., 1998). In addition to CK2, the MUT9-LIKE KINASEs (MLKs also known as PPKs/AELs) MLK1, MLK2, and MLK4 are known to interact with CCA1 and LHY (Su et al., 2017; Zheng et al., 2018), though whether these kinases affect CCA1/LHY transcriptional activity is unknown. Light sensitive proteins themselves, CCA1/LHY interact with photomorphogenesis factors ELONGATED HYPOCOTYL 5 (HY5), DE-ETIOLATED 1 (DET1), and FAR-RED ELONGATED HYPOCOTYL 3 (FHY3) (Andronis et al., 2008; Lau et al., 2011; Li et al., 2011). Within the core oscillator, CCA1

and LHY interact with other clock factors LNK1/LNK2 and heterodimerize with each other (Lu et al., 2009; Xie et al., 2014).

The family of PRR transcriptional regulators are expressed sequentially, beginning just after dawn in the order of PRR9>PRR7>PRR5>PRR3>PRR1/TOC1 (Matsushika et al., 2000). While their activity at the genetic level is well understood, the PRRs also participate in many protein interactions. Some of these interactions are with proteins that deposit post-translational modifications; PRR3/5 interact with and are phosphorylated by the protein kinase WITH NO LYSINE (K) KINASE 1 (WNK1) (Murakami-Kojima et al., 2002; Nakamichi et al., 2002); this family also physically interacts with several components of the E3 ubiquitin ligase pathway including ZEITLUPER (ZTL) (Más et al., 2003; Fujiwara et al., 2008; Wang et al., 2010), FLAVIN-BINDING KELCH REPEAT F-BOX 1 (FKF1) (Más et al., 2003; Yasuhara et al., 2004; Baudry et al., 2010), and LOV KELCH PROTEIN 2 (LKP2) (Más et al., 2003; Yasuhara et al., 2004; Baudry et al., 2010). In addition to these interactions, the PRRs also form within-family complexes: TOC1 interacts with PRR3/5/9 (Ito et al., 2003; Para et al., 2007; Fujiwara et al., 2008; Ito et al., 2008; Wang et al., 2010).

FIO1 is a functional U6 N^6-methyladenosine (m^6A) methyltransferase that regulates period length of the circadian clock in Arabidopsis (Kim et al., 2008; Wang et al., 2022; Xu et al., 2022). m^6A is a common mRNA modification found in eukaryotes that is thought to regulate mRNA metabolism (Zhao et al., 2017). Interestingly, m^6A modification of mRNA exhibits a circadian rhythm in mice (Wang et al., 2015). *FIO1* is one of the few Arabidopsis circadian clock genes to have a homolog in humans, called

METTL16 (Pendleton et al., 2017; Mendel et al., 2018). METTL16, however, has not been connected to circadian rhythms in mammals. There are very few studies focused on FIO1 and no protein interactions have been established for this protein.

Finally, JMJD5 is a jumonji C domain-containing (JMJ) putative histone demethylase that operates in the circadian oscillators of both Arabidopsis and humans (Jones et al., 2010; Lu et al., 2011; Jones et al., 2019). There are few studies specifically examining JMJD5 and no protein interactions have been validated for this protein in Arabidopsis. Interestingly, the human JMJD5 homolog interacts with the tumor suppressor gene p53 and is a potential therapeutic target for cancer treatments (Huang et al., 2015).

As summarized, some protein interactions have been identified for these core circadian clock components. However, a high throughput approach to protein interaction discovery has not been completed for these proteins. Here, we use affinity-purification coupled with mass-spectrometry (APMS) to identify novel protein-protein interactions for CCA1, LHY, PRR5, PRR7, PRR9, TOC1, JMJD5, and FIO1 on a proteomic scale (**Figure 3.1**). We coprecipitated hundreds of proteins and will make our APMS dataset publicly available on the STRING database (www.string-db.org) and on ProteomeXchange (www.proteomexchange.org). We followed up on an interaction identified between CCA1/LHY and CYCLING DOF FACTOR 2 (CDF2) using a yeast 2-hybrid assay and plan to continue our characterization of this and other interactions identified from this project. We summarize our findings here and highlight several high priority interactions

for each of these clock proteins. We hope that this public dataset will serve as a useful tool for future studies.

3.3 Results and Discussion

Affinity-tagged lines rescue mutant period phenotypes and show expected protein abundance patterns. To identify novel protein interactions within the Arabidopsis circadian clock, we created affinity-tagged versions of CCA1, LHY, FIO1, JMJD5, and TOC1. CCA1, LHY, FIO1, and JMJD5 were tagged with a 3x-FLAG-6x-His C-terminal (HFC) affinity tag while TOC1 was tagged at the C-terminus with a NanoLuc-3x-FLAG-10x-His tag (NL-3F10H). CCA1::CCA1-HFC, LHY::LHY-HFC, JMJD5::JMJD5-HFC, and TOC1::TOC1-NL-3F10H were driven by their endogenous promoters and transformed into the *cca1-1* CCA1::LUC, *lhy-20* CCA1::LUC, *jmjd5-1* CCR2::LUC, or *toc1-2* CCA1::LUC mutant backgrounds, respectively. 35S::FIO1-HFC was constitutively expressed from the Cauliflower Mosaic Virus (CaMV) 35S promoter and transformed into the Col-0 background. As FIO1 mRNA expression is not rhythmic (Kim et al., 2008), we anticipate that constitutive expression from the CaMV35S promoter will not significantly change expression patterns in terms of timing. We also examined protein interactions of PSEUDORESPONSE REGULATOR 5/7/9 (PRR5/7/9) using PRR5pro::FLAG-PRR5-GFP in *prr5*, PRR7pro::FLAG-PRR7-GFP in *prr7*, and PRR9pro::FLAG-PRR9-GFP in *prr9* that have been previously published (Kiba et al., 2007; Nakamichi et al., 2010).

To ensure that our affinity-tagged proteins function similarly to their native counterparts, we first examined the circadian period phenotype of plants carrying the transgene compared to their respective mutant backgrounds. The LHY-HFC construct

fully rescued the short period length of the *lhy-20* mutant back to wild-type levels while the other rescue lines showed partial rescue but were significantly different from the mutant background (**Figure 3.2B**). Constitutive expression of FIO1-HFC did not significantly alter the period length (**Figure 3.2D**). In addition to measuring the period phenotype of our affinity-tagged lines, we also examined protein abundance patterns over a 24-hour period under 12 hour light: 12 hour dark, 22 ℃ conditions (LDHH). We observed typical cycling patterns for CCA1, LHY, TOC1, and JMJD5 (Wang and Tobin, 1998a; Kim et al., 2003; Más et al., 2003; Song and Carré, 2005; Jones et al., 2010; Gan et al., 2014) with peak protein abundance at ZT3, ZT3, ZT12, and ZT15, respectively (**Figure 3.2F-J**). We did not observe cycling in protein abundance for FIO1-HFC (**Figure 3.2I**), which is consistent with previous reports showing that FIO1 does not have rhythmic mRNA expression (Kim et al., 2008). The FLAG-PRR5/7/9-GFP lines were previously characterized (Kiba et al., 2007; Nakamichi et al., 2010). We selected the time of tissue collection for APMS based on the time of peak protein abundance as determined by the 24-hour Western blots shown in **Figure 3.2** (**Figure 3.3**). Together, these experiments demonstrated that the affinity tagged lines exhibit expected protein abundance cycling patterns and function within the circadian clock, making them ideal reagents to capture native protein-protein interactions using APMS.

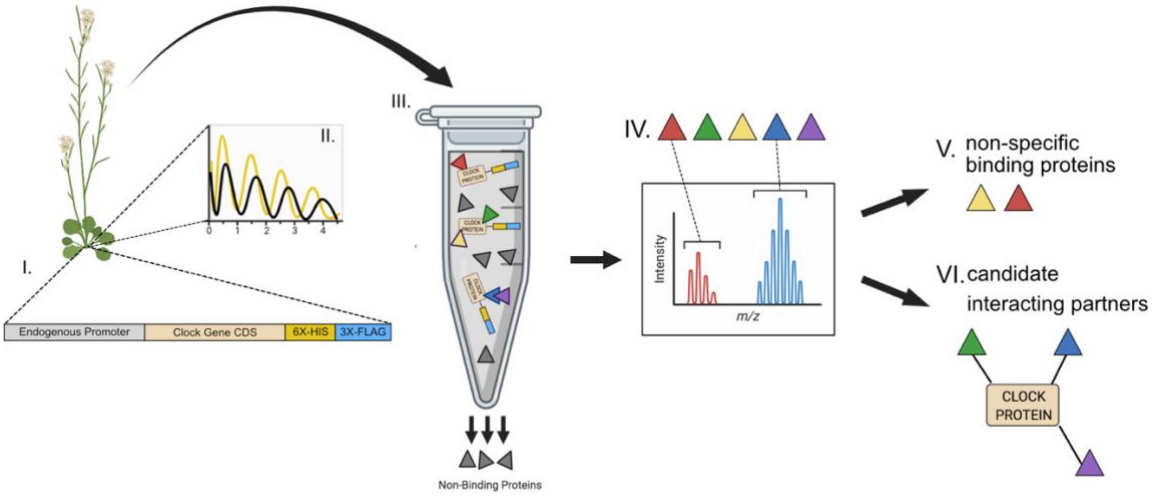

Figure 3.1 Graphical summary of APMS workflow
I) Arabidopsis thaliana ecotype Col-0 was engineered to express circadian clock proteins with a C-terminal 6X-His-3X-FLAG affinity tag. All lines except FIO1 were made in their respective mutant backgrounds so that the only version of the protein present in the cell is the tagged version. All lines except FIO1 are driven by their endogenous promoters. II) The circadian period phenotype of homozygous T3 lines is analyzed and lines that partially or fully rescue the mutant phenotype are selected to move forward. III) Protein extracts from affinity-tagged lines are created and used as the starting material for a FLAG immunoprecipitation followed by a His-tag isolation. Interacting proteins, as represented by colored triangles, are coprecipitated with clock baits in a direct or indirect manner. Non-binding proteins are washed away. IV) Interacting proteins are identified by their mass-to-charge ratio using mass spectrometry. V) Proteins identified in Col-0 or 35S::GFP-HFC negative control APMS experiments are filtered out of datasets as non-specific binding proteins. VI) Interactome networks of potential interactor partners can be constructed based on the remaining coprecipitated proteins.

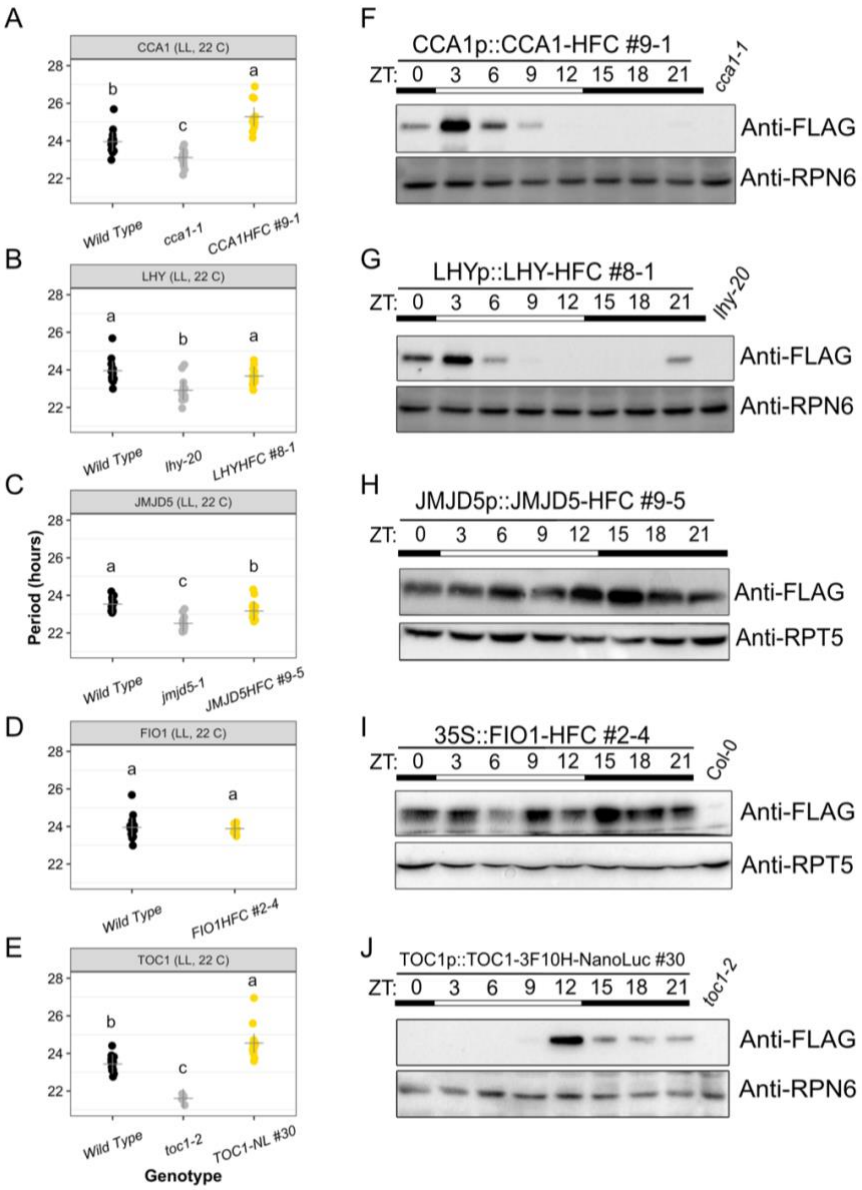

Figure 3.2 Characterization of affinity-tagged lines.
(A-E) Circadian luciferase reporter period analysis of selected T3 homozygous lines expressing (A) CCA1-HFC, (B) LHY-HFC, (C) JMJD5-HFC, (D) FIO1-HFC, or E) TOC1-NL-3F10H in their respective mutant backgrounds (*cca1-1*, *lhy-20*, *jmjd5-1*, Col-0, *toc1-2*). Each point represents the circadian period of an individual plant and the + symbol shows the average period for that genotype. Letters correspond to significantly different periods as determined by ANOVA with a Tukey's post-hoc test. Environmental conditions during imaging are included at the top of the plot (LL = constant light). (F-J) Time course Western blots showing cyclic protein abundance patterns of 10-day-old affinity tagged lines under 12 hr light: 12 hr dark 22 ℃ conditions. Affinity tagged lines are detected with anti-FLAG antibody. RPT5 or RPN6 were used to show loading. White and black bars indicate lights-on and lights-off, respectively Western blots and luciferase reporter assays were repeated at least 2 times. ZT= Zeitgeber Time.

Affinity purification-mass spectrometry (APMS) identifies novel interacting partners of CCA1, LHY, FIO1, JMJD5, TOC1, and PRR5/7/9. To identify protein-protein interactions on a proteomic scale, we used affinity purification-mass spectrometry (APMS). As protein levels cycle for all proteins under study except FIO1, we chose to collect tissue for APMS at the time of peak protein abundance using the 24-hour LDHH Western blots shown in **Figure 3.2**. We therefore collected tissue at the following timepoints during the LDHH cycle: CCA1/LHY were collected at ZT0 (in darkness), FIO1-HFC at ZT5, JMJD5 at ZT12 (in light), and TOC1-NL-3F10H at ZT18 (**Figure 3.3**). Based on previous reports of peak expression time, we collected FLAG-PRR9-GFP at ZT4, FLAG-PRR7-GFP at ZT6, and FLAG-PRR5-GFP at ZT8 (Kiba et al., 2007; Nakamichi et al., 2010) (**Figure 3.3**). A summary of the APMS experiments performed is provided in **Table S3.1**. For the TOC1-NL-3F10H and HFC-tagged lines, we performed a tandem affinity purification, first immunoprecipitating the FLAG epitope using FLAG antibody-coated magnetic beads and subsequently isolating for the 6x-His tag using nitrilotriacetic acid (NTA)-coated affinity beads. For the FLAG-PRR5/7/9-GFP lines, we performed the FLAG IP and concentrated the captured proteins using a trichloroacetic acid (TCA) precipitation.

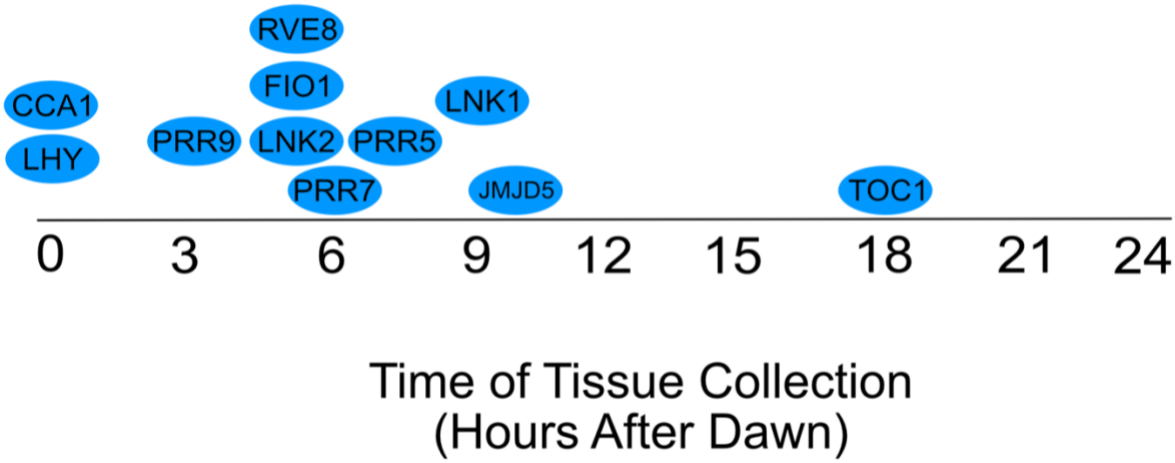

Figure 3.3 Time of tissue collection for APMS.
Timeline shows the time of day (hours after dawn) when we collected tissue for each affinity-tagged line. We selected these timepoints based on the time of peak protein abundance as determined by Western blots shown in **Figure 3.2**.

One challenge of using APMS to find novel protein interactions is identification of false positives. Native proteins may have non-specific affinity for the anti-FLAG or His-tag isolation beads, epitope tags, or even the bait proteins themselves. Additionally, highly abundant proteins can be carried over during APMS even through wash steps. We can decrease the number of false positive hits from our APMS experiments by using two affinity steps—non-specific binding proteins that have affinity for one epitope will hopefully not have affinity for a second. We also included two negative control samples: a 35S::GFP-HFC and a wild type Col-0. Any protein coprecipitated in these samples with more than 2 spectra assigned to it was considered a non-specific binding protein and was filtered out of the interactor lists for our target clock proteins. To simplify analysis, we have combined the data for CCA1/LHY-HFC and for FLAG-PRR5/7/9-GFP.

After filtering out non-specific binding proteins identified in the negative control samples, we found 501 proteins coprecipitated with CCA1/LHY-HFC, 234 proteins with

FIO1-HFC, 740 proteins with PRR5/7/9, 328 proteins with JMJD5, and 112 proteins with TOC1-NL-3F10H (**Dataset S3.1**). From these lists we prioritized interactors that met the following criteria: 1) its mRNA cycles with a circadian rhythm as determined in (Romanowski et al., 2020), 2) protein has been associated with circadian rhythms in the literature, or 3) the protein name or description includes one or more key words (transcription, light, circadian, temperature). After manual prioritization, we narrowed down our lists to 31 proteins for CCA1/LHY-HFC, 25 proteins for TOC1-NL-3F10H, 103 proteins for FLAG-PRR5/7/9-GFP, 31 proteins for JMJD5-HFC, and 24 proteins for FIO1-HFC (**Tables S3.2-3.6)**.

We created a Venn diagram to compare the complete filtered lists for CCA1/LHY-HFC, FIO1-HFC, JMJD5-HFC, TOC1-NL-3F10H, and FLAG-PRR5/7/9-GFP (**Figure 3.4**). We found significant overlap, with very few proteins exclusively coprecipitating with one bait protein/protein group. There were 10 proteins that exclusively coprecipitated with CCA1/LHY-HFC, 4 proteins exclusive to FIO1-HFC, 222 proteins exclusive to FLAG-PRR5/7/9-GFP, 5 proteins exclusive to JMJD5-HFC, and 3 proteins exclusive to TOC1-NL-3F10H (**Dataset S3.1**). As these proteins all function within the circadian clock, it is reasonable for there to be overlap in their interactor lists. We think the relatively high number of PRR5/7/9-exclusive proteins could be due to only performing one affinity purification step compared to the two purification steps for the HFC-tagged baits; there may be an increased number of transient or low abundance interactors in the FLAG-PRR5/7/9-GFP dataset or possibly more false positives. Despite the large overlap in interactor lists, the few proteins identified as exclusive interactors with one bait protein/protein group appear to provide insight into the function of these clock proteins.

For example, two of the TOC1-exclusive interactors are EARLY FLOWERING 4 (ELF4) and LUX ARRHYTHMO (LUX), two of the three members that make up the evening complex (EC) (Nusinow et al., 2011; Chow et al., 2012), suggesting that an important connection within the circadian clock is formed between TOC1 and the EC. This is supported by previous work showing that TOC1 is coprecipitated with ELF3, the third component of the EC (Huang et al., 2016). TOC1 is also involved in regulating the EC at the transcriptional level (Huang et al., 2012); thus, this new connection between TOC1 and the EC at the protein level presents an interesting possible new layer to the existing transcription-translation signaling pathway. In the next sections, we highlight some high priority interactions to follow up on.

CCA1/LHY-HFC interact with regulatory kinases and CDF2. Of the ten CCA1/LHY-HFC-exclusive interactors, six of them were subunits of casein kinase (CK): CKA1, CKA3, CKB1, CKB2, CKB3, and CKB4 (**Dataset S3.1**). CCA1/LHY-HFC also coprecipitated CKA2, CKA4, and all four family members of the MUT9-LIKE KINASES (MLKs), MLK1-4 (**Dataset S3.1, Table S3.2**). The CK subunits are well-known regulators of CCA1/LHY transcriptional activity (Sugano et al., 1998; Daniel et al., 2004) and MLKs1/2/4 have previously been shown to interact with these clock transcription factors (Su et al., 2017; Zheng et al., 2018). As CCA1/LHY are central regulators of numerous target loci (Nagel et al., 2015), perhaps this enrichment of protein interactions with regulatory kinases serves to provide tight control over the transcriptional activity of these important transcription factors.

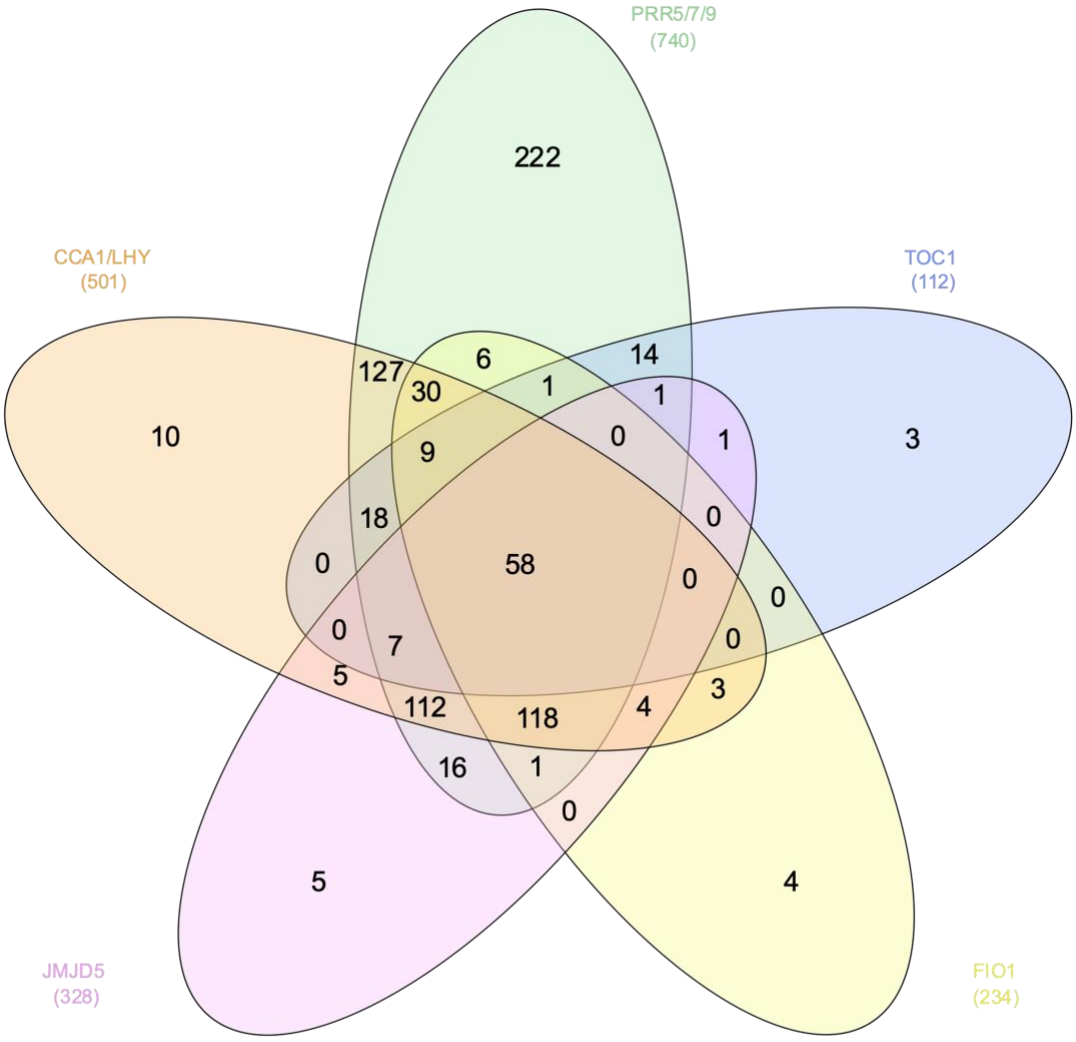

Figure 3.4 Venn diagram of APMS datasets from various clock proteins.
Protein lists were filtered to exclude any proteins that had 2 or more total spectra coprecipitated with 35S::GFP-HFC or Col-0 negative controls. Only the proteins identified with 2 or more spectra were included in analysis, except when proteins with only one peptide were identified in more than one biological replicate. Venn diagram was made with InveractiVenn (interactivenn.net).

Another CCA1/LHY-HFC-exclusive interactor was CYCLING DOF FACTOR 2 (CDF2). The family of CDFs regulates flowering time via repression of *CONSTANS* (*CO*) and has previously been linked to the circadian clock through its interaction with GIGANTEA (GI) (Fornara et al., 2009; Fornara et al., 2015; Krahmer et al., 2018). CDF2

also controls flowering via regulation of primary microRNA (miRNA) accumulation (Sun et al., 2015). *CDF2*, *CCA1*, and *LHY* have extremely similar mRNA expression patterns under LDHC conditions, which serves as further evidence that these proteins are coexpressed at the same time of day (**Figure 3.5**). We confirmed the interaction between CCA1/LHY and CDF2 using a yeast 2-hybrid system, validating that CDF2 is a novel interactor of these clock transcription factors (**Figure 3.6**).

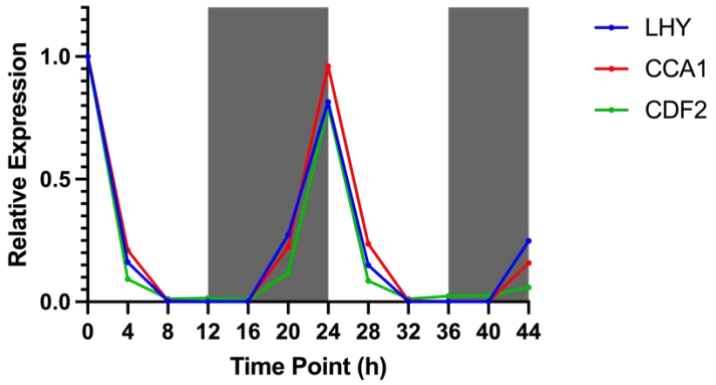

Figure 3.5 *CCA1, LHY,* and *CDF2* are coexpressed under LDHC cycles.
Normalized relative expression levels of mRNA under light:dark hot:cool cycles are plotted using microarray data available from www.mocklerlab.org. Maximum expression value for each gene was set to 1.0.

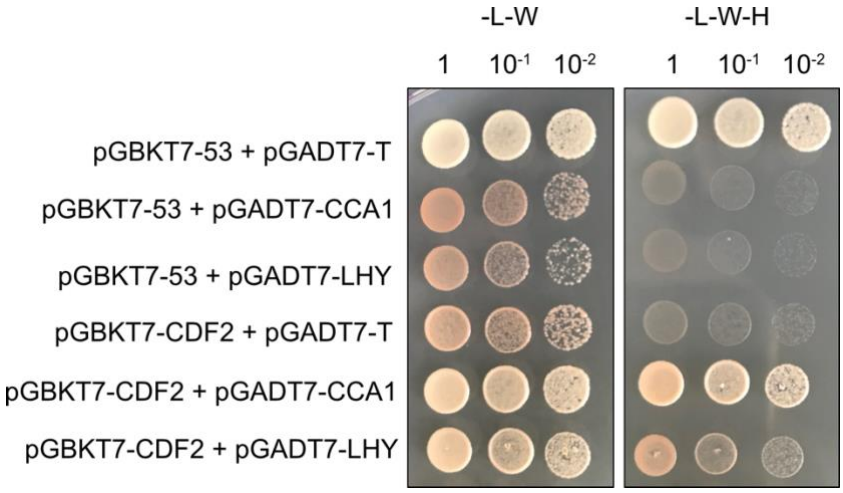

Figure 3.6 CDF2 interacts with CCA1 and LHY in a yeast 2-hybrid system.
Yeast strains Y2H Gold or Y187 expressing pGBKT7 (Gal4-DBD) or pGADT7 (Gal4-AD), respectively, were mated and plated onto selective media. Successful matings can grow on -Leucine/-Tryptophan media (-L-W) while positive interactors can grow on -Leucine/-Tryptophan/-Histidine (-L-W-H). pGBKT7-53 (p53) mated with pGADT7-T (large T-antigen protein) serves as a positive control interaction.

We next explored whether CDF2 influences clock function using a CCA1 promoter-driven luciferase reporter assay. Previous reports have shown that loss-of-function mutations in *cdf1/2/3/5* result in a short period phenotype (Fornara et al., 2015). We did not see a significant effect on CCA1::LUC period length in a *cdf2-1* knock-down mutant, likely due to the redundancy of the CDF family (**Figure 3.7**) (Fornara et al., 2009). We are also interested in looking at whether *CDF2* and *CCA1/LHY* function together in regulation of circadian rhythms by creating a *cdf2-1 cca1-1 lhy-11* CCA1::LUC triple mutant. As higher order *cdf* mutants and the *cca1-1 lhy-11* mutant exhibit short period phenotypes (Mizoguchi et al., 2002; Fornara et al., 2015), we hypothesize that the loss of *CDF2* will exacerbate the short period mutant phenotype of a *cca1-1 lhy-11* mutant. Based on the established role of CDF2 in transcriptional and posttranscriptional regulation of primary miRNAs, we propose that CDF2 could be recruited to CCA1/LHY miRNA target loci to regulate the expression of miRNAs that target genes involved in period length.

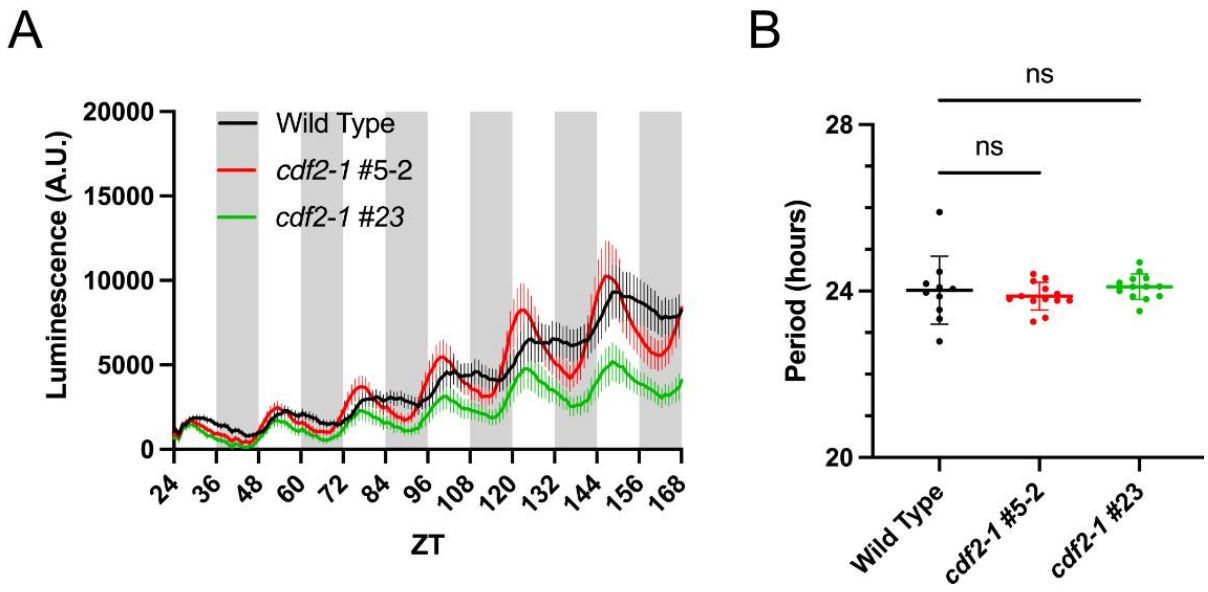

Figure 3.7 Loss-of-function of *CDF2* does not affect circadian period length.
A) Luciferase reporter assay. Plants expressing a CCA1::LUC reporter were grown for 7 days under LDHH conditions before being transferred to constant light (LL). Luminescence from the reporter was measured every hour for several days in LL using a super-cooled CCD camera. Traces are the average of N=16 plants with error bars = SEM. ZT= Zeitgeber Time; time after dawn. B) Period analysis of the traces shown in (A). Circadian period was calculated using Fast Fourier Transform Non-linear Least Squares (FFT-NLLS) analysis in BioDare2 (www.biodare2.ed.ac.uk). Each point represents the period calculated from the rhythms of an individual plant. Crosshair symbol shows the mean period. Asterisks indicate significant differences as determined by Welch ANOVA with multiple comparisons (ns = not significant).

FIO1 coprecipitates with phytochromes. Before our study, there were no confirmed FIO1 interaction partners. We noted that among the proteins coprecipitated with FIO1 were several members of the Phytochrome (Phy) family of light-sensing proteins: PhyC, PhyD, and PhyE (**Table S3.3, Dataset S3.1)**. Phys are red light photoreceptors that play a major role in light-driven development, or photomorphogenesis (Legris et al., 2019). They are also known regulators of light input to the circadian clock (Somers et al., 1998; Yeom et al., 2014). PhyD and PhyE fall into the same class as PhyB, the primary red-light phytochrome that is most well-studied (Legris et al., 2019); surprisingly, phyB was not coprecipitated with FIO1-HFC. The phytochrome-interacting

protein PHOTOPERIODIC CONTROL OF HYPOCOTYL 1 (PCH1) was also coprecipitated with FIO1-HFC, further implicating FIO1 in the Phy network (**Table S3.3, Dataset S3.1)**. Future work should include validation of the FIO1-Phy interactions using a yeast 2-hybrid or other orthologous approach.

An open question is why FIO1, a m6A methyltransferase (Wang et al., 2022; Xu et al., 2022), is interacting with photoreceptors. There is some existing evidence that the Phys regulate mRNA metabolism through interactions with RNA-binding proteins (Paik et al., 2012). Phys are also implicated in alternative splicing (Shikata et al., 2014). Notably, recent work has demonstrated that FIO1 regulates phytochrome-dependent hypocotyl elongation and this function requires an active methylase catalytic domain (Wang et al., 2022). Thus, we hypothesize that FIO1 could be recruited to target mRNAs by PhyC, PhyD, and PhyE—or through a Phy-containing complex—to deposit m6A and thereby regulate gene expression.

JMJD5 coprecipitates with UBP12 and UBP13. Among the most abundant coprecipitated proteins from the JMJD5-HFC APMS were UBIQUITIN-SPECIFIC PROTEASE 12 (UBP12) and UBP13 (**Table S3.4, Dataset S3.1**). These two UBPs have previously been linked to clock function and are known to interact with GI and ZTL (Cui et al., 2013; Lee et al., 2019) and one or both UBPs were also coprecipitated with CCA1-HFC, FIO1-HFC, FLAG-PRR5-GFP and FLAG-PRR7-GFP in this study (**Dataset S3.1**) and with LNK1-HFC, LNK2-HFC, RVE8-HFC and COLD REGULATED PROTEIN 27 (COR27) tagged with YFP in a previous study from our lab (Sorkin et al., 2022). Low

quantities of two other UBPs—UBP11 and UBP17—were also coprecipitated with FLAG-PRR7-GFP (**Dataset S3.1**).

UBP12/13 are predicted to stabilize GI, ZTL, and TOC1 by cleaving polyubiquitin from these proteins (Lee et al., 2019). Perhaps these UBPs are performing a similar function with JMJD5, stabilizing this protein at dusk (tissue was collected for JMJD5p::JMJD5-HFC at ZT12). To test this, we propose to examine JMJD5-HFC levels in wild-type, *ubp12-1,* and *ubp13-1* backgrounds. If UBP12/13 are involved in promoting JMJD5 protein stability, we predict that JMJD5 protein levels will decrease significantly in the *ubp12-1/ubp13-1* mutants. UBP12/13 are bridged to ZTL through GI (Lee et al., 2019). While we did not identify GI in our JMJD5p::JMJD5-HFC APMS, future studies should test whether JMJD5 interacts with GI and if JMJD5 directly interacts with UBP12/13. If not a direct interaction, it would be worth testing whether GI is the bridge protein that allows for UBP12/13 recruitment to JMJD5 (and other clock proteins) to stabilize it. As UBP12/13 were coprecipitated with several of circadian clock proteins in our studies (**Dataset S3.1**) (Sorkin et al., 2022), we think it is possible that these deubiquitylases could target many core clock components and serve as a key posttranslational regulatory mechanism in the clock.

TOC1 interacts with RNA-binding factors. We noticed an enrichment of RNA-binding or RNA-regulating factors in our TOC1-NL-3F10H APMS dataset (**Table 3.1**). The most abundant of these factors was a chloroplast-localized DEAD box RNA helicase, ATRH3, that regulates intron splicing and chloroplast ribosome biogenesis (**Table 3.1**) (Asakura et al., 2012). In a recent pre-print, TOC1 was shown to bind RNA and that this

activity is required for its transcriptional activity (Li et al., 2020). Additionally, a homolog of RH3 in the model fungus *Neurospora crassa* is essential for the formation of the FREQUENCY-WHITE COLLAR (FRQ-WC) complex that composes the core circadian oscillator in this organism (Cheng et al., 2005). The abundance of RNA-binding factors among the proteins coprecipitated with TOC1-NL-3F10H suggests that a role in RNA regulation exists for this core circadian clock protein. Future studies should identify specific RNA targets of TOC1 binding/regulation and examine whether any of the RNA-binding proteins identified here are important for this activity.

Table 3.1 RNA-binding proteins that coprecipitate with TOC1-NL-3F10H.
Values show total spectra identified for the corresponding protein in the given APMS biorep.

Protein Name	Gene Brief Description	AGI Locus Number	TOC1_ZT18_1	TOC1_ZT18_2	TOC1_ZT18_3
TOC1	Timing of CAB expression 1	AT5G61380‡	57	22	58
ATRH3	DEAD box RNA helicase (RH3)	AT5G26742	7	0	5
AT5G55670	RNA-Binding (RRM/RBD/RNP) family protein	AT5G55670	5	1	4
RH40	DEAD box RNA helicase family protein	AT3G06480‡	5	0	2
ATU2AF35A	U2 snRNP auxiliary factor	AT1G27650‡	3	0	0
IRP9	Cleavage/polyadenylation specificity factor	AT4G25550‡	3	1	3
ALBA1	Alba DNA/RNA-binding protein	AT1G76010	3	1	4
AT3G50370	Unknown protein (mRNA binding)	AT3G50370	2	0	1
XRN3	5'-3' EXORIBONUCLEASE 3	AT1G75660‡	2	0	0
RH14	DEAD box RNA helicase family protein	AT3G01540	2	0	0

CPL1	C-terminal domain phosphatase-like 1 (RNA-binding)	AT4G21670‡	2	0	0
SUS2	Pre-mRNA-processing-splicing factor	AT1G80070	1	0	1
RH11	DEA(D/H)-box RNA helicase family protein	AT3G58510‡	1	0	1

‡Indicates mRNA is rhythmic in constant light according to analysis in Romanowski et al. (2020) The Plant Journal.

PRR7 interacts with chromatin remodelers. Among the proteins coprecipitated with FLAG-PRR7-GFP were several factors characterized as being involved in chromatin remodeling (**Table S3.6**), including CHROMATIN REMODELING PROTEIN 2 (CHR2), CHR11, RINGLET 1 (RLT1), RLT2, and SWI/SNF ASSOCIATED PROTEIN 73 (SWP73A). Interestingly, CHR11 and RLT1/RLT2 physically interact and regulate the expression of genes involved in the transition from vegetative to reproductive growth (Li et al., 2012). With our APMS data, we may now propose that PRR7 interacts with this existing CHR-RLT complex, potentially to recruit these proteins to target chromatin. Further supporting a connection between the PRRs and these chromatin remodelers, PRR5 and PRR7 are significantly upregulated in a *rlt1-1 rlt2-1* double mutant microarray dataset (Li et al., 2012).

SWP73A is a chromatin remodeling protein that modulates histone-DNA interactions and DNA accessibility (Jégu et al., 2017). Some SWP73A targets include G-box-containing genes such as the PIFs, allowing SWP73A to regulate light-mediated growth (Jégu et al., 2017). Additionally, the mRNA of this gene is under circadian regulation, showing a similar expression pattern to TOC1/PRR1 (Jégu et al., 2017). In order to locate their target loci, SWI/SNF proteins interact with key transcription

factors/DNA-binding proteins like LEAFY, SEPALLATA3, and BROMODOMAIN-CONTAINING PROTEINS (BRDs) (Wu et al., 2012; Yu et al., 2021). Based on this information, we predict that PRR7 could be recruiting SWP73A to circadian targets to regulate chromatin accessibility at these loci.

It is possible that the other PRRs interact with these chromatin remodelers, but we did not capture those interactions in our APMS. Alternatively, perhaps there is a unique binding site to PRR7 that allows for these remodelers to stick to this PRR. Secondary validation approaches such as yeast 2-hybrid, BiFC, and *in vitro* co-IP can be used to determine which PRRs interact with these chromatin remodelers.

Visualization of interactome data using the STRING Database. To make our interactome data publicly available and easily interpretable, we have uploaded the networks of prioritized interactors for each bait group to the STRING database (www.string-db.org) (**Table 3.2**). STRING is a database of known and predicted protein-protein interactions that pulls data from five main sources: genomic context predictions, high-throughput lab experiments, co-expression, automated textmining, and previous knowledge in other databases, like BioGRID (www.thebiogrid.org). Users can also upload their own datasets to the existing STRING framework, allowing for easy visualization and accessibility of new data. **Figure 3.8** shows the prioritized interactions from our CCA1/LHY APMS experiments in a STRING network. Each “node” is a protein coprecipitated with CCA1/LHY-HFC and connecting “edges” show physical or functional interactions. STRING performs several analyses on a given network; for example, we chose to highlight nodes that fell into the Circadian Rhythm KEGG pathway in red (**Figure**

3.8). Additionally, STRING identified which SMART protein domains were enriched in this network. For our network, we chose to highlight proteins that contained casein kinase II regulatory subunits (blue), WD40 repeats (green), or Ser/Thr protein kinase catalytic domains (yellow) (**Figure 3.8**).

This analysis brought to our attention a potential protein complex containing CCA1, LHY, and three WD domain-containing proteins: LIGHT-REGULATED WD 1 (LWD1), (LWD2), and TOPLESS (TPL). Based on database mining, STRING identified a potential interaction between LWD1, LWD2 and TPL (blue edges), as putative homologs of these proteins are reported to interact in other organisms (**Figure 3.8**). LWD1 and LWD2 are known circadian clock proteins that regulate period length and photoperiodic flowering time (Wu et al., 2008; Wang et al., 2011). Furthermore, LWD1 has previously been linked to CCA1 as a coactivator of its expression in the morning (Wu et al., 2016). TPL is a transcriptional corepressor essential for proper embryogenesis that has many interaction partners (Causier et al., 2012). With our APMS data and the STRING database's predicted interactions, there is now evidence that the putative coactivators LWD1/LWD2 and the corepressor TPL interact with the core clock transcription factors CCA1 and LHY. Future studies should explore whether these coregulators interact with the CCA1/LHY MYB-like transcription factors to modulate their transcriptional activity. STRING networks of the prioritized interactions from FIO1-HFC, JMJD5-HFC, TOC1-NL-3F10H, and FLAG-PRR5/7/9-GFP are shown in **Figures S3.1** through **S3.4.**

In addition to performing enrichment analyses from various other databases (KEGG pathways, SMART protein domains, GO terms), STRING also provides helpful

link out options to TAIR (arabidopsis.org), UniProt (uniprot.org), NCBI (ncbi.nlm.nih.gov), and KEGG (genome.jp/kegg/). Users can also view putative protein crystal structures sourced from SWISS-MODEL (swissmodel.expasy.org), AlphaFold (alphafold.ebi.ac.uk), and others by clicking on a given node.

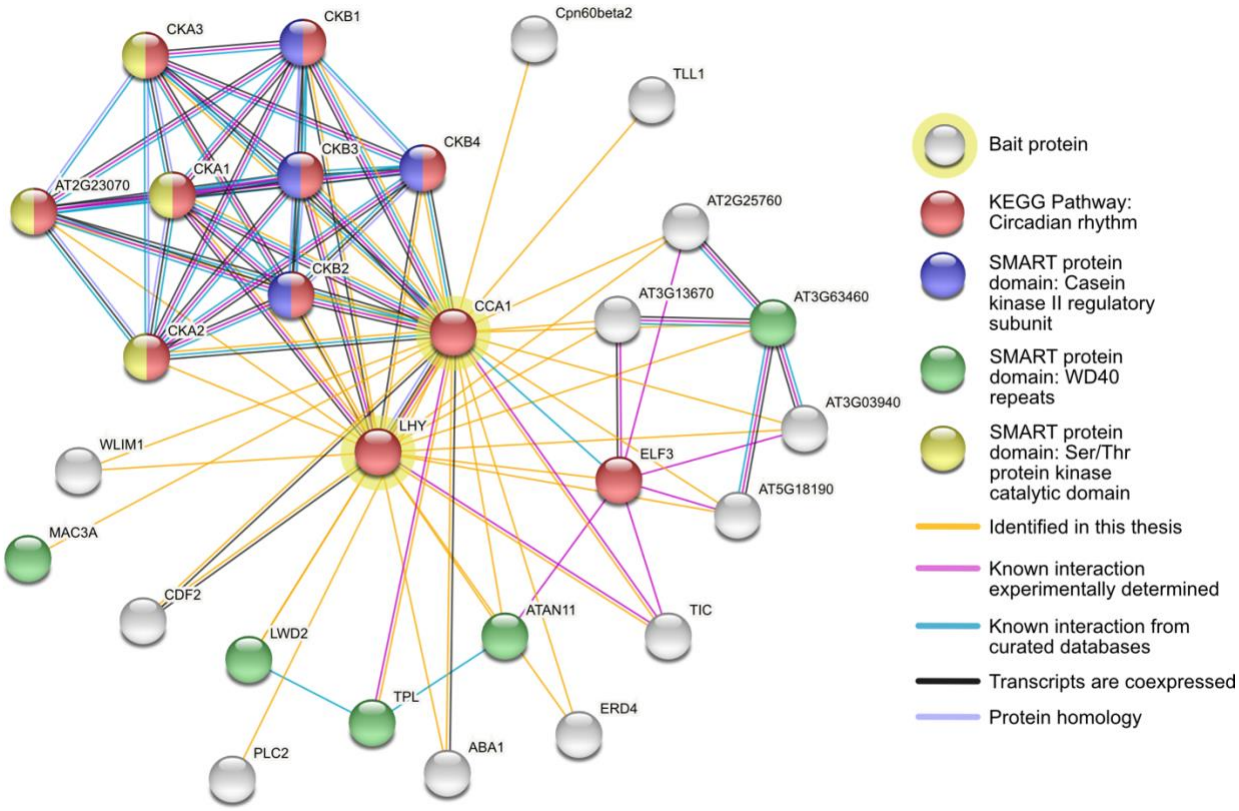

Figure 3.8 CCA1/LHY-HFC interactome visualized as a STRING network.
Prioritized interactions from the CCA1/LHY-HFC APMS experiments are shown here as nodes and edges using the STRING database (www.string-db.org). Nodes have been colored to highlight enriched terms as determined by the built-in analysis tab on STRING.

In conclusion, we have developed plant lines that express functional, affinity-tagged versions of several key circadian clock proteins and have used these transgenic lines to perform APMS and define protein-protein interaction networks for each bait protein. We hope that publishing our datasets publicly on STRING will allow future researchers to easily form or support hypotheses about the Arabidopsis circadian

network. **Table 3.2** provides readers with the unique STRING payload ID for each bait group used in this study and a permalink to a given network.

Table 3.2 STRING payload identifiers and permalinks to STRING networks projecting the prioritized interactions identified in this study.

Bait Group	STRING payload ID	Permalink to network
CCA1/LHY-HFC	b9FikCS0Fxxe	https://version-11-5.string-db.org/cgi/network?networkId=bY0U3G9x4WUm
FIO1-HFC	bS94RJLAsUjv	https://version-11-5.string-db.org/cgi/network?networkId=bPBUVw6rhVU4
JMJD5-HFC	bJn9AcDulUAo	https://version-11-5.string-db.org/cgi/network?networkId=bjxHvrPYf4Q6
TOC1-NL-3F10H	bQb0jQvAuZpQ	https://version-11-5.string-db.org/cgi/network?networkId=buRPgjTuE9cu
FLAG-PRR5/7/9-GFP	bFNTgEBDB0Yf	https://version-11-5.string-db.org/cgi/network?networkId=b5vgFw8u6H2o

3.4 Materials and Methods

Plant materials. The *cca1-1* null allele has been described previously (Green and Tobin, 1999). The *lhy-20* T-DNA mutant (SALK_031092) has been described previously (Michael et al., 2003). The hypomorphic *toc1-2* mutant has been described previously (Strayer et al., 2000). The *PRR5pro::FLAG-PRR5-GFP* in *prr5* (SALK_006280) was described previously and generously shared with us (Nakamichi Lab) (Kiba et al., 2007). The *PRR7pro::FLAG-PRR7-GFP* in *prr7* (SALK030430) and *PRR9pro::FLAG-PRR9-GFP* in *prr9* (SALK_106072) lines were previously characterized and generously shared (Nakamichi Lab) (Nakamichi et al., 2010). The *pB7 CCA1p::CCA1-HFC* in *cca1-1*

CCA1::LUC line was described previously (Kim et al., 2019). The *jmjd5-1 CCR2::LUC* line was described previously and generously shared with us (Harmer Lab) (Jones et al., 2010). The *lhy-20 CCA1::LUC* line was described previously and generously shared with us (José Pruneda-Paz, Kay Lab) (Pruneda-Paz et al., 2009).

Generation of epitope-tagged lines and plasmid construction pENTR-LHY-no stop and pENTR FIO1-no stop were generated by cloning the coding sequence from cDNA without the STOP codon of LHY and FIO1 using primers pDAN1076/1077 and pDAN1068/1069, respectively. The resulting PCR fragments were recombined into NotI/AscI-digested pENTR-MCS through In-Fusion HD cloning (Contech, Mountain View, California). pENTR-JMJD5-no stop was generated by cloning the coding sequence without the STOP codon using primers DN325/326 from cDNA. The resulting PCR fragment was recombined with pENTR-MCS through dTOPO cloning (Contech, Mountain View, California). To generate pB7 35S::LHY-HFC, pB7 35S::FIO1-HFC and pB7 35S::JMJD5-HFC, the pENTR-no stop versions of these genes were recombined using LR cloning (Thermo Fisher Scientific, Waltham, Massachusetts) into pB7-HFC (Huang et al., 2016), which is driven by the 35S Cauliflower Mosaic Virus (CaMV35S) promoter and contains the 6X-HIS 3X-FLAG C-terminal tag. To generate the endogenous promoter-driven lines for LHY and JMJD5, 1,811 bp from the LHY promoter and 2,280 bp from the JMJD5 promoter were cloned using primers pDAN1014/1015 and pDAN1037/1038, respectively. LHY promoter fragment was recombined into PmeI/SpeI-digested pB7 construct by In-Fusion HD cloning to make pB7-LHYp::LHY-HFC. JMJD5 promoter fragment was recombined into PmeI/HindIII-digested pB7 construct by In-Fusion HD cloning to make pB7-JMJD5p::JMJD5-HFC. We switched our JMJD5 construct into a

backbone with hygromycin resistance. To make a hygromycin resistant JMJD5 line, we digested pB7-JMJD5p::JMJD5-HFC and the pH7WG2 backbone (Karimi et al., 2002) with AgeI and KpnI and the resulting fragments were ligated.

pH7-JMJD5p::JMJD5-HFC and pB7-LHYp::LHY-HFC binary vectors were transformed into *jmjd5-1* CCR2::LUC and *lhy-20* CCA1::LUC mutant backgrounds, respectively, by agrobacterium-mediated transformation and positive transformants were selected by hygromycin or basta resistance. pB7-35S::FIO1-HFC was transformed into Col-0 through the same method. Generation of the TOC1p::TOC1-NanoLuc-3x-FLAG-10x-His in *toc1-2* CCA1::LUC (TOC1-NL-3F10H) line was described previously (Urquiza García, 2018).

To generate yeast 2-hybrid vectors, the gene of interest was cloned from its pENTR-STOP template using primers pDAN2349/pDAN2350 (**Table S3.7**) and recombined into pGADT7 digested with EcoRI using In-Fusion HD cloning (Clontech, Mountain View, California). For cloning into pGBKT7, primers pDAN2347/pDAN2348 (**Table S3.7**) were used to clone off the pENTR-STOP template and recombine into BamHI-digested pGBKT7 using In-Fusion HD cloning (Clontech, Mountain View, California).

Luciferase reporter assays. Individual 6-day-old seedlings expressing a CCA1::LUC reporter grown under LD cycles at 22℃ were arrayed on 1/2x MS + 1% Sucrose plates and sprayed with 5mM luciferin (GoldBio, Olivette, MO) prepared in 0.01% (v/v) Triton X-100 (Millipore Sigma-Aldrich, St. Louis, MO). Plants were transferred to an imaging chamber set to the appropriate free-run or entrainment program and images were taken every 60 minutes with an exposure of 10 minutes after a 3-minute delay after lights-

off to diminish signal from delayed fluorescence using a Pixis 1024 CCD camera (Princeton Instruments, Trenton, NJ). Images were processed to measure luminescence from each plant using the Metamorph imaging software (Molecular Devices, Sunnyvale, CA). Circadian period was calculated using fast Fourier transformed nonlinear least squares (FFT-NLLS) (Plautz et al., 1997) using the Biological Rhythms Analysis Software System 3.0 (BRASS) available at http://www.amillar.org or using BioDare 2 (biodare2.ed.ac.uk).

24-hour tissue collection, protein extraction, and Western blotting. Tissue from 10-day-old affinity-tagged plants grown under LD cycles at 22 ℃ was collected every three hours beginning at ZT0. Total protein was extracted from powdered tissue in SII buffer (100 mM sodium phosphate, pH 8.0, 150 mM NaCl, 5 mM EDTA, 5 mM EGTA, 0.1% Triton X-100, 1 mM PMSF, 1x protease inhibitor mixture (Roche, Basel, Switzerland), 1x Phosphatase Inhibitors II & III (Sigma- Aldrich), and 5 µM MG132 (Peptides International, Louisville, KY)) and sonicated using a duty cycle of 20 s (2 s on, 2 s off, total of 40 s) at 50% power. Extracts were clarified of cellular debris through 2x centrifugation for 10 min at ≥20,000 × g at 4 °C. Protein content was determined by DC Assay (Bio-Rad, Carlsbad, CA) and normalized to ~2.0 mg/mL. Extracts were loaded into an 8% acrylamide SDS-PAGE gel and transferred to a nitrocellulose membrane via semi-dry transfer.

FLAG-tagged proteins were detected with anti-FLAG-M2-Peroxidase conjugated antibody (Sigma-Aldrich, St. Louis, MO) diluted 1:10,000 in PBS + 0.1% Tween-20 and incubated at room temperature for 1 hour. RPT5 was detected using anti-RPT5-rabbit (ENZO Life Science, Farmingdale, New York) diluted to 1:5000 in PBS + 0.1% Tween-20

and incubated at room temperature for 1 hour. RPN6 was detected using anti-RPN6-rabbit (Agrisera, Sweden) diluted to 1:10,000 in PBS + 0.1% Tween-20 and incubated at room temperature for 1 hour.

Affinity purification. Affinity purification was performed as detailed in Sorkin and Nusinow (2022). Briefly, affinity-tagged lines were plated on 1/2x MS + 1% Sucrose and grown for 10 days under LD 22 ℃ conditions. On day 10 of growth, tissue was harvested at the time of peak protein abundance. To extract protein, powdered tissue was resuspended in SII buffer (100 mM sodium phosphate, pH 8.0, 150 mM NaCl, 5 mM EDTA, 5 mM EGTA, 0.1% Triton X-100, 1 mM PMSF, 1x protease inhibitor mixture (Roche, Basel, Switzerland), 1x Phosphatase Inhibitors II & III (Sigma- Aldrich), and 5 µM MG132 (Peptides International, Louisville, KY)) and sonicated using a duty cycle of 20 s (2 s on, 2 s off, total of 40 s) at 50% power. Extracts were clarified of cellular debris through 2x centrifugation for 10 min at ≥20,000 × g at 4 °C.

For HFC-tagged samples and TOC1-NL-3F10H, clarified extracts were incubated with FLAG-M2-conjugated Protein G Dynabeads (Thermo Fisher Scientific, Waltham, Massachusetts) for one hour. Captured proteins were eluted off FLAG beads using 500 µg/mL 3x-FLAG peptide (Sigma-Aldrich). Eluted proteins were then incubated with Dynabeads His-Tag Isolation and Pulldown (Thermo Fisher Scientific, Waltham, Massachusetts) for 20 minutes and then washed 5 x 1 minute in His-tag Isolation Buffer (100 mM Na-phosphate, pH 8.0, 150 mM NaCl, 0.025% Triton X-100). Washed bead pellet was washed 4x in 25mM ammonium bicarbonate and flash frozen in liquid N_2.

For FLAG-PRR5/7/9-GFP samples, the same protocol was followed through the FLAG elutions. Instead of continuing to the His-tag isolation, the FLAG eluates were

mixed with the precipitation agent trichloroacetic acid (TCA) (Sigma-Aldrich, St. Louis, MO) to a final volume of ~25% TCA and incubated on ice for 30 minutes and at -20 ℃ for 20 minutes. Precipitated eluates were spun down at max speed for 10 minutes at 4 ℃. Protein pellets were washed twice with ice cold acetone-HCl and then flash frozen in liquid N_2.

LC-MS/MS analysis of AP samples. Samples on affinity beads were resuspended in 50 mM ammonium bicarbonate, reduced (10 mM TCEP) and alkylated (25 mM Iodoacetamide) followed by digestion with Tryspin at 37°C overnight. Digest was separated from beads using a magnetic stand and acidified with 1%TFA before cleaned up with C18 tip (Thermo Fisher Scientific, Waltham, Massachusetts). The extracted peptides were dried down and each sample was resuspended in 10 µL 5% ACN/0.1% FA. 5 µL was analyzed by LC-MS with a Dionex RSLCnano HPLC coupled to a Orbitrap Fusion Lumos mass spectrometer (Thermo Fisher Scientific, Waltham, Massachusetts) using a 2h gradient. Peptides were resolved using 75 µm x 50 cm PepMap C18 column (Thermo Fisher Scientific, Waltham, Massachusetts).

Peptides were eluted at 300 nL/min from a 75 µm x 50 cm PepMap C18 column (Thermo Scientific) using the following gradient: Time = 0–4 min, 2% B isocratic; 4–8 min, 2–10% B; 8–83 min, 10–25% B; 83–97 min, 25–50% B; 97–105 min, 50–98%. Mobile phase consisted of A, 0.1% formic acid; mobile phase B, 0.1% formic acid in acetonitrile. The instrument was operated in the data-dependent acquisition mode in which each MS1 scan was followed by Higher-energy collisional dissociation (HCD) of as many precursor ions in 2 second cycle (Top Speed method). The mass range for the MS1 done using the FTMS was 365 to 1800 m/z with resolving power set to 60,000 @ 400 m/z and the

automatic gain control (AGC) target set to 1,000,000 ions with a maximum fill time of 100 ms. The selected precursors were fragmented in the ion trap using an isolation window of 1.5 m/z, an AGC target value of 10,000 ions, a maximum fill time of 100 ms, a normalized collision energy of 35 and activation time of 30 ms. Dynamic exclusion was performed with a repeat count of 1, exclusion duration of 30 s, and a minimum MS ion count for triggering MS/MS set to 5000 counts.

AP-MS Data Analysis. MS data were converted into mgf. Database searches were done using Mascot (Matrix Science, London, UK; v.2.5.0) using the TAIR10 database (20101214, 35,386 entries) and the cRAP database (http://www.thegpm.org/cRAP/) and assumes the digestion enzyme trypsin and 2 missed cleavages. Mascot was searched with a fragment ion mass tolerance of 0.60 Da and a parent ion tolerance of 10 ppm. Oxidation of methionine and carbamidomethyl of cysteine were specified in Mascot as variable modifications. Scaffold (Proteome Software Inc., Portland, OR; v.4.8) was used to validate MS/MS based peptide and protein identifications. Peptide identifications were accepted if they could be established at greater than 95.0% probability by the Peptide Prophet algorithm (Keller et al., 2002) with Scaffold delta-mass correction. The Scaffold Local FDR was used and only peptides probabilities with FDR <1% were used for further analysis. Protein identifications were accepted if they could be established at greater than 99.9% probability as assigned by the Protein Prophet algorithm (Nesvizhskii et al., 2003). Proteins that contained similar peptides and could not be differentiated based on MS/MS analysis alone were grouped to satisfy the principles of parsimony. Proteins sharing significant peptide evidence were grouped into clusters. Only the proteins identified with $\geq$ 2 spectra were further used in

the analysis, except when proteins with only one peptide were identified in more than one replicate. Proteins with ≥ 2 spectra identified in either the Col-0 no-tag, 35S::GFP-HFC, or 35S::NanoLuc-3F10H negative control APs were excluded from analysis.

Yeast 2-Hybrid (Y2H) Assay. We used the GAL4-based Matchmaker Gold Yeast 2-Hybrid System (Clontech, Mountain View, California) for all Y2H assays. All transformations were performed as detailed in the Yeast Protocols Handbook (Clontech, Mountain View, California). For Y2H, bait proteins were cloned into the pGBKT7 vector which encodes the GAL4 DNA binding domain and then transformed into the Y2H Gold strain (Clontech, Mountain View, California) and plated on SD/-Trp to select for positive transformants. Prey proteins were cloned into the pGADT7 vector which encodes the GAL4 activation domain, transformed into the Y187 strain (Clontech, Mountain View, California), and plated on SD/-Leu to select for positive transformants. All matings were performed as detailed in the Yeast Protocols Handbook (Clontech, Mountain View, California) using the 96-well plate format. Mated diploids were selected for on SD/-Leu/-Trp media. Single colonies of mated bait + prey strains were resuspended in YPDA and plated on SD/-Leu-Trp or SD/-Leu-Trp-His plates.

Uploading payload data to STRING-db. Arabidopsis Genome Initiative (AGI) Locus identifiers of the prioritized interactors from the CCA1/LHY-HFC, FIO1-HFC, JMJD5-HFC, TOC1-NL-3F10H, and FLAG-PRR5/7/9-GFP APMS (**Tables S3.2-3.6)** were input as “nodes” and interactions identified between baits and coprecipitated proteins were input at “edges” with evidence type denoted as “APMS”. We assigned a yellow halo to bait proteins to denote them as such in network diagrams. Only proteins

with 2≥ total spectra associated with them were included in analysis. Payload identifiers and permalinks to STRING networks can be found in **Table 3.2**.

3.5 Relative Contributions and Acknowledgements

MLS generated the HFC-affinity tagged lines with help from Rebecca Bindbeutel, He Huang, and DAN. The FLAG-PRR5/7/9-GFP constructs were previously characterized and generously shared with us by Dr. Norihito Nakamichi. The TOC1p::TOC1-NanoLuc-3F10H line was generated by Uriel Urquiza-García (Andrew Millar Lab) and generously shared with us. Sarah Pardi helped characterize the JMJD5-HFC line. LCMS was performed by Shin-Cheng (Newcity) Tzeng (Evans Lab, PMSF, DDPSC). Mass spectrometry analysis was performed by MLS and Shin-Cheng (Newcity) Tzeng. Dr. Noah Fahlgren helped MLS upload APMS data to the STRING database. MLS would also like to thank the technical support at STRING for helping with payload questions. MLS performed all other experiments and wrote this chapter.

3.6 Supplemental Material

Supplemental Dataset 3.1 Complete APMS dataset for CCA1/LHY-HFC, FIO1-HFC, JMJD5-HFC, TOC1-NL-3F10H, and FLAG-PRR5/7/9-GFP. (This dataset is provided as a separate attachment)

Table S 3.1 Summary of APMS Experiments performed in this study.
(this table is provided in as separate attachment)

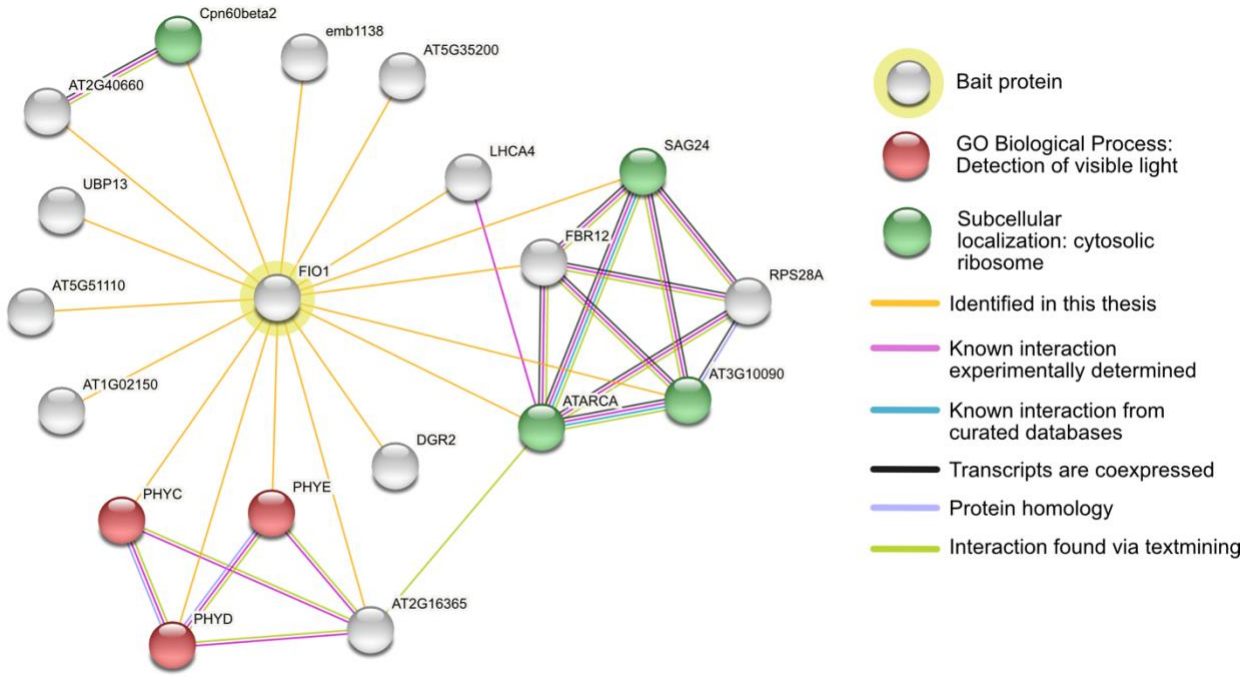

Figure S 3.1 FIO1-HFC interactome visualized as a STRING network.
Prioritized interactions from the FIO1-HFC APMS experiments are shown here as nodes and edges using the STRING database (www.string-db.org). Nodes have been colored to highlight enriched terms as determined by the built-in analysis tab on STRING.

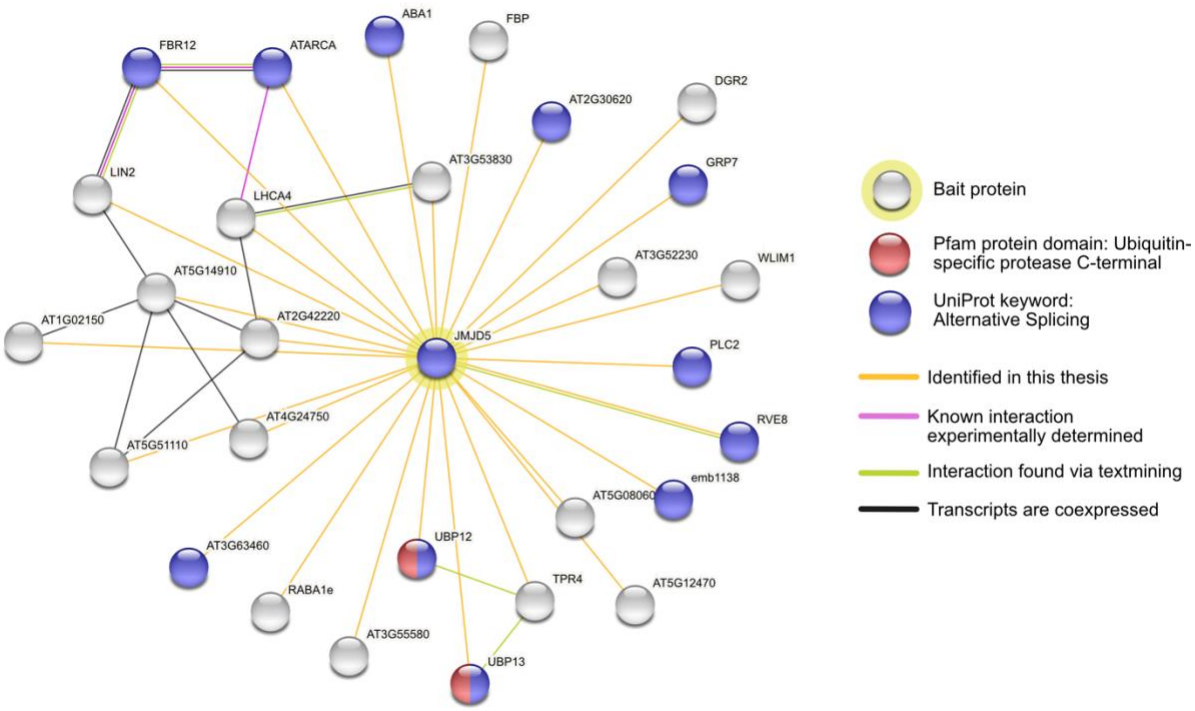

Figure S 3.2 JMJD5-HFC interactome visualized as a STRING network.
Prioritized interactions from the JMJD5-HFC APMS experiments are shown here as nodes and edges using the STRING database (www.string-db.org). Nodes have been colored to highlight enriched terms as determined by the built-in analysis tab on STRING.

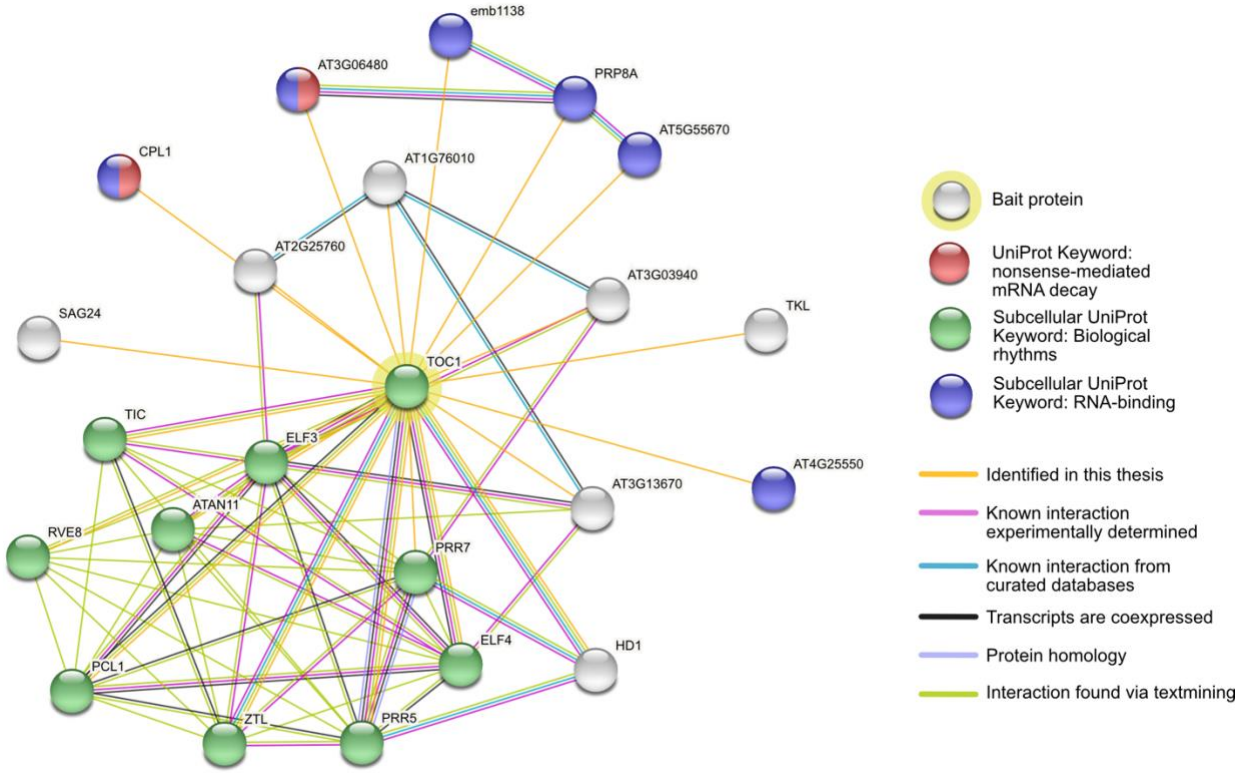

Figure S 3.3 TOC1-HFC interactome visualized as a STRING network.
Prioritized interactions from the TOC1-HFC APMS experiments are shown here as nodes and edges using the STRING database (www.string-db.org). Nodes have been colored to highlight enriched terms as determined by the built-in analysis tab on STRING.

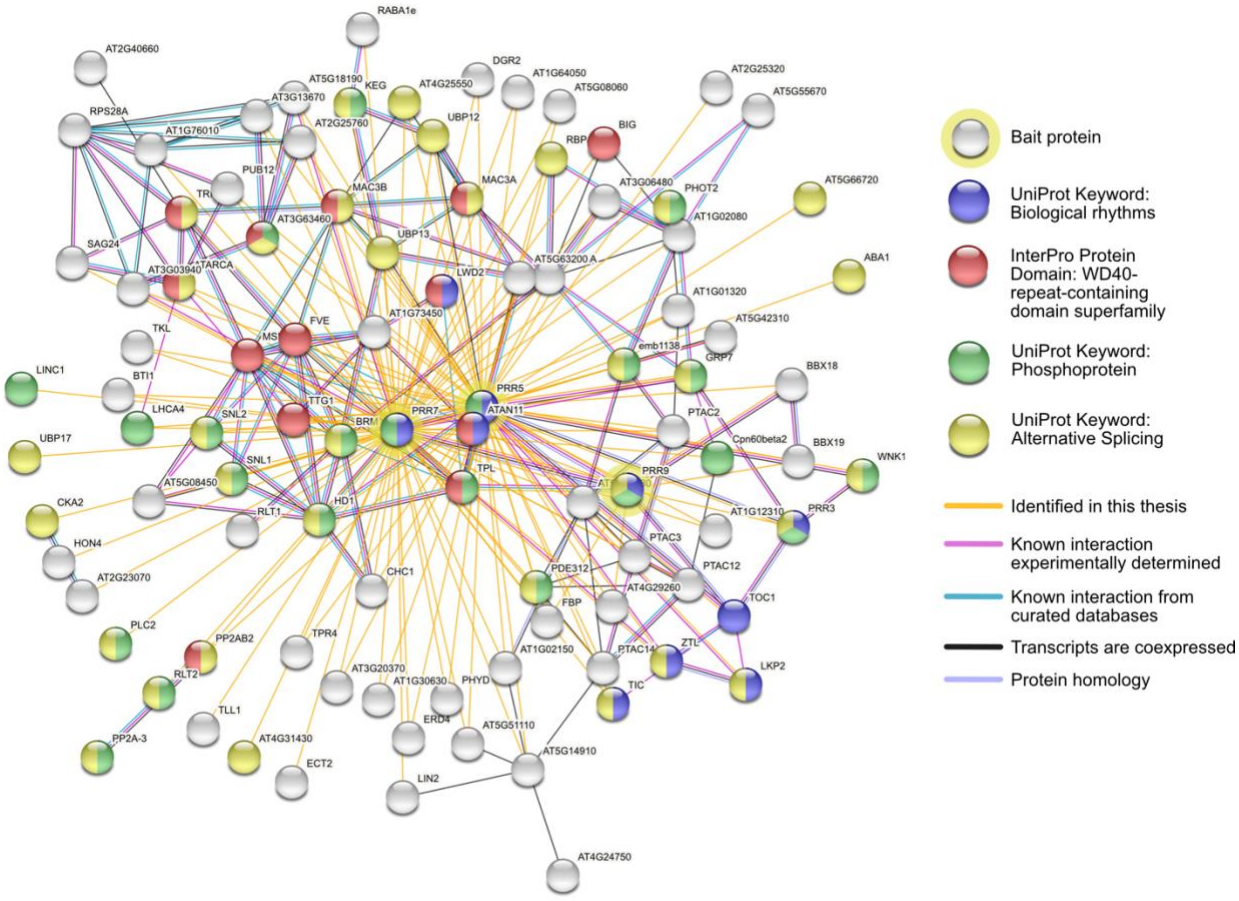

Figure S 3.4 PRR5/7/9-HFC interactome visualized as a STRING network.
Prioritized interactions from the PRR5/7/9-HFC APMS experiments are shown here as nodes and edges using the STRING database (www.string-db.org). Nodes have been colored to highlight enriched terms as determined by the built-in analysis tab on STRING.

Table S 3.2 Prioritized proteins coprecipitated with CCA1/LHY-HFC at ZT0.
Values show total spectra associated with a given interacting protein for a given biological replicate. Only 2 of 3 bioreps are shown.

Protein Name	AGI Locus Number	LHYHFC_ZT0_1	LHYHFC_ZT0_3	CCA1HFC_ZT0_1	CCA1HFC_ZT0_3
LHY	AT1G01060‡	326	300	132	173
CCA1	AT2G46830‡	95	75	425	510
CKA2	AT3G50000‡	83	85	94	102
CKA1	AT5G67380‡	75	70	78	88
CKA4	AT2G23070	71	67	75	85
CKA3	AT2G23080‡	41	42	50	53

CKB3	AT3G60250	23	17	17	22
CKB1	AT5G47080	22	21	18	25
CKB4	AT2G44680	21	17	18	19
CKB2	AT4G17640	15	15	14	19
TIC	AT3G22380	10	23	13	15
CDF2	AT5G39660	7	12	7	6
MLK2	AT3G03940	7	9	11	19
LWD1	AT1G12910‡	6	9	6	6
MLK4	AT3G13670‡	5	9	7	11
MLK1	AT5G18190	5	6	10	9
LWD2	AT3G26640‡	4	0	6	4
SEC31B	AT3G63460	4	0	2	5
ERD4	AT1G30360‡	3	2	7	7
MLK3	AT2G25760	2	3	3	7
ABA1	AT5G67030‡	1	1	2	4
WLIM1	AT1G10200‡	1	1	3	1
ELF3	AT2G25930‡	1	1	0	0
WSIP1	AT1G15750	1	0	5	2
CCR2	AT2G21660‡	1	0	0	1
PLC2	AT3G08510	0	0	2	2
MAC3A	AT1G04510‡	0	0	1	1
CPNB2	AT3G13470‡	0	0	15	0

‡Indicates mRNA is rhythmic in constant light according to analysis in Romanowski et al. (2020) The Plant Journal.

Table S 3.3 Prioritized proteins coprecipitated with FIO1-HFC at ZT5
Values show total spectra associated with a given interacting protein for a given biological replicate. 3 of 3 bioreps are shown.

Protein Name	AGI Locus Number	FIO1HFC_ZT5_1	FIO1HFC_ZT5_2	FIO1HFC_ZT5_3
FIO1	AT2G21070	252	268	101
PHYD	AT4G16250	13	1	0
ATRH3	AT5G26742	5	3	0
PHYE	AT4G18130‡	3	1	0
PHYC	AT5G35840	3	0	0
ENTH/ANTH/VHS superfamily protein	AT5G35200‡	2	4	1
ELF5A-2	AT1G26630‡	2	2	0

Protein of unknown function	AT5G25460‡	2	2	0
Nucleic acid-binding, OB-fold-like protein	AT2G40660‡	2	1	0
PCH1	AT2G16365	2	0	0
RAF2	AT5G51110‡	2	0	0
RACK1A	AT1G18080‡	1	2	0
CAB4	AT3G47470‡	1	2	0
Nucleic acid-binding, OB-fold-like protein	AT3G10090	1	1	0
UBP13	AT3G11910	1	1	0
CPNB2	AT3G13470‡	0	3	0
CCR16	AT1G02150‡	0	2	0
SAG24	AT1G66580‡	0	0	3

‡Indicates mRNA is rhythmic in constant light according to analysis in Romanowski et al. (2020) *The Plant Journal*

Table S 3.4 Prioritized proteins coprecipitated with JMJD5-HFC at ZT12.
Values show total spectra associated with a given interacting protein for a given biological replicate. 3 of 3 bioreps are shown.

Protein Name	AGI Locus Number	JMJD5HFC_ZT12_1	JMJD5HFC_ZT12_2	JMJD5HFC_ZT12_3
JMJD5	AT3G20810‡	343	420	449
UBP13	AT3G11910	38	47	42
UBP12	AT5G06600	29	35	33
TCF1	AT3G55580‡	25	24	23
RCC1L	AT3G53830‡	8	10	7
DGR2	AT5G25460‡	4	6	3
ABA1	AT5G67030‡	4	3	4
FINS1	AT1G43670‡	2	3	2
WLIM1	AT1G10200‡	2	2	2
CCR16	AT1G02150‡	1	2	3
RACK1A	AT1G18080‡	1	1	2
CCR2	AT2G21660‡	1	1	1
CAB4	AT3G47470‡	1	1	3

unknown protein	AT3G52230‡	1	1	2
FURRY	AT5G08060	1	1	0
RAF2	AT5G51110‡	1	1	2
TPR4	AT1G04530‡	0	1	2
HON2	AT2G30620‡	4	0	0
Heavy metal transport/detoxification superfamily protein	AT5G14910‡	1	0	2
Rhodanese/Cell cycle control phosphatase superfamily protein	AT2G42220‡	0	0	2
PLC2	AT3G08510	0	0	2
Rhodanese/Cell cycle control phosphatase superfamily protein	AT4G24750‡	0	0	2
RER4	AT5G12470‡	0	0	4

‡Indicates mRNA is rhythmic in constant light according to analysis in Romanowski et al. (2020) The Plant Journal

Table S 3.5 Prioritized proteins coprecipitated with TOC1-NL-3F10H at ZT18.
Values show total spectra associated with a given interacting protein for a given biological replicate. 3 of 3 bioreps are shown.

Protein Name	AGI Locus Number	TOC1_ZT18_1	TOC1_ZT18_2	TOC1_ZT18_3
TOC1	AT5G61380‡	57	22	58
TIC	AT3G22380	25	1	18
ELF3	AT2G25930‡	21	2	17
PRR7	AT5G02810‡	19	1	10
SAG24	AT1G66580‡	8	2	4
ATRH3	AT5G26742	7	0	5
LUX	AT3G46640	6	1	6
RNA-binding (RRM/RBD/RNP	AT5G55670	5	1	4

motifs) family protein				
MLK2	AT3G03940	5	0	4
RH40	AT3G06480‡	5	0	2
ZTL	AT5G57360	4	1	4
PRR5	AT5G24470‡	4	0	3
MLK3	AT2G25760	4	0	0
ALBA1	AT1G76010	3	1	4
IRP9	AT4G25550‡	3	1	3
LWD1	AT1G12910‡	3	0	3
MLK4	AT3G13670‡	3	0	0
ELF4	AT2G40080‡	2	0	2
HD1	AT4G38130	2	0	1
CPL1	AT4G21670‡	2	0	0
SUS2	AT1G80070	1	0	1
TKL	AT3G63180	1	0	1
RVE8	AT3G09600‡	0	1	1

‡Indicates mRNA is rhythmic in constant light according to analysis in Romanowski et al. (2020) *The Plant Journal*

Table S 3.6 Prioritized proteins coprecipitated with FLAG-PRR5/7/9-GFP at ZT8/6/4.
Values show total spectra associated with a given interacting protein for a given biological replicate. 2 of 3 bioreps are shown for each line.

Protein Name	AGI Locus Number	PRR5_ZT8_1	PRR5_ZT8_3	PRR7_ZT6_2	PRR7_ZT6_3	PRR9_ZT4_1	PRR9_ZT4_2
PRR5	AT5G24470‡	427	351	18	11	2	2
TIC1	AT3G22380	48	59	131	75	0	0
LWD1	AT1G12910‡	37	33	45	40	3	1
PRR7	AT5G02810‡	29	38	387	270	8	11
MLK2	AT3G03940	26	29	38	32	0	0
LWD2	AT3G26640‡	25	16	21	22	0	0
PRR9	AT2G46790‡	22	27	18	11	180	96
MLK4	AT3G13670‡	21	22	32	24	0	0
MLK1	AT5G18190	18	12	21	16	0	0
ZTL	AT5G57360	17	10	4	1	0	0

ATRH3	AT5G26742	17	5	26	26	0	0
TTG1	AT5G24520	14	15	36	21	1	0
MLK3	AT2G25760	13	17	22	15	0	0
TPL	AT1G15750	12	9	2	3	4	2
LKP2	AT2G18915	12	7	0	0	0	0
TOC1	AT5G61380‡	10	10	0	0	0	0
PRR3	AT5G60100	10	5	1	0	2	0
UBP13	AT3G11910	10	4	23	18	0	0
UBP12	AT5G06600	10	4	23	13	0	0
VSP3	AT4G29260	8	5	3	2	11	1
SNL2	AT5G15020	8	3	10	4	0	0
TRAF-like family protein	AT2G25320	8	1	0	0	0	0
SUS2	AT1G80070	8	0	18	19	0	0
Heavy metal transport/detoxification superfamily protein	AT5G14910‡	6	6	6	4	1	0
TKL	AT3G63180	5	8	18	9	0	0
MAC3B	AT2G33340	5	1	7	4	0	0
FLL2	AT1G01320‡	5	1	7	1	0	0
FINS1	AT1G43670‡	5	1	4	7	3	0
tetratricopeptide repeat (TPR)-containing protein	AT5G63200	5	0	7	4	0	0
PTAC2	AT1G74850	5	0	4	6	0	0
DGR2	AT5G25460‡	4	1	4	3	1	0
CAB4	AT3G47470‡	4	0	4	3	0	1
CCR16	AT1G02150‡	4	0	2	1	0	0
unknown protein	AT1G64050‡	3	3	11	6	0	0
HD1	AT4G38130	3	3	3	3	0	0
PP2A-3	AT2G42500	3	2	3	1	0	0
BBX19	AT4G38960‡	3	2	1	0	7	2
IRP9	AT4G25550‡	3	1	1	1	0	0
ERD4	AT1G30360‡	3	0	11	13	0	0
SEC31B	AT3G63460	3	0	4	2	0	0
SNL1	AT3G01320	3	0	3	1	0	0

ATB BETA	AT1G17720‡	3	0	2	2	0	0
MAC3A	AT1G04510‡	3	0	2	1	0	0
FURRY	AT5G08060	3	0	2	0	0	0
PHYD	AT4G16250	3	0	0	2	0	0
BBX18	AT2G21320‡	2	3	1	0	2	4
TRAF-like family protein	AT3G20370‡	2	2	4	5	1	0
Nucleic acid-binding, OB-fold-like protein	AT3G10090	2	2	4	2	2	0
PUB12	AT2G28830‡	2	2	3	3	1	0
PTAC14	AT4G20130‡	2	1	1	2	0	0
PTAC3	AT3G04260‡	2	0	6	3	0	0
PTAC10	AT3G48500	2	0	5	1	0	0
EPSILON1-COP	AT1G30630	2	0	4	3	0	0
TPR4	AT1G04530‡	2	0	4	2	0	0
BTI1	AT4G23630‡	2	0	4	1	0	0
RACK1A	AT1G18080‡	2	0	3	3	1	0
RH40	AT3G06480‡	2	0	3	0	0	0
CCR2	AT2G21660‡	2	0	2	3	0	0
RBP45B	AT1G11650‡	2	0	2	1	0	0
RAF2	AT5G51110‡	2	0	1	2	1	0
ABA1	AT5G67030‡	2	0	0	1	0	0
WNK1	AT3G04910‡	2	0	0	0	0	0
Protein phosphatase 2C family protein	AT5G66720	2	0	0	0	0	0
CHC1	AT5G14170‡	2	0	4	0	0	0
MSI1	AT5G58230	1	3	4	2	0	0
Calcium-binding EF-hand family protein	AT1G12310	1	2	8	9	0	0
BIG	AT3G02260	1	0	5	2	0	0
TRIP-1	AT2G46280	1	0	4	1	0	0
NOT1	AT1G02080	1	0	2	2	0	0
RNA-binding (RRM/RBD/R	AT5G55670	1	0	1	0	0	0

NP motifs) family protein							
Rhodanese/Cell cycle control phosphatase superfamily protein	AT4G24750‡	1	0	0	1	0	0
Nucleic acid-binding, OB-fold-like protein	AT2G40660‡	1	0	0	0	1	0
SAG24	AT1G66580‡	0	7	26	23	0	0
CPNB2	AT3G13470‡	0	5	35	25	0	0
HON4	AT3G18035	0	0	8	14	0	0
ALBA1	AT1G76010	0	0	4	3	0	0
CKA4	AT2G23070	0	0	4	3	0	0
KAKU4	AT4G31430	0	0	4	1	0	0
KEG	AT5G13530	0	0	3	3	0	0
CRP1	AT5G42310‡	0	0	3	2	0	0
CKA2	AT3G50000‡	0	0	3	1	0	0
RLT1	AT1G28420	0	0	3	0	0	0
RLT2	AT5G44180	0	0	2	3	0	0
FVE	AT2G19520	0	0	2	1	0	0
HMR	AT2G34640‡	0	0	2	1	0	0
PLC2	AT3G08510	0	0	2	1	0	0
ECT2	AT3G13460	0	0	2	1	0	0
HDC1	AT5G08450	0	0	2	1	0	0
PHOT2	AT5G58140	0	0	2	1	0	0
LNK2	AT1G03475	0	0	2	0	0	0
LINC1	AT1G67230	0	0	2	0	0	0
DYRKP-2B	AT1G73450‡	0	0	2	0	0	0
TLL1	AT1G45201‡	0	0	1	1	0	0
CHR2	AT2G46020	0	0	1	1	0	0
RABA1e	AT4G18430	0	0	1	1	0	0
SOT1	AT5G46580‡	0	0	0	2	0	0

‡Indicates mRNA is rhythmic in constant light according to analysis in Romanowski et al. (2020) *The Plant Journal*

Table S 3.7 Primers used in this study.

Primer Name	Sequence (5' -> 3')	Template	Purpose
pDAN2349	GGAGGCCAGTGAATTAGGCTCC GCGGCCGCC	pENTR-STOP clones	In-Fusion HD cloning for entry into pGADT7 digested with EcoRI
pDAN2350	CACCCGGGTGGAATTAGCTGGG TCGGCGCGCCC	pENTR-STOP clones	In-Fusion HD cloning for entry into pGADT7 digested with EcoRI
pDAN2347	GAATTCCCGGGGATCGCAGGCT CCGCGGCCGCC	pENTR-STOP clones	In-Fusion HD cloning for entry into pGBKT7 digested with BamHI
pDAN2348	GCAGGTCGACGGATCAGCTGGG TCGGCGCGCCC	pENTR-STOP clones	In-Fusion HD cloning for entry into pGBKT7 digested with BamHI
pDAN1068	GCAGGCTCCGCGGCCGCCCCCT TCACCATGCGGAGTGGGAAGAA GAGAGCTCG	cDNA	Forward primer for FIONA1 (AT2G21070.1) cloning for In-Fusion HD into pENTR-MCS
pDAN1069	AGCTGGGTCGGCGCGCCCACCC TTCCGGCAAAATTTGGACTTCAA AC	cDNA	Reverse primer for FIONA1-NO STOP (AT2G21070.1) cloning for In-Fusion HD into pENTR-MCS
pDAN1076	GCAGGCTCCGCGGCCGCCCCCT TCACCATGGATACTAATACATCT GG	cDNA	Forward primer for LHY cloning for In-Fusion HD into pENTR-MCS
pDAN1077	AGCTGGGTCGGCGCGCCCACCC TTTGTAGAAGCTTCTCCTTCCAAT C	cDNA	Reverse primer for LHY-NO STOP cloning for In-Fusion HD into pENTR-MCS
DN325	CACCATGTCAGGAGCTACCACCG CTT	cDNA	Forward primer for JMJD5 cloning for dTOPO cloning
DN326	CGAGCTAGAAGATTCTGCTTCA	cDNA	Reverse primer for JMJD5-NO STOP cloning for dTOPO cloning
pDAN1014	TCAAACACTGATAGTTTCAAATAA CTGTTATGTCCTAG	Genomic DNA	LHY promoter cloning, forward
pDAN1015	AAACTTGTGATATCACTAGAACA GGACCGGTGCAGCTA	Genomic DNA	LHY promoter cloning, reverse
pDAN1037	TCAAACACTGATAGTTTATAGATG GCGATTACGCCCC	Genomic DNA	JMJD5 promoter cloning, forward
pDAN1038	CACCTTTGAAATCTCCAGAAGCT	Genomic DNA	JMJD5 promoter cloning, reverse

3.7 References

Alabadí D, Oyama T, Yanovsky MJ, Harmon FG, Más P, Kay SA (2001) Reciprocal Regulation Between TOC1 and LHY / CCA1 Within the Arabidopsis Circadian Clock. Science (80-) **293**: 880–883

Andronis C, Barak S, Knowles SM, Sugano S, Tobin EM (2008) The clock protein CCA1 and the bZIP transcription factor HY5 physically interact to regulate gene expression in Arabidopsis. Mol Plant **1**: 58–67

Asakura Y, Galarneau E, Watkins KP, Barkan A, van Wijk KJ (2012) Chloroplast RH3 DEAD box RNA helicases in maize and Arabidopsis function in splicing of specific group II introns and affect chloroplast ribosome biogenesis. Plant Physiol **159**: 961–974

Baudry A, Ito S, Song YH, Strait AA, Kiba T, Lu S, Henriques R, Pruneda-Paz JL, Chua NH, Tobin EM, et al (2010) F-Box Proteins FKF1 and LKP2 Act in Concert with ZEITLUPE to Control Arabidopsis Clock Progression. Plant Cell **22**: 606–622

Causier B, Ashworth M, Guo W, Davies B (2012) The TOPLESS interactome: A framework for gene repression in Arabidopsis. Plant Physiol **158**: 423–438

Cheng P, He Q, He Q, Wang L, Liu Y (2005) Regulation of the Neurospora circadian clock by an RNA helicase. Genes Dev **19**: 234

Chow BBY, Helfer A, Nusinow D a., Kay S a. (2012) ELF3 recruitment to the PRR9 promoter requires other Evening Complex members in the Arabidopsis circadian clock. Plant Signal Behav **7**: 170–173

Cui X, Lu F, Li Y, Xue Y, Kang Y, Zhang S, Qiu Q, Zheng XC, Cui X, Zheng S, et al (2013) Ubiquitin-specific proteases UBP12 and UBP13 act in circadian clock and photoperiodic flowering regulation in Arabidopsis. Plant Physiol **162**: 897–906

Daniel X, Sugano S, Tobin EM (2004) CK2 phosphorylation of CCA1 is necessary for its circadian oscillator function in Arabidopsis. Proc Natl Acad Sci U S A **101**: 3292–3297

Doyle MR, Davis SJ, Bastow RM, McWatters HG, Kozma-Bognár L, Nagy F, Millar AJ (2002) The ELF4 gene controls circadian rhythms and flowering time in Arabidopsis thaliana. Nature **419**: 74–77

Farré EM, Harmer SL, Harmon FG, Yanovsky MJ, Kay SA (2005) Overlapping and Distinct Roles of PRR7 and PRR9 in the Arabidopsis Circadian Clock. Curr Biol **15**: 47–54

Fornara F, De Montaigu A, Sánchez-Villarreal A, Takahashi Y, Ver Loren Van Themaat E, Huettel B, Davis SJ, Coupland G (2015) The GI-CDF module of Arabidopsis affects freezing tolerance and growth as well as flowering. Plant J **81**: 695–706

Fornara F, Panigrahi KCS, Gissot L, Sauerbrunn N, Rühl M, Jarillo JA, Coupland G (2009) Arabidopsis DOF transcription factors act redundantly to reduce CONSTANS expression and are essential for a photoperiodic flowering response. Dev Cell **17**: 75–86

Fujiwara S, Wang L, Han L, Suh SS, Salomé PA, McClung CR, Somers DE (2008)

Post-translational regulation of the Arabidopsis circadian clock through selective proteolysis and phosphorylation of pseudo-response regulator proteins. J Biol Chem **283**: 23073–23083

Gan ES, Xu Y, Wong JY, Geraldine Goh J, Sun B, Wee WY, Huang J, Ito T (2014) Jumonji demethylases moderate precocious flowering at elevated temperature via regulation of FLC in Arabidopsis. Nat Commun. doi: 10.1038/ncomms6098

Green RM, Tobin EM (1999) Loss of the circadian clock-associated protein 1 in Arabidopsis results in altered clock-regulated gene expression. Proc Natl Acad Sci U S A **96**: 4176–9

Huang H, Alvarez S, Bindbeutel R, Shen Z, Naldrett MJ, Evans BS, Briggs SP, Hicks LM, Kay SA, Nusinow DA, et al (2016) Identification of Evening Complex Associated Proteins in Arabidopsis by Affinity Purification and Mass Spectrometry. Mol Cell Proteomics **15**: 201–217

Huang W, Pérez-García P, Pokhilko A, Millar AJ, Antoshechkin I, Riechmann JL, Mas P (2012) Mapping the core of the Arabidopsis circadian clock defines the network structure of the oscillator. Science (80-) **335**: 75–79

Huang X, Zhang S, Qi H, Wang Z, Chen HW, Shao J, Shen J (2015) JMJD5 interacts with p53 and negatively regulates p53 function in control of cell cycle and proliferation. Biochim Biophys Acta **1853**: 2286–2295

Ito S, Matsushika A, Yamada H, Sato S, Kato T, Tabata S, Yamashino T, Mizuno T (2003) Characterization of the APRR9 Pseudo-Response Regulator Belonging to the APRR1/TOC1 Quintet in Arabidopsis thaliana. Plant Cell Physiol **44**: 1237–1245

Ito S, Niwa Y, Nakamichi N, Kawamura H, Yamashino T, Mizuno T (2008) Insight into missing genetic links between two evening-expressed pseudo-response regulator genes TOC1 and PRR5 in the circadian clock-controlled circuitry in Arabidopsis thaliana. Plant Cell Physiol **49**: 201–213

Jégu T, Veluchamy A, Ramirez-Prado JS, Rizzi-Paillet C, Perez M, Lhomme A, Latrasse D, Coleno E, Vicaire S, Legras S, et al (2017) The Arabidopsis SWI/SNF protein BAF60 mediates seedling growth control by modulating DNA accessibility. Genome Biol **18**: 1–16

Jones MA, Covington MF, DiTacchio L, Vollmers C, Panda S, Harmer SL (2010) Jumonji domain protein JMJD5 functions in both the plant and human circadian systems. Proc Natl Acad Sci U S A **107**: 21623–21628

Jones MA, Morohashi K, Grotewold E, Harmer SL (2019) Arabidopsis JMJD5 / JMJ30 Acts Independently of LUX ARRHYTHMO Within the Plant Circadian Clock to Enable Temperature Compensation. **10**: 1–12

Karimi M, Inzé D, Depicker A (2002) GATEWAY™ vectors for Agrobacterium-mediated plant transformation. Trends Plant Sci **7**: 193–195

Keller A, Nesvizhskii AI, Kolker E, Aebersold R (2002) Empirical statistical model to estimate the accuracy of peptide identifications made by MS/MS and database search. Anal Chem **74**: 5383–5392

Kenigsbuch D, Tobin EM (1995) A region of the arabidopsis Lhcb1*3 promoter that binds to CA-1 activity is essential for high expression and phytochrome regulation. Plant Physiol **108**: 1023–1027

Kiba T, Henriques R, Sakakibara H, Chua NH (2007) Targeted Degradation of PSEUDO-RESPONSE REGULATOR5 by an SCFZTL Complex Regulates Clock Function and Photomorphogenesis in Arabidopsis thaliana. Plant Cell **19**: 2516–2530

Kim J, Kim Y, Yeom M, Kim JH, Nam HG (2008) FIONA1 is essential for regulating period length in the Arabidopsis circadian clock. Plant Cell **20**: 307–319

Kim JY, Song HR, Taylor BL, Carre IA (2003) Light-regulated translation mediates gated induction of the Arabidopsis clock protein LHY. EMBO J **22**: 935–944

Kim SC, Nusinow DA, Sorkin ML, Pruneda-Paz J, Wanga X (2019) Interaction and Regulation Between Lipid Mediator Phosphatidic Acid and Circadian Clock Regulators. Plant Cell **31**: 399–416

Krahmer J, Goralogia GS, Kubota A, Zardilis A, Johnson RS, Song YH, MacCoss MJ, LeBihan T, Halliday KJ, Imaizumi T, et al (2018) Time-resolved Interaction Proteomics of the GIGANTEA Protein Under Diurnal Cycles in Arabidopsis. FEBS Lett 1873-3468.13311

Lau OS, Huang X, Charron J-B, Lee J-H, Li G, Deng XW (2011) Interaction of Arabidopsis DET1 with CCA1 and LHY in mediating transcriptional repression in the plant circadian clock. Mol Cell **43**: 703–712

Lee CM, Li MW, Feke A, Liu W, Saffer AM, Gendron JM (2019) GIGANTEA recruits the UBP12 and UBP13 deubiquitylases to regulate accumulation of the ZTL photoreceptor complex. Nat Commun. doi: 10.1038/s41467-019-11769-7

Legris M, Ince YÇ, Fankhauser C (2019) Molecular mechanisms underlying phytochrome-controlled morphogenesis in plants. Nat Commun. doi: 10.1038/s41467-019-13045-0

Li G, Siddiqui H, Teng Y, Lin R, Wan XY, Li J, Lau OS, Ouyang X, Dai M, Wan J, et al (2011) Coordinated transcriptional regulation underlying the circadian clock in Arabidopsis. Nat Cell Biol **13**: 616–622

Li G, Zhang J, Li J, Yang Z, Huang H, Xu L (2012) Imitation Switch chromatin remodeling factors and their interacting RINGLET proteins act together in controlling the plant vegetative phase in Arabidopsis. Plant J **72**: 261–270

Li Y, Chang Y-G, Nagel DH, Chen T, Rugnone ML, Liwang A, Kay SA (2020) A Novel Regulatory Role for the Circadian Clock Protein TOC1 via RNA binding. bioRxiv. doi: 10.1101/2020.05.06.071340

Lu SX, Knowles SM, Andronis C, Ong MS, Tobin EM (2009) CIRCADIAN CLOCK ASSOCIATED1 and LATE ELONGATED HYPOCOTYL Function Synergistically in the Circadian Clock of Arabidopsis. Plant Physiol **150**: 834–843

Lu SX, Knowles SM, Webb CJ, Celaya RB, Cha C, Siu JP, Tobin EM (2011) The Jumonji C Domain-Containing Protein JMJ30 Regulates Period Length in the

Arabidopsis Circadian Clock. Plant Physiol **155**: 906

Más P, Kim W-Y, Somers DE, Kay SA (2003) Targeted degradation of TOC1 by ZTL modulates circadian function in Arabidopsis thaliana. Nature **426**: 567–570

Matsushika A, Makino S, Kojima M, Mizuno T (2000) Circadian waves of expression of the APRR1/TOC1 family of pseudo-response regulators in Arabidopsis thaliana: Insight into the plant circadian clock. Plant Cell Physiol **41**: 1002–1012

Mendel M, Chen KM, Homolka D, Gos P, Pandey RR, McCarthy AA, Pillai RS (2018) Methylation of Structured RNA by the m6A Writer METTL16 Is Essential for Mouse Embryonic Development. Mol Cell **71**: 986-1000.e11

Michael TP, Salome PA, Yu HJ, Spencer TR, Sharp EL, McPeek MA, Alonso JM, Ecker JR, McClung CR (2003) Enhanced Fitness Conferred by Naturally Occurring Variation in the Circadian Clock. Science (80-) **302**: 1049–1053

Millar AJ, Straume M, Chory J, Chua N, Kay SA (1995) The Regulation of Circadian Period by Phototransduction Pathways in Arabidopsis. Science **267**: 1163–1166

Mizoguchi T, Wheatley K, Hanzawa Y, Wright L, Mizoguchi M, Song H, Carre IA, Coupland G, Weg CVL (2002) LHY and CCA1 Are Partially Redundant Genes Required to Maintain Circadian Rhythms in Arabidopsis. Dev Cell **2**: 629–641

Murakami-Kojima M, Nakamichi N, Yamashino T, Mizuno T (2002) The APRR3 Component of the Clock-Associated APRR1/TOC1 Quintet is Phosphorylated by a Novel Protein Kinase Belonging to the WNK Family, the Gene for which is also Transcribed Rhythmically in Arabidopsis thaliana. Plant Cell Physiol **43**: 675–683

Nagel DH, Doherty CJ, Pruneda-Paz JL, Schmitz RJ, Ecker JR, Kay SA (2015) Genome-wide identification of CCA1 targets uncovers an expanded clock network in Arabidopsis. Proc Natl Acad Sci 4802–4810

Nakamichi N, Kiba T, Henriques R, Mizuno T, Chua N-H, Sakakibara H (2010) PSEUDO-RESPONSE REGULATORS 9, 7, and 5 Are Transcriptional Repressors in the Arabidopsis Circadian Clock. Plant Cell **22**: 594–605

Nakamichi N, Kita M, Ito S, Yamashino T, Mizuno T (2005) PSEUDO-RESPONSE REGULATORS, PRR9, PRR7 and PRR5, Together play essential roles close to the circadian clock of Arabidopsis thaliana. Plant Cell Physiol **46**: 686–698

Nakamichi N, Murakami-Kojima M, Sato E, Kishi Y, Yamashino T, Mizuno T (2002) Compilation and characterization of a novel wnk family of protein kinases in arabiodpsis thaliana with reference to circadian rhythms. Biosci Biotechnol Biochem **66**: 2429–2436

Nesvizhskii AI, Keller A, Kolker E, Aebersold R (2003) A statistical model for identifying proteins by tandem mass spectrometry. Anal Chem **75**: 4646–4658

Nusinow DA, Helfer A, Hamilton EE, King JJ, Imaizumi T, Schultz TF, Farré EM, Kay SA (2011) The ELF4–ELF3–LUX complex links the circadian clock to diurnal control of hypocotyl growth. Nature **475**: 398–402

Paik I, Yang S, Choi G (2012) Phytochrome regulates translation of mRNA in the cytosol.

Proc Natl Acad Sci U S A **109**: 1335–1340

Para A, Farré EM, Imaizumi T, Pruneda-Paz JL, Harmon FG, Kay SA (2007) PRR3 Is a Vascular Regulator of TOC1 Stability in the Arabidopsis Circadian Clock. Plant Cell **19**: 3462–3473

Pendleton KE, Chen B, Liu K, Hunter O V., Xie Y, Tu BP, Conrad NK (2017) The U6 snRNA m6A Methyltransferase METTL16 Regulates SAM Synthetase Intron Retention. Cell **169**: 824-835.e14

Plautz JD, Kaneko M, Hall JC, Kay SA (1997) Independent photoreceptive circadian clocks throughout Drosophila. Science **278**: 1632–1635

Pruneda-Paz JL, Breton G, Para A, Kay SA (2009) A functional genomics approach reveals CHE as a component of the Arabidopsis circadian clock. Science (80-) **326**: 1481–1485

Romanowski A, Schlaen RG, Perez-Santangelo S, Mancini E, Yanovsky MJ (2020) Global transcriptome analysis reveals circadian control of splicing events in Arabidopsis thaliana. Plant J **103**: 889–902

Rugnone ML, Soverna AF, Sanchez SE, Schlaen RG, Hernando CE, Seymour DK, Mancini E, Chernomoretz A, Weigel D, Mas P, et al (2013) LNK genes integrate light and clock signaling networks at the core of the Arabidopsis oscillator. Proc Natl Acad Sci U S A **110**: 12120–12125

Schaffer R, Ramsay N, Samach A, Corden S, Putterill J, Carré IA, Coupland G (1998) The late elongated hypocotyl Mutation of Arabidopsis Disrupts Circadian Rhythms and the Photoperiodic Control of Flowering. Cell **93**: 1219–1229

Shikata H, Hanada K, Ushijima T, Nakashima M, Suzuki Y, Matsushita T (2014) Phytochrome controls alternative splicing to mediate light responses in Arabidopsis. Proc Natl Acad Sci U S A **111**: 18781–18786

Somers DE, Devlin PF, Kay SA (1998) Phytochromes and cryptochromes in the entrainment of the Arabidopsis circadian clock. Science (80-) **282**: 1488–1490

Song HR, Carré IA (2005) DET1 regulates the proteasomal degradation of LHY, a component of the Arabidopsis circadian clock. Plant Mol Biol **57**: 761–771

Sorkin ML, Nusinow DA (2022) Using Tandem Affinity Purification to Identify Circadian Clock Protein Complexes from Arabidopsis. *In* D Staiger, S Davis, AM Davis, eds, Plant Circadian Networks Methods Protoc. Springer US, New York, NY, pp 189–203

Sorkin ML, Tzeng S-C, Romanowski A, Kahle N, Bindbeutel R, Hiltbrunner A, Yanovsky MJ, Evans BS, Nusinow DA (2022) COR27/28 Regulate the Evening Transcriptional Activity of the RVE8-LNK1/2 Circadian Complex. bioRxiv 2022.05.16.492168

Strayer C, Oyama T, Schultz TF, Raman R, Somers DE, Mas P, Panda S, Kreps JA, Kay SA (2000) Cloning of the Arabidopsis clock gene TOC1, an autoregulatory response regulator homolog. Science (80-) **289**: 768–771

Su Y, Wang S, Zhang F, Zheng H, Liu Y, Huang T, Ding Y (2017) Phosphorylation of

Histone H2A at Serine 95: A Plant-Specific Mark Involved in Flowering Time Regulation and H2A.Z Deposition. Plant Cell **29**: 2197–2213

Sugano S, Andronis C, Green RM, Wang ZY, Tobin EM (1998) Protein kinase CK2 interacts with and phosphorylates the Arabidopsis circadian clock-associated 1 protein. Proc Natl Acad Sci U S A **95**: 11020–11025

Sun Z, Guo T, Liu Y, Liu Q, Fang Y (2015) The Roles of Arabidopsis CDF2 in Transcriptional and Posttranscriptional Regulation of Primary MicroRNAs. PLoS Genet **11**: 1–19

Urquiza García JMU (2018) A Mathematical Model in Absolute Units for the Arabidopsis Circadian Oscillator. The University of Edinburgh

Wang C, Yang J, Song P, Zhang W, Lu Q, Yu Q, Jia G (2022) FIONA1 is an RNA N 6-methyladenosine methyltransferase affecting Arabidopsis photomorphogenesis and flowering. Genome Biol. doi: 10.1186/s13059-022-02612-2

Wang CY, Yeh JK, Shie S Sen, Hsieh IC, Wen MS (2015) Circadian rhythm of RNA N6-methyladenosine and the role of cryptochrome. Biochem Biophys Res Commun **465**: 88–94

Wang L, Fujiwara S, Somers DE (2010) PRR5 regulates phosphorylation, nuclear import and subnuclear localization of TOC1 in the Arabidopsis circadian clock. EMBO J **29**: 1903–1915

Wang Y, Wu J-F, Nakamichi N, Sakakibara H, Nam H-G, Wu S-H (2011) LIGHT-REGULATED WD1 and PSEUDO-RESPONSE REGULATOR9 form a positive feedback regulatory loop in the Arabidopsis circadian clock. Plant Cell **23**: 486–98

Wang Z-Y, Kenigsbuch D, Sun L, Harel E, Ong MS, Tobin EM (1997) A Myb-Related Transcription Factor Is Involved in the Phytochrome Regulation of an Arabidopsis Lhcb Gene. The Plant **9**: 491–507

Wang Z-Y, Tobin EM (1998a) Constitutive Expression of the CIRCADIAN CLOCK ASSOCIATED 1 (CCA1) Gene Disrupts Circadian Rhythms and Suppresses Its Own Expression. Cell **93**: 1207–1217

Wang ZY, Tobin EM (1998b) Constitutive expression of the CIRCADIAN CLOCK ASSOCIATED 1 (CCA1) gene disrupts circadian rhythms and suppresses its own expression. Cell **93**: 1207–1217

Wu J-F, Tsai H-L, Joanito I, Wu Y-C, Chang C-W, Li Y-H, Wang Y, Hong JC, Chu J-W, Hsu C-P, et al (2016) LWD-TCP complex activates the morning gene CCA1 in Arabidopsis. Nat Commun **7**: 13181

Wu J-F, Wang Y, Wu S-H (2008) Two new clock proteins, LWD1 and LWD2, regulate Arabidopsis photoperiodic flowering. Plant Physiol **148**: 948–59

Wu MF, Sang Y, Bezhani S, Yamaguchi N, Han SK, Li Z, Su Y, Slewinski TL, Wagner D (2012) SWI2/SNF2 chromatin remodeling ATPases overcome polycomb repression and control floral organ identity with the LEAFY and SEPALLATA3 transcription factors. Proc Natl Acad Sci U S A **109**: 3576–3581

Xie Q, Wang P, Liu X, Yuan L, Wang L, Zhang C, Li Y, Xing H, Zhi L, Yue Z, et al (2014) LNK1 and LNK2 Are Transcriptional Coactivators in the Arabidopsis Circadian Oscillator. Plant Cell **26**: 2843–2857

Xu T, Wu X, Wong CE, Fan S, Zhang Y, Zhang S, Liang Z, Yu H, Shen L (2022) FIONA1-Mediated m6A Modification Regulates the Floral Transition in Arabidopsis. Adv Sci **9**: 2103628

Yasuhara M, Mitsui S, Hirano H, Takanabe R, Tokioka Y, Ihara N, Komatsu A, Seki M, Shinozaki K, Kiyosue T (2004) Identification of ASK and clock-associated proteins as molecular partners of LKP2 (LOV kelch protein 2) in Arabidopsis. J Exp Bot **55**: 2015–2027

Yeom M, Kim H, Lim J, Shin AY, Hong S, Kim J Il, Nam HG (2014) How do phytochromes transmit the light quality information to the circadian clock in arabidopsis? Mol Plant **7**: 1701–1704

Yu Y, Fu W, Xu J, Lei Y, Song X, Liang Z, Zhu T, Liang Y, Hao Y, Yuan L, et al (2021) Bromodomain-containing proteins BRD1, BRD2, and BRD13 are core subunits of SWI/SNF complexes and vital for their genomic targeting in Arabidopsis. Mol Plant **14**: 888–904

Zhao BS, Roundtree IA, He C (2017) Post-transcriptional gene regulation by mRNA modifications. Nat Rev Mol Cell Biol **18**: 31

Zheng H, Zhang F, Wang S, Su Y, Ji X, Jiang P, Chen R, Hou S, Ding Y (2018) MLK1 and MLK2 Coordinate RGA and CCA1 Activity to Regulate Hypocotyl Elongation in Arabidopsis thaliana. Plant Cell **30**: 67–82

4 COR27/28 Regulate the Evening Transcriptional Activity of the RVE8-LNK1/2 Circadian Complex

This chapter is currently under review at *Plant Physiology* and posted as a pre-print on bioRxiv as:

Sorkin ML, Tzeng S-C, Romanowski A, Kahle N, Bindbeutel R, Hiltbrunner A, Yanovsky MJ, Evans BS, Nusinow DA (2022) COR27/28 Regulate the Evening Transcriptional Activity of the RVE8-LNK1/2 Circadian Complex. bioRxiv 2022.05.16.492168

4.1 Abstract

The timing of many molecular and physiological processes in plants occurs at a specific time of day. These daily rhythms are driven by the circadian clock, a master timekeeper that uses daylength and temperature to maintain rhythms of approximately 24 hours in various clock-regulated phenotypes. The circadian MYB-like transcription factor REVEILLE 8 (RVE8) interacts with its transcriptional coactivators NIGHT LIGHT INDUCIBLE AND CLOCK REGULATED 1 (LNK1) and LNK2 to promote the expression of evening-phased clock genes and cold tolerance factors. While genetic approaches have commonly been used to discover new connections within the clock and between other pathways, here we use affinity purification coupled with mass spectrometry to discover time-of-day-specific protein interactors of the RVE8-LNK1/2 complex. Among the interactors of RVE8/LNK1/LNK2 were COLD REGULATED GENE 27 (COR27) and COR28, which were coprecipitated in an evening-specific manner. In addition to COR27/28, we found an enrichment of temperature-related interactors that led us to establish a novel role for LNK1/2 in temperature entrainment of the clock. We established that RVE8, LNK1, and either COR27 or COR28 form a tripartite complex in yeast and that the effect of this interaction *in planta* serves to antagonize transcriptional activation of RVE8 target genes through mediating RVE8 protein degradation in the evening. Together, these results illustrate how a proteomic approach identified time-of-day-specific protein interactions and a novel RVE8-LNK-COR protein complex that implicates a new regulatory mechanism for circadian and temperature signaling pathways.

4.2 Introduction

Daily and seasonal patterns in daylength and temperature cycles are two of the most dependable environmental cues an organism experiences. As such, lifeforms in every kingdom have evolved a mechanism to anticipate and synchronize their biology with the earth's predictable 24-hour and 365-day cycles (Ouyang et al., 1998; Rosbash, 2009; Edgar et al., 2012). This mechanism is called the circadian clock, which in plants consists of approximately 20-30 genes that participate in transcription-translation feedback loops to produce rhythms with a period of about 24 hours (Creux and Harmer, 2019). These core oscillator genes respond to the environment by producing a physiological response appropriate for a particular time of day or year (Webb et al., 2019). In plants, the clock regulates a variety of phenotypic outputs, including the transition from vegetative to reproductive growth, biotic defense responses, and protection from abiotic stressors such as extreme warm or cold temperature (Greenham and Mcclung, 2015).

Identification of circadian-associated genes has been critical in understanding the generation of biological rhythms. Core oscillator components often exhibit rhythmic gene expression with a period of ~24 hours and a set phase—or time of peak and trough expression. For example, two of the first genes to be defined as core oscillator components in the model plant *Arabidopsis thaliana* (Arabidopsis) are the morning-phased MYB-like transcription factors *CIRCADIAN CLOCK ASSOCIATED 1* (*CCA1*) and *LATE ELONGATED HYPOCOTYL* (*LHY*) (Schaffer et al., 1998; Wang and Tobin, 1998; Green and Tobin, 1999). These genes are highly expressed at dawn and repress the expression of the afternoon- and evening-phased *PSEUDO RESPONSE REGULATOR* genes *PRR1/ TIMING OF CAB EXPRESSION 1* (*TOC1*), *PRR5*, *PRR7*, and *PRR9*

(Alabadí et al., 2001; Farré et al., 2005; Kamioka et al., 2016). The *PRRs* reciprocally repress *CCA1*/*LHY*, completing one of the negative feedback loops that define the clock. In the evening, *EARLY FLOWERING 3* (*ELF3*), *ELF4*, and *LUX ARRHYTHMO* (*LUX*) interact in the nucleus to form a tripartite protein complex called the evening complex, which represses *PRR9*, *CCA1*/*LHY*, and other clock and growth-promoting factors (Dixon et al., 2011; Nusinow et al., 2011; Chow et al., 2012; Herrero et al., 2012). As we discover new connections within and between the clock, we enhance our understanding of this important system.

In this study, we used affinity purification coupled with mass spectrometry (APMS) to identify protein-protein interactions associated with the REVEILLE 8 (RVE8)-NIGHT LIGHT-INDUCIBLE AND CLOCK-REGULATED 1 (LNK1)/LNK2 circadian transcriptional complex. The RVEs are an 8-member family of CCA1/LHY-like transcription factors of which some members interact with the LNK proteins to coregulate target gene expression (Rawat et al., 2011; Rugnone et al., 2013; Xie et al., 2014; Pérez-García et al., 2015; Gray et al., 2017). In the late morning, the RVE8-LNK1/2 transcriptional complex activates the expression of evening-expressed clock genes such as *TOC1* and *PRR5* via recruitment of the basal transcriptional machinery to these and other *RVE8* target promoters (Xie et al., 2014; Ma et al., 2018). Conversely, *LNK1/2* are also known to act as corepressors of other *RVE8* targets, such as the anthocyanin structural gene *UDP-GLUCOSE:FLAVONOID 3-O-GLUCOSYLTRANSFERASE (UF3GT)* (Pérez-García et al., 2015). Additionally, LNK1/2 interact with another transcription factor, MYB3, as corepressors to inhibit the expression of the phenylpropanoid biosynthesis gene *C4H*

(Zhou et al., 2017). The mechanism behind the corepressive function of the LNKs and how they switch between an activating and a repressive role is unknown.

LNK1/2 bind to RVE8 and MYB3 via two conserved arginine/asparagine-containing motifs called R1/R2 located in the LNK C-terminus (Xie et al., 2014; Zhou et al., 2017). Additionally, the Extra N-terminal Tail (ENT) domain present in LNK1/2 but not LNK3/4 is required for their repressive activity with MYB3 (Zhou et al., 2017). The LNKs have no other known functional protein domains apart from these regions. RVE8 and the other RVEs are characterized by the presence of a LHY-/CCA1-LIKE (LCL) domain, which can directly bind the LNKs, presumably at the C-terminus (de Leone et al., 2018; Ma et al., 2018). RVE8 target gene promoters frequently contain the canonical *CCA1*/*LHY*-binding motif called the evening element (EE) as well as G-box-like and morning element (ME)-like motifs (Hsu et al., 2013a).

In addition to regulating circadian rhythms, *RVE4*/8 regulate thermotolerance under both high and low temperatures (Li et al., 2019; Kidokoro et al., 2021). After exposure to heat shock, RVE4/8 upregulate the expression of *ETHYLENE RESPONSIVE FACTOR 53* (*ERF53*) and *ERF54*, boosting the plant's heat shock tolerance (Li et al., 2019). In another study, the authors found that *RVE4*/8 also appear to promote freezing tolerance via activation of *DEHYDRATION-RESPONSIVE ELEMENT BINDING PROTEIN 1A* (*DREB1A*, also referred to as *C-REPEAT BINDING FACTOR 3, CBF3*) when grown at 4℃ (Kidokoro et al., 2021). A corresponding association between temperature and the LNKs has not been well studied, although EC-mediated induction of *LNK1* expression under warm nights suggests a role for the LNKs in temperature responses (Mizuno et al., 2014).

Our proteomic approach presented here establishes novel protein interactions with the RVE8-LNK1/2 transcriptional complex at ZT5 and ZT9. Although these clock bait proteins exhibit peak mRNA expression in the early morning hours, we found that LNK1 and RVE8 interact with more protein partners at the later ZT9 timepoint than at ZT5. Temperature response related GO terms were significantly enriched among the coprecipitated proteins, prompting us to explore and establish a role for LNK1/2 in temperature entrainment of the clock. Among the temperature-related coprecipitated proteins were COLD REGULATED GENE 27 (COR27) and COR28, which only coprecipitated with RVE8/LNK1/LNK2 at ZT9. Furthermore, we found that the CORs interact with RVE8 and LNK1 in a tripartite complex in a yeast 3-hybrid system. By performing APMS using 35S::YFP-COR27 and 35S::GFP-COR28, we validated the interaction with LNK1, LNK2, and RVE8, and identified additional novel interactions between the CORs and RVE5, RVE6, and several light signaling proteins. Further investigation into the role of the RVE8-LNK1/2-COR27/28 interaction suggested that the CORs antagonize activation of RVE8 target genes via regulation of RVE8 protein stability in the evening. Thus, by taking a proteomic approach to study a core circadian transcriptional complex, we identified a novel, evening-phased RVE8-LNK-COR protein complex that presents a new regulatory mechanism for circadian and temperature signaling pathways.

4.3 Results

Characterization of affinity-tagged lines. To identify new interactions with known clock proteins, we created endogenous promoter-driven, 3x-FLAG-6x-His C-terminal (HFC) affinity-tagged versions of RVE8, LNK1, and LNK2. RVE8-HFC was

transformed into the *rve8-1 CCR2::LUC* mutant background while LNK1-HFC and LNK2-HFC were introduced into *lnk1/2/3/4* quadruple mutant (*lnkQ)* (de Leone et al., 2018) *CCA1::LUC.* By transforming our tagged LNKs into the *lnkQ* background, we could eliminate co-precipitating interactors that could be formed through a complex between our tagged LNKs and the endogenous LNKs. To ensure the tagged versions of our proteins of interest functioned similarly to their native counterparts, we selected T3 homozygous lines that rescued the long period mutant phenotype of *rve8-1* or *lnkQ* mutants (Rawat et al., 2011; Xie et al., 2014) (**Fig. 4.1A-C**). LNK1-HFC/LNK2-HFC did not fully restore the circadian period back to wild-type levels, but the lengthened period is consistent with the absence of the other three LNKs after the introduction of the tagged LNK into the *lnkQ* quadruple mutant (Xie et al., 2014; de Leone et al., 2018). We also determined that the HFC-tagged proteins exhibit rhythmic protein abundance patterns under 12 hr light: 12 hr dark (LD) conditions, as would be expected for these proteins (**Fig. 4.1D-G**). While mRNA expression for *RVE8*, *LNK1*, and *LNK2* peaks at ZT1, ZT5, and ZT2, respectively, peak protein abundance occurred at ZT6, ZT9, and ZT6—about 4-5 hours after peak mRNA expression (Mockler et al., 2007) (**Fig. 4.1D-G, Fig. S4.1**). This lag in protein abundance after transcription is consistent with previously reported data showing a peak in RVE8-HA abundance three to six hours after dawn (Rawat et al., 2011). These experiments demonstrate that our affinity-tagged clock proteins behaved similarly to the native protein and are functional, making them ideal tools for capturing relevant protein interactions.

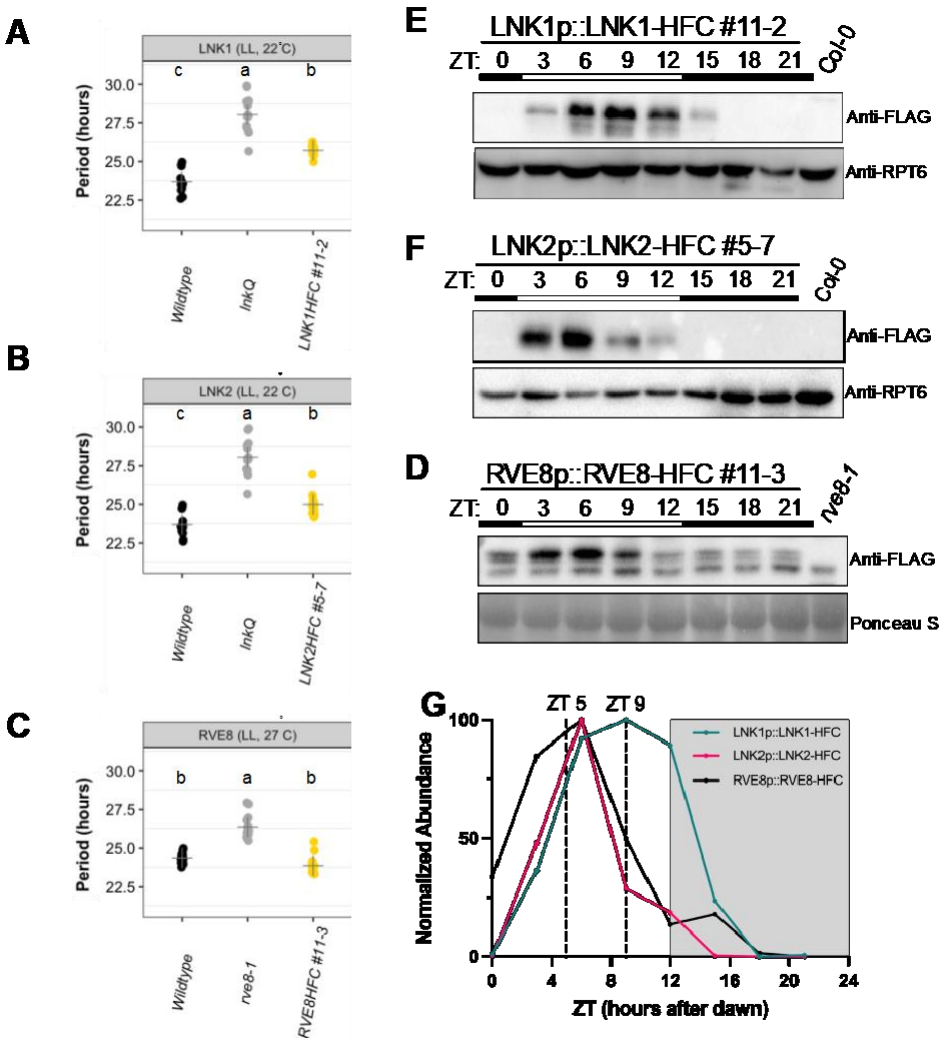

Figure 4.1 Characterization of affinity-tagged lines used for APMS
(A-C) Circadian luciferase reporter period analysis of selected T3 homozygous lines expressing (A) LNK1-HFC, (B) LNK2-HFC, or (C) RVE8-HFC in their respective mutant backgrounds (*rve8-1* or *lnkQ*). Each point represents the circadian period of an individual plant and the + symbol shows the average period for that genotype. Letters correspond to significantly different periods as determined by ANOVA with a Tukey's post-hoc test. LNK1 and LNK2 luciferase assays were performed together and include the same wildtype and *lnkQ* data. Environmental conditions during imaging are included at the top of the plot (LL = constant light). (D-F) Time course Western blots showing cyclic protein abundance patterns of 10-day-old affinity tagged lines under 12 hr light: 12 hr dark 22 ℃ conditions. Affinity tagged lines are detected with anti-FLAG antibody. RPT5 or Ponceau S staining was used to show loading. Col-0 CCA1::LUC (Col-0) or *rve8-1* CCR2::LUC (*rve8-1*) were used as negative controls. White and black bars indicate lights-on and lights-off, respectively (D) 24-hour protein expression patterns of affinity tagged lines normalized to Ponceau S or RPT5 quantified by densitometry of Western blots shown in D-F. Vertical dotted lines indicate time of tissue collection for APMS. White and grey shading indicates lights-on and lights-off, respectively. Western blots and luciferase reporter assays were repeated at least 2 times. ZT= Zeitgeber Time.

Affinity purification-mass spectrometry (APMS) identifies novel time-of-day-specific interacting partners for RVE8, LNK1, and LNK2. We selected two timepoints for APMS based on the protein abundance patterns for RVE8-HFC, LNK1-HFC, and LNK2-HFC **(Fig. 4.1G**). RVE8-HFC and LNK2-HFC exhibited the highest protein abundance between ZT3 and ZT6, while LNK1-HFC protein was highest between ZT6 and ZT9. Considering this, we chose to examine protein-protein interactions at ZT5 and ZT9.

We identified a total of 392 proteins that coprecipitated with either RVE8-HFC, LNK1-HFC, or LNK2-HFC at ZT5 or ZT9 but did not coprecipitate in our GFP-HFC nor Col-0 negative controls (**Fig. 4.2A, Dataset S4.1**). Consistent with the time of peak LNK1-HFC and LNK2-HFC protein abundance (ZT9 and ZT5, respectively; **Fig. 4.1G**), we saw higher total spectra mapping to LNK1-HFC at ZT9 (621) and LNK2-HFC at ZT5 (497) compared to the other timepoint (**Tables S4.1 and S4.2**). Similarly, the number of coprecipitated proteins was greatest at ZT9 for LNK1-HFC and at ZT5 for LNK2-HFC (**Fig. 4.2B-C, Dataset S1**). Total spectra mapping to the bait protein RVE8-HFC were similar between the two timepoints (**Tables 1 and 2**). Despite the similarity in RVE8-HFC total spectra between timepoints, we precipitated more ZT9-specific interactors than ZT5-specific interactors with RVE8-HFC (**Fig. 4.2D**). Overall, we identified more RVE8/LNK1/LNK2-binding partners at ZT9 (364) versus the earlier timepoint of ZT5 (281) (**Fig. 4.2A**) and found that 111 out of 392 (28.3%) total proteins coprecipitated were ZT9-specific; these proteins were not coprecipitated in any APMS experiment performed at ZT5. In summary, the enrichment of coprecipitated proteins at ZT9 suggests an important post-translational role for the RVE8-LNK1/2 complex in the evening.

We used gene ontology (GO) analysis to categorize coprecipitated proteins at ZT5, ZT9, and ZT5/9 (**Fig. 4.2A**). Proteins coprecipitated at ZT5 only were mostly assigned GO biological process terms associated with homeostasis and general metabolism while proteins found at ZT9 only or ZT5/ZT9 fell into relevant categories such as 'regulation of circadian rhythm', 'response to light stimulus', and 'photoperiodism' (**Fig. 4.2A**). We also noted that GO terms associated with temperature response were enriched in our interactor dataset ('response to cold', 'response to temperature stimulus', and 'response to heat') (**Fig. 4.2A**). This analysis suggested that we identified biologically relevant interacting partners involved in circadian rhythms in our APMS experiments and that there is an enrichment of temperature-related factors among these interactors. We also cross-referenced our lists of coprecipitated proteins with known cycling genes (Romanowski et al., 2020) and found that 71.0% of ZT5 and 71.1% of ZT9 proteins exhibited cyclic mRNA expression (**Dataset S4.1**), demonstrating that our bait circadian clock proteins mostly interacted with proteins whose expression also cycles.

Among the top interactors for LNK1-HFC, LNK2-HFC, and RVE8-HFC were four cold-response proteins: COLD REGULATED GENE 27 (COR27), COR28, and two regulator of chromosome condensation family proteins, TOLERANT TO CHILLING/FREEZING 1 (TCF1), and a homolog of TCF1 that we named REGULATOR OF CHROMOSOME CONDENSATION 1-LIKE (*RCC1L*, AT3G53830) (**Tables S4.1-S4.2**). We characterized these as high-priority interactors based on their subcellular localization prediction and mRNA expression patterns; all four proteins are predicted to be nuclear localized according to the SUBACon subcellular localization consensus algorithm (Hooper et al., 2014), which stands in agreement with being interactors of the

nuclear-localized RVE8/LNK1/LNK2 proteins; additionally, the mRNA expression for these genes is rhythmic under constant light conditions, suggesting circadian regulation of their expression (**Fig. 4.2E-H**). TCF1 and RCC1L were coprecipitated with RVE8/LNK1/LNK2 at both ZT5 and ZT9 while COR27/28 were ZT9-specific interactors **(Tables S4.1-S4.2**).

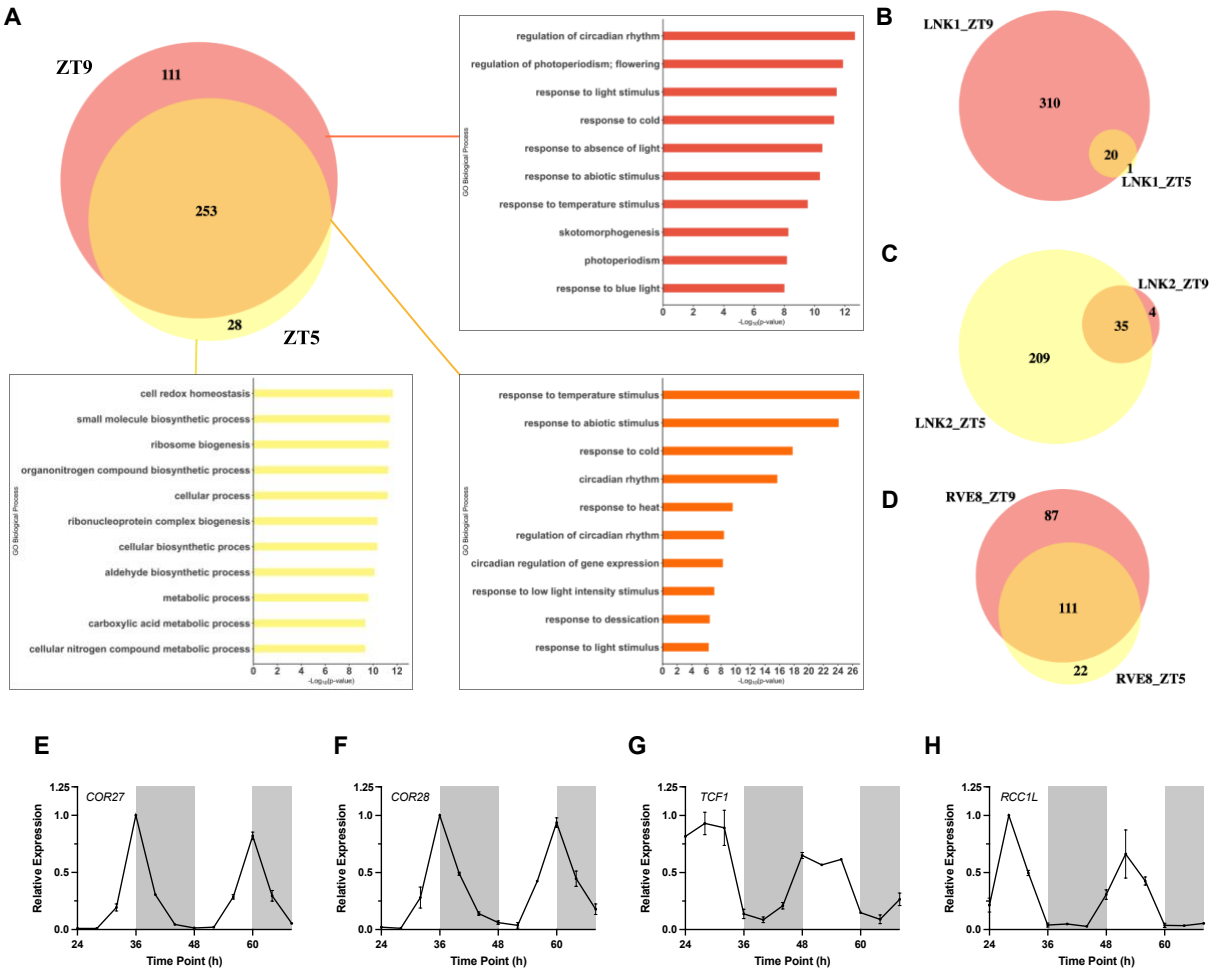

Figure 4.2 Analysis of proteins coprecipitated with RVE8/LNK1/LNK2-HFC by time-of-day affinity purification-mass spectrometry
(A) Venn diagram showing number of proteins coprecipitated with RVE8/LNK1/LNK2 at ZT5, ZT9, or at both timepoints. Corresponding bar charts show enriched GO biological process terms with -Log10$_{(p\text{-value})}$. (B-D) Venn diagrams of coprecipitated proteins at ZT5 and ZT9 separated by bait protein (B, LNK1-HFC, C, LNK2-HFC, or D, RVE8-HFC). (E-H) mRNA expression profiles in constant light of four cold-response proteins identified as RVE8/LNK1/LNK2 interactors. RNA-seq data for E-H taken from Romanowski et al. (2020) *The Plant Journal*. ZT= Zeitgeber Time

TCF1 and *RCC1L* are homologs of the regulator of chromosome condensation (RCC) family protein, RCC1 (Ji et al., 2015) and share 49.7% identity in an amino acid alignment (**Fig. S4.2**). RCC1 is a highly conserved guanine nucleotide exchange factor

(GEF) for the GTP-binding protein RAN and is involved in nucleocytoplasmic export along with regulation of the cell cycle via chromosome condensation during mitosis (Ren et al., 2020). While there are no previous publications characterizing *RCC1L,* its sister gene *TCF1* is a known negative regulator of cold tolerance in Arabidopsis via the lignin biosynthesis pathway (Ji et al., 2015). *RCC1L* expression is downregulated upon cold treatment (**Table S4.3**), but no formal studies have been made into its role in cold tolerance nor chromatin biology.

COR27/28 have no known protein domains and are repressors of genes involved in cold tolerance, circadian rhythms and photomorphogenesis (Li et al., 2016; Wang et al., 2017; Kahle et al., 2020; Li et al., 2020; Zhu et al., 2020). Notably, COR27/28 repress the same clock and cold tolerance genes that are activated by RVE8; *PRR5*, *TOC1*, and *DREB1A* are repressed by the CORs and activated by RVE8 (Rawat et al., 2011; Kidokoro et al., 2021). Null or knock-down mutants of *cor27*/*cor28* exhibit a long period mutant phenotype, similar to that observed for *lnk* and *rve8* mutants (Rawat et al., 2011; Rugnone et al., 2013; Li et al., 2016). As the CORs do not contain a known DNA-binding domain, it is not understood how, mechanistically, these factors alter transcription.

Among the 111 evening-specific interactors were COR27, COR28, CONSTITUTIVELY PHOTOMORPHOGENIC 1 (COP1), and SUPPRESSOR OF PHYA-105 (SPA1) (**Table S4.2**). COP1 and SPA1 were RVE8-HFC-specific interactors while COR27/28 coprecipitated at ZT9 with LNK1/LNK2/RVE8-HFC. We hypothesized that this time-of-day-specific coprecipitation could be explained by the relative abundance of these proteins at ZT5 versus ZT9 due to diurnal changes in gene expression over the course of the day. To investigate this hypothesis, we overlayed the LD mRNA expression patterns

of these ZT9-specific interactors on top of the protein abundance levels of RVE8-HFC, LNK1-HFC, and LNK2-HFC that were determined by time course Western blots shown in **Figure 4.1D-F** (**Fig. S3**). There is very little overlap in expression between the *CORs* and *RVE8/LNK1/LNK2* at ZT5 (**Fig. S4.3)**, indicating that COR27/28 may have only coprecipitated at ZT9 due to increased expression at that timepoint. In contrast, there was not a clear time-of-day distinction in expression overlap between COP1/SPA1 and the clock bait proteins, suggesting the ZT9-specific interaction between COP1/SPA1 and RVE8-HFC is possibly due to a factor other than expression level, such as recruitment through other proteins (such as COR27 or COR28) (**Fig. S4.3**).

COR27 and COR28 interact with circadian and light signaling proteins. To better understand the role of COR27/28 at the protein level, we performed APMS using 35S::YFP-COR27 and 35S::GFP-COR28 lines (Li et al., 2016) collected at ZT9. Through this experiment, we validated the interactions between the CORs and RVE8/LNK1/LNK2 and additionally coprecipitated RVE5 and RVE6, further supporting the connection between COR27/28 and the RVE/LNK proteins (**Table S4.4, Dataset S4.1**). Previous studies have shown an interaction between COR27/28 and PHYTOCHROME B (PHYB), COP1, and SPA1 (Kahle et al., 2020; Li et al., 2020; Zhu et al., 2020). Our affinity purification captured these known interactions and additionally identified PHYD and SPA2/3/4, supporting the previously demonstrated role for the CORs in photomorphogenesis (**Table S4.4**) (Kahle et al., 2020; Li et al., 2020; Zhu et al., 2020). TCF1, one of the cold-tolerance proteins (Ji et al., 2015) to coprecipitate with RVE8/LNK1/LNK2, was also captured with COR27 (**Table S4.4**), which further implicates the CORs in freezing tolerance. In total, we identified 268 proteins that coprecipitated with

YFP-COR27 or GFP-COR28 (**Dataset S4.1**). Of these, we found 58.9% exhibited circadian-regulated mRNA (Romanowski et al., 2020) (**Dataset S4.1**). Together, the COR27/28 APMS provides strong evidence that these proteins are important factors in circadian and light signaling networks.

RVE8, LNK1, and COR27/28 form a protein complex. We used a yeast 2-hybrid system to validate the interactions identified in our APMS between RVE8/LNK1/LNK2 with COR27/28. Surprisingly, we did not see a positive interaction between these components when using a binary yeast 2-hybrid (**Fig. S4.4)**. Since APMS can identify both direct and indirect protein-protein interactions, we hypothesized that RVE8-LNK1/2-COR27/28 could be forming a protein complex where the CORs can only bind when both RVE8 and LNK1 are present. To test this, we used a yeast 3-hybrid system in which a linker protein is expressed in addition to the bait and prey proteins. We used N- and C-terminal truncations of LNK1 since full-length LNK1 autoactivates in yeast, as has been shown previously and here **(Fig. S4.5**) (Xie et al., 2014). Using this method, we found that yeast expressing RVE8, the C-terminus of LNK1, and COR27 or COR28 were able to grow on selective media in a higher order complex (**Fig. 4.3**). Yeast strains where COR27 or COR28 was paired with either LNK1 or RVE8 alone were unable to grow on selective media, indicating that indeed all three components must be present for the CORs to bind (**Fig. 4.3, S4.4**). We also confirmed that RVE8 interacts with the C-terminus of LNK1 (**Fig. S4.4**), in agreement with previous studies (Xie et al., 2014). In combination with our time-of-day APMS, these results show the CORs interact with RVE8/LNK1 in a complex that is present at ZT9.

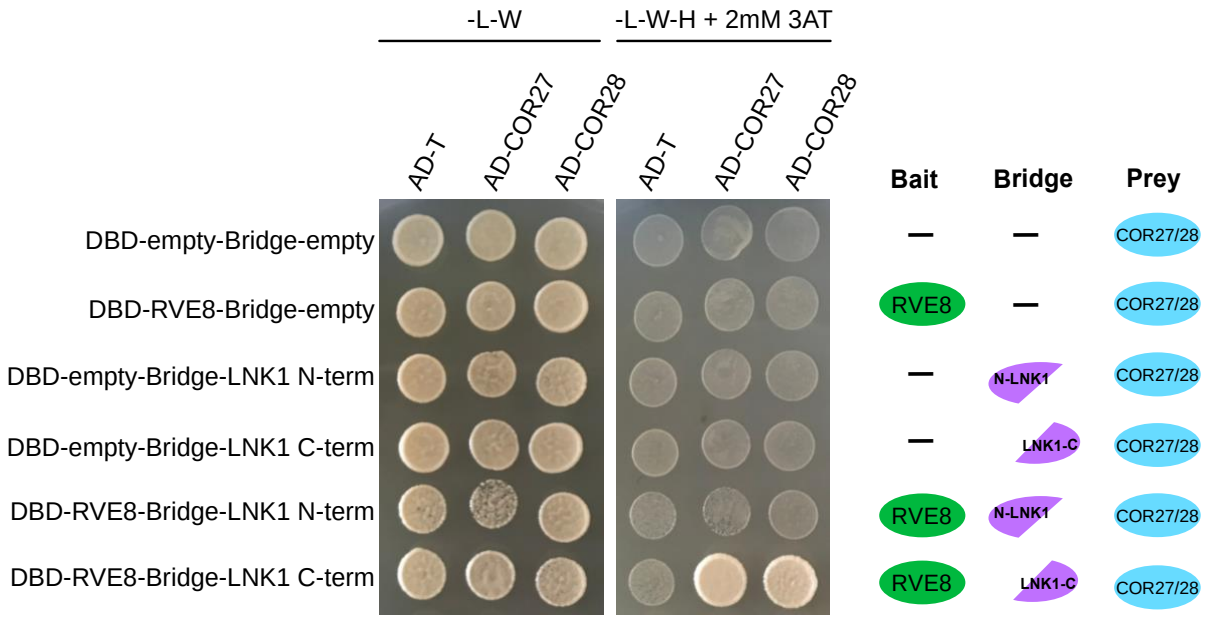

Figure 4.3 COR27/28 interact with RVE8/LNK1 in a yeast 3-hybrid system.
Yeast strains Y2H Gold or Y187 expressing pBridge (GAL4-DBD and a Bridge protein) or pGADT7 (GAL4-AD), respectively, were mated and plated onto selective media. Successful matings can grow on -Leucine/-Tryptophan media (-L-W) while positive interactors can grow on -Leucine/-Tryptophan/-Histidine + 2mM 3-amino-1,2,4-triazole (3AT) (-L-W-H + 2mM 3AT). A graphical depiction of different combinations is shown to the right. AD-T (large T-antigen protein) is a negative control for prey interactions. Experiment was repeated at least twice.

COR27/28 alter diurnal RVE8 protein abundance patterns and antagonize activation of the RVE8 target gene *TOC1*. We next sought to determine the biological relevance of the RVE8-LNK1/2-COR27/28 interaction. COR27/28 are post-translationally regulated via degradation by 26S proteasome (Kahle et al., 2020; Li et al., 2020; Zhu et al., 2020). As COR27/28 were identified as ZT9-specific RVE8-HFC interactors (**Table S4.2**), we hypothesized that COR27/28 target the RVE8-LNK complex for degradation in the evening, thus blocking expression of RVE8 target genes late in the day. To determine if RVE8-HFC abundance patterns are driven by a post-translational mechanism, we examined protein abundance of RVE8-HFC in seedlings treated with either the 26S proteasome inhibitor bortezomib (bortz) or DMSO (mock). The mock treated seedlings

showed the typical pattern for RVE8-HFC protein abundance (**Fig. 4.1F**) with decreasing RVE8-HFC from ZT6 to ZT15 (**Fig. S4.6**). Treatment with bortz led to increased RVE8-HFC accumulation during this time frame, indicating 26S-proteasome degradation is involved in the observed decrease of RVE8-HFC from ZT6 to ZT15 (**Fig. S4.6**).

Next, we tested if COR27 and COR28 regulate RVE8 protein abundance by examining cyclic protein abundance in RVE8p::RVE8-HFC versus RVE8p::RVE8-HFC in *cor27-2 cor28-2*. While RVE8-HFC abundance in the wild-type background exhibits rhythmic protein abundance with peak protein levels at ZT6, RVE8-HFC abundance is significantly higher in the *cor27-2 cor28-2* background during the evening and nighttime hours (**Fig. 4.4A-C**). This result is consistent with the hypothesis that in the absence of COR27/28, RVE8-HFC should be stabilized specifically in the evening—when it would normally be degraded through its interaction with the CORs. As the circadian rhythm of *RVE8* mRNA expression under LD cycles was shown to be unchanged in the *cor27-2 cor28-2* background (Wang et al., 2017), our results indicate that COR27/28 regulate RVE8-HFC protein abundance at the post-translational level.

We then tested the effect of the CORs on RVE8/LNK1 transcriptional activity using a transactivation assay in *Nicotiana benthamiana* (**Fig. 4.4D**). RVE8 binds to the evening element cis-regulatory motif in the *TOC1* promoter to activate its expression (Rawat et al., 2011). When LNK1 and RVE8 were transiently expressed together in *N. benthamiana* along with a *TOC1* promoter-driven luciferase reporter, we observed activation of the reporter, as expected (**Fig. 4.4D**). When COR27 or COR28 was added to the inoculation cocktail, activation of the reporter was reduced, indicating that the CORs antagonize RVE8/LNK1 transcriptional activity *in vivo* (**Fig 4.4D**). Taken together, our results indicate

that the RVE8-COR27/28-LNK1/2 interaction serves to block activation of RVE8 target genes via degradation of RVE8 in the evening.

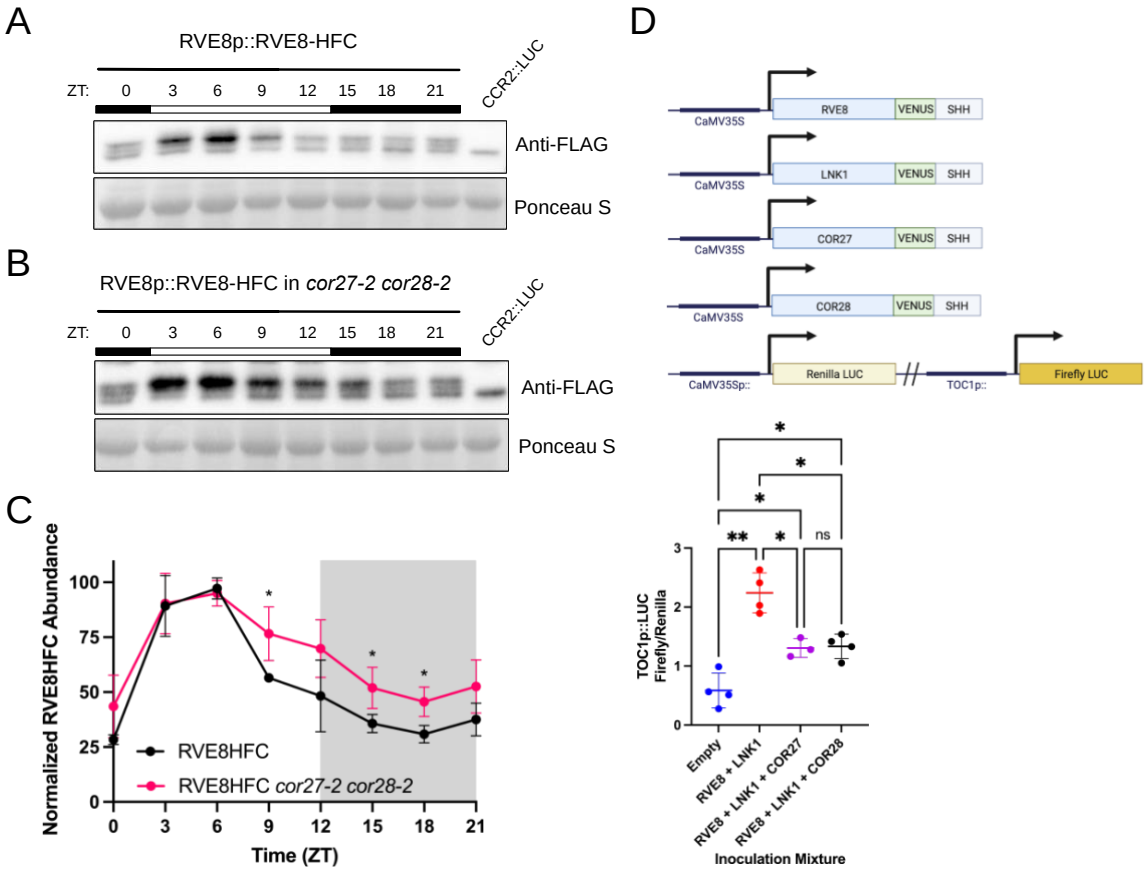

Figure 4.4 COR27/28 alter RVE8-HFC protein abundance patterns and inhibit RVE8/LNK1-mediated activation of *TOC1*.
(A-B) 24-hour protein expression patterns of RVE8-HFC in wild type (A) or cor27-2 cor28-2 (B) backgrounds analyzed by Western blot. Tissue was collected every 3 hours from 12-day-old plants grown under 12 hr light: 12 hr dark 22 ℃ conditions. Anti-FLAG antibody was used to detect RVE8-HFC and Ponceau S staining was used to show loading. White and black bars indicate lights-on and lights-off, respectively. Col-0 CCR2::LUC was used as the negative control. (C) Densitometry quantification of (A) and (B) RVE8-HFC 24-hour abundance normalized to Ponceau S in wild type and cor27-2 cor28-2 backgrounds. Points represent the average normalized RVE8-HFC abundance from 3 (WT) or 4 (cor27-2 cor28-2) independent bioreps. Asterisks indicate significant differences between genotypes based on Welch's t-test (* p< 0.05). Error bars = SD. (D) Dual luciferase assay in 3–4-week-old Nicotiana benthamiana. Schematic of expression constructs infiltrated are shown at the top (SHH = 2X-StrepII-HA-His6 tag). Luminescence from a dual firefly/renilla luciferase reporter was measured after coinfection with 35S::RVE8-VENUS-SHH, 35S::LNK1-VENUS-SHH, 35S::COR27-VENUS-SHH, or 35S::COR28-VENUS-SHH. Luminescence was normalized to constitutively expressed renilla luciferase luminescence to control for infection efficiency. Points represent the normalized luminescence from 3-4 independent experiments with N=12. Mean normalized luminescence is indicated by the crosshair symbol and error bars = SD. Asterisks indicate significant differences by unpaired t-test with Welch correction (ns= not significant, * p< 0.05, ** p< 0.01). ZT= Zeitgeber Time. Empty = reporter alone.

The RVEs are important for cold temperature induction of COR27/28. *COR27/28* contain evening elements in their promoters that are important for their cold induction and could be targets of RVE8 transcriptional regulation (Mikkelsen and Thomashow, 2009; Wang et al., 2017). Additionally, *COR27/28* are significantly upregulated in an inducible RVE8:GR line according to a previously published RNA-seq dataset (Hsu et al., 2013b). Both COR27/28 and RVE4/8 regulate cold tolerance in Arabidopsis; *COR27/28* expression is induced by cold temperature (16 ℃ and 4 ℃) within 3 hours and the *cor27-1 cor28-2* loss-of-function mutant shows increased freezing tolerance, suggesting these genes are negative regulators of the plant's response to freezing temperatures (Li et al., 2016). In contrast, RVE4/8 are activators of cold tolerance (Kidokoro et al., 2021). Upon cold treatment (4℃ for 3 hours), RVE4/8 localize to the nucleus and upregulate *DREB1A* to promote freezing tolerance (Kidokoro et al., 2021).

To determine if the RVE transcription factors are regulators of *COR27*/*28* cold-induction, we examined *COR27*/*28* expression at 22 ℃ and 4 ℃ in Col-0, *rve8-1, rve34568,* and *lnkQ* mutants. We found that *COR27*/*28* cold-induction was greatly attenuated in *rve34568* and *lnkQ* mutants, consistent with the *CORs* being targets of the RVE-LNK transcriptional complex (**Fig. S4.7A-B)**. The absence of an effect in the *rve8-1* single mutant suggests there is redundancy among the *RVE* family in the regulation of *COR27*/*28*. Indeed, we found that the LNKs coprecipitated RVE3/4/5/6/8 in our APMS (**Tables S4.1 and S4.2**), suggesting multiple RVE/LNK complexes could influence the regulation of the *CORs*. Interestingly, we saw little effect of RVEs/LNKs on *COR27/28* expression at 22 ℃ at ZT12 (**Fig. S4.7C-D**), suggesting these clock factors only have an

effect under cold stress or that there may be a greater effect on expression at 22 ℃ at a different time of day.

LNK1 and LNK2 are important for temperature entrainment of the clock. The enrichment of temperature response GO terms among the list of coprecipitated proteins in our APMS (**Fig. 4.2A**), as well as the existing evidence linking RVE8 to temperature regulation (Blair et al., 2019; Kidokoro et al., 2021) prompted us to investigate whether *LNK1/2* are important for temperature input to the clock. While light is the primary entrainment cue for the plant clock, daily temperature cycles are known to be another major environmental input cue (Devlin and Kay, 2001; Salomé and Robertson Mcclung, 2005; Avello et al., 2019). To examine temperature entrainment, we examined rhythms from a CCA1::LUC reporter in wild type and *lnk1-1, lnk2-4,* and *lnk1-1 lnk2-4* mutant plants that were first grown under constant light and then transferred into a temperature entrainment condition. Under constant light, the *lnk* mutants exhibited their canonical long period mutant phenotype (Rugnone et al., 2013) (**Fig. 4.5**). Upon entering a temperature entrainment condition of 12 hr 20 ℃: 12 hr 22 ℃, the *lnk1/2* mutants were unable to resynchronize their circadian rhythms to that of wild type (**Fig. 4.5A-B**). This defect was ameliorated when the difference between the minimum and maximum temperature was increased from 2 ℃ to 4 ℃; when provided temperature cycles of 12 hr 18 ℃: 12 hr 22 ℃, most *lnk* mutants were able to realign with the wild-type acrophase (peak reporter expression) by the third day of temperature entrainment (**Fig. 4.5 C-D**). However, this resynchronization was still slower than when the *lnk* mutants were provided with photocycles—upon the transition from constant light to LD cycles, all mutants were able to immediately re-align their rhythms to wild type, indicating that the *lnk* mutants are

specifically impaired in their ability to use temperature as an entrainment cue (**Fig. 4.5E-F**).

The temperature entrainment programs used in **Figure 4.5A-D** are non-ramping, meaning the temperature shifts immediately from the cool to warm temperatures. To better simulate environmental conditions, we also employed a ramping, natural temperature entrainment which gradually oscillates between a low temperature of 16 ℃ and a high of 22 ℃. We observed a similar delay in the ability of the *lnk* mutants to assimilate to wild-type acrophase under natural temperature cycles, demonstrating that this defect is not a byproduct of non-ramping temperature changes (**Fig. S4.8**).

As the LNKs form a four-member family, we also examined whether LNK3/4 play a role in temperature entrainment. The *lnk3-1 lnk4-1* double mutant showed little difference from wild-type rhythms under constant light nor temperature entrainment, indicating LNK1/2 are the primary family members important for temperature entrainment (**Fig. S4.9**). In summary, we have demonstrated a previously unknown role for LNK1/2 in temperature entrainment of the clock.

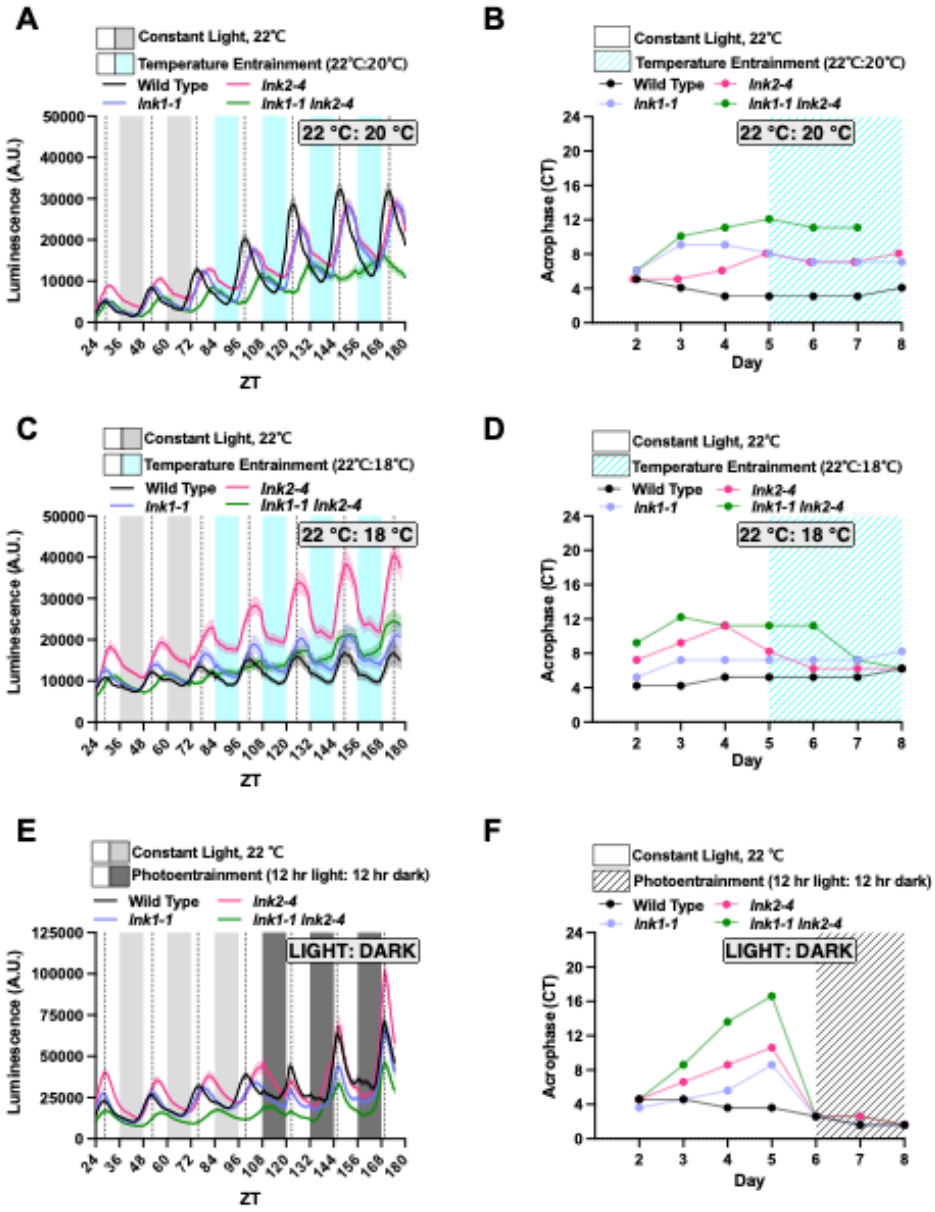

Figure 4.5 LNK1/2 are important for temperature entrainment of the clock.
(A,C,E) Plants were grown for 7 days under 12 hr light: 12 hr dark 22 ℃ conditions for initial entrainment. On day 7, seedlings were transferred to imaging chamber and luminescence was measured for at least 3 days in continuous light and temperature (22 ℃) before the chamber was switched to either a temperature- (A,C) or photo- (E) entrainment program. Temperature entrainment consisted of a day temperature of 22 ℃ and nighttime temperature of 20 ℃ (A) or 18 ℃ (C). Photoentrainment consisted of 12 hr light followed by 12 hr darkness (22 ℃). Lines represent the average luminescence from n=16 seedlings with errors bars = SEM. Vertical dotted lines correspond to the acrophase, or time of peak reporter expression, of the CCA1::LUC reporter in wild type plants. (B,D,F) Acrophase is plotted for each genotype for each day of imaging in constant light and the temperature entrainment condition (B, D) or under photoentrainment (F). Each point represents the acrophase of the averaged luminescence trace shown in (A,C,E). CT = Circadian Time. A.U. = Arbitrary Units. ZT=Zeitgeber Time.

4.4 Discussion

Daily and seasonal temperature cycles are important cues for the entrainment of the plant circadian clock (Salomé and Clung, 2005). In parallel to this, the clock is essential for proper response to temperature stimuli (Salomé and Robertson Mcclung, 2005; Thines and Harmon, 2010). In this study, we have identified a novel, time-of-day-specific interaction between two established components of the circadian and temperature response pathways: the circadian clock transcriptional activation complex containing RVE8 and LNK1/LNK2 and the cold response proteins COR27/COR28. Previous studies have demonstrated that RVE8 and COR27/COR28 both regulate the transcription of the master cold response regulator *DREB1A* and the core circadian oscillator genes *PRR5* and *TOC1*; however, RVE8 acts as a transcriptional activator of these targets while the CORs act as repressors (Rawat et al., 2011; Li et al., 2016; Wang et al., 2017; Kidokoro et al., 2021). In addition to sharing transcriptional targets, RVE8 and COR27/COR28 also affect similar phenotypes, including period lengthening in the null or knock-down mutants and regulation of photoperiodic flowering time (Rawat et al., 2011; Li et al., 2016). Despite these established overlaps in function between the RVE8-LNK1/LNK2 complex and the CORs, a mechanistic connection between these factors has until now been lacking. In this study, we have demonstrated that COR27/COR28 physically interact with and regulate the protein stability of the RVE8-LNK1/LNK2 complex in the evening and that the CORs antagonize RVE8/LNK1-mediated activation of *TOC1* expression.

Our time-of-day-specific APMS experiments demonstrated that RVE8, LNK1, and LNK2 interact with different protein partners at ZT5 versus four hours later at ZT9 (**Fig.**

4.2A-D). LNK1 and RVE8 interacted with more protein partners at the later timepoint, ZT9, while LNK2 coprecipitated more interactors at ZT5 (**Fig. 4.2B-D)**. For LNK1 and LNK2, their time of peak protein abundance (**Fig. 4.1D**) aligned with the time of day when they coprecipitated the most interactors (**Fig. 4.2B-C**), suggesting that increased abundance of these clock bait proteins led to an increased number of captured interactions. Interestingly, while our 24-hour time course Western blots showed a higher abundance of RVE8-HFC at ZT5, we coprecipitated more interactors at ZT9 than at ZT5. This might indicate that even though protein levels of RVE8-HFC are lower at ZT9, perhaps there is an important bridge protein expressed in the evening that links in RVE8-HFC interactors only in the evening. Alternatively, perhaps there are more RVE8-HFC protein interacting partners expressed at ZT9 than at ZT5. By performing APMS at two different time points, we have established that these circadian clock proteins interact with different partners depending on the time of day.

For example, COR27, COR28, COP1, and SPA1 were coprecipitated with RVE8/LNK1/LNK2 at ZT9 but not ZT5 (**Tables S4.1-S4.2**). We have considered the following hypotheses for what is driving this time-of-day-specific interaction: 1) The diurnal expression patterns of these components produces high gene expression overlap at ZT9 but not ZT5, 2) There is a third protein component that is expressed at ZT9 that allows for the interaction between these factors via bridging or by inducing a conformational change in one of the participating proteins, or 3) APMS is not an exclusionary method and could simply have not detected a low abundance peptide that was coprecipitated at ZT5. When we examined the LD mRNA expression patterns for *COR27, COR28, COP1,* and *SPA1*, we found that COR27 and COR28 are most likely ZT9-specific interactors due

to their mRNA expression levels having a higher overlap with RVE8/LNK1/LNK2-HFC protein abundance at ZT9 (**Fig. S4.3**). Indeed, the *CORs* have very low mRNA expression at ZT5 and thus are likely absent from the cell and not interacting with the RVE8-LNK1/2 proteins (**Fig. S4.3**). COP1 and SPA1, in contrast, do not show higher expression overlap with RVE8-HFC at ZT9 over ZT5 (**Fig. S4.3**). We instead think it is possible that COP1/SPA1 could be recruited to RVE8 via COR27/COR28 and thus can only be coprecipitated at ZT9 (hypothesis #2). However, future studies are needed to validate this possibility.

As COR27/28 are post-translationally regulated by 26S proteasome-mediated degradation (Kahle et al., 2020; Li et al., 2020; Zhu et al., 2020), we predicted that the interaction between RVE8/LNK1/LNK2 and COR27/28 could function to target the circadian transcriptional module for degradation in the evening. We found that RVE8-HFC cyclic protein abundance patterns were disrupted in a *cor27-2 cor28-2* mutant background, with higher RVE8-HFC levels observed specifically during the evening and nighttime hours (**Fig. 4.4A-C**). This suggests that COR27/28 are important for degradation of RVE8 in the evening. As COP1/SPA1 were also identified as ZT9-specific RVE8 binding proteins, we suggest that the CORs recruit the COP1-SPA1 E3 ubiquitin ligase complex to RVE8-LNK1/2 to target it for degradation by the proteasome, though this has yet to be directly tested. We also coprecipitated *UBIQUITIN-SPECIFIC PROTEASE 12* (*UBP12*) and *UBP13* and the E3 ubiquitin ligases *PLANT U-BOX 12* (*PUB12*) and *PUB13* in RVE8/LNK1/LNK2 APMS experiments and these factors may also play a role in time-of-day-specific complex degradation (**Tables S4.1-S4.2, Dataset S4.1**) (Zhou et al., 2021). In tobacco transactivation assays, we observed that presence

of COR27/28 reduced the ability of RVE8-LNK1 to activate the expression of a *TOC1* promoter-driven reporter, demonstrating that the CORs have an antagonistic effect on the transcriptional activity of this circadian module (**Fig. 4.4D**).

The CORs do not have identifiable DNA-binding domains and do not bind to DNA *in vitro* (Li et al., 2020); therefore, the CORs must work with a DNA-binding protein to affect transcription of their target genes. Previous work supported this hypothesis by showing that COR27/28 interact with the major photomorphogenic transcription factor ELONGATED HYPOCOTYL 5 (HY5) and regulate some of the same HY5 target loci (Li et al., 2020). Perhaps a similar mechanism is at work here, with the CORs interacting with the RVE-LNK complex to alter its transcriptional activity. The mechanism behind how the CORs change or potentially change the activity of these transcription factors is an open question.

Finally, as *COR27/28* expression is induced under cold stress and RVE8 accumulates in the nucleus upon cold treatment, this presents an interesting possibility that the interaction between RVE8 and the CORs could serve to connect cold temperature response and the circadian clock. Notably, COR27/28 and RVE8 oppositely regulate freezing tolerance; the CORs repress expression of *DREB1A* to decrease freezing tolerance while RVE4/8 activate *DREB1A* expression (Li et al., 2016; Kidokoro et al., 2021). Thus, we anticipate that the interaction between the CORs and the RVE8-LNK complex is antagonistic in its nature.

In summary, we used affinity purification-mass spectrometry (APMS) to identify novel circadian-associated proteins using the RVE8/LNK1/LNK2 core circadian oscillator proteins as baits. By performing APMS at two time points during the 24-hour cycle, we

identified time-of-day-specific interactors, including COR27 and COR28, which only coprecipitated with these three clock baits at the later timepoint, ZT9 **(Fig. 4.6A, Tables S4.1 and S4.2**). The obligate higher order nature of this complex that we established using a yeast 3-hybrid demonstrates a powerful advantage of using an *in vivo* method like APMS over another screening system—screens such as the yeast 2-hybrid library system can only identify binary interactions and thus would never have identified the interaction described here between RVE8, the C-terminus of LNK1, and COR27/28. Taken together, we propose the following model **(Fig. 4.6B**): In the morning–early afternoon, when the *CORs* are not expressed, the RVE8-LNK1/2 complex is free to perform its canonical duty as an activating force in the circadian oscillator and in cold tolerance. As evening approaches, *COR27*/28 expression rises and the RVE8-LNK1/2-COR27/28 complex is formed, which antagonizes RVE8-LNK1/2 transcriptional activity via regulating RVE8 protein abundance. Future studies examining this complex's role in circadian and cold tolerance phenotypes will be of great interest.

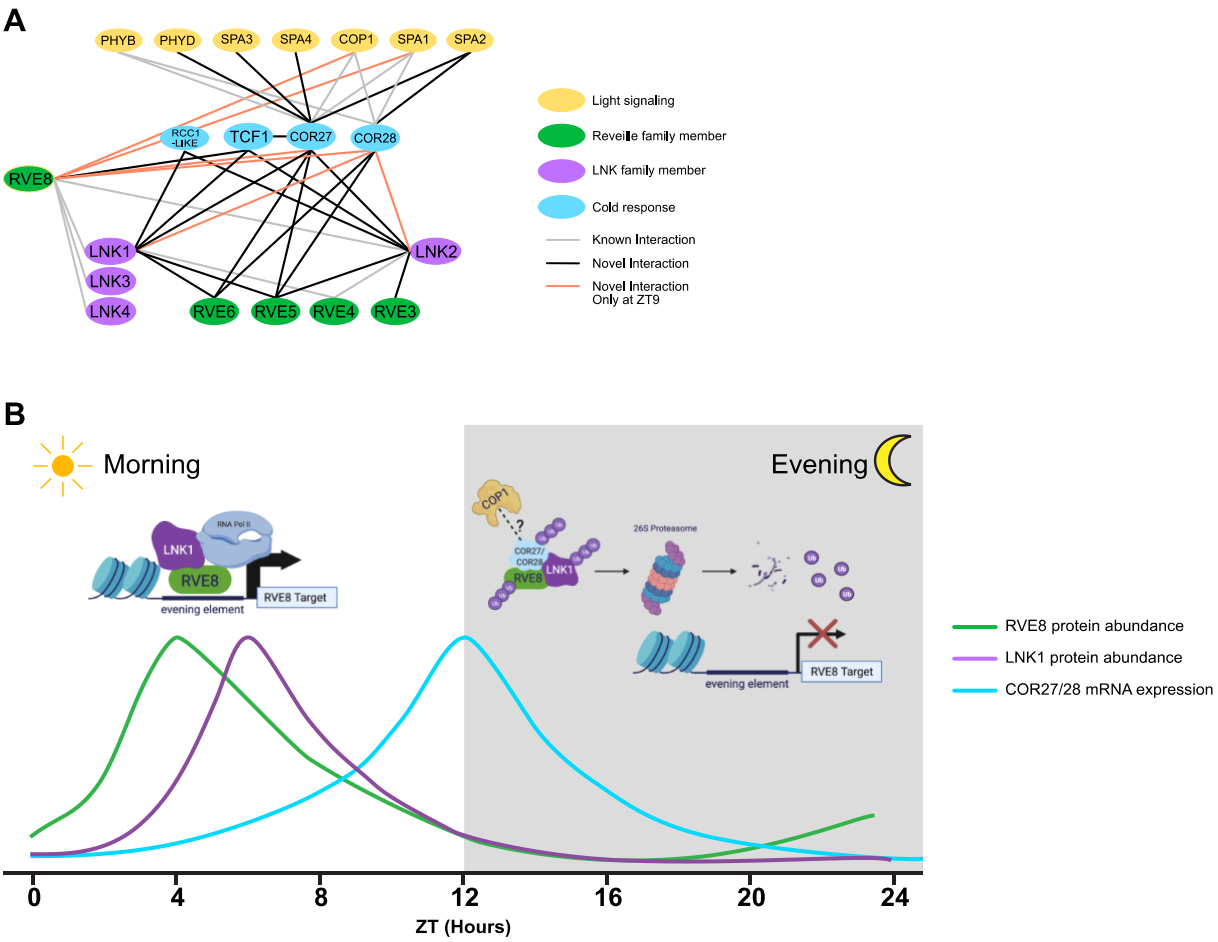

Figure 4.6 The RVE8-LNK1/2-COR27/28 complex is a novel post-translational regulatory mechanism in the circadian clock.
(A) Protein interaction network compiled from APMS experiments using RVE8-HFC, LNK1-HFC, LNK2-HFC, YFP-COR27, and GFP-COR28 as bait proteins at ZT5 and ZT9. Black lines indicate novel interactions identified in this study, grey lines show previously published interactions validated in this study, and orange lines show novel interactions that were identified only at ZT9. (B) Model of hypothesized role of the RVE-LNK-COR interaction during a 24-hour period. In the morning, RVE8-LNK1/2 interact to coactivate the expression of target genes such as evening-phased circadian clock genes and cold-response genes. Towards the evening, COR27/28 are expressed and interact with the RVE8-LNK1/2 complex, potentially recruiting a ubiquitin E3 ligase such as COP1 to target the entire complex for degradation by the 26S proteasome, thus blocking activation of RVE8 targets in the evening. Green and purple lines show approximate protein abundance patterns of RVE8 and LNK1, respectively, while the blue line shows approximate *COR27/28* mRNA expression.

4.5 Methods

Plant Materials. T-DNA disrupted lines used in this study: rve8-1 (SALK_053482C), lnk1-1 (SALK_024353), lnk2-1 (GK_484F07), lnk2-4 (GK_484F07), lnk3-1 (SALK_085551C), lnk4-1 (GK_846C06), cor27-2 (SALK_042072C), and cor28-2 (SALK_137155C) (Alonso et al., 2003). The lnkQ CCA1::LUC line was generated by transforming the lnkQ mutant background (de Leone et al., 2020) with a binary vector containing CCA1::LUC and Basta resistance (from Harmer Lab). The *lnk3-1 lnk4-1* CCA1::LUC line was generated by crossing *lnk3-1 lnk4-1* to the CCA1::Luc reporter. The 35S::YFP-COR27 and 35S::GFP-COR28 lines were described previously (Li et al., 2016) and generously shared with us by Dr. Hongtao Liu. The rve8-1 CCR2::LUC line was described previously (Rawat et al., 2011) and generously shared with us by Dr. Stacey Harmer. The lnk1-1 CCA1::LUC, lnk2-4 CCA1::LUC, and lnk1-1 lnk2-4 CCA1::LUC lines were a generous gift from Dr. Xiaodong Xu (Xie et al., 2014). All plants used were in the Col-0 background.

Seeds were gas sterilized and plated on 1/2X Murashige and Skoog basal salt medium with 0.8% agar + 1% (w/v) sucrose. After stratification for 2 days, plates were transferred to a Percival incubator (Percival-Scientific, Perry, IA) set to a constant temperature of 22 °C. Light entrainment was 12 hr light/12 hr dark (LD) cycles, with light supplied at 80 µmol/m^2/s. 24-hour tissue collections were performed under white light during the daytime timepoints and under dim green light during the nighttime timepoints.

Generation of Epitope-tagged Lines and Plasmid Construction. To generate pB7-RVE8p::RVE8-HFC, RVE8 was cloned from genomic DNA without the stop codon

using primers pDAN1127 and pDAN1128 (**Table S4.5**) and cloned into NotI/AscI-digested pENTR-MCS through In-Fusion HD cloning (Clontech, Mountain View, California). pENTR-RVE8-no stop was then recombined using LR Clonase (Thermo Fisher Scientific, Waltham, Massachusetts) into pB7-HFC (Huang et al., 2016a), which contains the 6X-HIS 3X-FLAG C-terminal tag, to generate pB7-RVE8-HFC. To generate the endogenous promoter driven line, the sequence upstream of the RVE8 transcription start site to the stop codon of the upstream gene was cloned (945 bases) using primers pDAN1129 and pDAN1130 (**Table S4.5**). The 35S Cauliflower Mosaic Virus (CaMV35S) promoter was excised from pB7-RVE8-HFC via PmeI/SpeI digest and replaced with the RVE8 promoter fragment through In-Fusion HD cloning (Clontech, Mountain View, California) to generate pB7-RVE8P::RVE8-HFC. pB7 RVE8p::RVE8-HFC binary vector was transformed into rve8-1 CCR2::LUC (Rawat et al., 2011) by agrobacterium mediated transformation and positive transformants were identified through basta resistance (Clough and Bent, 1998).

To generate pH7WG2-LNK1p::LNK1-HFC and pH7WG2-LNK2p::LNK2-HFC, LNK1 and LNK2 coding sequences were cloned from cDNA without the stop codon using primers pDAN0990/pDAN0991 (LNK1) and pDAN1066/pDAN1067 (LNK2) (**Table S4.5**) and recombined into pENTR-MCS through dTOPO cloning or In-Fusion HD cloning (Contech, Mountain View, California), respectively. pENTR-LNK1-no stop and pENTR-LNK2-no stop were then recombined using LR Clonase (Thermo Fisher Scientific, Waltham, Massachusetts) into pB7-HFC to generate pB7-LNK1-HFC and pB7-LNK2-HFC. To make the endogenous promoter driven construct, the LNK1 promoter was cloned from the LNK1 transcription start site to the upstream gene's 5' UTR (1709 bp) using primers pDAN1016 and pDAN1017 (**Table S4.5**). This promoter fragment was

swapped with CaMV35S via PmeI/SpeI digest and In-Fusion HD cloning (Clontech, Mountain View, California) to generate pB7-LNK1p::LNK1-HFC. Similarly, the LNK2 promoter was cloned from just before the start of the upstream gene through 142 bases into exon 4 from genomic DNA using primers pDAN1018 and pDAN1019 (**Table S4.5**) and inserted into pB7-HFC PmeI/BglII digest and In-Fusion HD cloning (Clontech, Mountain View, California) to generate pB7-LNK2p::LNK2-HFC. To make pH7WG2-LNK1p::LNK1-HFC and pH7WG2-LNK2p::LNK2-HFC, pB7-LNK1p::LNK1-HFC, pB7-LNK2p::LNK2-HFC, and pH7WG2 (Karimi et al., 2002) were digested with KpnI and AgeI and the resulting fragments were ligated. pH7-LNK1p::LNK1-HFC and pH7-LNK2p::LNK2-HFC binary vector were transformed into lnkQ CCA1::LUC by agrobacterium mediated transformation and positive transformants were identified through hygromycin resistance (Clough and Bent, 1998).

To make LNK1 truncations, the N-terminus of LNK1 from the start codon through amino acid 296 was cloned using primers pDAN1954/pDAN2010 (**Table S4.5**), adding a stop codon. The LNK1 C-terminal fragment was cloned using primers pDAN2011/pDAN1955 (**Table S4.5**) with the first amino acid starting at amino acid number 297. Gene fragments were recombined into pENTR-MCS through In-Fusion HD cloning (Clontech, Mountain View, California) to make pENTR-LNK1-N-term-STOP and pENTR-LNK1-C-term-STOP.

To generate pK7-VENUS (VEN)-2x-StrepII-HA-6X-His-C-terminus (SHHc), we first made pK7-SHHc by PCR amplifying the 2X-SII-HA-6X-His C-terminal (SHHc) tag from pB7-SHHc (Huang et al., 2016b) and digesting pK7FWG2 (Karimi et al., 2002) with BstXI and KpnI. The PCR fragment containing the SHHc tag was combined with the

digested backbone using In-Fusion HD cloning (Clontech, Mountain View, California) to make pK7-SHHc. Venus was cloned from plasmid mVENUS C1 (Koushik et al., 2006) using primers pDAN0869 and pDAN0870 and recombined with pK7SHHc digested with AvrII using In-Fusion HD cloning (Clontech, Mountain View, California) to generate pK7-VEN-SHHc.

pENTR-no stop clones of COR27 and COR28 were generated by amplifying the coding sequences of COR27 (AT5G24900.1) and COR28 (AT4G33980.1) using primers pDAN1906/pDAN1908, and pDAN1909/pDAN1911, respectively (**Table S4.5**). The resulting amplicons were cloned into NotI/AscI-digested pENTR-MCS through In-Fusion HD cloning (Clontech, Mountain View, California) to make pENTR-COR27-no stop and pENTR-COR28-no stop. To generate pK7-RVE8-VEN-SHHc, pK7-LNK1-VEN-SHHc, pK7-COR27-VEN-SHHc, and pK7-COR28-VEN-SHHc, the pENTR-no stop versions of these genes were recombined to the pK7-VEN-SHHc binary vector using LR Clonase (Thermofisher). These C-terminally tagged proteins are driven from the CaMV35S promoter. To generate the dual luciferase reporter pGreenII 0800-LUC-TOC1p, 2098 bp of the TOC1 promoter was cloned using primers pDAN2735/pDAN2736 (**Table S4.5**) and inserted via In-Fusion HD cloning (Clontech, Mountain View, California) into the pGreenII 0800-LUC plasmid (Hellens et al., 2005) digested with BamHI. The resulting vector (pGreenII 0800-LUC-TOC1p) constitutively expresses renilla luciferase from the CaMV35S promoter and contains the gene for firefly luciferase driven by the TOC1 promoter.

To generate yeast 2-/3-hybrid vectors, the gene of interest was cloned from its pENTR-STOP template using primers pDAN2349/pDAN2350 (**Table S4.5**) and

recombined into pGADT7 digested with EcoRI using In-Fusion HD cloning (Clontech, Mountain View, California). For cloning into pGBKT7, primers pDAN2347/pDAN2348 (**Table S4.5**) were used to clone off the pENTR-STOP template and recombine into BamHI-digested pGBKT7 using In-Fusion HD cloning (Clontech, Mountain View, California). For cloning into the pBridge vector (Clontech, Mountain View, California), the gene of interest was cloned from its pENTR-STOP template using primers pDAN2441/pDAN2442 (**Table S4.5**) and recombined into the first MCS of pBridge digested with EcoRI using In-Fusion HD cloning (Clontech, Mountain View, California) or using primers pDAN2443/pDAN2444 (**Table S4.5**) to recombine into the second MCS of pBridge digested with BglII using In-Fusion HD cloning (Clontech, Mountain View, California).

Affinity Purification. Affinity purification was performed as detailed in Sorkin and Nusinow (2022). Briefly, affinity-tagged lines were plated on 1/2x MS + 1% Sucrose and grown for 10 days under LD 22 ℃ conditions. On day 10 of growth, tissue was harvested at either ZT5 or ZT9. To extract protein, powdered tissue was resuspended in SII buffer (100 mM sodium phosphate, pH 8.0, 150 mM NaCl, 5 mM EDTA, 5 mM EGTA, 0.1% Triton X-100, 1 mM PMSF, 1x protease inhibitor mixture (Roche, Basel, Switzerland), 1x Phosphatase Inhibitors II & III (Sigma- Aldrich), and 5 µM MG132 (Peptides International, Louisville, KY)) and sonicated using a duty cycle of 20 s (2 s on, 2 s off, total of 40 s) at 50% power. Extracts were clarified of cellular debris through 2x centrifugation for 10 min at ≥20,000 × g at 4 °C.

For HFC-tagged samples, clarified extracts were incubated with FLAG-M2-conjugated Protein G Dynabeads (Thermo Fisher Scientific, Waltham, Massachusetts) for one hour. Captured proteins were eluted off FLAG beads using 500 µg/mL 3x-FLAG peptide (Sigma-Aldrich). Eluted proteins were then incubated with Dynabeads His-Tag Isolation and Pulldown (Thermo Fisher Scientific, Waltham, Massachusetts) for 20 minutes and then washed 5 x 1 minute in His-tag Isolation Buffer (100 mM Na-phosphate, pH 8.0, 150 mM NaCl, 0.025% Triton X-100). Washed bead pellet was washed 4x in 25mM ammonium bicarbonate and flash frozen in liquid N_2.

For YFP-COR27 and GFP-COR28, clarified extracts were incubated with GFP-TRAP Magnetic Agarose affinity beads (ChromoTek GmbH, Planegg-Martinsried, Germany) for one hour. Captured proteins were washed 3 x 1 minute in His-tag Isolation Buffer (100 mM Na-phosphate, pH 8.0, 150 mM NaCl, 0.025% Triton X-100) and 4x in 25mM ammonium bicarbonate and then flash frozen in liquid N_2.

LCMS/MS analysis of AP samples. Samples on affinity beads were resuspended in 50 mM ammonium bicarbonate, reduced (10 mM TCEP) and alkylated (25 mM Iodoacetamide) followed by digestion with Tryspin at 37°C overnight. Digest was separated from beads using a magnetic stand and acidified with 1%TFA before cleaned up with C18 tip (Thermo Fisher Scientific, Waltham, Massachusetts). The extracted peptides were dried down and each sample was resuspended in 10 µL 5% ACN/0.1% FA. 5 µL was analyzed by LC-MS with a Dionex RSLCnano HPLC coupled to a Orbitrap Fusion Lumos mass spectrometer (Thermo Fisher Scientific, Waltham, Massachusetts)

using a 2h gradient. Peptides were resolved using 75 µm x 50 cm PepMap C18 column (Thermo Fisher Scientific, Waltham, Massachusetts).

Peptides were eluted at 300 nL/min from a 75 µm x 50 cm PepMap C18 column (Thermo Scientific) using the following gradient: Time = 0–4 min, 2% B isocratic; 4–8 min, 2–10% B; 8–83 min, 10–25% B; 83–97 min, 25–50% B; 97–105 min, 50–98%. Mobile phase consisted of A, 0.1% formic acid; mobile phase B, 0.1% formic acid in acetonitrile. The instrument was operated in the data-dependent acquisition mode in which each MS1 scan was followed by Higher-energy collisional dissociation (HCD) of as many precursor ions in 2 second cycle (Top Speed method). The mass range for the MS1 done using the FTMS was 365 to 1800 m/z with resolving power set to 60,000 @ 400 m/z and the automatic gain control (AGC) target set to 1,000,000 ions with a maximum fill time of 100 ms. The selected precursors were fragmented in the ion trap using an isolation window of 1.5 m/z, an AGC target value of 10,000 ions, a maximum fill time of 100 ms, a normalized collision energy of 35 and activation time of 30 ms. Dynamic exclusion was performed with a repeat count of 1, exclusion duration of 30 s, and a minimum MS ion count for triggering MS/MS set to 5000 counts.

APMS Data Analysis. MS data were converted into mgf. Database searches were done using Mascot (Matrix Science, London, UK; v.2.5.0) using the TAIR10 database (20101214, 35,386 entries) and the cRAP database (http://www.thegpm.org/cRAP/) and assuming the digestion enzyme trypsin and 2 missed cleavages. Mascot was searched with a fragment ion mass tolerance of 0.60 Da and a parent ion tolerance of 10 ppm. Oxidation of methionine and carbamidomethyl of cysteine were specified in Mascot as

variable modifications. Scaffold (Proteome Software Inc., Portland, OR; v.4.8) was used to validate MS/MS based peptide and protein identifications. Peptide identifications were accepted if they could be established at greater than 95.0% probability by the Peptide Prophet algorithm (Keller et al., 2002) with Scaffold delta-mass correction. The Scaffold Local FDR was used and only peptides probabilities with FDR <1% were used for further analysis. Protein identifications were accepted if they could be established at greater than 99.9% probability as assigned by the Protein Prophet algorithm (Nesvizhskii et al., 2003). Proteins that contained similar peptides and could not be differentiated based on MS/MS analysis alone were grouped to satisfy the principles of parsimony. Proteins sharing significant peptide evidence were grouped into clusters. Only the proteins identified with ≥ 2 unique peptides were further used in the analysis, except when proteins with only one peptide were identified in more than one replicate.

Yeast 2-Hybrid (Y2H) and Yeast 3-Hybrid Assays. We used the GAL4-based Matchmaker Gold Yeast 2-Hybrid System (Clontech, Mountain View, California) for all Y2H and Y3H assays. All transformations were performed as detailed in the Yeast Protocols Handbook (Clontech, Mountain View, California). For Y2H, bait proteins were cloned into the pGBKT7 vector which encodes the GAL4 DNA binding domain and then transformed into the Y2H Gold strain (Clontech, Mountain View, California) and plated on SD/-Trp to select for positive transformants. Prey proteins were cloned into the pGADT7 vector which encodes the GAL4 activation domain, transformed into the Y187 strain (Clontech, Mountain View, California), and plated on SD/-Leu to select for positive transformants. All matings were performed as detailed in the Yeast Protocols Handbook

(Clontech, Mountain View, California) using the 96-well plate format. Mated diploids were selected for on SD/-Leu/-Trp media. Single colonies of mated bait + prey strains were resuspended in YPDA and plated on SD/-Leu-Trp or SD/-Leu-Trp-His plates.

For Y3H, bait and linker proteins were cloned into the appropriate position of the pBridge vector (Clontech, Mountain View, California), which encodes a GAL4 DNA binding domain and a linker protein, transformed into the Y2H Gold strain, and plated on SD/-Trp to select for positive transformants. pBridge strains were mated with pGADT7 prey strains and plated on SD/-Trp/-Leu to select for diploids. Single colonies of mated strains were resuspended in YPDA plated on SD/-Leu-Trp or SD/-Leu-Trp-His plates.

Luciferase Reporter Assays. Individual 6-day-old seedlings expressing a CCA1::LUC reporter grown under LD cycles at 22℃ were arrayed on 1/2x MS + 1% Sucrose plates and sprayed with 5mM luciferin (GoldBio, Olivette, MO) prepared in 0.01% (v/v) Triton X-100 (Millipore Sigma-Aldrich, St. Louis, MO). Plants were transferred to an imaging chamber set to the appropriate free-run or entrainment program and images were taken every 60 minutes with an exposure of 10 minutes after a 3-minute delay after lights-off to diminish signal from delayed fluorescence using a Pixis 1024 CCD camera (Princeton Instruments, Trenton, NJ). Images were processed to measure luminescence from each plant using the Metamorph imaging software (Molecular Devices, Sunnyvale, CA). Circadian period was calculated using fast Fourier transformed nonlinear least squares (FFT-NLLS) (Plautz et al., 1997) using the Biological Rhythms Analysis Software System 3.0 (BRASS) available at http://www.amillar.org.

***N. benthamiana* Transient Transformation.** Transient transformation of 3-4 week-old *Nicotiana benthamiana* plants was performed as in (Lasierra and Prat, 2018). Briefly, overnight saturated cultures of *Agrobacterium tumefaciens* strain GV3101 carrying pGreenII 0800-LUC-TOC1p, pK7-RVE8-VEN-SHHc, pK7-LNK1-VEN-SHHc, pK7-COR27-VEN-SHHc, pK7-COR28-VEN-SHHc, or 35S::P19-HA (Chapman et al., 2004) were pelleted and resuspended in 5 mL of resuspension buffer (10mM $MgSO_4$, 10mM MES (pH 5.8), 150 µM Acetosyringone) for 2-3 hours. Cultures were diluted to OD_{600}= 0.4 in resuspension buffer and inoculation mixtures were prepared by mixing the selected constructs together with the volume of 35S::P19-HA being varied to ensure that an equal amount of agrobacteria was added to each mixture relative to the reporter, regardless of the total number of effectors being introduced. Mixtures were inoculated into one quadrant of a mature leaf per one mixture. Four different mixtures could be inoculated into a single leaf. Three leaves per plant were inoculated and four plants were used for a total of 12 biological replicates per mixture.

Dual-Luciferase Assay. The dual luciferase assay was performed using the Dual-Glo Luciferase Assay System (Promega, Madison, Wisconsin). Briefly, 3-4 week-old tobacco plants were inoculated with *Agrobacterium tumefaciens* expressing pGreenII 0800-LUC-TOC1p and a combination of other proteins: pK7-RVE8-VEN-2x-StrepII-HA-6X-His-C-terminus (SHHc), pK7-LNK1-VEN-SHHc, pK7-COR27-VEN-SHHc, or pK7-COR28-VEN-SHHc. This reporter firefly luciferase driven by the 3 leaf disks were collected per infiltration site from 3-day-post-infiltrated tobacco plants and frozen in liquid N_2. Tissue was homogenized and resuspended in 200 µL of Cell Culture Lysis Reagent

(100 mM potassium phosphate, pH 7.8, 1 mM EDTA, 7mM 2-mercaptoethanol, 1% Triton X-100, 10% glycerol). Lysates were centrifuged at max speed for 5 minutes and 5 µL of undiluted extract was used for the Dual Luciferase Assay input. 40 µL of Luciferase Assay Buffer was added to undiluted extract in a black 96-well plate and incubated for at least 10 minutes. Luminescence was measured over a 10-minute exposure using a Pixis 1024 CCD camera (Princeton Instruments, Trenton, NJ). 40 µL of Stop & Glo Reagent was added to wells to quench the firefly luciferase signal and provide the substrate for renilla luciferase. After at least 10 minutes incubation, luminescence was measured over a 10-minute exposure using the CCD camera. Firefly luciferase signal was divided by renilla signal to calculate normalized luminescence.

Densitometry Analysis. Densitometry analysis was performed in FIJI (https://imagej.net/software/fiji/) on high resolution (600 dpi), greyscale images of Western blots captured with the same exposure time. Mean grey value was measured from ROIs of equal area for each protein band and for background regions as well as for loading controls (Ponceau S stain) and loading control background regions. Inverted pixel density of background regions was subtracted from the inverted pixel density of protein bands and loading controls to generate the net pixel density value. To calculate normalized abundance, the ratio of the net protein band value over the net loading control value was taken.

Quantitative RT-PCR. Seedlings were gas sterilized and grown on 1/2x MS + 1% Sucrose plates with Whatman filter paper under 12 hr light: 12 hr dark, 22 ℃ conditions.

On day 7 of growth at ZT10, plates were transferred to a different chamber set to either 22 ℃ or 4 ℃ for two hours. Tissue was collected at ZT12. Total RNA was extracted from powdered tissue using the RNeasy Plant Mini kit (Qiagen, Hilden, Germany). 1 µg of total RNA was used as the template to synthesize cDNA using the iScript RT-PCR kit (Bio-Rad, Carlsbad, CA). qPCR was performed with the SYBR Green I nucleic acid gel stain (Sigma-Aldrich) using a QuantStudio 5 Real-Time PCR System (ThermoFisher). PCR was set up as follows: 3 min at 95˚C, followed by 40 cycles of 10 s at 95˚C, 10 s at 55˚C and 20 s at 72˚C. A melting curve analysis was conducted right after all PCR cycles are done. APA1 (At1g11910), expression of which remain stable during the diurnal cycle, was used as the normalization control. Primers for qPCR are listed in **Table S4.5**.

4.6 Acknowledgements

We acknowledge support by the National Science Foundation under Grant No. DBI-1827534 for acquisition of the Orbitrap Fusion Lumos LC-MS/MS and from the NIH award 5R01GM141374 to DAN. MLS was supported by NSF GRF award DGE-1745038 and by the William H. Danforth Plant Science Fellowship from the Donald Danforth Plant Science Center. This study was also supported by the German Research Foundation (DFG) under Germany's Excellence Strategy (CIBSS - EXC 2189 – Project ID 390939984) and DFG grant HI 1369/6-1 to AH and by Agencia Nacional de Promoción Científica y Tecnológica (ANPCyT) to MJY.

4.7 Relative Contributions

MLS, NK, AH, MJY, AR, BSE and DAN designed the research project. The research was performed by MLS, ST, and RB. AR contributed new analysis to the chapter. MLS, ST, and DAN wrote the chapter.

4.8 Supplemental Material

Supplemental Dataset 4.1. Full APMS dataset for RVE8-HFC, LNK1-HFC, LNK2-HFC, YFP-COR27, and GFP-COR28. (this file is provided as a separate attachment).

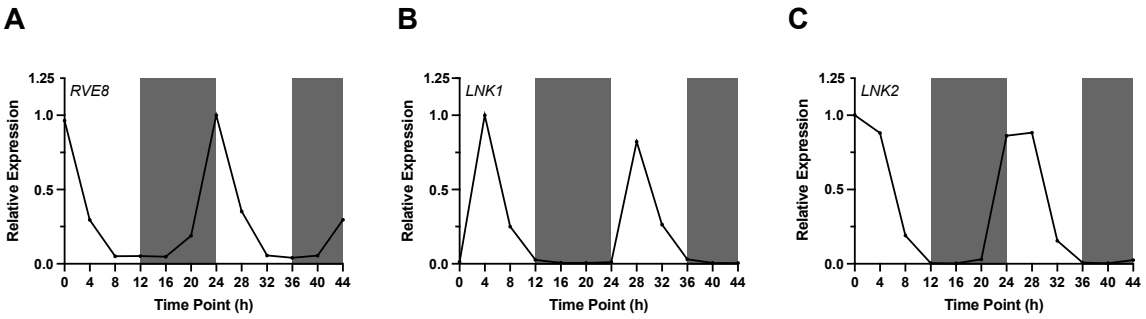

Figure S 4.1 mRNA expression patterns of RVE8, LNK1, and LNK2 under photocycles (12 hr light: 12 hr dark).
White and dark grey shading indicates lights-on and lights-off, respectively. Microarray data from diurnal.mocklerlab.com.

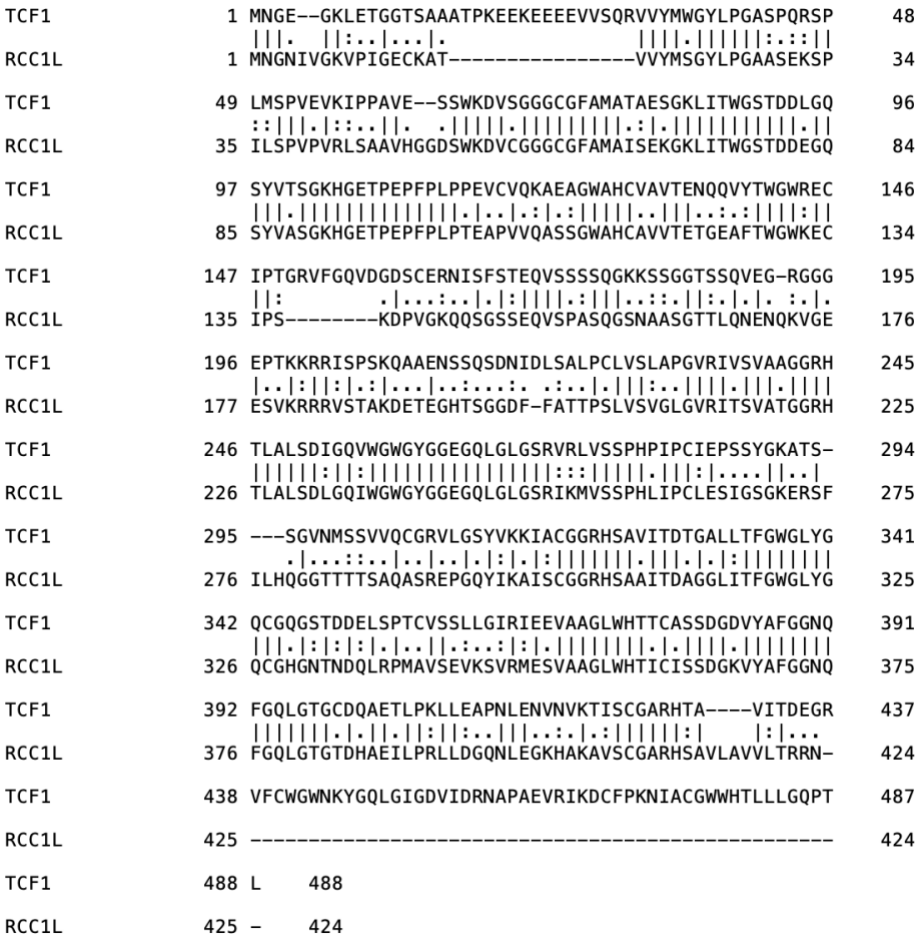

Figure S 4.2 Protein alignment of TCF1 (AT3G55580) and RCC1L (AT3G53830).
Protein sequences were aligned using the needle algorithm using the EBLOSUM62 matrix, a gap penalty of 10.0, and an extend penalty of 0.5. Sequences share 49.7% identity.

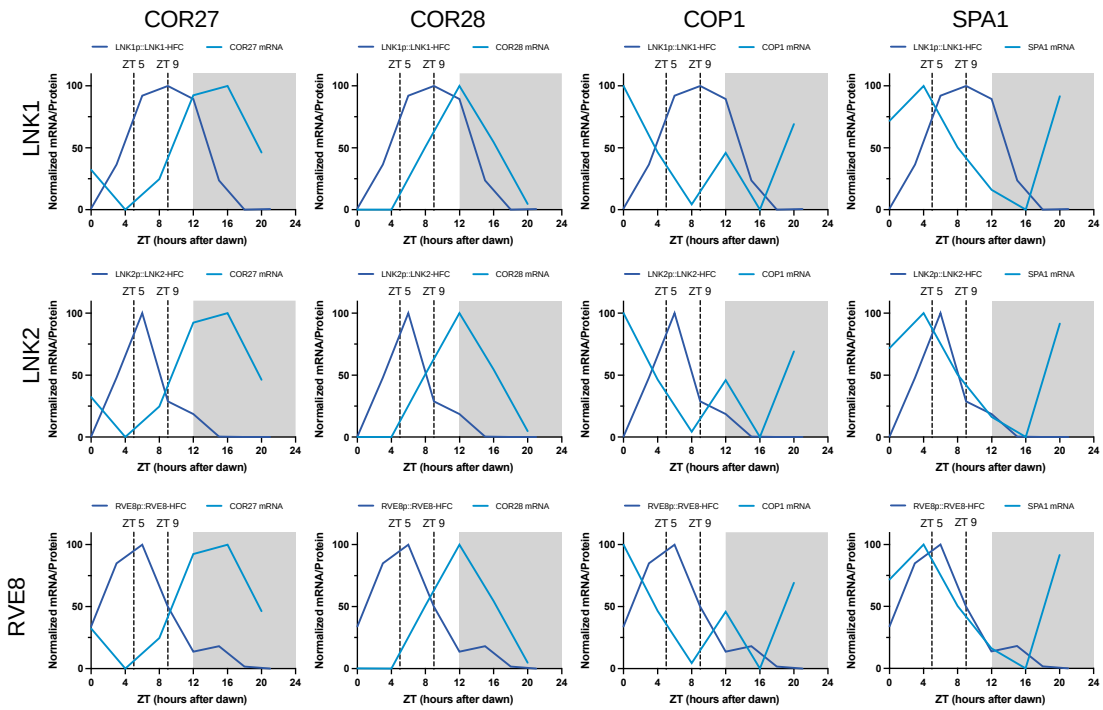

Figure S 4.3 Comparison of HFC-tagged protein abundance with *COR27/28*, *COP1*, and *SPA1* mRNA expression profiles.
24-hour (12 hr light: 12 hr dark, 22 ℃ (LDHH)) protein abundance (dark blue) is quantified from Western blots shown in Figure 4.1D-F. LDHH mRNA data from diurnal.mocklerlab.com (light blue) is overlayed. Vertical dotted lines show the time of day when tissue was collected for APMS. White and grey shading indicated lights-on and lights-off, respectively.

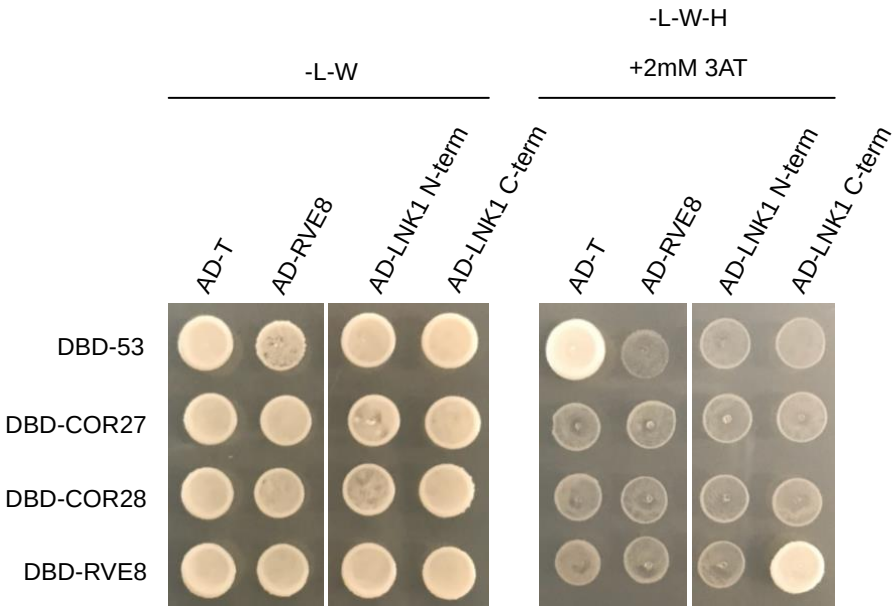

Figure S 4.4 COR27/28 do not interact with RVE8 or LNK1 in a binary Y2H system
Yeast strains Y2H Gold or Y187 expressing pGBKT7 (Gal4-DBD) or pGADT7 (Gal4-AD), respectively, were mated and plated onto selective media. Successful matings were able to grow on -Leucine/-Tryptophan media (-L-W) while positive interactors can grow on -Leucine/-Tryptophan/-Histidine + 2mM 3-amino-1,2,4-triazole (3AT) (-L-W-H +3AT). Only the positive controls DBD-53 (p53) + AD-T (large T-antigen protein) and DBD-RVE8 + AD-LNK1 C-term show an interaction.

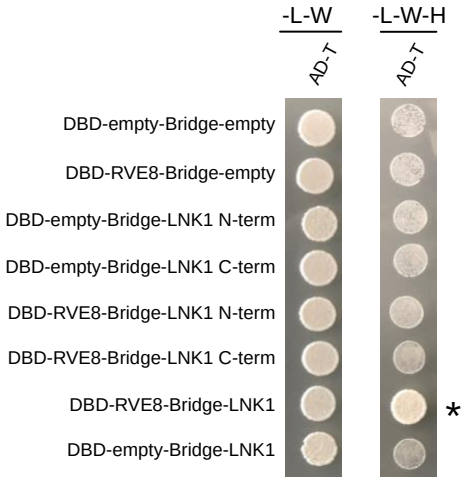

Figure S 4.5 Full-length LNK1 auto-activates in yeast when paired with a DBD-containing protein

Yeast strains Y2H Gold or Y187 expressing pBridge (Gal4-DBD and a Bridge protein) or pGADT7 (Gal4-AD), respectively, were mated and plated onto selective media. Successful matings were able to grow on -Leucine/-Tryptophan media (-L-W). Full length LNK1 (bridge protein, no AD domain) paired with the transcription factor RVE8 (*) can aberrantly activate the expression of the histidine biosynthesis reporter, allowing it to grow on -Leucine/-Tryptophan/-Histidine (-L-W-H) when paired with the negative control large T-antigen protein (T). LNK1 N- and C-terminal truncations do not autoactivate.

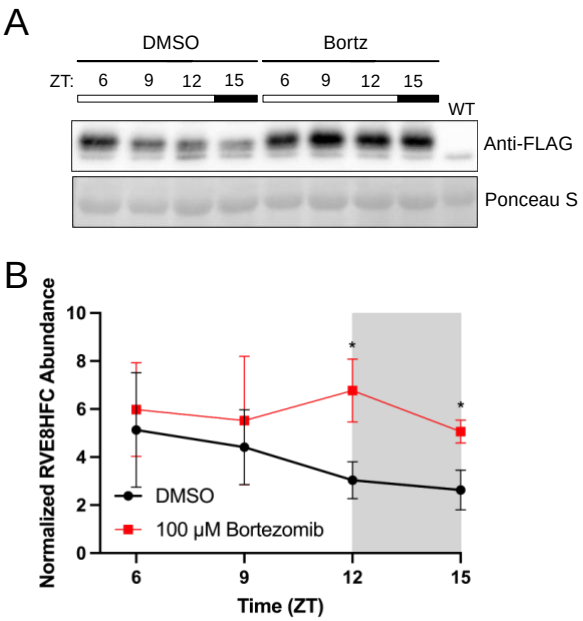

Figure S 4.6 RVE8-HFC protein abundance patterns are regulated by the 26S proteasome

(A) Representative Western blot showing protein expression patterns of RVE8-HFC plants treated with DMSO or 100 µM bortezomib. At ZT5, 12-day-old seedlings growing under 12 hr light: 12 hr dark, 22 ℃ conditions were immersed in 1/2X MS media containing either 100 µM bortezomib or DMSO. Tissue was collected every 3 hours starting at ZT6. RVE8-HFC was detected with anti-FLAG and Ponceau S staining was used to show loading. (B) Densitometry quantification of RVE8-HFC abundance in (A) normalized to Ponceau S. Points represent the average normalized RVE8-HFC abundance from 3 independent bioreps. Asterisks indicate significant differences between genotypes based on Welch's t-test (* $p<0.05$). Error bars = SD. White and grey shading indicate lights-on and lights-off, respectively. ZT= Zeitgeber Time.

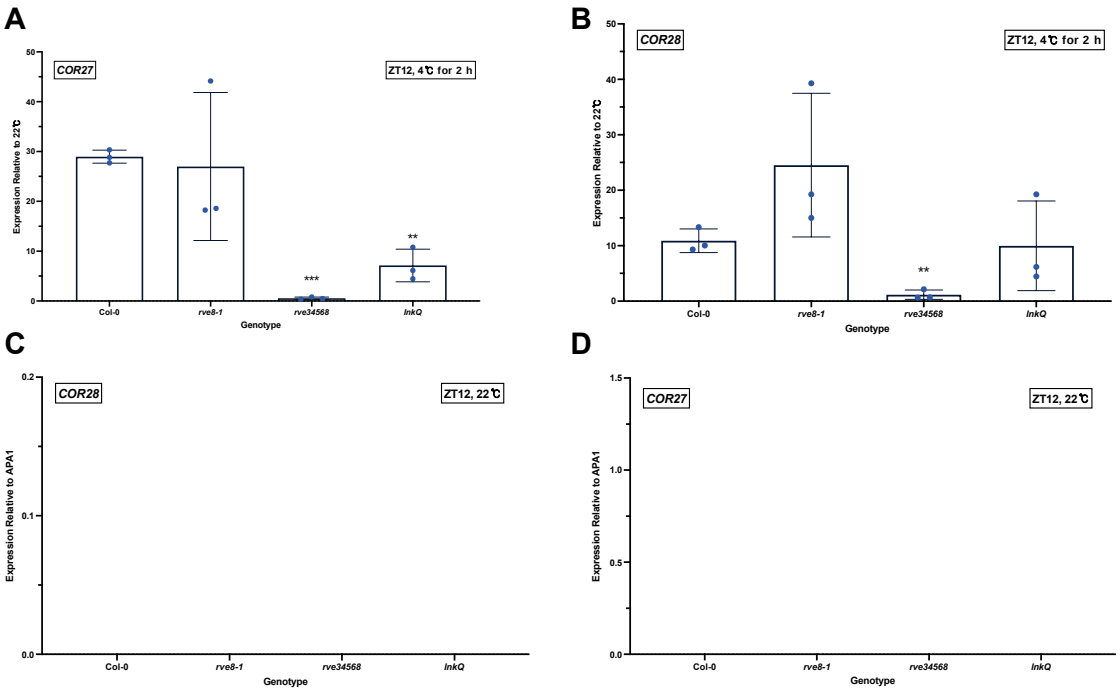

Figure S 4.7 The RVEs and LNKs are important for cold induction of *COR27/28*. Seedlings were grown on 1/2X MS + 1% sucrose for seven days under 12 hr light; 12 hr dark 22 ℃ conditions and then transferred at ZT10 to either 22 ℃ or 4 ℃ for two hours and tissue was collected at ZT12. (A-B) show the induction of *COR27/28* expression at 4 ℃ compared to 22 ℃. Figures (C-D) show *COR27/28* expression levels at 22 ℃. Expression was normalized to the endogenous control gene APA1. Bars show average expression with error bars = SD from 3 independent bioreps (points) for each genotype. Asterisks indicate significant differences as determined by Welch's t-test (** p<0.01, *** P<0.001).

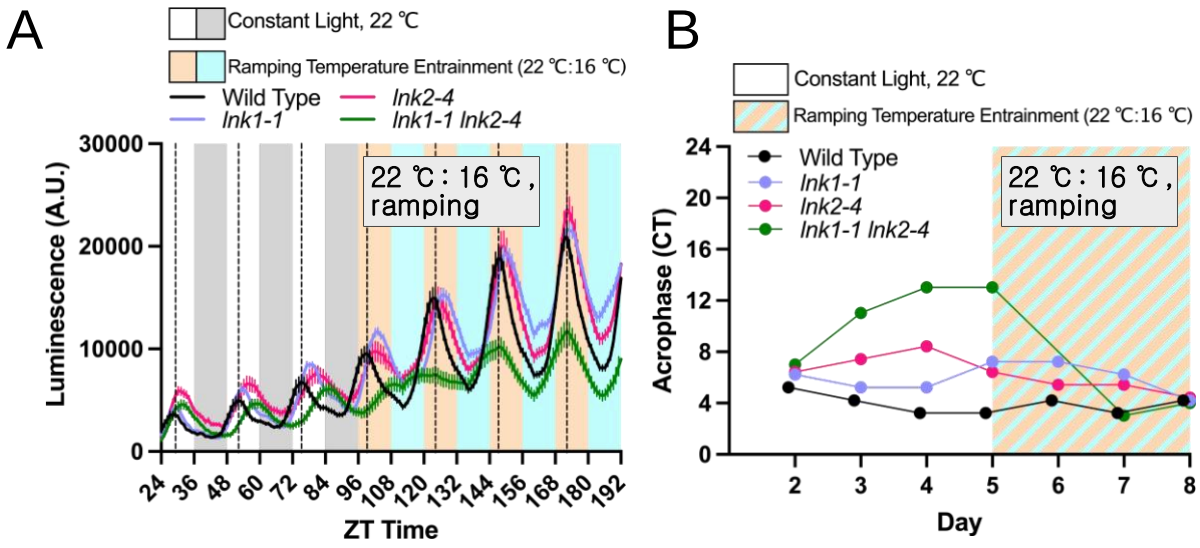

Figure S 4.8 LNK1/2 mutants are also impaired in temperature entrainment under ramping temperature cycles

(A) Luminescence from 7-day-old plants entrained under 12 hr light: 12 hr dark, 22 ℃ conditions expressing a CCA1p::LUC reporter was imaged for at least 3 days in continuous light and temperature (22 ℃) before the chamber was switched to a ramping temperature entrainment program that gradually oscillated between a low temperature of 16 ℃ at ZT16 and a high of 22 ℃ at ZT4. Lines represent the average luminescence from n=16 seedlings with errors bars = SEM. Vertical dotted lines correspond to the peak expression time (acrophase) of the CCA1p::LUC reporter in wild type plants. (B) Acrophase, or time of peak reporter expression, is plotted for each genotype for each day of imaging in constant light and the temperature entrainment condition. Each point represents the acrophase of the averaged luminescence trace shown in (A). CT = Circadian Time. A.U. = Arbitrary Units. ZT= Zeitgeber Time.

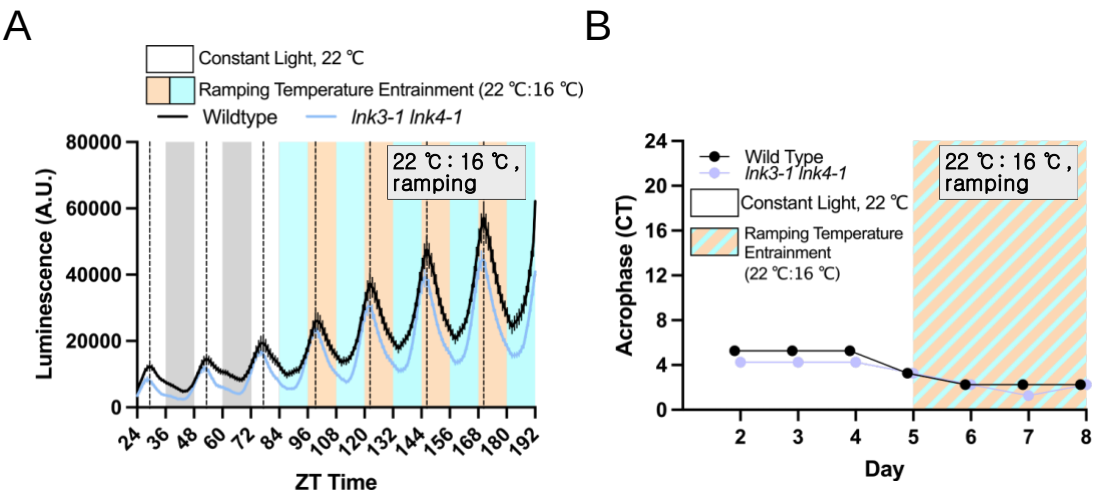

Figure S 4.9 *lnk3/4* mutants are not impaired in temperature entrainment
(A) Luminescence from 7-day-old plants expressing a CCA1p::LUC reporter were grown for at least 3 days in continuous light and temperature (22 ℃) before the chamber was switched to a ramping temperature entrainment program that gradually oscillates between a low temperature of 16 ℃ at ZT16 and a high of 22 ℃ at ZT4. Lines represent the average luminescence from n=16 seedlings with errors bars = SEM. Vertical dotted lines correspond to the peak expression time of the CCA1p::LUC reporter in wild type plants. (B) Acrophase, or time of peak reporter expression, is plotted for each genotype for each day of imaging in constant light and the temperature entrainment condition. Each point represents the acrophase of the averaged luminescence trace shown on the right. CT = Circadian Time. A.U. = Arbitrary Units. ZT=Zeitgeber Time.

Table S 4.1 Proteins coprecipitated with RVE8/LNK1/LNK2-HFC at ZT5.
Total spectra for a given coprecipitated protein is shown for each independent ZT5 sample. The curated table excludes coprecipitated proteins that were identified in the GFP-HFC or Col-0 negative control APMS experiments, see Dataset S1 for all identifications.

Protein Name	AGI Locus Number	M.W. (kDa)	LNK1HFC_ ZT5_1	LNK1HFC_ ZT5_2	LNK2HFC_ ZT5_1	LNK2HFC_ ZT5_2	RVE8HFC_ ZT5_1	RVE8HFC_ ZT5_2
LNK1	AT5G64170‡	70	173	56	0	0	107	87
LNK2	AT3G54500‡	81	0	0	468	497	154	149
RVE8	AT3G09600‡	40	22	13	206	223	272	267
RVE6	AT5G52660	36	28	14	79	87	0	0
TCF1	AT3G55580‡	51	16	8	37	39	7	4
RVE5	AT4G01280‡	34	16	8	27	33	0	0
RCC1L	AT3G53830‡	49	4	2	8	8	0	0
RVE4	AT5G02840‡	31	4	0	85	84	0	0
CCR16	AT1G02150‡	60	1	0	0	0	0	0
RVE3	AT1G01520‡	33	0	0	10	11	0	0
GRXS17	AT4G04950	53	0	0	10	9	0	0
UBP12	AT5G06600	131	0	0	8	9	0	0
UBP13	AT3G11910	131	0	0	6	7	1	0
RACK1A	AT1G18080‡	36	0	0	2	4	0	0
DGR2	AT5G25460‡	40	0	0	4	3	1	0
PICALM3	AT5G35200‡	61	0	0	4	2	0	0
TRA1A	AT2G17930	436	0	0	0	2	0	0
CAB4	AT3G47470‡	28	0	0	1	1	0	0
BTI1	AT4G23630‡	31	0	0	1	1	0	0
PUB12	AT2G28830‡	107	0	0	0	1	0	0
ABA1	AT5G67030‡	74	0	0	0	1	0	0
FLL2	AT1G01320‡	199	0	0	1	0	0	0
WLIM1	AT1G10200‡	21	0	0	1	0	0	0
FINS1	AT1G43670‡	37	0	0	1	0	0	0
PP2A-3	AT2G42500	36	0	0	1	0	0	0
Nucleic acid-binding, OB-fold-like protein	AT3G10090	7	0	0	1	0	0	0
CPNB2	AT3G13470‡	63	0	0	0	0	31	26
LNK3	AT3G12320‡	30	0	0	0	0	24	25
SAG24	AT1G66580‡	25	0	0	0	0	4	0
LNK4	AT5G06980	32	0	0	0	0	3	3
ATRH3	AT5G26742	81	0	0	0	0	1	0

‡Indicates mRNA is circadian regulated in constant light according to analysis in Romanowski et al. (2020) The Plant Journal

Table S 4.2 Identified proteins coprecipitated with RVE8/LNK1/LNK2-HFC at ZT9
Total spectra for a given coprecipitated protein is shown for each independent ZT9 sample. The curated table excludes coprecipitated proteins that were identified in the GFP-HFC or Col-0 negative control APMS experiments, see Dataset S1 for all identifications.

Protein Name	AGI Locus Number	M.W. (kDa)	LNK1HFC_Z T9_1	LNK1HFC_Z T9_2	LNK2HFC_Z T9_1	LNK2HFC_Z T9_2	RVE8HFC_Z T9_1	RVE8HFC_Z T9_2
LNK1	AT5G64170‡	70	435	621	0	0	66	90
LNK2	AT3G54500‡	81	0	0	140	151	109	137
RVE8	AT3G09600‡	40	71	101	33	52	285	317
RVE6	AT5G52660	36	86	113	21	22	4	3
RVE5	AT4G01280‡	34	32	51	12	12	0	0
TCF1	AT3G55580‡	51	32	49	20	30	13	13
RVE4	AT5G02840‡	31	31	43	0	7	0	0
RCC1L	AT3G53830‡	49	20	25	3	10	0	0
COR28	AT4G33980‡	26	11	15	6	6	26	29
RVE3	AT1G01520‡	33	8	10	0	0	0	0
CCR16	AT1G02150‡	60	3	8	0	0	0	1
TRA1A	AT2G17930	436	3	7	0	0	0	0
DGR2	AT5G25460‡	40	3	4	0	0	2	5
ENTH/ANTH/VHS superfamily protein	AT5G35200‡	61	2	3	0	0	0	0
FLL2	AT1G01320‡	199	0	3	0	0	0	1
Nucleic acid-binding, OB-fold-like protein	AT2G40660‡	42	3	2	0	0	0	0
UBP12	AT5G06600	131	0	1	0	0	0	0
PHOT2	AT5G58140	102	1	2	0	0	0	0
MLK4	AT3G13670‡	79	0	2	0	0	6	6
UBP13	AT3G11910	131	0	2	0	0	1	4
COR27	AT5G42900	27	2	1	0	1	4	7
WLIM1	AT1G10200‡	21	1	1	0	0	1	2
CAB4	AT3G47470‡	28	1	1	0	0	1	1
MLK2	AT3G03940	78	0	0	1	1	6	7
GRXS17	AT4G04950	53	0	0	0	0	1	2
CPNB2	AT3G13470‡	63	0	0	0	0	35	41
LNK3	AT3G12320‡	31	0	0	0	0	18	23
LNK4	AT5G06980	32	0	0	0	0	2	6
COP1	AT2G32950‡	76	0	0	0	0	3	4
MLK1	AT5G18190	77	0	0	0	0	3	4
SPA1	AT2G46340‡	115	0	0	0	0	1	4
MLK3	AT2G25760	76	0	0	0	0	3	0

‡Indicates mRNA is circadian regulated in constant light according to analysis in Romanowski et al. (2020) *The Plant Journal*

Table S 4.3 RCC1L (AT3G53830) expression is downregulated by cold treatment.
Data taken from Kidokoro et al. (2021) PNAS. Wild-type (Col-0) plants were transferred to 4 °C at LL2 (T=0; 2 hours after dawn) and tissue for RNA sequencing was collected at 3 hours and 12 hours after transfer to cold conditions. RCC1L is significantly downregulated after 12 hours under 4 °C treatment.

Condition	log fold change over T=0	adjusted p-value
3 hours at 4℃	-0.047	9.50E-01
12 hours at 4℃	-1.963	5.70E-39

Table S 4.4 Identified proteins coprecipitated with YFP-COR27/GFP-COR28 at ZT9.
Total spectra for a given coprecipitated protein is shown for each independent ZT9 sample. The curated table excludes coprecipitated proteins that were identified in the GFP-HFC or Col-0 negative control APMS experiments, see Dataset S1 for all identifications.

Protein Name	AGI Locus Number	M.W. (kDa)	YFP-COR27 _ZT9_1	YFP-COR27_ ZT9_2	YFP-COR27_ ZT9_3	YFP-COR27_ ZT9_4	GFP-COR28_ ZT9_1	GFP-COR28_ ZT9_2	GFP-COR28_ ZT9_3	GFP-COR28_ ZT9_4
COR27	AT5G42900	27	89	85	95	80	0	0	0	0
COR28	AT4G33980‡	26	0	0	0	0	22	18	8	10
COP1	AT2G32950‡	76	16	12	19	16	6	6	1	2
SPA1	AT2G46340‡	115	16	12	16	13	4	6	1	0
MLK4	AT3G13670‡	79	16	11	15	12	0	0	0	0
MLK2	AT3G03940	78	13	12	15	12	0	0	0	0
PHYD	AT4G16250	129	8	7	13	11	0	0	0	0
MLK1	AT5G18190	77	10	10	12	10	0	0	0	0
SPA4	AT1G53090	89	8	4	11	7	0	0	0	0
SPA2	AT4G11110	115	8	6	10	6	0	1	0	0
SF1	AT5G51300	87	7	12	7	5	0	0	0	0
RVE8	AT3G09600‡	40	7	5	7	6	3	4	0	3
LNK2	AT3G54500‡	81	6	5	6	3	0	1	0	0
MLK3	AT2G25760	76	5	6	6	8	0	0	0	0
LNK1	AT5G64170‡	70	4	4	5	4	4	3	1	0
SPA3	AT3G15354‡	93	4	4	4	4	0	0	0	0
RVE6	AT5G52660	36	3	3	4	1	1	0	0	0
RVE5	AT4G01280‡	34	1	1	2	0	1	0	0	0
CCR2	AT2G21660‡	17	1	0	1	1	0	0	0	0
TCF1	AT3G55580‡	51	0	0	1	0	0	0	0	0
PHYE	AT4G18130‡	123	1	0	0	0	0	0	0	0

‡Indicates mRNA is circadian regulated in constant light according to analysis in Romanowski et al. (2020) The Plant Journal

Table S 4.5 Oligonucleotides used in this study.

Description	Primer Name	Primer Sequence (5' -> 3')
RVE8 genomic cloning fwd	pDAN1127	GCAGGCTCCGCGGCCGCCCCCTTCACCATGAGCTCGTCGCCGTCA
RVE8 genomic cloning rev	pDAN1128	AGCTGGGTCGGCGCGCCCACCCTTTGCTGATTTGTCGCTTGTTGAG
RVE8 promoter cloning	pDAN1129	TCAAACACTGATAGTTTCAAAACAGTTAAAATGAAAAAATTG
RVE8 promoter cloning	pDAN1130	AACTTGTGATATCACTAGCGGTTATTTTTCAGATAAAGACA
LNK1 cDNA cloning fwd	pDAN0990	CACCATGGGTAGTGGAACAAACCATC
LNK1 cDNA cloning rev	pDAN0991	ATTGTTGTCACTTGTTACAACTTCTG
LNK2 cDNA cloning fwd	pDAN1066	GCAGGCTCCGCGGCCGCCCCCTTCACCATGTTTGATTGGGAAGAAGAAGAG
LNK2 cDNA cloning rev	pDAN1067	AGCTGGGTCGGCGCGCCCACCCTTCAATTTTCTTTTGTTTCCTTGGG
LNK1 promoter cloning fwd	pDAN1016	TCAAACACTGATAGTTTGATCAAAGGATCTCTCCCGGC
LNK1 promoter cloning rev	pDAN1017	AACTTGTGATATCACTAGATTCCTCCCAACTTCAGACTC
LNK2 promoter cloning fwd	pDAN1018	TCAAACACTGATAGTTTGTGGCCCTTCTTGTGCTGCA
LNK2 promoter cloning rev	pDAN1019	CTCAGTTCTAATATCCAATCCTAGA
mVenus cloning fwd	pDAN0869	CTTGTACAAAGTGGTGCGAATGGTGAGCAAGGGCGAGG
mVenus cloning rev	pDAN0870	GGCTCCAGCTTCCACCCCTAGACTTGTACAGCTCGTCCA
COR27 cDNA cloning fwd	pDAN1906	GCAGGCTCCGCGGCCGCCCCCTTCACCATGGTTGGTGATTACAGA
COR27 cDNA cloning rev	pDAN1908	AGCTGGGTCGGCGCGCCCACCCTTAGAAACAGACTTCAAATTTACG
COR28 cDNA cloning fwd	pDAN1909	GCAGGCTCCGCGGCCGCCCCCTTCACCATGGAGAATGATTGCACG
COR28 cDNA cloning rev	pDAN1911	AGCTGGGTCGGCGCGCCCACCCTTACGAAAACAAACACCAATCCTA
TOC1 promoter cloning fwd	pDAN2736	GCAGCCCGGGGGATCCTTCTCTGAGGAATTTCATCAAACA
TOC1 promoter cloning rev	pDAN2735	TAGAACTAGTGGATCGATCAGATTAACAACTAAACCCACA
LNK1 cDNA N-terminus cloning fwd	pDAN1954	GCAGGCTCCGCGGCCGCCCCCTTCACCATGGGTAGTGGAACAAAC
LNK1 cDNA N-terminus cloning rev	pDAN2010	AGCTGGGTCGGCGCGCCCACCCTTTTACTTCTTCTCAAGATTTGCCTCT
LNK1 cDNA C-terminus fwd	pDAN2011	GCAGGCTCCGCGGCCGCCCCCTTCACCATGACTGATCATCTTCAT
LNK1 cDNA C-terminus rev	pDAN1955	AGCTGGGTCGGCGCGCCCACCCTTTTAATTGTTGTCACTTGTTACAACT
Universal fwd cloning from pENTR for entry into pGBKT7 digested with BamHI	pDAN2347	GAATTCCCGGGGATCGCAGGCTCCGCGGCCGCC
Universal rev cloning from pENTR for entry into pGBKT7 digested with BamHI	pDAN2348	GCAGGTCGACGGATCAGCTGGGTCGGCGCGCCC
Universal fwd cloning from pENTR for entry into pGADT7 digested with EcoRI	pDAN2349	GGAGGCCAGTGAATTAGGCTCCGCGGCCGCC
Universal rev cloning from pENTR for entry into pGADT7 digested with EcoRI	pDAN2350	CACCCGGGTGGAATTAGCTGGGTCGGCGCGCCC
Universal fwd cloning from pENTR for entry into the first MCS of pBridge digested with EcoRI	pDAN2441	TGTATCGCCGGAATTAGGCTCCGCGGCCGCC

Universal rev cloning from pENTR for entry into the first MCS of pBridge digested with EcoRI	pDAN2442	GGATCCCCGGGAATTAGCTGGGTCGGCGCGCCC
Universal fwd cloning from pENTR for entry into the second MCS of pBridge digested with BglII	pDAN2443	ATTAGCCCGAAGATCAGGCTCCGCGGCCGCC
Universal rev cloning from pENTR for entry into the second MCS of pBridge digested with BglII	pDAN2444	ATCAGCCCGAAGATCAGCTGGGTCGGCGCGCCC
COR27 fwd qPCR	pDAN2838	CGCGTGACCACGACCAAATCAGCG
COR27 rev qPCR	pDAN2839	CATCTTCTTCGAGCTTCCGTTTTCGCC
COR28 fwd qPCR	pDAN2842	GGGAACTACTGTCCAAGGAGATG
COR28 rev qPCR	pDAN2843	TCATCGTTATTTGCTTCTCTTTCTC
APA1 fwd qPCR	pDAN0282	CTCCAGAAGAGTATGTTCTGAAAG
APA1 rev qPCR	pDAN0281	TCCCAAGATCCAGAGAGGTC

4.9 References

Alonso JM, Stepanova AN, Leisse TJ, Kim CJ, Chen H, Shinn P, Stevenson DK, Zimmerman J, Barajas P, Cheuk R, et al (2003) Genome-wide insertional mutagenesis of Arabidopsis thaliana. Science (80-) **301**: 653–657

Avello PA, Davis SJ, Ronald J, Pitchford JW (2019) Heat the Clock: Entrainment and Compensation in *Arabidopsis* Circadian Rhythms. J Circadian Rhythms **17**: 5

Blair EJ, Bonnot T, Hummel M, Hay E, Marzolino JM, Quijada IA, Nagel DH (2019) Contribution of time of day and the circadian clock to the heat stress responsive transcriptome in Arabidopsis. Sci Rep **9**: 4814

Chapman EJ, Prokhnevsky AI, Gopinath K, Dolja V V., Carrington JC (2004) Viral RNA silencing suppressors inhibit the microRNA pathway at an intermediate step. Genes Dev **18**: 1179–1186

Clough SJ, Bent AF (1998) Floral dip: A simplified method for Agrobacterium-mediated transformation of Arabidopsis thaliana. Plant J **16**: 735–743

Devlin PF, Kay SA (2001) CIRCADIAN PHOTOPERCEPTION. Annu Rev Physiol **63**: 677–694

Gray JA, Shalit-Kaneh A, Chu DN, Yingshan Hsu P, Harmer SL (2017) The REVEILLE Clock Genes Inhibit Growth of Juvenile and Adult Plants by Control of Cell Size. Plant Physiol **173**: 2308–2322

Hellens RP, Allan AC, Friel EN, Bolitho K, Grafton K, Templeton MD, Karunairetnam S, Gleave AP, Laing WA (2005) Transient expression vectors for functional genomics, quantification of promoter activity and RNA silencing in plants. doi: 10.1186/1746-4811-1-13

Hooper CM, Tanz SK, Castleden IR, Vacher MA, Small ID, Millar AH (2014) Data and text mining SUBAcon: a consensus algorithm for unifying the subcellular localization data of the Arabidopsis proteome. **30**: 3356–3364

Hsu PY, Devisetty UK, Harmer SL (2013a) Accurate timekeeping is controlled by a cycling activator in Arabidopsis. Elife **2**: e00473

Hsu PY, Devisetty UK, Harmer SL (2013b) Accurate timekeeping is controlled by a cycling activator in Arabidopsis. Elife. doi: 10.7554/eLife.00473

Huang H, Alvarez S, Bindbeutel R, Shen Z, Naldrett MJ, Evans BS, Briggs SP, Hicks LM, Kay SA, Nusinow DA, et al (2016a) Identification of Evening Complex Associated Proteins in Arabidopsis by Affinity Purification and Mass Spectrometry. Mol Cell Proteomics **15**: 201–217

Huang H, Yoo CY, Bindbeutel R, Goldsworthy J, Tielking A, Alvarez S, Naldrett MJ, Evans BS, Chen M, Nusinow DA (2016b) PCH1 integrates circadian and light-signaling pathways to control photoperiod-responsive growth in Arabidopsis. Elife **5**: 1–27

Ji H, Wang Y, Cloix C, Li K, Jenkins GI, Wang S, Shang Z, Shi Y, Yang S, Li X (2015) The Arabidopsis RCC1 Family Protein TCF1 Regulates Freezing Tolerance and Cold Acclimation through Modulating Lignin Biosynthesis. PLOS Genet **11**: e1005471

Kahle N, Sheerin DJ, Fischbach P, Koch LA, Schwenk P, Lambert D, Rodriguez R, Kerner K, Hoecker U, Zurbriggen MD, et al (2020) COLD REGULATED 27 and 28 are targets of CONSTITUTIVELY PHOTOMORPHOGENIC 1 and negatively affect phytochrome B signalling. Plant J **104**: 1038–1053

Karimi M, Inzé D, Depicker A (2002) GATEWAY^{TM} vectors for Agrobacterium-mediated plant transformation. Trends Plant Sci **7**: 193–195

Keller A, Nesvizhskii AI, Kolker E, Aebersold R (2002) Empirical statistical model to estimate the accuracy of peptide identifications made by MS/MS and database search. Anal Chem **74**: 5383–5392

Kidokoro S, Hayashi K, Haraguchi H, Ishikawa T, Soma F, Konoura I, Toda S, Mizoi J, Suzuki T, Shinozaki K, et al (2021) Posttranslational regulation of multiple clock-related transcription factors triggers cold-inducible gene expression in Arabidopsis. Proc Natl Acad Sci. doi: 10.1073/PNAS.2021048118

Koushik S V, Chen H, Thaler C, Puhl HL 3rd, Vogel SS (2006) Cerulean, Venus, and VenusY67C FRET reference standards. Biophys J **91**: L99–L101

Lasierra P, Prat S (2018) Transient Transactivation Studies in Nicotiana benthamiana Leaves. *In* L Oñate-Sánchez, ed, Two-Hybrid Syst. Methods Protoc. Springer New York, New York, NY, pp 311–322

de Leone MJ, Hernando CE, Romanowski A, García-Hourquet M, Careno D, Casal J, Rugnone M, Mora-García S, Yanovsky MJ, De Leone MJ, et al (2018) The LNK Gene Family: At the Crossroad between Light Signaling and the Circadian Clock. Genes (Basel) **10**: 2

de Leone MJ, Hernando CE, Vázquez M, Schneeberger K, Yanovsky MJ (2020)

Bacterial Infection Disrupts Clock Gene Expression to Attenuate Immune Responses. Curr Biol **30**: 1–8

Li B, Gao Z, Liu X, Sun D, Tang W (2019) Transcriptional Profiling Reveals a Time-of-Day-Specific Role of REVEILLE 4/8 in Regulating the First Wave of Heat Shock-Induced Gene Expression in Arabidopsis. Plant Cell **31**: 2353–2369

Li X, Liu C, Zhao Z, Ma D, Zhang J, Yang Y, Liu Y, Liu H (2020) COR27 and COR28 are Novel Regulators of the COP1-HY5 Regulatory Hub and Photomorphogenesis in Arabidopsis. Plant Cell Adv Publ. doi: 10.1105/tpc.20.00195

Li X, Ma D, Lu SX, Hu X, Huang R, Liang T, Xu T, Tobin EM, Liu H (2016) Blue Light- and Low Temperature-Regulated COR27 and COR28 Play Roles in the Arabidopsis Circadian Clock. Plant Cell **28**: 2755–2769

Ma Y, Gil S, Grasser KD, Mas P (2018) Targeted Recruitment of the Basal Transcriptional Machinery by LNK Clock Components Controls the Circadian Rhythms of Nascent RNAs in Arabidopsis. Plant Cell **30**: 907–924

Mikkelsen MD, Thomashow MF (2009) A role for circadian evening elements in cold-regulated gene expression in Arabidopsis. Plant J **60**: 328–339

Mizuno T, Takeuchi A, Nomoto Y, Nakamichi N, Yamashino T (2014) The LNK1 night light-inducible and clock-regulated gene is induced also in response to warm-night through the circadian clock nighttime repressor in Arabidopsis thaliana. Plant Signal Behav. doi: 10.4161/psb.28505

Mockler TC, Michael TP, Priest HD, Shen R, Sullivan CM, Givan SA, Mcentee C, Kay SA, Chory J (2007) The diurnal project: Diurnal and circadian expression profiling, model-based pattern matching, and promoter analysis. Cold Spring Harb Symp Quant Biol **72**: 353–363

Nesvizhskii AI, Keller A, Kolker E, Aebersold R (2003) A statistical model for identifying proteins by tandem mass spectrometry. Anal Chem **75**: 4646–4658

Pérez-García P, Ma Y, Yanovsky MJ, Mas P (2015) Time-dependent sequestration of RVE8 by LNK proteins shapes the diurnal oscillation of anthocyanin biosynthesis. Proc Natl Acad Sci U S A **112**: 5249–53

Plautz JD, Kaneko M, Hall JC, Kay SA (1997) Independent photoreceptive circadian clocks throughout Drosophila. Science **278**: 1632–1635

Rawat R, Takahashi N, Hsu PY, Jones MA, Schwartz J, Salemi MR, Phinney BS, Harmer SL (2011) REVEILLE8 and PSEUDO-REPONSE REGULATOR5 Form a Negative Feedback Loop within the Arabidopsis Circadian Clock. PLoS Genet **7**: e1001350

Ren X, Jiang K, Zhang F (2020) The Multifaceted Roles of RCC1 in Tumorigenesis. Front Mol Biosci **7**: 225

Romanowski A, Schlaen RG, Perez-Santangelo S, Mancini E, Yanovsky MJ (2020) Global transcriptome analysis reveals circadian control of splicing events in Arabidopsis thaliana. Plant J **103**: 889–902

Rugnone ML, Soverna AF, Sanchez SE, Schlaen RG, Hernando CE, Seymour DK,

Mancini E, Chernomoretz A, Weigel D, Mas P, et al (2013) LNK genes integrate light and clock signaling networks at the core of the Arabidopsis oscillator. Proc Natl Acad Sci U S A **110**: 12120–12125

Salomé PA, Clung C (2005) What makes the Arabidopsis clock tick on time? A review on entrainment. Plant, Cell Environ **28**: 21–38

Salomé PA, Robertson Mcclung C (2005) PSEUDO-RESPONSE REGULATOR 7 and 9 Are Partially Redundant Genes Essential for the Temperature Responsiveness of the Arabidopsis Circadian Clock. Plant Cell **17**: 791–803

Sorkin ML, Nusinow DA (2022) Using Tandem Affinity Purification to Identify Circadian Clock Protein Complexes from Arabidopsis. *In* D Staiger, S Davis, AM Davis, eds, Plant Circadian Networks Methods Protoc. Springer US, New York, NY, pp 189–203

Thines B, Harmon FG (2010) Ambient temperature response establishes ELF3 as a required component of the core Arabidopsis circadian clock. Proc Natl Acad Sci **107**: 3257–3262

Wang P, Cui X, Zhao C, Shi L, Zhang G, Sun F, Cao X, Yuan L, Xie Q, Xu X (2017) *COR27* and *COR28* encode nighttime repressors integrating *Arabidopsis* circadian clock and cold response. J Integr Plant Biol **59**: 78–85

Xie Q, Wang P, Liu X, Yuan L, Wang L, Zhang C, Li Y, Xing H, Zhi L, Yue Z, et al (2014) LNK1 and LNK2 Are Transcriptional Coactivators in the Arabidopsis Circadian Oscillator. Plant Cell **26**: 2843–2857

Zhou M, Zhang K, Sun Z, Yan M, Chen C, Zhang X, Tang Y, Wu Y (2017) LNK1 and LNK2 Corepressors Interact with the MYB3 Transcription Factor in Phenylpropanoid Biosynthesis 1. Plant Physiol **174**: 1348–1358

Zhou Y, Park SH, Soh MY, Chua NH (2021) Ubiquitin-specific proteases UBP12 and UBP13 promote shade avoidance response by enhancing PIF7 stability. Proc Natl Acad Sci U S A. doi: 10.1073/pnas.2103633118

Zhu W, Zhou H, Lin F, Zhao X, Jiang Y, Xu D, Deng XW (2020) COLD-REGULATED GENE 27 Integrates Signals from Light and the Circadian Clock to Promote Hypocotyl Growth in Arabidopsis. Plant Cell Adv Publ. doi: 10.1105/tpc.20.00192

5 Conclusions and Future Directions

5.1 Summary

My thesis work began with a proteomic screen to identify protein interactions for 11 core circadian clock factors: CIRCADIAN CLOCK ASSOCIATED 1 (CCA1), LATE ELONGATED HYPOCOTYL (LHY), PSEUDORESPONSE REGULATOR 5 (PRR5), PRR7, PRR9, TIMING OF CAB 1 (TOC1)/PRR1, FIONA 1 (FIO1), JUMONJI DOMAIN-CONTAINING 5 (JMJD5), NIGHT LIGHT-INDUCIBLE AND CLOCK-REGULATED 1 (LNK1), LNK2, and REVEILLE 8 (RVE8). While this is not an exhaustive list of the core components of the Arabidopsis circadian clock, we believe the protein-protein "interactome" produced from this work will serve as a useful resource for the plant circadian community. Our datasets have been uploaded to the STRING database (www.string-db.org), where users can visualize our data as a network using an interactive webtool with useful link out options provided. Additionally, the raw mass spec data have or will be made publicly available on ProteomeXchange (www.proteomexchange.org). We hope this project will open the door for many future discoveries.

The key methodology used for this study is affinity purification-mass spectrometry (APMS). We developed and optimized an APMS protocol that was published as a book chapter in *Springer Protocols* (Sorkin and Nusinow, 2022). In Chapter 2, we provide this protocol and discuss our efforts to improve it. While we believe our approach is highly effective at identifying novel protein-protein interactions, we also here include a case study of a non-specific binding protein, FTIP1, that was found in our APMS (see **Appendix I**). While our hypothesis that FTIP1 was involved in intercellular communication of circadian rhythms remains unproven, the literature review undertaken during that period of my thesis work was published as a review in *Trends in Plant Science* that

provides an overview of our understanding of tissue-specific clocks and intercellular communication of circadian rhythms (see *Appendix II*) (Sorkin and Nusinow, 2021).

In Chapter 3 we discuss the key findings from completing APMS for the 11 chosen circadian clock proteins. We generated plant lines expressing affinity-tagged versions of these clock proteins that behaved similarly to their native counterparts. All but 35S::FIO1-HFC were driven by their endogenous promoter. Using these lines, we were able to identify hundreds of protein-protein interactions. While we chose to follow up with an in-depth study of one set of interesting interactions in Chapter 4, there are a multitude of other coprecipitated proteins that could prove interesting as well. For each group of bait proteins (CCA1/LHY, FIO1, JMJD5, PRR5/7/9, or TOC1), we highlight several coprecipitated proteins that we think could be promising interactions to follow up with.

We chose to follow up on an interaction between RVE8/LNK1/LNK2 and two proteins previously unrelated to these clock components, COLD RESPONSE PROTEIN 27 (COR27) and COR28. We found that these proteins form a complex in the early evening that serves to regulate RVE8 protein stability and to block the transcriptional activity of RVE8-LNK1/2. Also among the RVE8/LNK1/LNK2 interactors were several proteins associated with temperature response-related GO terms. As temperature cycles are a known input to the circadian clock, we thus examined the role of the LNKs in temperature entrainment and found that loss of LNK1 and/or LNK2 results in impaired ability of the plant to return to wildtype rhythms when provided with temperature cycles. Together, our study on the RVE8/LNK1/LNK2 interactome has led to the identification of

a novel post-translational regulatory mechanism for the clock involving COR27/28 and the finding that LNK1/LNK2 are important for temperature entrainment.

5.2 Major Findings

Affinity-purification mass-spectrometry (APMS) is a powerful tool for protein-protein interaction discovery. To properly understand a protein's function, awareness of its interaction partners is often important. The key circadian clock genes that have been identified in Arabidopsis thaliana have been discovered using primarily genetic approaches (**Chapter 1, Table 1.1**). Before this thesis, a high-throughput screen of protein interactions for the core Arabidopsis circadian clock proteins had not been performed. In total, we established protein interaction networks for 11 core components of the circadian clock: CCA1, LHY, FIO1, JMJD5, LNK1, LNK2, RVE8, TOC1/PRR1, PRR5, PRR7, and PRR9. While this is not an exhaustive list, we believe our dataset provides a rich source of information that will be valuable to the circadian community and beyond. We identified hundreds of protein interactions and demonstrated the efficacy of this approach by following up on interactions between RVE8/LNK1/LNK2 and COR27/COR28 and between CCA1/LHY and CYCLING DOF FACTOR 2 (CDF2). We demonstrated that our lists contain proteins that are likely true interactors of the bait proteins by performing GO enrichment analysis and finding expected, relevant terms such as photoperiodism and response to light stimulus (**Chapter 4, Fig. 4.2**).

To help other scientists use this methodology in their own work, we optimized and published our protocol for affinity purification of FLAG/His-tagged proteins. Through our optimization studies, we established that using detergent, while harmful to mass

spectrometry equipment if used in high quantities, is essential for effective capture of interacting proteins (**Chapter 2, Figs. 2.3-2.4, Table 2.1**). We suggest using Triton X-100 at a concentration of no higher than 0.1% in buffers used during affinity purification. Additionally, final washes of affinity beads to be submitted for LCMS analysis should be conducted in 25 mM ammonium bicarbonate without detergents. We also highlight that including a no-tag wild-type background AP, in addition to a 35S::GFP-HFC AP, is an important negative control (**Chapter 2, Appendix I**).

COR27/28 interact with the RVE8-LNK1/2 complex at ZT9, likely as a higher order complex. One significant advantage of using an *in vivo* technique such as APMS over an orthogonal high-throughput system like yeast 2-hybrid library screening is the ability to identify both binary and higher-order interactions. Our study into the interaction between COR27/28 and the RVE8-LNK1/2 transcriptional complex is a nice case study of this advantage. After coprecipitating the CORs in our RVE8/LNK1/LNK2-HFC APMS, we sought to validate this interaction in yeast. However, we did not see a positive interaction between any of these components in a yeast 2-hybrid system (**Chapter 4, Fig. S4.4**). Since we knew that RVE8 and the LNKs form a complex, we sought to determine if both RVE8 and LNK1 or LNK2 needed to be present in order for the CORs to bind. By using a yeast 3-hybrid system, we demonstrated that, indeed, a positive interaction was observed when RVE8, the C-terminus of LNK1, and either COR27 or COR28 were present in the system (**Chapter 4, Fig. 4.3)**. Thus, this complex interaction would have never been identified using a yeast 2-hybrid library screen, which is the most commonly used method for high-throughput discovery of protein-protein interactions.

Another advantage of using an *in vivo* approach like APMS is the ability to find protein interactions under biologically relevant conditions. For circadian clock proteins, time is an important variable to consider when performing experiments. Here, we examined the interactome of RVE8/LNK1/LNK2 at two different times of day: ZT5 and ZT9 (**Chapter 4**). We hoped to identify time-of-day-specific interactions that might offer insight into time-dependent functions for this complex. Indeed, COR27/28 were coprecipitated with our complex at ZT9 but not ZT5, likely due to coincidence of expression levels at ZT9 and the absence of coincidence earlier in the day, when the CORs are not as highly expressed (**Chapter 4, Fig. S4.3**). Again, this nuance of the interaction would have been lost in an orthogonal approach. Full time-resolved affinity purification experiments that take place over the course of a full 24-hour period (such as in (Krahmer et al., 2018)) would be a valuable follow up effort to our work.

COR27/28 regulate the protein stability and transcriptional activity of RVE8. Having identified the RVE8-LNK1/2-COR27/28 interaction, we sought to determine the biological role of this complex in the plant. To understand why COR27/28 interact with this circadian transcriptional complex, we examined the previously published reports on these genes. Previous work demonstrated that an E3 ubiquitin ligase complex consisting of CONSTITUTIVELY PHOTOMORPHOGENIC 1 (COP1) and SUPPRESSOR OF PHYA-105 1 (SPA1) physically interacts with COR27/28 and promotes their degradation by the 26S proteasome in the dark (Kahle et al., 2020; Li et al., 2020; Zhu et al., 2020). Additionally, COR27/28 interact with several major transcription factors: phytochrome B (phyB), phyA, and ELONGATED HYPOCOTYL 5 (HY5) (Kahle et al., 2020; Li et al., 2020; Zhu et al., 2020). Having no identifiable DNA-binding domains nor possessing DNA-

binding activity *in vitro* (Li et al., 2016; Li et al., 2020), it is unlikely that the CORs themselves are transcription factors. Rather, it appears COR27/28 regulate gene expression through their interactions with these three transcription factors. Given these facts, we hypothesize that the CORs are recruiting the COP1-SPA complex to target these transcription factors for degradation.

In our work we demonstrate that the CORs interact with yet another family transcription factors: the RVEs (RVE5/6/8) (**Chapter 4**) (Sorkin et al., 2022). Furthermore, COR27/28 previously had been shown to repress the expression of two RVE8 target genes—PRR5 and TOC1—specifically in the evening (Li et al., 2016; Wang et al., 2017). Thus, the CORs are negative regulators of the same genes that the RVE8-LNK1/2 complex activates (Rawat et al., 2011; Hsu et al., 2013a; Xie et al., 2014). Therefore, we hypothesized that the CORs were negatively regulating RVE8-LNK1/2 transcriptional activity. Since we identified this connection through APMS, we predicted this regulation occurred at the post-translational level.

We found support for this hypothesis: RVE8-HFC levels were stabilized, specifically in the evening, in a *cor27-2 cor28-2* double mutant (**Chapter 4, Fig. 4.4**). Additionally, activation of a RVE8 target gene, TOC1, was blocked when COR27 or COR28 were added to a tobacco transactivation assay (**Chapter 4, Fig. 4.4**). Together, these experiments supported our idea that the CORs antagonize RVE8 transcriptional activity, possibly through destabilizing this protein in the evening. Whether this activity is COP1-dependent is an open question.

LNK1/2 are important for temperature entrainment. Among the top GO terms enriched in our RVE8/LNK1/LNK2 APMS dataset were those related to temperature response (**Chapter 4, Fig. 4.2**). Indeed, we found four cold response-related proteins among our prioritized interactors for RVE8/LNK1/LNK2: COR27, COR28, TOLERANT TO CHILLING/FREEZING 1 (TCF1) and a family member of TCF1 we named REGULATOR OF CHROMOSOME CONDENSATION 1-LIKE (RCC1L) (AT3G53830) that is also cold responsive.

Daily temperature patterns are an input cue to entrain the circadian oscillator and the oscillator, in turn, regulates the response to ambient temperatures (Salomé and Robertson Mcclung, 2005; Thines and Harmon, 2010; Dong et al., 2011; Chow et al., 2014; Avello et al., 2019). Previous work has shown that members of the RVE and LNK families are involved in the circadian output of regulating the response to temperature (Mizuno et al., 2014; Kidokoro et al., 2021). In contrast, we know very few of the factors involved in temperature entrainment of the clock. To test whether the LNKs could be involved in temperature entrainment, we examined circadian rhythms of a CCA1::LUCIFERASE (LUC) reporter in wild-type plants and in *lnk1/2* mutants. Under constant light (LL), *lnk1/2* mutants display a long period mutant phenotype (**Chapter 4, Fig. 4.5**) (Rugnone et al., 2013; Xie et al., 2014). In our experiment, we measured reporter rhythms for several days under constant light and temperature before switching the chamber to a temperature entrainment program with warm-cool cycles. Under constant conditions, we found that the rhythms of the *lnk1/2* mutants became out of sync with those of wild-type plants due to the long period phenotype of the *lnk1/2* plants. When switched to a temperature entrainment program, the *lnk1/2* mutant reporter rhythms eventually

synced back up with wild-type rhythms, but it took several days, indicating the mutants were impaired in their ability to use temperature information for entrainment (**Chapter 4, Fig. 4.5**). In contrast, when provided with photocycles, the mutants immediately realigned their rhythms with wild type, indicating that *lnk1/2* mutants aren't defective in entrainment in general, but rather are specifically impaired in their ability to use temperature cycles. As there is yet much to learn about temperature entrainment of the plant circadian clock, we believe this contribution will be of high value to the clock community.

5.3 Open Questions

Is COP1 involved in RVE8 degradation? In Chapter 4, we demonstrated that RVE8 interacts with COR27/28 in a time-of-day-dependent manner and that this interaction appears to regulate the stability of RVE8, thus affecting its transcriptional function (Sorkin et al., 2022). An open question is by what mechanism RVE8 is being degraded. Previous studies have demonstrated that COR27/28 stability is regulated by the E3 ubiquitin ligase COP1 (Kahle et al., 2020; Li et al., 2020; Zhu et al., 2020). Notably, COP1 and its partner SPA1 coprecipitated with RVE8 at ZT9 but not ZT5 (Sorkin et al., 2022). This is surprising given that all three proteins should be present in the cell at ZT5 based on their rhythmic mRNA/protein abundance patterns (Sorkin et al., 2022). This suggests to us that there could be an important bridge protein expressed at ZT9 that bridges the interaction between RVE8 and the COP1-SPA complex. Since COR27/28 are only coprecipitated with the RVE8-LNK1/2 complex at ZT9 and also interact with COP1/SPA1, we hypothesize that the CORs allow the COP1-SPA complex to interact with RVE8/LNK1/LNK2 to target this transcriptional unit for degradation (Sorkin et al., 2022).

To follow up on this interaction, we propose to first validate whether RVE8 binds to COP1 directly or if COR27/28 are required for a complex to form. To test this, yeast 2- and 3-hybrid assays can be performed. First, we anticipate that RVE8 will not bind COP1 in a yeast 2-hybrid system. Instead, we think addition of one of the CORs as a linker protein using a yeast 3-hybrid will result in a positive interaction. It is possible that the LNKs, too, must be present for the full complex to form. Another approach we propose is to also perform APMS on plants expressing RVE8p::RVE8-HFC in *cor27-2 cor28-2*. Without COR27/28, we expect that COP1/SPA1 will no longer coprecipitate with RVE8-HFC at ZT9. From these experiments, we hope to demonstrate that COR27/28 bridge the interaction between the COP1-SPA complex and the RVE8-LNK1/2 complex. It is possible that RVE8 binds to COP1-SPA directly, but since we found that RVE8 stability is dependent on the presence of COR27/28, we posit that these factors are necessary for this interaction.

COR27/28 interact with COP1 via a conserved Val-Pro (VP) peptide motif (Kahle et al., 2020). Mutation of this peptide to Ala-Ala (AA) blocks this interaction and stabilizes COR27/28-VPAA (Kahle et al., 2020). By using these endogenous promoter-driven COR27/28-VPAA lines, we can determine whether the COR-COP1 interaction is important for regulation of RVE8 stability. First, we can examine RVE8-HFC protein levels over the course of the day in a COR27/28-VPAA mutant background. Without the ability to recruit the COP1-SPA complex, we predict that RVE8-HFC levels should phenocopy the pattern seen in a *cor27-2 cor28-2* double mutant, in which RVE8-HFC levels remained high in the evening instead of decreasing at nightfall as in wild type (Sorkin et al., 2022). Likewise, we hypothesize that in a TOC1p::LUC reporter assay, addition of COR27/28-

VPAA to an inoculation mixture containing RVE8 and LNK1/2 would have no effect on reporter signal, whereas addition of the wild-type proteins would decrease reporter signal. This hypothesis assumes that wild-type COR27/28 decrease reporter signal via degradation of the activator RVE8 in a COP1-dependent manner.

There could, however, be other COP1-bridging proteins that interact with RVE8 or perhaps transient binding of COP1 directly to RVE8. In this scenario, absence of the CORs or loss of the COR27/28-COP1 interaction would not prohibit COP1 from degrading RVE8. Thus, we also suggest examining RVE8-HFC levels in the *cop1-4* hypomorph, as full loss of COP1 is lethal (McNells et al., 1994).

To further connect the CORs and COP1 to RVE8 transcriptional activity, RVE8-HFC enrichment at target gene promoters could be examined in *cop1-4* using chromatin immunoprecipitation (ChIP). Relative to wild type, RVE8-HFC occupancy at its cis-regulatory motif in the promoter of TOC1 should increase in the *cop1-4, cor27-2 cor28-2*, and COR27/28-VPAA mutants. Specifically, this effect should only be significant in the evening, at which time COR27/28 are interacting with the RVE8-LNK1/2 complex and promoting their degradation via the COP1-SPA complex and the 26S proteasome. We expect that earlier in the day, when the CORs are not expressed, RVE8-HFC enrichment at TOC1 should be unchanged. These results would highlight the unique time-of-day specificity that is conferred by this posttranslational mechanism.

Is the RVE8-LNK1/2 complex stabilized by UBP12/13? We also coprecipitated two deubiquitylases, UBIQUITIN-SPECIFIC PROTEASE 12 (UBP12) and UBP13 with members of the RVE8-LNK1/2 complex at ZT5 and ZT9 (Sorkin et al., 2022). Previous

work has established that UBP12/13 interact with the circadian clock proteins GIGANTEA (GI) and ZEITLUPE (ZTL) to stabilize these factors presumably through cleaving of polyubiquitin (Krahmer et al., 2018; Lee et al., 2019). Additionally, loss of UBP12/13 results in early flowering and shortens the period of *CCA1, LHY,* and *TOC1* mRNA expression (Cui et al., 2013). While our work investigating the interaction with COR27/28 suggests these factors promote degradation of RVE8-LNK1/2 in the evening, perhaps UBP12/13 are acting in an opposing role to stabilize this complex. The mRNA and protein abundance of UBP12/13 is rhythmic under constant light and driven conditions (Cui et al., 2013), suggesting there could be a specific time-of-day when these factors act upon the RVE8-LNK1/2 complex, as is the case with COR27/28 (Sorkin et al., 2022).

To follow up on the interaction between RVE8, LNK1/2, and UBP12/13, we first suggest confirming whether these factors interact directly using a yeast 2-hybrid approach. As UBP12/13 require GI to bridge the interaction with ZTL, we think it is possible that GI or another linker protein is required for these proteins to complex with RVE8/LNK1/LNK2. A yeast 3-hybrid can be used to test different linker proteins if a direct interaction is not found using the 2-hybrid approach. It may also be useful to perform APMS on UBP12/13 to identify more of their targets.

Based on the established function of the UBPs, we hypothesize that UBP12/13 cleave polyubiquitin from RVE8/LNK1/LNK2 to stabilize these clock proteins. To test this, we can examine RVE8/LNK1/LNK2-HFC protein abundance over the course of 24-hours in wild-type and *ubp12-1 ubp13-1* backgrounds, anticipating that protein levels will be decreased in the double mutant. To determine whether the deubiquitylation activity of the

UBPs is required for protein abundance phenotypes, we can use mutant forms of UBP12/13, UBP12C208S and UBP13C207S, in which the conserved cysteine residue of the deubiquitylase enzymatic active site is substituted with a serine (Cui et al., 2013). If UBP12/13 stabilize RVE8/LNK1/LNK2 through cleaving of polyubiquitin, protein abundance patterns in the UBP12C208S/UBP13C207S mutants should phenocopy the *ubp12-1/ubp13-1* mutants. Downstream effects of RVE8-LNK1/2 destabilization in UBP12/13 mutants can be monitored via ChIP-qPCR and tobacco transactivation assays; decreased abundance of this complex should lead to decreased occupation of/activation of RVE8 target genes such as *TOC1*.

RVE8-LNK1/2-mediated activation of evening-phased circadian clock genes like *TOC1* and *PRR5* during the late morning is critical for maintaining proper circadian rhythms (Hsu et al., 2013b; Xie et al., 2014). To sustain precise timing of circadian rhythms, we propose that a balance between stabilization of the RVE8-LNK1/2 complex by UBP12/13 and targeted degradation by COR27/28 must be modulated throughout the day.

What are the characteristics of the RVE8-LNK1/2-COR27/28 complex *in vivo*?

While our yeast 3-hybrid experiment demonstrated that RVE8, the C-terminus of LNK1, and either COR27 or COR28 can form a tripartite complex in yeast, we do not know the stoichiometry or orientation of this complex *in vivo*. For example, perhaps there are more than just three proteins involved in the complex in the plant cell. Very likely, the nature of this protein complex is highly dynamic, with different proteins continuously binding and releasing.

We are curious why COR27/28 cannot bind RVE8 or LNK1 in yeast in a binary manner. As these components can form a complex in a 3-hybrid system, we hypothesize that a binding pocket on either RVE8 or LNK1 is made available to the CORs only when RVE8-LNK1 have formed a dimer (or higher order complex). To test this hypothesis, we first propose to identify the protein domains necessary for complex formation by creating truncation mutants of RVE8 and LNK1 and testing their ability to interact with the CORs in a yeast 3-hybrid assay. In addition, we would like to examine the crystal structure of RVE8 when it is alone versus when bound by LNK1 and when bound by LNK1 and COR27/28. To investigate the stoichiometry of this complex *in vivo*, we could use single-molecule localization microscopy (SMLM) (Fricke et al., 2015; Singh et al., 2020) and native PAGE gel electrophoresis.

Are COR27/28 evolutionarily conserved proteins that target major transcription factors for COP1-mediated degradation? Previous phylogenetic analysis of COR27/28 demonstrated that these genes are conserved from angiosperms to algae, with homologs in early land plants like *Physcomitrella patens* and in the charophyte alga *Chara braunii* (Kahle et al., 2020). While sequence similarity between most COR27/28 homologs is only 20-30%, there are five conserved motifs that are present in almost all the species with identified homologs. One of these conserved motifs contains the VP peptide, which mediates the interaction between COP1 and COR27/28 (Kahle et al., 2020). This suggests that regulation of protein stability via COR27/28-COP1 binding could be an ancestral trait conserved through millions of years of evolution in the plant kingdom.

We propose to examine the evolutionary history of COR27/28, COP1, and RVE8/LNK1/LNK2. To determine whether these proteins have conserved their function from early land plants to angiosperms, we can perform crossspecies complementation experiments in which the Arabidopsis versions of these genes are swapped out for the homologs identified in the moss *Physcomitrella patens*. If the *P. patens* COR27/28 homologs function in photomorphogenesis and circadian rhythms, we would expect for expression of these genes in an Arabidopsis *cor27-2/cor28-2* mutant to rescue the short hypocotyl and long period mutant phenotypes, respectively. It would be interesting to identify whether homologs from some species only rescue circadian phenotypes while others rescue photomorphogenesis phenotypes. If this were the case, perhaps we could then identify the evolved sequences important for connecting the COR-COP1 regulatory module to light-mediated growth and circadian pathways.

As previously mentioned, COR27/28 interact with a number of important transcription factors: PhyB, PhyA, HY5, and RVE8 (Kahle et al., 2020; Li et al., 2020; Zhu et al., 2020; Sorkin et al., 2022). Together, with the COP1/SPA1 interaction, we propose that the CORs are negative regulators of phytochrome, RVE8, and HY5 target loci via recruitment of the COP1-SPA complex to target these transcription factors for degradation by the proteasome. It would be interesting to test whether copies of COR27/28 from the relatives of early land plants, like mosses, also participate in these protein interactions using yeast 2/3-hybrids and whether they affect the activity of these transcription factors through transcriptional assays or ChIP-qPCR.

5.4 References

Avello PA, Davis SJ, Ronald J, Pitchford JW (2019) Heat the clock: Entrainment and compensation in arabidopsis circadian rhythms. J Circadian Rhythms **17**: 5

Chow BY, Sanchez SE, Breton G, Pruneda-Paz JL, Krogan NT, Kay SA (2014) Transcriptional Regulation of LUX by CBF1 Mediates Cold Input to the Circadian Clock in Arabidopsis. Curr Biol **24**: 1518–1524

Cui X, Lu F, Li Y, Xue Y, Kang Y, Zhang S, Qiu Q, Zheng XC, Cui X, Zheng S, et al (2013) Ubiquitin-specific proteases UBP12 and UBP13 act in circadian clock and photoperiodic flowering regulation in Arabidopsis. Plant Physiol **162**: 897–906

Dong MA, Farré EM, Thomashow MF (2011) CIRCADIAN CLOCK-ASSOCIATED 1 and LATE ELONGATED HYPOCOTYL regulate expression of the C-REPEAT BINDING FACTOR (CBF) pathway in Arabidopsis. Proc Natl Acad Sci **108**: 7241–7246

Fricke F, Beaudouin J, Eils R, Heilemann M (2015) One, two or three? Probing the stoichiometry of membrane proteins by single-molecule localization microscopy OPEN. Sci RepoRts | **5**: 14072

Hsu PY, Devisetty UK, Harmer SL (2013a) Accurate timekeeping is controlled by a cycling activator in Arabidopsis. Elife **2**: e00473

Hsu PY, Devisetty UK, Harmer SL (2013b) Accurate timekeeping is controlled by a cycling activator in Arabidopsis. Elife. doi: 10.7554/eLife.00473

Kahle N, Sheerin DJ, Fischbach P, Koch LA, Schwenk P, Lambert D, Rodriguez R, Kerner K, Hoecker U, Zurbriggen MD, et al (2020) COLD REGULATED 27 and 28 are targets of CONSTITUTIVELY PHOTOMORPHOGENIC 1 and negatively affect phytochrome B signalling. Plant J **104**: 1038–1053

Kidokoro S, Hayashi K, Haraguchi H, Ishikawa T, Soma F, Konoura I, Toda S, Mizoi J, Suzuki T, Shinozaki K, et al (2021) Posttranslational regulation of multiple clock-related transcription factors triggers cold-inducible gene expression in Arabidopsis. Proc Natl Acad Sci. doi: 10.1073/PNAS.2021048118

Krahmer J, Goralogia GS, Kubota A, Zardilis A, Johnson RS, Song YH, MacCoss MJ, LeBihan T, Halliday KJ, Imaizumi T, et al (2018) Time-resolved Interaction Proteomics of the GIGANTEA Protein Under Diurnal Cycles in Arabidopsis. FEBS Lett 1873-3468.13311

Lee CM, Li MW, Feke A, Liu W, Saffer AM, Gendron JM (2019) GIGANTEA recruits the UBP12 and UBP13 deubiquitylases to regulate accumulation of the ZTL photoreceptor complex. Nat Commun. doi: 10.1038/s41467-019-11769-7

Li X, Liu C, Zhao Z, Ma D, Zhang J, Yang Y, Liu Y, Liu H (2020) COR27 and COR28 are Novel Regulators of the COP1-HY5 Regulatory Hub and Photomorphogenesis in Arabidopsis. Plant Cell Adv Publ. doi: 10.1105/tpc.20.00195

Li X, Ma D, Lu SX, Hu X, Huang R, Liang T, Xu T, Tobin EM, Liu H (2016) Blue Light- and Low Temperature-Regulated COR27 and COR28 Play Roles in the Arabidopsis Circadian Clock. Plant Cell **28**: 2755–2769

McNells TW, Von Arnim AG, Araki T, Komeda Y, Miséra S, Deng XW (1994) Genetic and molecular analysis of an allelic series of cop1 mutants suggests functional

roles for the multiple protein domains. Plant Cell **6**: 487–500

Mizuno T, Takeuchi A, Nomoto Y, Nakamichi N, Yamashino T (2014) The LNK1 night light-inducible and clock-regulated gene is induced also in response to warm-night through the circadian clock nighttime repressor in Arabidopsis thaliana. Plant Signal Behav. doi: 10.4161/psb.28505

Rawat R, Takahashi N, Hsu PY, Jones MA, Schwartz J, Salemi MR, Phinney BS, Harmer SL (2011) REVEILLE8 and PSEUDO-REPONSE REGULATOR5 Form a Negative Feedback Loop within the Arabidopsis Circadian Clock. PLoS Genet **7**: e1001350

Rugnone ML, Soverna AF, Sanchez SE, Schlaen RG, Hernando CE, Seymour DK, Mancini E, Chernomoretz A, Weigel D, Mas P, et al (2013) LNK genes integrate light and clock signaling networks at the core of the Arabidopsis oscillator. Proc Natl Acad Sci U S A **110**: 12120–12125

Salomé PA, Robertson Mcclung C (2005) PSEUDO-RESPONSE REGULATOR 7 and 9 Are Partially Redundant Genes Essential for the Temperature Responsiveness of the Arabidopsis Circadian Clock. Plant Cell **17**: 791–803

Singh A, Van Slyke AL, Sirenko M, Song A, Kammermeier PJ, Zipfel WR (2020) Stoichiometric analysis of protein complexes by cell fusion and single molecule imaging. Sci Reports 2020 101 **10**: 1–12

Sorkin ML, Nusinow DA (2021) Time Will Tell: Intercellular Communication in the Plant Clock. Trends Plant Sci **26**: 706–719

Sorkin ML, Nusinow DA (2022) Using Tandem Affinity Purification to Identify Circadian Clock Protein Complexes from Arabidopsis. *In* D Staiger, S Davis, AM Davis, eds, Plant Circadian Networks Methods Protoc. Springer US, New York, NY, pp 189–203

Sorkin ML, Tzeng S-C, Romanowski A, Kahle N, Bindbeutel R, Hiltbrunner A, Yanovsky MJ, Evans BS, Nusinow DA (2022) COR27/28 Regulate the Evening Transcriptional Activity of the RVE8-LNK1/2 Circadian Complex. bioRxiv 2022.05.16.492168

Thines B, Harmon FG (2010) Ambient temperature response establishes ELF3 as a required component of the core Arabidopsis circadian clock. Proc Natl Acad Sci **107**: 3257–3262

Wang P, Cui X, Zhao C, Shi L, Zhang G, Sun F, Cao X, Yuan L, Xie Q, Xu X (2017) *COR27* and *COR28* encode nighttime repressors integrating *Arabidopsis* circadian clock and cold response. J Integr Plant Biol **59**: 78–85

Xie Q, Wang P, Liu X, Yuan L, Wang L, Zhang C, Li Y, Xing H, Zhi L, Yue Z, et al (2014) LNK1 and LNK2 Are Transcriptional Coactivators in the Arabidopsis Circadian Oscillator. Plant Cell **26**: 2843–2857

Zhu W, Zhou H, Lin F, Zhao X, Jiang Y, Xu D, Deng XW (2020) COLD-REGULATED GENE 27 Integrates Signals from Light and the Circadian Clock to Promote Hypocotyl Growth in Arabidopsis. Plant Cell Adv Publ. doi: 10.1105/tpc.20.00192

6 Appendix I: FTIP1 as a case study of a non-specific binding protein

6.1 Background and Motivation

One of the most abundant proteins coprecipitated in our FLAG-His tandem APMS experiments was FLOWERING LOCUS T-INTERACTING PROTEIN 1 (FTIP1) (**Table 6.1**). In a previous APMS experiment in our lab, FTIP1 was also identified as a top interactor of ELF3 and ELF4, two components of the circadian evening complex (Huang et al., 2016). We were therefore interested in following up on FTIP1 as a potential novel interactor of several core circadian clock proteins.

The FTIP1 protein contains three C2 domains, a C-terminal transmembrane domain, and is localized to the membrane of the ER (Liu et al., 2012). In Arabidopsis, FTIP1 is part of a 16-member family of multiple C2 transmembrane proteins (MCTPs) that have a wide variety of expression patterns (Liu et al., 2018a). FTIP1 expression is highest in the root although its function has primarily been examined in the companion cells of the phloem, where expression is also high. More broadly, FTIP1 is a homolog of calcium/lipid-binding proteins that include ferlins, synaptotagmins, tricalbins, and MCTPs, which are conserved across kingdoms. A common function of all of these protein families is that they are typically involved in inter- and intra-cellular transport (Lek et al., 2012). For example, in mammals, synaptotagmins are essential for forming the vesicles that carry neurotransmitters between synapses in the brain (Südhof and Rizo, 1996). While FTIP1 shares homology with calcium/lipid-binding proteins, it has yet to be demonstrated that these substrates are bound in this case. Notably, two homologs of FTIP1—FTIP3 and FTIP4—have also been shown to play a role in protein trafficking (Liu et al., 2018b). FTIP3/4 physically interact with the homeobox protein SHOOT MERISTEMLESS (STM)

to regulate intracellular trafficking of this meristem maintenance factor between the plasma membrane and the nucleus.

Table 6.1 FTIP1 is coprecipitated with several clock factors.
Total spectra associated with FTIP1 (AT5G06850.1) are shown for APMS experiments using CCA1-HFC, LHY-HFC, FIONA 1 (FIO1)-HFC, GFP-HFC, and Col-0.

Protein Name	Gene ID	CCA1-HFC	LHY-HFC	FIO1-HFC	GFP-HFC	Col-0
FTIP1	AT5G06850.1	67	56	64	0	63

FTIP1 was not identified in any of the 12 separate 35S::GFP-HFC negative control samples and it is not listed as a common contaminant of plant affinity purification experiments (Van Leene et al., 2015). This suggested to us that FTIP1 was a true positive interactor of many circadian clock proteins. Based on its known role in FT trafficking, we hypothesized that FTIP1 was performing a similar role here—facilitating intercellular transport of circadian clock transcription factors. As Arabidopsis is known to possess tissue-specific clocks (Shimizu et al., 2015; Endo, 2016; Sorkin and Nusinow, 2021), we proposed that FTIP1-mediated transport of clock proteins served to coordinate rhythms over long distances between tissues.

6.2 Results and Discussion

FTIP1 is non-specific binding protein that is not involved in circadian rhythms. As many circadian clock-associated genes exhibit rhythmic mRNA or protein expression patterns (Huang and Nusinow, 2016), we prioritize APMS interactors that show rhythmic gene/protein expression patterns under diurnal and/or free-running conditions. Upon identifying FTIP1 as a top interactor for several circadian clock bait proteins (**Table 6.1**), we thus checked whether this gene exhibits rhythmic mRNA

expression. By checking publicly available expression datasets, we determined that FTIP1 mRNA does not cycle under free-running conditions nor under diurnal light:dark cycles (Bonnot et al.; Covington et al., 2008; Hsu and Harmer, 2012; Romanowski et al., 2020) (**Figure 6.1A**). We also examined FTIP1 expression at the protein level by performing a time course Western blot using plants expressing FTIP1p::4HA-FTIP1 in *ftip1-1* (hereafter referred to as 4HA-FTIP1). Similar to the mRNA expression profile, FTIP1 protein levels did not fluctuate in a rhythmic manner over the course of the day under light:dark cycles **(Figure 6.1B**). While we anticipated to see rhythmic expression patterns for FTIP1, not all circadian clock genes cycle (Kim et al., 2008); therefore, we did not eliminate FTIP1 as a possible circadian-associated factor despite the absence of cycling.

Although we did not find discernable daily rhythms in FTIP1 mRNA expression or protein abundance, we decided to further explore if FTIP1 had a circadian phenotype. Most circadian-associated loci exhibit defects in period length, rhythm amplitude, or rhythm phase upon mutation (Hsu and Harmer, 2014). We thus examined circadian rhythms in *ftip1-1* CCA1::LUC and 35S::FTIP1 CCA1::LUC lines, hypothesizing that the period of the CCA1 promoter-driven luciferase reporter would significantly deviate from 24 hours. However, both the null mutant and overexpression line exhibited ~24-hour periods similar to Col-0 (**Figure 6.1C**). Overall amplitude of the reporter was lower in the mutants compared to the wildtype, although we were unsure if this reflected a true genetic effect on the reporter or if this was simply due to the expression level of the background reporter line used to generate the null and overexpression reporter lines. It is possible

that these are conditional mutants that would have shown a circadian phenotype under a specific environmental condition, but we did not explore this hypothesis further.

The absence of cycling and the lack of a circadian phenotype in null and overexpression mutants suggested that FTIP1 is not involved in circadian rhythms. As FTIP1 was one of the most abundant proteins coprecipitated in our clock bait APMS experiments (**Table 6.1**), we were surprised to find that this protein had no apparent role in circadian rhythms. As FTIP1 was not identified in our 35S::GFP-HFC negative control APMS samples, we did not suspect that it was a "sticky", non-specific binding protein. To validate the interaction between FTIP1 and the clock proteins, we performed a small-scale anti-FLAG coimmunoprecipitation *in vitro* using protein extracts made from pB7 CCA1p::CCA1-HFC FTIP1p::4HA-FTIP1 in *ftip1-1 cca1-1* CCA1::LUC. These extracts were incubated with anti-FLAG magnetic affinity beads for one hour. We also included a negative control sample that incubated extracts from the 4HA-FTIP1 line (without the -HFC tagged bait) with the anti-FLAG beads. Presence/absence of the tagged proteins in the input, IP, or flow-through was determined by Western blot probing with anti-FLAG to visualize CCA1-HFC and anti-HA for 4HA-FTIP1. Notably, we observed that 4HA-FTIP1 incubated with anti-FLAG beads alone could bind non-specifically to the beads (**Figure 6.1D, lane 6**). This indicated to us that FTIP1 was a non-specific binding protein that was showing up as a false positive in our APMS experiments.

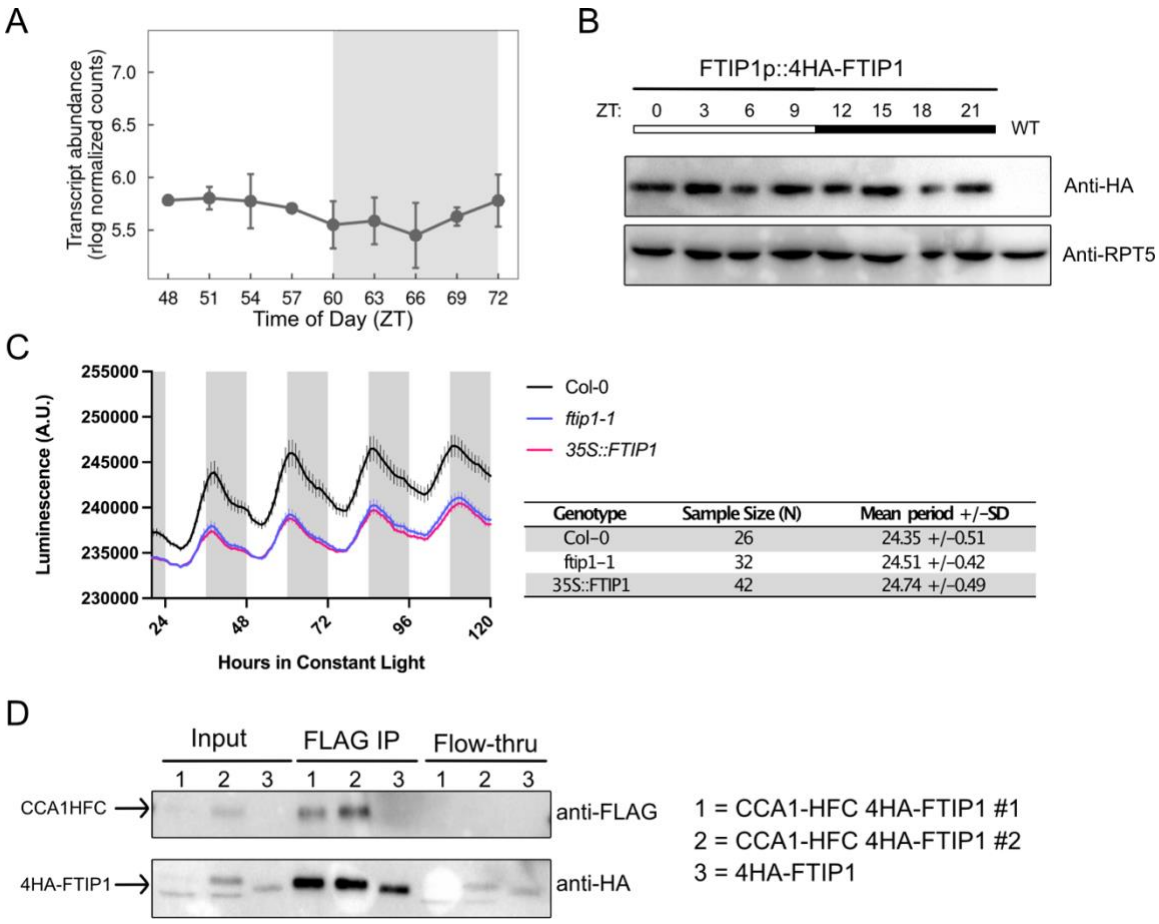

Figure 6.1 FTIP1 is a non-specific binding protein that is not involved in circadian rhythms

(A) FTIP1 mRNA expression does not cycle under constant light, 22 ℃ conditions. RNA-seq data is provided from CAST-R (Bonnot et al., 2021). (B) 4HA-FTIP1 abundance does not cycle under 12 hr light: 12 hr dark 22 ℃ conditions. Tissue was collected every three hours from 10-day-old seedlings. 4HA-FTIP1 was detected using an anti-HA antibody while anti-RPT5 was used for loading control. (C) FTIP1 does not perturb circadian rhythms under constant light, 22 ℃ conditions. Luminescence from a CCA1p::LUC reporter in *ftip1-1* or 35S::FTIP1 plants was imaged for several days under constant light/temperature using a super-cooled CCD camera. Table shown to the right shows the calculated period for each genotype as determined by fast Fourier transformed nonlinear least squares (FFT-NLLS) (Plautz et al., 1997) using the Biological Rhythms Analysis Software System 3.0 (BRASS) available at http://www.amillar.org. (D) Anti-FLAG coIP shows 4HA-FTIP1 binds non-specifically to anti-FLAG affinity beads. Protein extracts from 2 individual lines (#1 and #2) expressing FTIP1p::4HA-FTIP1 (4HA-FTIP1) and CCA1p::CCA1-3X-FLAG-6X-His (CCA1-HFC) were incubated with anti-FLAG Dynabeads and detected by Western blot. Extracts from a plant only expressing FTIP1p::4HA-FTIP1 were incubated with anti-FLAG beads as a negative control.

As previously mentioned, FTIP1 was not coprecipitated in GFP-HFC APMS. However, based on our follow-up experiments, we had evidence that FTIP1 was indeed

a non-specific binding that was not identified in our negative control. We hypothesized that the overexpression of GFP-HFC and high affinity of this tagged protein for the anti-FLAG and His-isolation beads outcompeted FTIP1 in GFP-HFC control samples, causing FTIP1 to not co-precipitate in these samples. To test this hypothesis, we performed a Col-0 control AP in which wild type protein extracts were used for the large-scale tandem affinity purification. By using this approach, we could identify native proteins that bind our affinity beads non-specifically. In agreement with our hypothesis, we found that FTIP1 was one of the top proteins identified in our Col-0 control APMS.

By performing follow-up experiments investigating the role of FTIP1 in the circadian clock and using a secondary method to validate our large-scale APMS findings, we were able to determine that FTIP1 was a non-specific binding protein that does not involved in circadian rhythms. This line of inquiry helped us establish that including a wild type, no-tag control APMS is critical for proper identification of non-specific binding proteins. While the GFP-HFC control APMS is helpful in identifying proteins that might non-specifically bind to the HFC tag, a wild-type, no-tag control will help identify proteins that bind to the affinity resins themselves.

6.3 Methods

Plant Materials. The *ftip1-1* (SALK013179C) T-DNA mutant was obtained from the ABRC and confirmed homozygous by PCR genotyping using primers listed in **Supplemental Table S6.1**. The *ftip1-1* CCA1::LUC and 35S::FTIP1 CCA1::LUC reporter lines were generated by crossing. The FTIP1p::4HA-FTIP1 in *ftip1-1* line was generously shared with us by Dr. Hao Yu (Liu et al., 2012). pB7 CCA1p::CCA1-HFC in *cca1-1* CCA1::LUC has been described previously (Kim et al., 2019). The

CCA1p::CCA1-HFC FTIP1p::4HA-FTIP1 in *ftip1-1 cca1-1* CCA1::LUC line was generated by crossing. Plants were grown under 12 hr light: 12 hr dark photoperiods (LD) at 22 ℃ on 1/2X Murashige and Skoog basal salt medium with 0.8% agar + 1% (w/v) sucrose unless otherwise noted.

Luciferase Reporter Assay. Individual 6-day-old seedlings expressing a CCA1::LUC reporter grown under LD cycles at 22 ℃ were arrayed on 1/2x MS + 1% Sucrose plates and sprayed with 5mM luciferin (GoldBio, Olivette, MO) prepared in 0.01% (v/v) Triton X-100 (Millipore Sigma-Aldrich, St. Louis, MO). Plants were transferred to an imaging chamber set to the appropriate free-run or entrainment program and images were taken every 60 minutes with an exposure of 4 minutes after a 3-minute delay after lights-off to diminish signal from delayed fluorescence using a Pixis 1024 CCD camera (Princeton Instruments, Trenton, NJ). Images were processed to measure luminescence from each plant using the Metamorph imaging software (Molecular Devices, Sunnyvale, CA). Circadian period was calculated using fast Fourier transformed nonlinear least squares (FFT-NLLS) (Plautz et al., 1997) using the Biological Rhythms Analysis Software System 3.0 (BRASS) available at http://www.amillar.org.

24-hour tissue collection, protein extraction, and Western blotting. Tissue from 10-day-old plants grown under LD 22 ℃ was harvested every 3 hours starting at ZT0 and ending at ZT21. Collections during the dark period were performed under dim green light. Total protein was extracted in SII buffer (100 mM sodium phosphate, pH 8.0, 150 mM NaCl, 5 mM EDTA, 5 mM EGTA, 0.1% Triton X-100, 1 mM PMSF, 1x

protease inhibitor mixture (Roche, Basel, Switzerland), 1x Phosphatase Inhibitors II & III (Sigma-Aldrich), and 5 µM MG132 (Peptides International, Louisville, KY)) and sonicated using a duty cycle of 20 s (2 s on, 2 s off, total of 40 s) at 50% power. Extracts were clarified of cellular debris through 2x centrifugation for 10 min at ≥20,000 × g at 4 °C. Protein content was determined by DC Assay (Bio-Rad, Carlsbad, CA) and normalized to 2.9 mg/mL. Extracts were loaded into an 8% acrylamide SDS-PAGE gel and transferred to a nitrocellulose membrane via semi-dry transfer.

HA-tagged proteins were probed with Anti-HA-HRP (Roche, Pleasanton, California) diluted 1:2000 in PBS + 0.1% Tween-20 and incubated at room temperature for 1 hour. FLAG-tagged proteins were detected with anti-FLAG-M2-Peroxidase conjugated antibody (Sigma-Aldrich, St. Louis, MO) diluted 1:10,000 in PBS + 0.1% Tween-20 and incubated at room temperature for 1 hour. RPT5 was detected using anti-RPT5-rabbit (ENZO Life Science, Farmingdale, New York) diluted to 1:5000 in PBS + 0.1% Tween-20 and incubated at room temperature for 1 hour.

FLAG Co-immunoprecipitation (IP). For *in vivo* co-IP experiment, 2 mg of protein extracts of lines expressing CCA1p::CCA1-HFC in *cca1-1* CCA1::LUC and FTIP1p::4HA-FTIP1 in *ftip1-1* were incubated with anti-FLAG-M2 antibody (Sigma-Aldrich, St. Louis, MO) crosslinked to Protein G Dynabeads (ThermoFisher Scientific, Waltham, MA). A line expressing only FTIP1p::4HA-FTIP1 in *ftip1-1* incubated with anti-FLAG-M2 beads was used as a negative control. 5 µg antibodies conjugated to 30 µL of Dynabeads were used for each FLAG-IP and were incubated with protein extracts for 1 hour at 4 ℃ with rotation. Beads were washed three times in SII buffer and remaining

proteins were eluted from beads and denatured by adding 2X SDS sample buffer and incubated at 75 ℃ for 10 minutes. Results were visualized via Western blot as described above.

6.4 Supplementary Information

Table S 6.1 Primers used in this study

Primer Name	Sequence (5' -> 3')	Purpose
pDAN0012	ATTTTGCCGATTTCGGAAC	Genotyping, LB primer for SALK T-DNA
pDAN1398	GCTTATATTTGCGTCGACCAC	Genotyping, RP primer for *ftip1-1* genotyping
pDAN1397	GTTCTTCAAATGGCTCTGCAG	Genotyping, LP primer for *ftip1-1* genotyping

6.5 References

Bonnot T, Gillard MB, Nagel DH CAST-R: An application to visualize circadian and heat stress-responsive genes in plants. doi: 10.1093/plphys/kiac121

Covington MF, Maloof JN, Straume M, Kay SA, Harmer SL (2008) Global transcriptome analysis reveals circadian regulation of key pathways in plant growth and development. Genome Biol **9**: 10.1186/gb-2008-9-8-r130

Endo M (2016) Tissue-specific circadian clocks in plants. Curr Opin Plant Biol **29**: 44–49

Hsu PY, Harmer SL (2012) Circadian Phase Has Profound Effects on Differential Expression Analysis. PLoS One **7**: e49853

Hsu PY, Harmer SL (2014) Wheels within wheels: The plant circadian system. Trends Plant Sci **19**: 240–249

Huang H, Alvarez S, Bindbeutel R, Shen Z, Naldrett MJ, Evans BS, Briggs SP, Hicks LM, Kay SA, Nusinow DA, et al (2016) Identification of Evening Complex Associated Proteins in Arabidopsis by Affinity Purification and Mass Spectrometry. Mol Cell Proteomics **15**: 201–217

Huang H, Nusinow DA (2016) Into the Evening: Complex Interactions in the Arabidopsis Circadian Clock. Trends Genet **32**: 674–686

Kim J, Kim Y, Yeom M, Kim JH, Nam HG (2008) FIONA1 is essential for regulating period length in the Arabidopsis circadian clock. Plant Cell **20**: 307–319

Kim SC, Nusinow DA, Sorkin ML, Pruneda-Paz J, Wanga X (2019) Interaction and Regulation Between Lipid Mediator Phosphatidic Acid and Circadian Clock Regulators. Plant Cell **31**: 399–416

Van Leene J, Eeckhout D, Cannoot B, De Winne N, Persiau G, Van De Slijke E,

Vercruysse L, Dedecker M, Verkest A, Vandepoele K, et al (2015) An improved toolbox to unravel the plant cellular machinery by tandem affinity purification of Arabidopsis protein complexes. Nat Protoc **10**: 169–187

Lek A, Evesson FJ, Sutton RB, North KN, Cooper ST (2012) Ferlins: Regulators of Vesicle Fusion for Auditory Neurotransmission, Receptor Trafficking and Membrane Repair. Traffic **13**: 185–194

Liu L, Li C, Liang Z, Yu H (2018a) Characterization of Multiple C2 Domain and Transmembrane Region Proteins in Arabidopsis. Plant Physiol **176**: 2119–2132

Liu L, Li C, Song S, Teo ZWN, Shen L, Wang Y, Jackson D, Yu H (2018b) FTIP-Dependent STM Trafficking Regulates Shoot Meristem Development in Arabidopsis. Cell Rep **23**: 1879–1890

Liu L, Liu C, Hou X, Xi W, Shen L, Tao Z, Wang Y, Yu H (2012) FTIP1 is an essential regulator required for florigen transport. PLoS Biol **10**: e1001313

Romanowski A, Schlaen RG, Perez-Santangelo S, Mancini E, Yanovsky MJ (2020) Global transcriptome analysis reveals circadian control of splicing events in Arabidopsis thaliana . Plant J **3**: 1–14

Shimizu H, Katayama K, Koto T, Torii K, Araki T, Endo M, Doherty CJ, Kay SA, Barclay JL, Tsang AH, et al (2015) Decentralized circadian clocks process thermal and photoperiodic cues in specific tissues. Nat Plants **1**: 10.1038/NPLANTS.2015.163

Sorkin ML, Nusinow DA (2021) Time Will Tell: Intercellular Communication in the Plant Clock. Trends Plant Sci **26**: 706–719

Südhof TC, Rizo J (1996) Synaptotagmins: C2-Domain Proteins That Regulate Membrane Traffic. Neuron **17**: 379–388

7 Appendix II: Intercellular Communication in the Plant Clock

This Appendix was previously published as: **Sorkin ML, Nusinow DA. Time Will Tell: Intercellular Communication in the Plant Clock. Trends Plant Sci. 2021**

7.1 Abstract

Multicellular organisms have evolved local and long-distance signaling mechanisms to synchronize development and response to stimuli among a complex network of cells, tissues, and organs. Biological timekeeping is one such activity that is suggested to be coordinated within an organism to anticipate and respond to daily and seasonal patterns in the environment. New research into the plant clock suggests circadian rhythms are communicated between cells and across long distances. However, further clarity is required on the nature of the signaling molecules and the mechanisms underlying signal translocation. This review summarizes the roles and properties of tissue-specific circadian rhythms, discusses the evidence for local and long-distance clock communication, and evaluates the potential signaling molecules and transport mechanisms involved in this system.

7.2 Multicellular organisms communicate circadian information between cells, tissues, and organs

In all domains of life, organisms have evolved an endogenous timekeeper named the circadian clock that anticipates and responds to daily and seasonal patterns in the environment (Pittendrigh, 1960; Ouyang et al., 1998; O'neill et al., 2011; Edgar et al., 2012). In plants, the clock includes ~20 transcriptional regulators that participate in interlocking transcription-translation feedback loops to produce 24-hour rhythms in circadian-regulated processes (Pokhilko et al., 2012). These core oscillator genes exhibit time-of-day-specific gene expression and activity. For example, in *Arabidopsis thaliana,* the partially redundant MYB-like transcription factors *CIRCADIAN CLOCK ASSOCIATED1* (*CCA1*) and *LATE ELONGATED HYPOCOTYL* (*LHY*) have peak

expression at dawn, while afternoon- and evening-phased genes include *PSEUDO-RESPONSE REGULATORS 5/7/9*, *TIMING OF CAB EXPRESSION 1* (*TOC1* aka *PRR1*), and members of the evening complex–*LUX ARRHYTHMO* (*LUX* aka *PCL1*), *EARLY FLOWERING 3* (*ELF3*), and *EARLY FLOWERING 4* (*ELF4*). Environmental input from day length and temperature modulates the expression and activity levels of these core oscillator transcripts and proteins, which themselves regulate the expression of genes involved in various circadian-regulated output pathways such as vegetative growth, reproductive development, and abiotic/biotic stress responses (Hicks et al., 2001; Niwa et al., 2007; Creux and Harmer, 2019; de Leone et al., 2020). With so many important biological processes under the control of the clock, it is unsurprising that harmonizing biological rhythms with the natural 24-hour cycles in light and temperature confers a fitness benefit (Ouyang et al., 1998; Dodd et al., 2005; Yerushalmi et al., 2011).

The multicellular nature of land plants implies there is a process in place that coordinates individual cellular rhythms to produce synchronous, whole-plant phenotypes. Mammalian species have achieved this inter-organ synchrony via a central clock called the suprachiasmatic nucleus (SCN), which sends synchronizing signals to peripheral organ clocks from its location in the brain (Dibner et al., 2010). As plants do not have a central nervous system, plant biologists have questioned if and how plant clocks are synchronized. Is there a dominant organ clock, as in animals? Are circadian rhythms cell-autonomous in all plant cells? In other multicellular model species, similar research is ongoing to explore intercellular communication of circadian rhythms.

Early investigation into long-distance communication of circadian rhythms in *Arabidopsis thaliana* suggested that each plant cell possessed an independently

functioning, autonomous clock that can sense inputs and regulate outputs (Thain et al., 2000). In this foundational experiment, the authors exposed the two cotyledons of an arabidopsis seedling to an entrainment protocol where the time of dawn and dusk was opposite for each leaf (Thain et al., 2000). Remarkably, the rhythms from a circadian luciferase reporter maintained the distinct phases in the cotyledons over several days. With the clocks in each cotyledon appearing to operate independently, the authors reasoned that the impact of cell-to-cell circadian synchronization is negligible.

Developments in micrografting techniques, single-cell methods, tissue-specific technologies, and computational modeling have challenged this view that plant cell clocks are functionally independent and that there is no significant cell-to-cell nor long-distance communication in the plant clock. One might assume a clock coordinating mechanism would be unnecessary if each plant cell reacted similarly to the same environmental input. However, the numerous internal and external stimuli considered input signals to the clock might be differentially sensed and decoded by different cell types in the plant (James et al., 2008; Bordage et al., 2016; Nimmo, 2018; Greenwood et al., 2019). For instance, belowground tissues (roots) experience changes in light and temperature differently from aboveground tissues (stems and leaves), and photosynthetic tissues host diurnal fluctuations in sugar production distinct from other cell types. Different sensitivities to environmental entrainment cues would result in cell-to-cell variation in clock activity, leading to asynchronies in the absence of a coupling mechanism. Thus, it is likely that a coordination system between circadian networks exists.

This review discusses cell-type- and tissue-specific properties of the plant clock, evidence for local and long-distance communication of circadian information, and

potential signaling molecules and methods of signal transport. We define three properties of the plant circadian clock communication system: 1) tissue-specific clocks regulate specific phenotypic outputs, 2) cell-autonomous clocks are weakly synchronized via local coupling, and 3) plant clocks function within a hierarchical network structure with multiple synchronization hubs. Clarity into how tissue clocks interpret clock input cues and communicate this information to distal parts of the plant will be necessary for future breeding and bioengineering projects targeting circadian rhythms.

7.3 The Clock has Tissue-Specific Properties and Functions

Circadian rhythms have primarily been observed at the whole-plant level, using tissue from whole seedlings to measure the 24-hour oscillations in mRNA expression or bioluminescence from luciferase reporters (Millar et al., 1992; Harmer et al., 2000). With the development of micrografting, tissue-specific approaches, and single-cell technologies (**Figure 7.1**), several studies have revealed that the *A. thaliana* clock has cell-type-specific properties that deviate from the strict 24-hour period and expression levels observed globally (James et al., 2008; Endo et al., 2014; Takahashi et al., 2015; Gould et al., 2018; Lee and Seo, 2018; Román et al., 2020). Apart from the cotyledons, which maintain a 24-hour period even under constant light conditions, the hypocotyl, root, and root tip have significantly longer free-running periods (Greenwood et al., 2019). Interestingly, single-cell imaging of CCA1-YFP and near-single-cell imaging of *GIGANTEA* (*GI*)*::LUC* showed that a small portion of cells in the root tip exhibited a short period, indicating that tissue-specific circadian function is more complex than a simple delineation between shoot and root (Gould et al., 2018; Greenwood et al., 2019). Another

study demonstrated that guard cells of the cotyledon have delayed expression of CCA1-HA-YFP and a longer period compared to the surrounding mesophyll and epidermal cells, demonstrating further, sub-cotyledon partitioning of clock activity (Yakir et al., 2011).

In addition to differences in their free-running period, transcript abundance of core circadian regulators differs between cell types (Para et al., 2007; James et al., 2008; Endo et al., 2014; Lee and Seo, 2018). Evening-peaking clock gene transcripts tend to be more abundant in the root and vascular tissue, suggesting evening genes are important for clock function in these organs (Para et al., 2007; Endo et al., 2014; Lee and Seo, 2018). In contrast, morning-phased genes have low transcript abundance in the root and high expression in the mesophyll (Endo et al., 2014). In agreement with reduced activity in the roots, the morning-expressed CCA1 and LHY transcription factors decrease binding activity to target genes promoters in the root tissue, reducing their repressive activity in this organ (James et al., 2008).

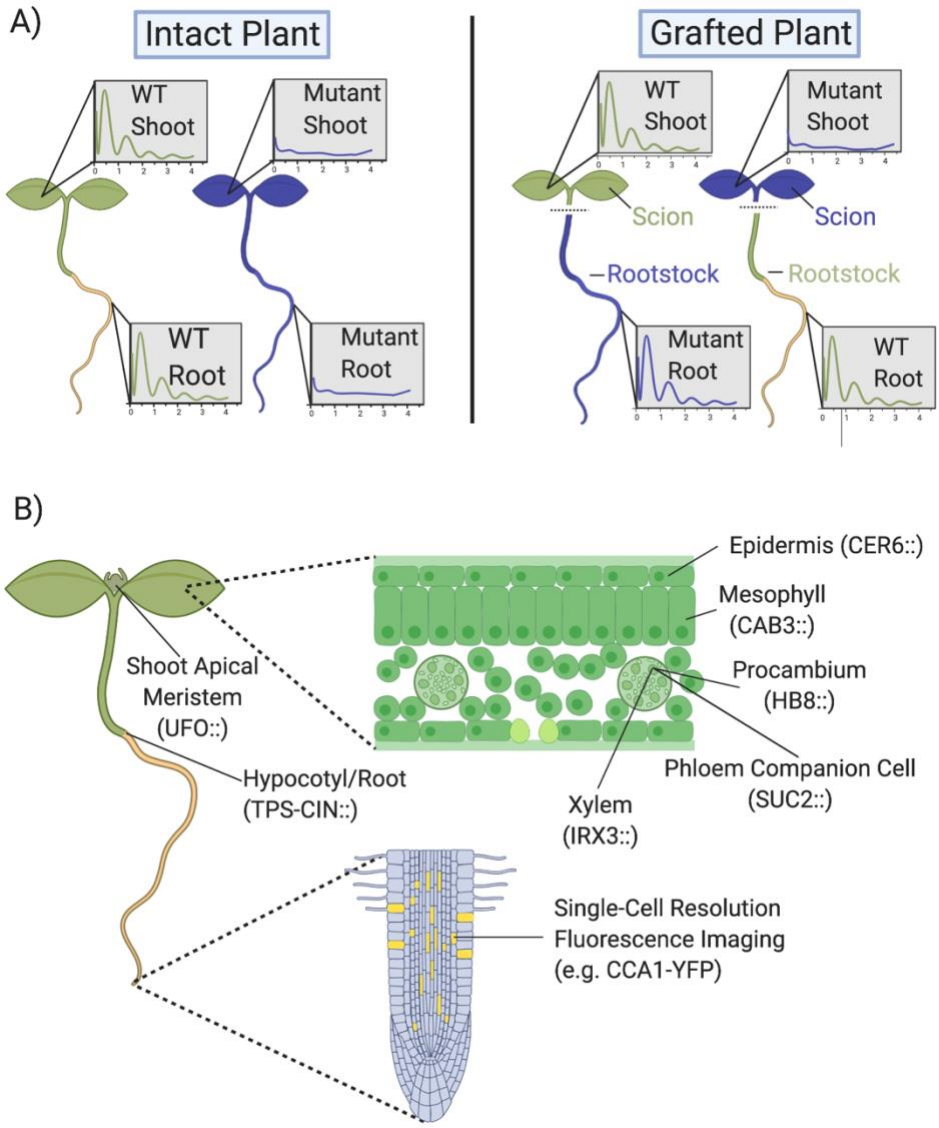

Figure 7.1 Tissue-specific techniques.
(A) Schematic of a micrografting experiment. Rhythms of an intact wild-type (WT) plant (green) and an arrhythmic clock mutant (blue) are shown to the left, while reciprocal grafts using the shoot as the scion and the hypocotyl/roots as the rootstock are shown to the right. WT scions (specifically, the shoot apical meristem) are able to confer WT rhythms to mutant rootstocks, while WT rootstocks cannot rescue rhythms in a mutant shoot [22]. Broken horizontal line indicates graft location. (B) Tissue-specific promoters and single-cell reporter systems have enabled spatiotemporal study of the clock in plants. Abbreviations: CAB3, CHLOROPHYLL A/B BINDING PROTEIN 3; CER6, 3-KETOACYL-COA SYNTHASE 6; HB8, HOMEOBOX GENE 8; IRX3, IRREGULAR XYLEM 3; SUC2, SUCROSE-PROTON SYMPORTER 2; TPS-CIN, TERPENE SYNTHASE-LIKE SEQUENCE-1,8-CINEOLE; UFO, UNUSUAL FLORAL ORGANS. Figure created with BioRender.com.

The mechanism behind organ-specific circadian rhythms is unknown. One possibility is that every tissue may possess different sensitivity to environmental stimuli such as light and temperature. For instance, the epidermis is the first cell layer that intercepts temperature information and is thus a logical location where the clock might act on temperature cues. Indeed, perturbation of the epidermal clock by overexpressing *CCA1* from the epidermis-specific *CER6* promoter resulted in hypersensitive temperature-dependent cell elongation (**Figure 7.2B**), while *CCA1-OX* in the vasculature or the mesophyll did not (Shimizu et al., 2015). Light-piping via the vascular system may point to the vasculature clock playing a role in the systemic transmission of light signaling in plants (Nimmo, 2018). Lastly, the long period observed in roots may result from differential input of light and sucrose signals to this organ (James et al., 2008; Bordage et al., 2016; Nimmo, 2018; Greenwood et al., 2019). It will be interesting to see if other abiotic and biotic inputs to the clock are perceived via specific organs. For example, perhaps circadian-regulated immune responses are primarily triggered in guard cells of the epidermis (Melotto et al., 2006), while the root clock might be highly sensitive to changes in water availability or ion concentration.

With the vast differences in clock properties in different tissues, it is not surprising that several studies have noted different organ clocks regulate specific phenotypic outputs (Endo et al., 2014; Shimizu et al., 2015; VoB et al., 2015). Disruption of clock activity in the phloem companion cells decreases *FT* expression and leads to delayed flowering, indicating that precise clock function in the vasculature is required for proper circadian regulation of reproductive development (Endo et al., 2014; Shimizu et al., 2015). Similar disruption of the mesophyll or epidermal clocks had no effect on flowering time

(Shimizu et al., 2015). As previously mentioned, the epidermal clock is critical for temperature-regulated cell elongation (Shimizu et al., 2015). Finally, loss of the core clock gene *TOC1* or global overexpression of *CCA1* or its homolog *LHY* leads to defects in lateral root emergence, suggesting the root clock could be important for this developmental process (VoB et al., 2015). However, additional tissue-specific experiments are needed to substantiate this claim (**Figure 7.2B**).

7.4 Local Coupling Synchronizes Neighboring Cell Clocks

Arabidopsis has cell-autonomous clocks that can maintain circadian rhythms when given an entrainment cue (Box 1) (**Figure 7.2A**) (Thain et al., 2000; Yakir et al., 2011). While this mechanism allows for the continuous entrainment of each cell clock with the environment, several studies have suggested that a weak cell-to-cell coupling phenomenon plays a role in clock synchronization (Fukuda et al., 2007; James et al., 2008; Fukuda et al., 2012; Wenden et al., 2012; Takahashi et al., 2015; Muranaka and Oyama, 2016). In *Lemna gibba* (duckweed), single-cell resolution data from a AtCCA1::LUC reporter showed that individual cells in constant light rapidly desynchronize and exhibit a range of free-running periods (Muranaka and Oyama, 2016). This suggests that noise in cellular clocks can result in highly variable rhythms without an entrainment cue. However, neighboring cells within a radius of 0.5 mm showed lower period length variation, suggesting that short-range coupling allows these cells to synchronize their clocks (Muranaka and Oyama, 2016). Additionally, local coupling has been observed in arabidopsis and positively correlates with cell density (Gould et al., 2018), as has been reported in mammals (Aton et al., 2005). The root tip, for example, shows high coupling (Gould et al., 2018). The significance of this regional variance on coupling strength is not

known. Perhaps counterintuitively, the root tip also exhibits the highest level of cell-to-cell variability in period length in an arabidopsis seedling (Gould et al., 2018). Thus, we think it is possible that recently differentiated cells have a higher stochastic circadian gene expression requiring stronger coupling to harmonize with the environment and neighboring cells during early cell programming.

There is high cell-to-cell variability in clock gene expression and other environmental-response genes despite the presence of synchronizing cues such as light and temperature cycles (Muranaka and Oyama, 2016; Cortijo et al., 2019). Stochasticity could confer plasticity to the plant's response to unpredictable stressors in the environment, serving as an evolutionarily advantageous bet-hedging strategy (Cortijo et al., 2019; Webb et al., 2019; Cortijo and Locke, 2020). Although there is heterogeneity in cell-to-cell clock gene expression, plants grown under free-running conditions do not exhibit spatially randomized phases, implicating that an endogenous process, such as cell-to-cell coupling, serves as a synchronizing force (Wenden et al., 2012; Greenwood et al., 2019).

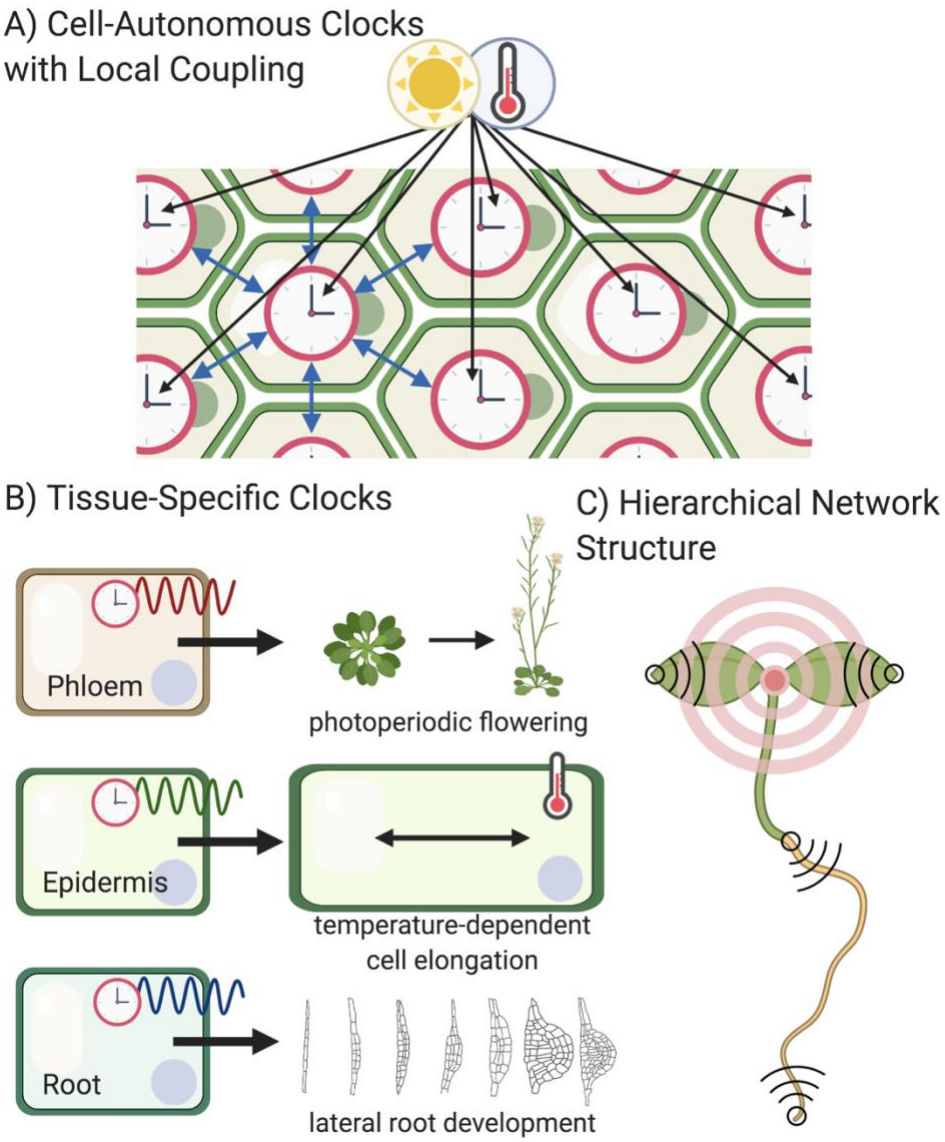

Figure 7.2 Key properties of the plant clock network.
(A) Each cell in the plant clock possesses a complete circadian oscillator that can use entrainment cues to produce rhythms cell autonomously. These cells do not operate independently but rather are weakly synchronized to neighboring cells via local coupling (represented by blue arrows). (B) The plant has tissue-specific clocks that regulate specific processes. For example, the phloem clock regulates photoperiodic flowering; the epidermis clock plays a role in temperature-dependent cell elongation; and the root clock is involved with lateral root development. (C) The architecture of the plant circadian signaling network is made up of a hierarchical system with multiple synchronization hubs. The shoot apical meristem possesses a dominant clock (red signal), but there are other synchronization points potentially located at the root tip, the base of the root, and the leaf edges (black signals). Figure created with BioRender.com.

In the mammalian system, cell-to-cell coupling produces spatial waves of clock gene expression in the central SCN clock (Welsh et al., 2010). There is experimental and

mathematical evidence that spatial waves of gene expression also exist in plants, albeit with multiple origins instead of one synchronization location (**Figure 7.2C**) (Rascher et al., 2001; Fukuda et al., 2007; Fukuda et al., 2012; Ukai et al., 2012; Wenden et al., 2012; Gould et al., 2018; Greenwood et al., 2019). For instance, waves of CCA1-YFP expression are present in the arabidopsis root, where they originate from the root tip and the top of the root closer to the hypocotyl (Gould et al., 2018). Waves of CCA1::LUC expression have also been observed in leaf tissue in arabidopsis and lettuce (Ukai et al., 2012; Wenden et al., 2012). Mathematical modeling incorporating organ-specific periods and local coupling recapitulated the spatial waves observed in experimental setups, confirming that these factors are sufficient to produce this spatiotemporal clock gene expression (Greenwood et al., 2019). These precisely timed spatial oscillations imply that there could be a diffusible or actively transported molecular signal communicated between adjacent cells that enables rhythmic coupling. Together, these experiments demonstrate weak local coupling maintains synchrony between neighboring cells and contributes to producing spatial waves of gene expression across organs. We speculate that strong coupling between cells would theoretically eliminate the observed tissue-specific differences in period and other clock parameters, yielding a plant that exhibits circadian uniformity. Perhaps weak local coupling provides a low level of buffering against cell-to-cell variability in circadian rhythms while still enabling regional functional partitioning.

7.5 Long-distance clock communication follows a hierarchical model with multiple synchronization points

In addition to local synchronization of clock activity, evidence for long-distance signaling of circadian information has helped define the network architecture of the clock communication system in plants. Perturbations in clock activity in one part of the plant can affect the clock in a distal location (Endo et al., 2014; Takahashi et al., 2015). However, there does not appear to be a single clock dominant to all other tissue clocks in plants. Instead, there is possibly a hierarchy of synchronization hubs that transmit circadian information throughout the plant, with the shoot apical meristem (SAM) serving as a dominant clock (**Figure 7.2C**) (Takahashi et al., 2015).

Formative work using micrografting in arabidopsis demonstrated that the SAM clock is dominant to the root clock, establishing hierarchy in the plant clock network (Takahashi et al., 2015). This study showed that joining a wild-type shoot apex scion with an arrhythmic clock mutant rootstock (*cca1-1/lhy-11* or *elf3-2*) restored wild-type rhythms in the root. In contrast, grafting a wild-type rootstock to a clock mutant SAM did not recover shoot rhythms, suggesting the shoot apex clock is uniquely capable of transmitting circadian information from the shoot to the root (**Figure 7.1**). Interestingly, the arrhythmic mutant SAM did not send an overriding “arrhythmic signal” to the wild-type root, which maintained normal 24-hour rhythms. The mechanism behind this genotype-specific SAM dominance over the root clock as not been established. While the SAM appears to have a dominant role in the clock network hierarchy, it is not required for clock function in other parts of the plant, as detached roots can sustain circadian rhythmicity for several days before dampening (Bordage et al., 2016; Li et al., 2020). Additionally, when grown under opposite light-dark entrainment cycles, the root and shoot clocks can operate in antiphase, indicating that synchronization by light input is dominant to any

tissue-specific signals (Bordage et al., 2016). Transmission of circadian information between the shoot and the root is also supported by earlier work showing chemical inhibition of sucrose production in photosynthetic leaf tissue disrupts the root clock, suggesting sucrose or a photosynthesis-related signal from the shoot is important for root rhythms (James et al., 2008).

The multiple origin points for spatial waves of gene expression include the SAM, root tip, the base of the root near the hypocotyl, and the edge of the leaf tissue (**Figure 7.2C**) (Ukai et al., 2012; Wenden et al., 2012; Takahashi et al., 2015; Gould et al., 2018). Areas of high cell density such as the root and shoot meristems are associated with increased coupling and, interestingly, are also proposed signaling hubs for clock communication (Takahashi et al., 2015; Gould et al., 2018). This is comparable to the mechanism in mammals where tight intercellular coupling in the SCN helps maintain robust rhythms (Liu et al., 2007). Perhaps the high cell density found in plant meristems is a quality that makes these ideal signaling hubs.

7.6 There are multiple candidates for potential signaling molecules mediating clock communication

Research is ongoing to identify the signal and signal transmission mechanism behind clock communication. Some possible signaling molecule(s) include mobile RNA species, photosynthetic sucrose (James et al., 2008; Philippou et al., 2019), protein molecules (Lee and Seo, 2018; Greenwood et al., 2019; Chen et al., 2020), and ions (Ruiz et al., 2018) (**Figure 7.3**). Among these candidates, there is direct evidence that demonstrates sucrose and the clock protein ELF4 are signaling molecules in the clock (James et al., 2008; Chen et al., 2020).

While mobile RNAs play a role in other signaling pathways (Kragler and Kehr, 2018), there is no direct evidence that these molecules are involved in cell-to-cell circadian synchronization to date. However, analysis of a study examining mobile transcripts in an ecotype heterograft of arabidopsis (Thieme et al., 2015) showed that 495 (24.6%) of the 2006 transcripts identified as cell-to-cell mobile also exhibit circadian-regulated expression under constant light conditions (unpublished, diurnal.mocklerlab.org). Also, within this list of 2006 mobile mRNAs are those of *LUX*, *GI*, *TOC1*, *CCA1 HIKING EXPEDITION (CHE)*, *LIGHT-INSENSITIVE PERIOD 1* (*LIP1*), and *TANDEM ZINC KNUCKLE PLUS3* (*TZP*), all of which are circadian-associated genes (**Table 7.1**). It will be interesting to explore whether these circadian-regulated mobile mRNAs help transmit circadian information across the plant.

Photosynthate is both an input and output of the circadian clock (Haydon et al., 2013; Haydon et al., 2017; Seki et al., 2017; Philippou et al., 2019) and has been shown to be involved in intercellular clock communication (James et al., 2008). Inhibiting photosynthesis using 3-(3,4-dichlorophyenyl)-1,1-dimethylurea (DCMU) treatment dampens the rhythmic expression of some clock genes in the roots while leaving shoots unaffected, suggesting sucrose signals from photosynthetic tissue sustains clock function below ground (James et al., 2008; Takahashi et al., 2015). In contrast, a 2016 study argued that tissue-specific light intensity was a more powerful determinant of shoot versus root rhythms than sucrose signaling when they observed no difference in rhythms when plants were grown with or without 1% sucrose (Bordage et al., 2016). However, this study supplied sucrose via the growth media, whereas it might be more biologically relevant to disrupt photosynthetic production of sugars using low light and CO_2, or an inhibitor like

DCMU. While further work is needed to clarify these discrepancies, there is strong evidence that shoot-to-root sucrose signaling is involved in circadian communication.

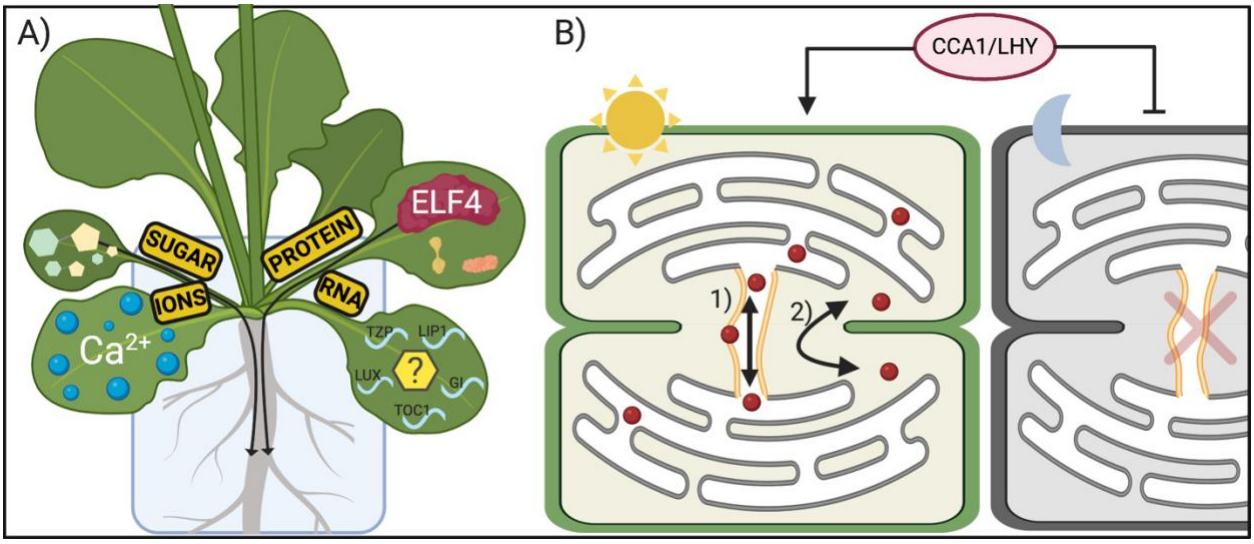

Figure 7.3 Potential signals and transport mechanisms.
(A) Potential signaling molecules include sucrose; ions such as Ca^{2+}; mobile RNA such as LUX, CHE, TZP, LIP1, GI, and TOC1; and proteins including ELF4. Sucrose and ELF4 have known shoot-to-root signaling activity. (B) Potential circadian signaling molecules likely travel via the plasmodesmata (PD). The clock gates PD transport during the day and decreases transport at night in arabidopsis and *Nicotiana benthamiana*. In tobacco, the CCA1/LHY homolog mediates gating of PD transport. Red spheres represent the potential clock signaling molecule(s). The desmotubule is highlighted in yellow. PD transport could be (i) targeted transport that requires interaction with the PD membrane or (ii) nontargeted diffusion through the PD channel. Figure created with BioRender.com.

Mobile proteins can act non-cell-autonomously to communicate information between cell types within tissues and to distal organs in plants, as is the case for SHORTROOT (SHR) (Nakajima et al., 2001), ELONGATED HYPOCOTYL5 (HY5) (Chen et al., 2016), and FLOWERING LOCUS T (FT) (Jaeger and Wigge, 2007). Recently, the core circadian oscillator component, ELF4 was proposed as a shoot-to-root mobile signaling protein involved in communicating aboveground temperature information to the root clock (Chen et al., 2020) (**Figure 7.3**). ELF4 is part of the core clock oscillator in arabidopsis in a tripartite protein complex called the evening complex (EC) where it functions to enhance EC activity (Nusinow et al., 2011; Herrero et al., 2012; Silva et al.,

2020). ELF4 is a small protein (12,375 Da) with a high isoelectric point (pI= 9.16) that is similar to other mobile proteins such as HY5 and FT. Micrografting the shoot apex scion of an *ELF4-GFP* overexpression line onto an arrhythmic *elf4*-1 mutant rootstock (hypocotyl and roots) resulted in the restoration of wild-type rhythms in the roots, consistent with previous grafting experiments (Takahashi et al., 2015). GFP signal in this graft could be observed in the vasculature and root tissue, suggesting that ELF4-GFP may travel long distances in the plant to regulate the root clock (Chen et al., 2020) (**Figure 7.3**). Importantly, injecting purified ELF4 protein into leaves of *elf4-1* seedlings also rescued root rhythms, demonstrating that the transmissible molecule is ELF4 protein and not its mRNA. The small size of ELF4 protein is important for its shoot-to-root trafficking, as rescue of root rhythms was blocked in a graft of an *ELF4-3xGFP* apex and *elf4-1* roots. Adding to the established roles for the EC in temperature response (Mizuno et al., 2014a; Mizuno et al., 2014b; Jung et al., 2020), the authors also showed that ELF4 shoot-to-root movement decreases with warmer temperatures and thus produces faster rhythms in the root. ELF4 is the first identified cell-to-cell mobile core circadian clock protein that participates in the communication of temperature information from the shoot to the root.

Several other proteins have characteristics that could make them ideal mobile signaling molecule candidates in clock communication (**Table 7.1**). The mobile transcriptional regulator HY5 is a potential circadian signaling molecule based on its shoot-to-root movement and regulation of circadian rhythms (Andronis et al., 2008; Chen et al., 2016; Hajdu et al., 2018; Greenwood et al., 2019). Another protein candidate is the core clock component GI, which is among the list of mobile mRNAs (Thieme et al., 2015). GI has highest tissue-specific mRNA expression in the shoot (Lee and Seo, 2018), yet

the *gi-2* mutant has dampened circadian rhythms exclusively in the root tissue (Lee and Seo, 2018), indicating GI has tissue specific and perhaps non-cell-autonomous activity. Based on studies performed in the root, approximately one-fifth of all transcription factors are cell-to-cell mobile (Lee et al., 2006; Gallagher et al., 2014), indicating that a mobile protein signal could likely be an important factor of cell-to-cell synchronization of circadian rhythms.

Calcium (Ca^{2+}) can move as a rapid, systemic signaling molecule in response to wounding, salt stress, and other abiotic and biotic stressors in a cell-type-specific manner (Wood et al., 2001; Martí et al., 2013; Choi et al., 2014). Additionally, Ca^{2+} is considered both an entrainment input and physiological output of the plant circadian clock, with rhythmic cytosolic Ca^{2+} levels peaking towards the middle-to-end of the day under constant light or light/dark cycles (Johnson et al., 1995; Love et al., 2004; Dodd et al., 2007; Ruiz et al., 2018). Dark-induced transient increases in Ca^{2+} originate from green tissue, providing the possibility that this shoot-specific signal would need to be communicated to the root (Ruiz et al., 2020). While future work is required to test this hypothesis, these characteristics support Ca^{2+} as another potential signaling molecule involved in clock communication.

While this list is not exhaustive, we would also like to highlight that ROS-mediated salicylic acid (SA) has been shown to propagate systemic period lengthening and rhythm dampening from a local *Pseudomonas syringae* infection and could be a circadian signal (Li et al., 2018). Indeed, in addition to SA, any mobile signaling molecule that acts as an input to the circadian clock could be co-opted as a proxy signal to communicate circadian information; perhaps Ca^{2+}, SA, glutamate (Gutierrez et al., 2008; Toyota et al., 2018), and

other ions, metabolites, or hormones fall under this proxy signal role. We expect that multiple signaling molecules contribute to the transmission of circadian information in the plant.

7.7 The plasmodesmata are a likely conduit for circadian transport

Plasmodesmata (PD), the channels that connect adjacent cells via the cytoplasm, are a logical conduit for circadian communication (Lee and Frank, 2018; Petit et al., 2019) (**Figure 7.3**). PD transport is regulated by light and the circadian clock in arabidopsis and *Nicotiana benthamiana*, with the clock gating light-induced PD transport during the day in a *CCA1/LHY*-mediated manner in *N. benthamiana* (Brunkard and Zambryski, 2019). The mechanism by which the clock regulates PD transport is unclear, but does not appear to involve changing callose deposition at the PD (Brunkard and Zambryski, 2019). However, increasing callose deposition at PD using the *CALS3* gain-of-function mutant (*cals3-d*) (Vatén et al., 2011) dampened rhythms in the roots but not the shoots, supporting a role for PD transport in shoot-to-root clock communication (Takahashi et al., 2015).

Symplastic transport could play a role in both local and long-distance signaling. At the local level, spatial waves of gene expression could be propagated cell-to-cell via a signal moving through PD. On a larger scale, PD connecting the cells in the phloem could regulate the long-distance trafficking of a signaling molecule. For example, the flowering regulator FT is transported from the companion cell of the phloem into the sieve tube element where it mobilizes to the apical meristem to promote reproductive development (Jaeger and Wigge, 2007; Mathieu et al., 2007).

Movement of molecules through the PD can occur in a targeted or non-targeted manner (Crawford and Zambryski, 2001). Targeted movement is named after the distinct puncta that a protein forms on the desmotubule of the PD, indicating that the protein is interacting with PD components to regulate its transport. FT appears to be transported in a targeted manner, working with the ER-membrane-localized FT-INTERACTING PROTEIN 1 (FTIP1) in the PD channel for efficient transport to the sieve tube (Liu et al., 2012). In non-targeted movement, a molecule moves via simple diffusion between cells. The floral identity transcription factor LEAFY (LFY) is an example of a protein that moves in a non-targeted fashion (Wu et al., 2003). The mechanism by which ELF4 moves has yet to be determined. Proteins that are small enough (about 40 kDa) to move through the PD without changing the size exclusion limit of the channel's aperture may move by diffusion (**Table 7.1**) (Gallagher and Benfey, 2005; Gallagher et al., 2014). Currently, there is little evidence that transcription factors move apoplastically through the extracellular space (Gallagher et al., 2014).

Table 7.1 Circadian-associated genes that encode predicted mobile proteins and/or mobile transcripts

Shaded rows indicate proteins whose molecular weight is less than 40,000 Da and thus may be able to move via passive diffusion, depending on their solubility (Gallagher et al., 2014).

Protein	Molecular weight (Da)	Isoelectric Point (pI)	AGI Locus Code
ELF4	12,375.50	9.16	AT2G40080
HY5	18,463.10	10.19	AT5G11260
FT	19,808.40	8.05	AT1G65480
CHE‡	24,751.10	10.20	AT5G08330
LNK3	30,553.70	3.97	AT3G12320
LNK4	31,959.70	4.11	AT5G06980
RVE4	32,206.80	5.09	AT5G02840
RVE2	32,436.10	7.54	AT5G37260
RVE3	32,795.20	10.18	AT1G01520

RVE8	32,800.80	9.79	AT3G09600
RVE5	33,890.10	9.73	AT4G01280
LUX‡	35,011.40	5.85	AT3G46640
RVE6	36,264.00	9.45	AT5G52660
LIP1‡	37,741.10	9.18	AT5G64813
LWD1	39,088.30	4.57	AT1G12910
LWD2	39,091.30	4.49	AT3G26640
XCT	39,239.50	6.62	AT2G21150
TOC1‡	60,194.80	7.59	AT5G61380
COP1‡	76,187.00	6.83	AT2G32950
TZP‡	90,613.20	4.99	AT5G43630
GI‡	127,874.00	7.04	AT1G22770
PHYB‡	129,330.20	5.69	AT2G18790

‡ indicates genes whose transcripts were identified as cell-to-cell mobile in Thieme et al. (2015).

7.8 Concluding Remarks and Future Perspectives

Evidence of tissue-specific clocks, local synchronization between neighboring cells, and non-cell-autonomous effects of clock perturbation supports the existence of communication of circadian information in plants. This intercellular communication may be in place to maintain whole-plant synchrony amongst the noisy clock gene expression observed on a cell-to-cell basis (Cortijo et al., 2019) and tissue clocks with distinct circadian period and expression profiles. It would be interesting to test this hypothesis by inhibiting the signaling molecule or mechanism of communication and determine if rhythms rapidly dampen due to loss of synchronization.

Expanding our knowledge on the tissue-specific roles of the clock could help guide future engineering efforts. Time-resolved single-cell RNA-sequencing—as has been completed using the mouse SCN (Pembroke et al., 2015; Wen et al., 2020)—would be a useful tool for expanding our understanding of cell-type-specific clocks. For example, crop improvement projects targeting circadian-regulated flowering time may benefit from specifically engineering the phloem companion cell clock instead of manipulating the clock in all tissues, which could produce unintended phenotypes.

Identification of shoot- and root-specific circadian functions provides the opportunity to utilize grafting as a crop improvement tool targeting clock-regulated traits. Grafting has been used primarily in woody plants like fruit trees, but more recently been adapted in vegetable crops to confer resistance to soil-borne pathogens and heartiness against abiotic stressors like drought, cold, and nutrient stress (Savvas et al., 2010; Warschefsky et al., 2016; Kyriacou et al., 2017; Grieneisen et al., 2018). Additionally, a large amount of work has been done studying transport across the graft junction to produce systemic changes in root and shoot tissue (Gaut et al., 2019; Thomas and Frank, 2019). Because mutations in circadian clock genes can result in highly pleiotropic phenotypes (Creux and Harmer, 2019), a clock mutant may positively affect one phenotype while simultaneously decreasing the plant's fitness via another pathway (Zhang et al., 2019). Grafting together specific clock mutants could circumvent this, allowing a beneficial root-specific clock mutant phenotype to coexist in a plant with a wild-type shoot ecotype that is unaffected by the clock mutation, for example. With the accumulating evidence of tissue-specific clock functions and long-distance signaling of circadian rhythms, we anticipate that heterografts targeting clock phenotypes like

flowering time and abiotic stress response will add to the repertoire of high-value crops produced via this methodology.

7.9 References

Andronis C, Barak S, Knowles SM, Sugano S, Tobin EM (2008) The clock protein CCA1 and the bZIP transcription factor HY5 physically interact to regulate gene expression in Arabidopsis. Mol Plant **1**: 58–67

Aton SJ, Colwell CS, Harmar AJ, Waschek J, Herzog ED (2005) Vasoactive intestinal polypeptide mediates circadian rhythmicity and synchrony in mammalian clock neurons. Nat Neurosci **8**: 476–483

Bordage S, Sullivan S, Laird J, Millar AJ, Nimmo HG (2016) Organ specificity in the plant circadian system is explained by different light inputs to the shoot and root clocks. New Phytol **212**: 136–149

Brunkard JO, Zambryski P (2019) Plant Cell-Cell Transport via Plasmodesmata Is Regulated by Light and the Circadian Clock. Plant Physiol **181**: 1459–1467

Chen WW, Takahashi N, Hirata Y, Ronald J, Porco S, Davis SJ, Nusinow DA, Kay SA, Mas P (2020) A mobile ELF4 delivers circadian temperature information from shoots to roots. Nat Plants **6**: 416–426

Chen X, Yao Q, Gao X, Jiang C, Harberd NP, Fu Correspondence X (2016) Shoot-to-Root Mobile Transcription Factor HY5 Coordinates Plant Carbon and Nitrogen Acquisition. Curr Biol **26**: 640–646

Choi W-G, Toyota M, Kim S-H, Hilleary R, Gilroy S (2014) Salt stress-induced Ca 2+ waves are associated with rapid, long-distance root-to-shoot signaling in plants. Proc Natl Acad Sci **111**: 6497–6502

Cortijo S, Aydin Z, Ahnert S, Locke JC (2019) Widespread inter-individual gene expression variability in Arabidopsis thaliana. Mol Syst Biol **15**: 1–16

Cortijo S, Locke JCW (2020) Does Gene Expression Noise Play a Functional Role in Plants? Trends Plant Sci 1–11

Crawford KM, Zambryski PC (2001) Non-Targeted and Targeted Protein Movement through Plasmodesmata in Leaves in Different Developmental and Physiological States. Plant Physiol **125**: 1802–1812

Creux N, Harmer S (2019) Circadian Rhythms in Plants. Cold Spring Harb Perspect Biol. doi: 10.1101/cshperspect.a034611

Dibner C, Schibler U, Albrecht U (2010) The Mammalian Circadian Timing System: Organization and Coordination of Central and Peripheral Clocks. Annu Rev Physiol **72**: 517–549

Dodd AN, Gardner MJ, Hotta CT, Hubbard KE, Dalchau N, Love J, Assie J-M, Robertson FC, Jakobsen MK, Goncalves J, et al (2007) The Arabidopsis Circadian Clock Incorporates a cADPR-Based Feedback Loop. Science **318**: 1789–1792

Dodd AN, Salathia N, Hall A, Kévei E, Tóth R, Nagy F, Hibberd JM, Millar AJ, Webb A a R (2005) Plant circadian clocks increase photosynthesis, growth, survival, and competitive advantage. Science **309**: 630–633

Edgar RS, Green EW, Zhao Y, Van Ooijen G, Olmedo M, Qin X, Xu Y, Pan M, Valekunja UK, Feeney KA, et al (2012) Peroxiredoxins are conserved markers of circadian rhythms. Nature **485**: 459–464

Endo M, Shimizu H, Nohales MA, Araki T, Kay SA (2014) Tissue-specific clocks in Arabidopsis show asymmetric coupling. Nature **515**: 419–422

Fukuda H, Nakamichi N, Hisatsune M, Murase H, Mizuno T (2007) Synchronization of Plant Circadian Oscillators with a Phase Delay Effect of the Vein Network. Phys Rev Lett **99**: 10.1103/PhysRevLett.99.098102

Fukuda H, Ukai K, Oyama T (2012) Self-arrangement of cellular circadian rhythms through phase-resetting in plant roots. Phys Rev E **86**: 10.1103/PhysRevE.86.041917

Gallagher KL, Benfey PN (2005) Not just another hole in the wall: Understanding intercellular protein trafficking. Genes Dev **19**: 189–195

Gallagher KL, Sozzani R, Lee C-M (2014) Intercellular Protein Movement: Deciphering the Language of Development. Annu Rev Cell Dev Biol **30**: 207–233

Gaut BS, Miller AJ, Seymour DK (2019) Living with Two Genomes: Grafting and Its Implications for Plant Genome-to-Genome Interactions, Phenotypic Variation, and Evolution. Annu Rev Genet **53**: 195–215

Gould PD, Domijan M, Greenwood M, Tokuda IT, Rees H, Kozma-Bognar L, Hall AJ, Locke JC (2018) Coordination of robust single cell rhythms in the Arabidopsis circadian clock via spatial waves of gene expression. Elife **7**: https://doi.org/10.7554/eLife.31700

Greenwood M, Domijan M, Gould PD, Hall AJW, Locke JCW (2019) Coordinated circadian timing through the integration of local inputs in Arabidopsis thaliana. PLoS Biol **17**: 10.1371/journal.pbio.3000407

Grieneisen ML, Aegerter BJ, Stoddard CS, Zhang M (2018) Yield and fruit quality of grafted tomatoes, and their potential for soil fumigant use reduction. A meta-analysis. Agron Sustain Dev **38**: https://doi.org/10.1007/s13593-018-0507-5

Gutierrez RA, Stokes TL, Thum K, Xu X, Obertello M, Katari MS, Tanurdzic M, Dean A, Nero DC, McClung CR, et al (2008) Systems approach identifies an organic nitrogen-responsive gene network that is regulated by the master clock control gene CCA1. Proc Natl Acad Sci **105**: 4939–4944

Hajdu A, Dobos O, Domijan M, Azs B Alint B, An Nagy I, Nagy F, Aszl O Kozma-Bogn Ar L (2018) ELONGATED HYPOCOTYL 5 mediates blue light signalling to the Arabidopsis circadian clock. Plant J **96**: 1242–1254

Harmer SL, Hogenesch JB, Straume M, Chang H-S, Han B, Zhu T, Wang X, Kreps JA, Kay SA (2000) Orchestrated Transcription of Key Pathways in Arabidopsis by the Circadian Clock. Science **290**: 2110–2113

Haydon MJ, Mielczarek O, Frank A, Román Á, Webb AAR (2017) Sucrose and Ethylene Signaling Interact to Modulate the Circadian Clock. Plant Physiol **175**: 947–958

Haydon MJ, Mielczarek O, Robertson FC, Hubbard KE, Webb A a R (2013) Photosynthetic entrainment of the Arabidopsis thaliana circadian clock. Nature **502**: 689–92

Herrero E, Kolmos E, Bujdoso N, Yuan Y, Wang M, Berns MC, Uhlworm H, Coupland G, Saini R, Jaskolski M, et al (2012) EARLY FLOWERING4

Recruitment of EARLY FLOWERING3 in the Nucleus Sustains the Arabidopsis Circadian Clock. Plant Cell **24**: 428–443
Hicks KA, Albertson TM, Wagner DR (2001) EARLY FLOWERING3 Encodes a Novel Protein That Regulates Circadian Clock Function and Flowering in Arabidopsis. Plant Cell **13**: 1281–1292
Jaeger KE, Wigge PA (2007) FT Protein Acts as a Long-Range Signal in Arabidopsis. Curr Biol **17**: 1050–1054
James AB, Monreal JA, Nimmo GA, Kelly CL, Herzyk P, Jenkins GI, Nimmo HG (2008) The circadian clock in Arabidopsis roots is a simplified slave version of the clock in shoots. Science **322**: 1832–1835
Johnson CH, Knight MR, Kondo T, Masson P, Sedbrook J, Haley A, Trewavas A (1995) Circadian Oscillations of Cytosolic and Chloroplastic Free Calcium in Plants. Science **269**: 1863–1865
Jung J-H, Barbosa AD, Hutin S, Kumita JR, Gao M, Derwort D, Silva CS, Lai X, Pierre E, Geng F, et al (2020) A prion-like domain in ELF3 functions as a thermosensor in Arabidopsis. Nature. doi: 10.1038/s41586-020-2644-7
Kragler F, Kehr J (2018) Long distance RNA movement. New Phytol **218**: 29–40
Kyriacou MC, Rouphael Y, Colla G, Zrenner R, Schwarz D (2017) Vegetable Grafting: The Implications of a Growing Agronomic Imperative for Vegetable Fruit Quality and Nutritive Value. Front Plant Sci **8**: 10.3389/fpls.2017.00741
Lee HG, Seo PJ (2018) Dependence and independence of the root clock on the shoot clock in Arabidopsis. Genes Genomics **40**: 1063–1068
Lee J-Y, Colinas J, Wang JY, Mace D, Ohler U, Benfey PN (2006) Transcriptional and posttranscriptional regulation of transcription factor expression in Arabidopsis roots. Proc Natl Acad Sci **103**: 6055–6060
Lee J-Y, Frank M (2018) Plasmodesmata in phloem: different gateways for different cargoes. Curr Opin Plant Biol **43**: 119–124
de Leone MJ, Hernando CE, Vázquez M, Schneeberger K, Yanovsky MJ (2020) Bacterial Infection Disrupts Clock Gene Expression to Attenuate Immune Responses. Curr Biol **30**: 1–8
Li Y, Wang L, Yuan L, Song Y, Sun J, Jia Q, Xie Q, Xu X (2020) Molecular investigation of organ-autonomous expression of Arabidopsis circadian oscillators. Plant Cell Environ 1–12
Li Z, Bonaldi K, Uribe F, Pruneda-Paz JL (2018) A Localized Pseudomonas syringae Infection Triggers Systemic Clock Responses in Arabidopsis. Curr Biol **28**: 630-639.e4
Liu AC, Welsh DK, Ko CH, Tran HG, Zhang EE, Priest AA, Buhr ED, Singer O, Meeker K, Verma IM, et al (2007) Intercellular Coupling Confers Robustness against Mutations in the SCN Circadian Clock Network. Cell **129**: 605–616
Liu L, Liu C, Hou X, Xi W, Shen L, Tao Z, Wang Y, Yu H (2012) FTIP1 is an essential regulator required for florigen transport. PLoS Biol **10**: e1001313
Love J, Dodd AN, Webb AAR (2004) Circadian and Diurnal Calcium Oscillations Encode Photoperiodic Information in Arabidopsis. Plant Cell **16**: 956–966
Martí MC, Stancombe MA, Webb AAR (2013) Cell-and stimulus type-specific intracellular free Ca2+ signals in Arabidopsis. Plant Physiol **163**: 625–634
Mathieu J, Warthmann N, Küttner F, Schmid M (2007) Export of FT Protein from

Phloem Companion Cells Is Sufficient for Floral Induction in Arabidopsis. Curr Biol **17**: 1055–1060

Melotto M, Underwood W, Koczan J, Nomura K, He SY (2006) Plant Stomata Function in Innate Immunity against Bacterial Invasion. Cell **126**: 969–980

Millar AJ, Short SR, Chua N-H, Kay SA (1992) A Novel Circadian Phenotype Based on Firefly Luciferase Expression in Transgenic Plants. Plant Cell **4**: 1075–1087

Mizuno T, Kitayama M, Oka H, Tsubouchi M, Takayama C, Nomoto Y, Yamashino T (2014a) The EC Night-Time Repressor Plays a Crucial Role in Modulating Circadian Clock Transcriptional Circuitry by Conservatively Double-Checking Both Warm-Night and Night-Time-Light Signals in a Synergistic Manner in Arabidopsis thaliana. Plant Cell Physiol **55**: 2139–2151

Mizuno T, Nomoto Y, Oka H, Kitayama M, Takeuchi A, Tsubouchi M, Yamashino T (2014b) Ambient Temperature Signal Feeds into the Circadian Clock Transcriptional Circuitry Through the EC Night-Time Repressor in Arabidopsis thaliana. Plant Cell Physiol **55**: 958–976

Muranaka T, Oyama T (2016) Heterogeneity of cellular circadian clocks in intact plants and its correction under light-dark cycles. Sci Adv **2**: e1600500

Nakajima K, Sena G, Nawy T, Benfey PN (2001) Intercellular movement of the putative transcription factor SHR in root patterning. Nature **413**: 307–311

Nimmo HG (2018) Entrainment of Arabidopsis roots to the light:dark cycle by light piping. Plant Cell Environ **41**: 1742–1748

Niwa Y, Ito S, Nakamichi N, Mizoguchi T, Niinuma K, Yamashino T, Mizuno T (2007) Genetic Linkages of the Circadian Clock-Associated Genes, TOC1, CCA1 and LHY, in the Photoperiodic Control of Flowering Time in Arabidopsis thaliana. Plant Cell Physiol **48**: 925–937

Nusinow DA, Helfer A, Hamilton EE, King JJ, Imaizumi T, Schultz TF, Farré EM, Kay SA (2011) The ELF4–ELF3–LUX complex links the circadian clock to diurnal control of hypocotyl growth. Nature **475**: 398–402

O'neill JS, Van Ooijen G, Dixon LE, Troein C, Corellou F, Bouget F-Y, Reddy AB, Millar AJ (2011) Circadian rhythms persist without transcription in a eukaryote. Nature **469**: 554–558

Ouyang Y, Andersson CR, Kondo T, Golden SS, Johnson CH (1998) Resonating circadian clocks enhance fitness in cyanobacteria in silico. Proc Natl Acad Sci **95**: 8660–8664

Para A, Farré EM, Imaizumi T, Pruneda-Paz JL, Harmon FG, Kay SA (2007) PRR3 Is a Vascular Regulator of TOC1 Stability in the Arabidopsis Circadian Clock. Plant Cell **19**: 3462–3473

Pembroke WG, Babbs A, Davies KE, Ponting CP, Oliver PL (2015) Temporal transcriptomics suggest that twin-peaking genes reset the clock. Elife **4**: e10518

Petit JD, Li ZP, Nicolas WJ, Grison MS, Bayer EM (2019) Dare to change, the dynamics behind plasmodesmata-mediated cell-to-cell communication. Curr Opin Plant Biol **2020**: 80–89

Philippou K, Ronald J, Sánchez-Villarreal A, Davis AM, Davis SJ (2019) Physiological and genetic dissection of sucrose inputs to the Arabidopsis thaliana circadian system. Genes (Basel) **10**: doi:10.3390/genes10050334

Pittendrigh CS (1960) Circadian rhythms and the circadian organization of living

systems. Cold Spring Harb Symp Quant Biol **25**: 159–184
Pokhilko A, Fernández AP, Edwards KD, Southern MM, Halliday KJ, Millar AJ (2012) The clock gene circuit in Arabidopsis includes a repressilator with additional feedback loops. Mol Syst Biol **8**: 1–13
Rascher U, Hutt M-T, Siebke K, Osmond B, Beck F, Luttge U (2001) Spatiotemporal variation of metabolism in a plant circadian rhythm: The biological clock as an assembly of coupled individual oscillators. Proc Natl Acad Sci **98**: 11801–11805
Román Á, Golz JF, Webb AAR, Graham IA, Haydon MJ (2020) Combining GAL4 GFP enhancer trap with split luciferase to measure spatiotemporal promoter activity in Arabidopsis. Plant J **102**: 187–198
Ruiz MCM, Hubbard KE, Gardner MJ, Jung HJ, Aubry S, Hotta CT, Mohd-Noh NI, Robertson FC, Hearn TJ, Tsai Y-C, et al (2018) Circadian oscillations of cytosolic free calcium regulate the Arabidopsis circadian clock. Nat Plants **4**: 690–698
Ruiz MCM, Jung HJ, Webb AAR (2020) Circadian gating of dark-induced increases in chloroplast-and cytosolic-free calcium in Arabidopsis. New Phytol **225**: 1993–2005
Savvas D, Colla G, Rouphael Y, Schwarz D (2010) Amelioration of heavy metal and nutrient stress in fruit vegetables by grafting. Sci Hortic (Amsterdam) **127**: 156–161
Seki M, Ohara T, Hearn TJ, Frank A, Da Silva VCH, Caldana C, Webb AAR, Satake A (2017) Adjustment of the Arabidopsis circadian oscillator by sugar signalling dictates the regulation of starch metabolism. Sci Rep **7**: 10.1038/s41598-017-08325-y
Shimizu H, Katayama K, Koto T, Torii K, Araki T, Endo M, Doherty CJ, Kay SA, Barclay JL, Tsang AH, et al (2015) Decentralized circadian clocks process thermal and photoperiodic cues in specific tissues. Nat Plants **1**: 10.1038/NPLANTS.2015.163
Silva CS, Nayak A, Lai X, Hutin S, Hugouvieux V, Jung J-H, López-Vidriero I, Franco-Zorrilla JM, Panigrahi KCS, Nanao MH, et al (2020) Molecular mechanisms of Evening Complex activity in Arabidopsis. Proc Natl Acad Sci **117**: 6901–6909
Takahashi N, Hirata Y, Takahashi N, Hirata Y, Aihara K, Mas P (2015) A Hierarchical Multi-oscillator Network Orchestrates the Arabidopsis Circadian System. Cell **163**: 148–159
Thain SC, Hall A, Millar AJ (2000) Functional independence of circadian clocks that regulate plant gene expression. Curr Biol **10**: 951–956
Thieme CJ, Rojas-Triana M, Stecyk E, Schudoma C, Zhang W, Yang L, Miñambres M, Walther D, Schulze WX, Paz-Ares J, et al (2015) Endogenous Arabidopsis messenger RNAs transported to distant tissues. Nat Plants **1**: 10.1038/NPLANTS.2015.25
Thomas HR, Frank MH (2019) Connecting the pieces: uncovering the molecular basis for long-distance communication through plant grafting. New Phytol **223**: 582–589
Toyota M, Spencer D, Sawai-Toyota S, Jiaqi W, Zhang T, Koo AJ, Howe GA, Gilroy S (2018) Glutamate triggers long-distance, calcium-based plant defense signaling. Science **361**: 1112–1115
Ukai K, Inai K, Nakamichi N, Ashida H, Yokota A, Hendrawan Y, Murase H, Fukuda H (2012) Traveling waves of circadian gene expression in lettuce. Environ Control Biol **50**: 237–246

Vatén A, Dettmer J, Wu S, Stierhof Y-D, Miyashima S, Yadav SR, Roberts CJ, Campilho A, Bulone V, Lichtenberger R, et al (2011) Callose Biosynthesis Regulates Symplastic Trafficking during Root Development. Cell **21**: 1144–1155

VoB U, Wilson MH, Kenobi K, Gould PD, Robertson FC, Peer WA, Lucas M, Swarup K, Casimiro I, Holman TJ, et al (2015) The circadian clock rephases during lateral root organ initiation in Arabidopsis thaliana. Nat Commun **6**: 10.1038/ncomms8641

Warschefsky EJ, Klein LL, Frank MH, Chitwood DH, Londo JP, von Wettberg EJB, Miller AJ (2016) Rootstocks: Diversity, Domestication, and Impacts on Shoot Phenotypes. Trends Plant Sci **21**: 418–437

Webb AAR, Seki M, Satake A, Caldana C (2019) Continuous dynamic adjustment of the plant circadian oscillator. Nat Commun **10**: https://doi.org/10.1038/s41467-019-08398-5

Welsh DK, Takahashi JS, Kay SA (2010) Suprachiasmatic Nucleus: Cell Autonomy and Network Properties. Rev Adv Annu Rev Physiol **72**: 551–577

Wen S, Ma D, Zhao M, Xie L, Wu Q, Gou L, Zhu C, Fan Y, Wang H, Yan J (2020) Spatiotemporal single-cell analysis of gene expression in the mouse suprachiasmatic nucleus. Nat Neurosci **23**: 456–467

Wenden B, Toner DLK, Hodge SK, Grima R, Millar AJ (2012) Spontaneous spatiotemporal waves of gene expression from biological clocks in the leaf. Proc Natl Acad Sci **109**: 6757–6762

Wood NT, Haley A, Viry-Moussaïd M, Johnson CH, Van der Luit AH, Trewavas AJ (2001) The calcium rhythms of different cell types oscillate with different circadian phases. Plant Physiol **125**: 787–796

Wu X, Dinneny JR, Crawford KM, Rhee Y, Citovsky V, Zambryski PC, Weigel D (2003) Modes of intercellular transcription factor movement in the Arabidopsis apex. Development **130**: 3735–3745

Yakir E, Hassidim M, Melamed-Book N, Hilman D, Kron I, Green RM (2011) Cell autonomous and cell-type specific circadian rhythms in Arabidopsis. Plant J **68**: 520–531

Yerushalmi S, Yakir E, Green RM (2011) Circadian clocks and adaptation in Arabidopsis. Mol Ecol **20**: 1155–1165

Zhang Y, Bo C, Wang L (2019) Novel Crosstalks between Circadian Clock and Jasmonic Acid Pathway Finely Coordinate the Tradeoff among Plant Growth, Senescence and Defense. Int J Mol Sci **20**: 10.3390/ijms20215254